An investigation into the factors governing the performance of nedocromil sodium as a dry powder inhalation system

Clarke, Martyn James

Award date:
1999

Awarding institution:
University of Bath

An Investigation into the Factors Governing the Performance of Nedocromil Sodium as a Dry powder Inhalation System

Submitted by
Martyn James Clarke B.Pharm., M.R.Pharm.S.
for the degree of Doctor of Philosophy of
the University of Bath
1999

ProQuest LLC
789 East Eisenhower Parkway
P.O. Box 1346
Ann Arbor, MI 48106-1346

Acknowledgements

I would like to thank both of my supervisors, John Staniforth and Mike Tobyn, for their help and support throughout my research. I would also like to thank the members of CDFS, old and new, for all their help over the past three years.

In addition, I am grateful to the members of Electron Optics for their technical help throughout the project.

My thanks are also due to all of my friends, old and new, within the department of Pharmacy and Pharmacology.

Finally, I would like to thank my family. Without their continued love, support and encouragement my time at Bath would never have been possible. I dedicate this work to them.

Abstract

Nedocromil sodium is a high dose anti-allergic drug currently formulated as a pressurised metered dose inhaler for the prophylactic treatment of bronchial asthma. There are currently no marketed dry powder inhalation formulations, which is due in part to a poor understanding of the physicochemical properties of nedocromil sodium and how these properties affect the interparticle interactions governing the aerosol performance of the powder systems. Therefore, the physicochemical properties of micronised nedocromil sodium trihydrate (NST) were characterised and are described.

Low temperature scanning electron microscopy (LTSEM), a technique considered novel to the characterisation of pharmaceutical particulate systems, is described. LTSEM provided useful information as to the particle size and shape of fully hydrated micronised NST as well as enabling the drug particles' distribution within carrier based powder systems to be characterised. The techniques of energy dispersive X-ray analysis (EDAX) and environmental scanning electron microscopy (ESEM), as they relate to the characterisation of this high dose dry powder inhalation systems, are also described.

NST was not amenable to conventional methods of dry powder inhaler formulation, including the preparation of coarse carrier and aggregated powder systems. The *in-vitro* aerosol performance of both systems was governed by the cohesive drug/drug interactions. Therefore, alternative powder formulation strategies (novel to NST) were developed in an attempt to physically disrupt the cohesive drug interactions and promote more efficient

regeneration of fine particle material upon aerosolisation. Further manipulation of these systems enabled excellent flow properties to be restored without adversely affecting the improved aerosol performance of the systems. Following each formulation procedure, improvements in the *in-vitro* aerosol performance of the systems, together with supportive LTSEM and ESEM images, were related to changes in the interparticle forces presumed to be governing the mixing and aerosolisation of the systems.

It was concluded that the efficient regeneration of fine particles of NST could be achieved by the intercalation of fine particle lactose within the aggregated NST system.

By comparing the milled and micronised NST (physicochemical and *in-vitro* aerosol performance), the strong cohesive interactions governing the aerosol performance of both carrier based and pure drug aggregated systems were related to the ultrafine nature of the micronised material. Imaging of the milled and micronised materials using LTSEM together with optimisation of the particle size measurement techniques, enabled alternative theories describing the deagggregation of both systems to be developed.

Table of Contents

List of Abbreviations

ACI	Andersen Cascade Impactor
AJS	Air Jet Sieved
AR	Angle of Repose
BNF	British National Formulary
BP	British Pharmacopoeia
CFCs	Chlorofluorocarbons
CI	Carr's index
D_{ae}	Effective Aerodynamic Diameter
DPF	Dry Powder Feeder
DPIs	Dry Powder Inhalers
DSC	Differential Scanning Calorimetry
DSCG	Disodium Cromoglycate
ED	Emitted Dose
ESEM	Environmental Scanning Electron Microscopy
FPD	Fine Particle Dose
FPF	Fine Particle Fraction
FPL	Fine Particle Lactose
HB	Hand Blended
HR	Hausner Ratio
HSM	Hot Stage Microscopy
KF	Karl Fischer
LALLS	Low Angle Laser Light Scattering
LTSEM	Low Temperature Scanning Electron Microscopy
LVC	Large Volume Cell
MDIs	Metered Dose Inhalers
MMI	Marple Miller Impactor
MSLI	Multistage Liquid Impinger
MP	Mortar and Pestle
NS	Nedocromil Sodium
NSHH	Nedocromil Sodium Heptahemihydrate

NSM	Nedocromil Sodium Monohydrate
NST	Nedocromil Sodium Trihydrate
RBB	Rotary Bladed Blender
RH	Relative Humidity
SEM	Scanning Electron Microscopy
SS	Salbutamol Sulphate
SVC	Small Volume Cell
SVP	Single Vessel Proccessor
TGA	Thermogravimetric Analysis
TOFABS	Time of Flight Aerosol Beam Spectroscopy
TS	Terbutaline Sulphate
TTM	Turbulent Tumbling Mixer
VMD	Volume Median Diameter
XRPD	X-Ray Powder Diffraction

CHAPTER 1

GENERAL INTRODUCTION

1.1 Introduction

Inhalation is now the principal route of administration for drugs whose site of action is the lungs (Asking and Olsson, 1997), having several recognised advantages over alternative routes of drug administration. Medication for the treatment of respiratory diseases reaches the site of action directly, allowing for a rapid and predictable onset of action (Timsina et al. 1994). The large pulmonary surface area and extensive blood supply provide an excellent site for drug absorption (Timsina et al. 1994). The hepatic first pass effect and degradation within the gastrointestinal tract are avoided. Therefore, lower doses are generally required reducing the potential for unwanted side effects (Newman and Clarke, 1983).

Currently, the main uses for medicinal aerosols are for the immediate and prophylactic treatment of asthma and chronic irreversible obstructive airway diseases (chronic bronchitis and emphysema) (Smith and Bernstein, 1996). The ultimate goals of asthma drug therapy are prevention of symptoms (by controlling bronchial hyperresponsiveness and inflammation) and preservation of lung function (Smith and Bernstein, 1996). The treatment of acute symptoms involves the use of selective β_2-adrenergic agonists, anticholinergic agents, theophylline and other xanthine oxidase inhibitors. Long term control of asthma usually involves the use of anti-inflammatory preparations containing corticosteriods and/or the antiallergic drugs, cromolyn sodium or nedocromil sodium (Holgate, 1996; Smith and Bernstein, 1996).

Recent advancements in biotechnology have led to a large increase in the number of large molecule drugs available (proteins and peptides). Due to their poor oral

bioavailability, the majority of these drugs are currently delivered by injection. However, many proteins and peptides are relatively well absorbed from the lung (Niven, 1995; Patton, 1996; Smith, 1997), making it a potential target for the delivery of locally and systemically acting biotherapeutics (Berressem, 1999).

Drugs for inhalation can be dissolved in aqueous based formulations for nebulisation or in liquefied propellant-based systems for delivery by a pressurised metered dose inhaler (MDI). Alternatively, fine drug particles can be formulated as suspensions (MDIs) or as dry powder inhaler (DPI) systems, reducing the problems associated with drug solubility and stability (Johnson, 1997).

Each of the delivery systems has advantages and disadvantages. MDIs are very compact and portable. However, the relatively large size and high initial velocity of the delivered droplets can lead to considerable drug loss in the oropharynx (Leach, 1999). These problems can be reduced by using auxiliary spacer devices which, provide additional time for reduction of the primary droplet size (by evaporation of the propellant) (Holzner and Müller, 1994), decrease droplet velocity (Vidgren et al. 1987a) and improve the patient's ability to co-ordinate actuation with inhalation.

Most currently marketed MDIs use chlorofluorocarbons (CFCs) as the system propellants. The potential adverse environmental effects of CFCs and the international regulations phasing out their production (Tansey, 1997) has led to the development of alternative systems for aerosolised drug delivery (Leach, 1995 and 1999). Despite significant formulation challenges (Tansey, 1997), MDIs containing alternative "ozone friendly" propellants (hydrofluorocarbons) have been developed (Leach, 1999). The

elimination of CFCs from MDIs has provided the opportunity to more optimally target formulations to the deep lung, whilst decreasing oropharynx drug deposition (Leach, 1999).

However, in addition to the formulation challenges, there continue to be issues relating to patients who find it difficult to co-ordinate their inhalation with the actuation of the MDI device (Crompton, 1982) although breath actuated MDIs are now available (Hickey and Dunbar, 1997; Newman et al. 1991a).

As a result of the problems associated with MDIs, a great deal of effort has been directed at improving the efficiency of DPI systems. Advantages associated with DPIs include the ease of operation (synchronisation of aerosol discharge with inspiration is inherent) and the formulations generally do not require the extensive use of excipients (Timsina et al. 1994).

Investigations in the present study have focused on factors influencing the performance of dry powders formulated for inhalation. The following sections review some of the important issues governing the aerosol performance and the *in-vitro* testing of dry powder systems.

1.2 Aerosol Properties

The particle size is considered to be the most critical factor determining the degree and site of drug deposition within the lung (Hinds, 1982; Staniforth, 1996). Particles for inhalation can be spherical, fibrous or complex aggregates of smaller particles with a highly irregular shape. Therefore, when characterising the properties of particles in an aerosol cloud, the aerodynamic equivalent diameter (D_{ae}), a parameter that considers the particle size, shape and density is used. The D_{ae} is defined as the diameter of a sphere of unit density (1000 m^3 kg^{-1}) which has the same terminal settling velocity in still air as the particle examined (Gonda, 1988). Assuming the particles do not deviate significantly from sphericity, the D_{ae} can be estimated by multiplying the volume median diameter (VMD) by the square root of the effective particle density (Hickey, 1990).

Therapeutic aerosols are generally polydisperse and are described by a log normal probability size distribution characterised by two parameters; the count mean diameter (CMD) and the geometric standard deviation (GSD) (Gonda, 1988). However, for biological applications where the mass of drug is related to activity, the particle size distribution is more meaningfully expressed according to particle mass or volume. The mass median diameter (MMD) is the particle diameter above which 50% of the aerosol mass is contained.

1.3 Factors Influencing the Deposition of Dry Powder Aerosols

For drug delivery using a DPI system, the quality of the aerosol cloud is governed by three interdependent factors; the patient, the design of the device and the dry powder formulation (Ganderton, 1992; Timsina et al. 1994; Zanen et al. 1992).

1.3.1 The Patient

Anatomy of the Respiratory Tract

The anatomical and physiological features of the respiratory tract as well as the patient's inhalation technique have a significant influence on the aerodynamic behaviour and hence the deposition of the inhaled particles (Auty et al. 1987; Vidgren et al. 1988a).

The human respiratory tract is composed of a series of branching airways which can be divided into three anatomically distinct regions; the upper respiratory tract or oropharyngeal region, the tracheobronchial or conducting airways and the alveolar or pulmonary region (Gerrity, 1990).

Particle deposition within the respiratory tract is a complex process caused principally by inertial impaction, gravitational sedimentation and diffusion mechanisms (Hinds, 1982).

Aerosol deposition in the upper airways occurs mainly due to inertial impaction. As the inspired air changes direction, the larger aerosol particles ($D_{ae} \geq 5$ μm) impact on the upper airway walls due to their increased momentum. It is generally accepted that for

deposition in the tracheobronchial and pulmonary regions of the lung, drug particles in the D_{ae} size range of 1-5 μm are required (Gonda, 1992; Hinds, 1982). Particle deposition in these regions is governed by gravitational sedimentation and diffusion (Hinds, 1982). The large surface area of the bronchioles and alveoli facilitate the rapid absorption of the inhaled drug and it is deposition in these regions that is generally assumed to be therapeutically important. Excessively small particles (D_{ae} <0.5 μm) have such a low terminal velocity that they hardly deposit within the deep lung and are therefore mainly exhaled (Zanen et al. 1994).

Mode of Inhalation

All DPIs in current use are breath actuated and the inhalation flow rate is critical to the operation and efficiency of the device. An increased inspiratory flow rate improves the deaggregation of the powder, increasing the generation of potentially respirable particles (Newman et al. 1991b). This benefit may to some extent be countered by the increased velocity and hence greater oropharnygeal impaction of the drug particles in the upper respiratory tract (Vidgren, 1994).

1.3.2 Device Design

The design of the DPI device has a significant effect on the deaggregation and subsequent fine particle deposition within the respiratory tract (Moren, 1992). A turbulent airflow is considered more effective for dispersing powder mixtures. However, the design principles employed to increase turbulence generally increase the resistance of the DPI device and therefore the inspiratory effort required of the patient (Clark and Hollingworth, 1993a).

A large number of dry powder inhalers are currently available, each with different designs and operating principles (Bell et al. 1971; Brindley et al. 1995; Steckel and Müller, 1997a; Wetterlin, 1988). Hickey and Dunbar (1997) provide a review of currently marketed DPI devices and possible future developments.

1.3.3 The Formulation

Powder Mixing

The early theory of powder mixing was based on a concept known as random mixing, suggested by Lacey in 1943 (Staniforth, 1987). Random mixing requires there to be no particle interactions between the components of a powder mix, assumptions which may have been approximately valid when mixing very coarse and dense powders (Staniforth, 1987).

However, when considering finer, less dense pharmaceutical powders, the assumption that the component particles are non-interacting is no longer valid (Staniforth, 1987). Fine particles have been shown to adhere onto the surface of coarser carrier particles (Travers and White, 1971) and this phenomenon has been described as ordered mixing (Hersey, 1975).

The fundamental difference which distinguishes an ordered mix from a random mix is the nature of the forces influencing the interparticle interactions (Staniforth, 1981). Particles in a random mix are mainly influenced by the force of gravity (in a totally random mix there will be no cohesive or adhesive interactions between particles). In an ordered mix, the fines particles are bound to the larger coarser particles by interparticle forces that result from electrostatic, van der Waals or surface tensional interactions. The

ordered units are however still influenced by gravity. However, in the ordered mix the gravitational force is weak in relation to the cohesive/adhesive interparticle interactions, in the random mix the reverse is true.

However, the formation of ideal random or ordered mixes probably never occurs in pharmaceutical powders (Staniforth, 1982). Staniforth (1981) suggested that the two mechanisms, ordering and randomisation, exist in a dynamic equilibrium and proposed the concept of total mixing. Total mixing encompasses situations in which particles are mixed randomly, non-randomly, by ordering, by partial ordered randomisation or by any combination of these mechanisms (Staniforth, 1981). Intermediate forms of total mixes, in which ordered units containing different number of adherent particles and total mixes containing discrete particles as well as ordered units (partially ordered random mixes) probably occur most frequently in pharmaceutical systems (Staniforth, 1982).

The area of contact between the two interacting particles governs the strength of the interparticle force. This is in turn influenced by the size, shape, separation distance and surface properties of the particles (Hickey et al. 1994).

The ultimate aim of all powders formulated for inhalation is the delivery of drug particles in the D_{ae} size range 1-5 μm by manipulating the powder system and/or optimising the design of the device. However, drug particles in this size range exist as cohesive powder systems with poor flow and adverse processing characteristics. Furthermore, the drug system is difficult to disperse upon patient inhalation due to the highly cohesive nature of fine particles (Hickey et al. 1994). Therefore, particles have

to be sufficiently fine for deep lung deposition but a coarse particle system helps ensure effective powder processing and efficient DPI discharge.

Where a formulation approach has been used to address this issue, two general strategies have been adopted. In the first (figure 1.1), the micronised drug particles are blended with coarse (e.g. 30-100 μm) excipient carrier particles. This manipulation of powders is traditionally considered to result in the formation of an ordered system (Hersey, 1975) in which micronised drug particles are bound at active sites on the carrier substrate surface (Staniforth, 1996). The inclusion of a coarse carrier also overcomes the problem of dose metering and dose uniformity when low dose potent substances are to be administered (Ganderton, 1992). The carrier particles are generally designed to have a size such that after inhalation, most of them remain in the inhaler or deposit in the mouth and upper airways. In order to reach the lower airways, drug particles must therefore dissociate from the carrier particles and become re-dispersed in the airflow.

For most drug substances this is an inefficient formulation strategy because: (1) most of the drug particles are not liberated from the coarser carrier when the patient inhales and (2) drug particles which separate from the surface can often exist as agglomerates which are themselves too large to enter the lower lungs.

An idealised interactive mix may be expected with many potent low dose drugs (having a drug to carrier ratio typically between 1:50 and 1:500) (Wong et al. 1995a). The mixing process may result in a monolayer of drug particles adhered onto the carrier surface. However, for high dose drug systems where the drug to carrier ratio is far greater (typically 1:1 to 1:10), a pure interactive mix is not possible. The active powder

in the carrier formulations may be present in a variety of possible states: a) individual drug particles; b) drug-drug agglomerates; c) drug particles bound to individual carrier particles in mono- or multi-layer configurations and d) as combined drug and carrier agglomerates (French et al. 1996; Wong et al. 1995b). The coarse components may assist in the mixing process by breaking down aggregates of fine powder, thus allowing the adhesion of single fine particles to the surface of the coarser constituents (Yeung and Hersey, 1979).

In the second strategy (figure 1.2), interactions between primary drug particles are modified using processing conditions selected to encourage the formation of agglomerated units of pure drug (Bell et al. 1971; Trofast and Falk, 1996; Wetterlin, 1988).

Both formulation strategies improve the flow properties of the drug system ensuring that downstream processing and subsequent device emptying are efficient. However, adhesive forces developed between the drug and carrier particles or the internal cohesive drug-drug interactions observed in agglomerated formulations may be of a magnitude that prevents efficient regeneration of the primary drug particles under clinically achievable inspiratory conditions (Zanen et al. 1992).

The aerosol performance of carrier based and agglomerated dry powder formulations is predominately influenced by the particle characteristics and interactions within these systems.

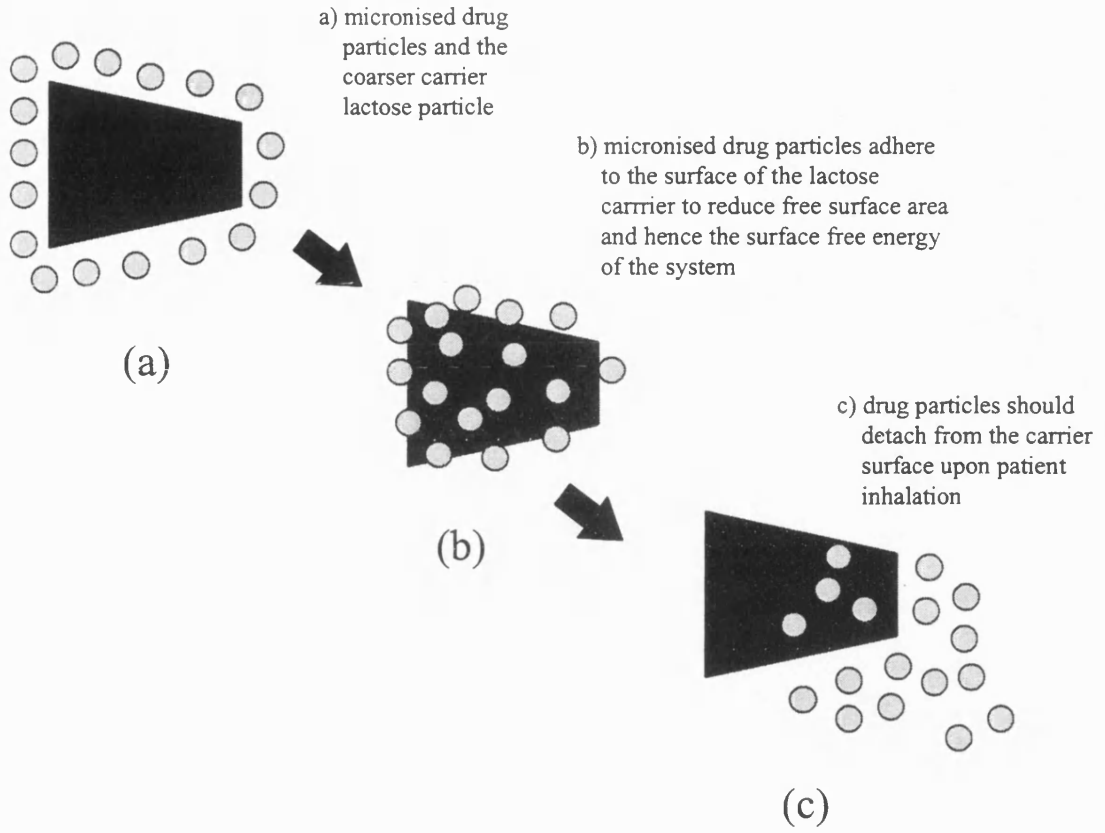

Figure 1.1 Diagrammatic representation of a coarse carrier based powder system

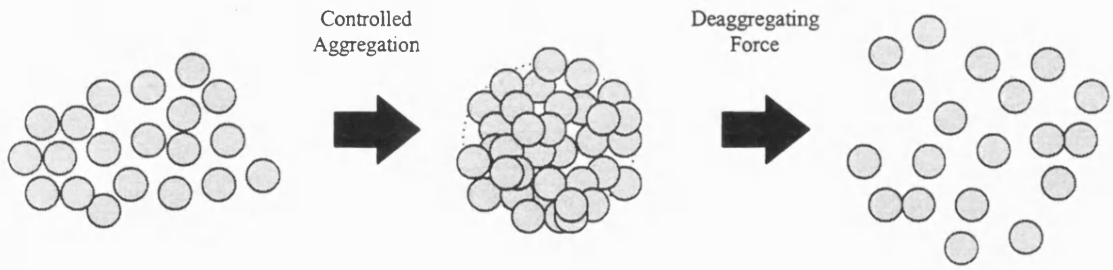

Figure 1.2 Diagrammatic representation of an aggregated powder system.

1.4 Interparticle Forces

The current generation of aerosol therapies has failed to fully exploit the potential of the pulmonary route for drug delivery (Hindle et al. 1998), due in part to a poor understanding of the interparticle forces dictating the performance of the systems.

Powder mixing, flow, fluidisation and dispersion are influenced by particle interactions (Stewart, 1986). For the majority of DPI formulations, powder deaggregation and dispersion currently relies solely on the energy harnessed by the device upon the patient's inhalation. To improve the effectiveness and reproducibility of the aerosol performance, a better understanding of the interparticle forces that govern the behaviour of drug powders formulated for inhalation is required.

Micronised drug particles present in DPI formulations are thermodynamically unstable, possessing excess surface free energy. The exposed surface area can be decreased by self-agglomeration or adhesion of the drug particles to the surface of a coarser carrier component (Staniforth, 1987).

The total force of interaction in a mixture will consist of a number of force components (Stewart, 1986). Particle interactions are primarily dictated by: van der Waals, electrical, electrostatic (coulomb) and capillary forces (Stewart, 1986, Visser, 1989). The relative contribution of these components to the total adhesion/cohesion in a particle system will depend on the interacting materials, environmental humidity and processing factors (Padmadisastra et al. 1994a). The size, shape, rugosity, hardness and

chemical composition of the interacting particles influence these interactions (Hickey et al. 1994).

1.4.1 Van der Waals Forces

Three types of van der Waals interactions exist; dipole, induction and dispersion or London-van der Waals forces (Corn, 1966). Of these examples, London-van der Waals interactions provide the major contribution to molecular forces (Corn, 1966).

London-van der Waals forces arise due to the random movement of electrons within an atom or molecule giving rise to the formation of temporary dipoles, which in turn induce complementary dipoles in nearby molecules (Visser, 1989). Attractive forces arise between the dipoles and the induced dipoles (Visser, 1989). Because of their limited charge, these forces have a very short distance of activity (Hiestand, 1966). However, when integrated over all the molecules in the contacting particles they are the major cause of particle cohesion (Visser, 1989). The van der Waals force ($Fvdv_{ss}$) acting between spherical particles of identical diameter separated by a distance (h) is given by;

$$F_{vdw\,ss} = \frac{Ar}{12h^2} \qquad \text{Equation 1.1}$$

Where r is the particle radius and A is the Hammaker constant.

A more appropriate model for low dose carrier based powder formulations is to consider the attractive interactions between a spherical particle and a flat surface;

$$F_{vdw\,sp} = \frac{Ar}{6h^2} \qquad \text{Equation 1.2}$$

where $Fvdw_{sp}$ is the van der Waals force acting between a sphere and a flat plane. The Hammaker constant is a material property that can be directly related to the molecular properties on the interacting particles (Visser, 1989).

Van der Waals forces are only noticeable when the particles become sufficiently close, i.e. separation distances of 0.2 to 1 nm (Visser, 1989). The magnitude of the van der Waals attraction becomes negligible compared with that of the gravitational force when the particle size exceeds a certain value. This value is of the order of a few microns (Visser, 1989).

Under "standard" conditions, i.e. no electrical charging and humidities <65% RH, the cohesive interactions of fine particles formulated for inhalation will be governed by the van der Waals interactions (French et al. 1996; Staniforth, 1995). The van der Waals interactions are very much dependent on the separation distance, the particles' properties (Hammaker constant) and the region of interaction (Visser, 1989). The separation distance (h) between fine particles is the single most important factor governing the van der Waals attraction (equation 1.1 and 1.2) therefore, any means to increase the interparticle distance will reduce the attractive forces.

Any effect that increases the area of contact between particles, without increasing the separation distance, will lead to an increase in interparticle interactions. Extended contact areas are found in particles having a partly flattened surface that may be due to their inherent structure, e.g. crystalline material.

1.4.2 Electrostatic Forces

Electrostatic forces can be formed by triboelectric charging (sliding/frictional forces involved) or by the formation of a potential difference when two dissimilar materials make and then break contact (Kulvanich and Stewart, 1987a). The charge that results from such processes will depend on the nature of the material, surface properties and environmental conditions (Mackin et al. 1993). The direction of charge transfer is governed by the difference in electron affinity of the two interacting materials (Kulvanich and Stewart, 1987a; Staniforth and Rees, 1982).

Triboelectrification is determined by many factors, such as particle properties (size, shape, physicochemical properties of the contacting surfaces), atmospheric conditions and processing parameters (particle motion, processing time) (Bailey, 1984). In most pharmaceutical processing conditions, the relative movement/collisions of particles provide an ideal environment for the development of contact potential or electrostatic charge (Kulvanich and Stewart, 1987a). Processes that may induce triboelectrification in pharmaceutical powders include; the preparation of fine particles (mechanical micronisation and spray drying), mixing and fluidisation in a turbulent airstream. During mechanical micronisation, the particle size is reduced by means of collisions between coarse particles so that the larger particles are broken up and fine particles are

produced. These collisions may produce high electrical charges on the micronised particles (Bailey, 1994).

Triboelectric charging and ionisation methods have been used to increase the stability of powder mixes (Staniforth and Rees, 1982). It has been reported that excipient powders generally charge negatively when contacted with metal or glass surfaces whereas many charge positively when contacted with plastic surfaces (Staniforth and Rees, 1982). Most pharmaceutical excipients have a low resistivity and therefore rapidly lose the electric charge. However, the short lived increase in electrical interactions may facilitate closer surface contact between interacting particles causing a more permanent increase in van der Waals forces (Staniforth, 1987, Visser, 1989).

Electrostatic charge and charge decay of both the drug and carrier material may also affect drug delivery from DPI systems (Peart, 1996).

At low humidities (<30% RH), electrostatic effects markedly influence the degree of interaction. However, at increased humidities (>65% RH), capillary forces arising due to water vapour condensation at the interface of the particle become more predominant (Kulvanich and Stewart, 1988).

1.4.3 Surface Tensional Forces

The RH influences the type of interparticle interactions predominating in the powder mix (Kulvanich and Stewart, 1988). The presence of moisture in a powder system can impair the flow properties of the material, adversely affect stability and influence the aerosol performance of the formulation (Genus et al. 1997; Zografi, 1988).

At a particular temperature and humidity, the amount of water associated with a solid will be dependent on its chemical affinity for the solid and the number of available sites for interaction (Konty, 1988). Water may be adsorbed onto the solid surface and/or may be absorbed into the bulk solid structure (Brittain et al. 1988; Khankari and Grant, 1995). In hydrates, water occupies definite positions in the crystal lattice usually forming hydrogen bonds and/or co-ordinate covalent bonds with the anhydrate drug molecules (Khankari and Grant, 1995).

For non-hydrating, crystalline materials, the moisture associated with the particles at low humidities is adsorbed water vapour (Coelho and Harnby, 1978a). At increased levels of humidity, water vapour condensation at the interface of the interacting particles may give rise to capillary forces (Coelho and Harnby, 1978a; Kulvanich and Stewart, 1988). The critical relative humidity at which condensation first occurs ranges from 65 to 80% (Coelho and Harnby, 1978a). As the critical humidity is reached, liquid bridges become stable and capillary forces should become the main component of the interparticle interaction (Coelho and Harnby, 1978b). In addition, if the material is very water soluble, formation of bridges of solid material at particle-particle contacts can occur as the liquid evaporates from the capillary region (Padmadisastra et al. 1994b).

When both adsorption and absorption occur, the term sorption is used.

Adsorbed moisture may increase the van der Waals interactions as the adsorbed layer may be regarded as part of the particle thus causing a decrease in the interparticle separation distance (Coelho and Harnby, 1978a). However, adsorbed moisture will reduce the electrostatic forces as humidity causes the surrounding air to become

conductive and therefore facilitates rapid discharge of the particles (Coelho and Harnby, 1978b).

1.4.4 Measurement of Interparticle Interactive Forces

Forces of adhesion/cohesion are generally determined by two approaches. In the first, measurements are based on the behaviour of a large number of particles and include, angle of repose determinations, vibration assessments (Staniforth, 1984; Staniforth and Rees, 1982 and 1983), shear stress and packing density measurements (Hiestand, 1966).

The second approach employs methods that determine the interparticle forces acting between individual powder particles and surfaces, e.g. pendulum impaction techniques (Concessio et al. 1988) and centrifugal methods (Kulvanich and Stewart, 1987b and 1987c; Staniforth et al. 1981).

The interactions of fine drug particles bound to larger carrier particles (or glass beads) have been assessed using a modified centrifuge cell (Kulvanich and Stewart, 1987b and 1988; Staniforth et al. 1981). More recent designs have used a scattering of coarse particles fixed to the centrifuge cell with drug particles then added to the experimental surface (Peart, 1996; Podczeck et al. 1995 and 1997). Centrifugal techniques have also been used to assess the influence of RH on the adhesive properties of model drug-carrier interactive systems (Kulvanich and Stewart, 1988; Podczeck et al. 1996 and 1997).

The removal of individual particles from carrier surfaces can be studied using the atomic force microscope, potentially allowing greater characterisation of the isolated sites of adhesion (Bowen et al. 1998; Mizes, 1994).

1.5 Pre-Formulation Aspects of Dry Powder Aerosols

A number of physicochemical properties of the constituent particles must be optimised to ensure efficient powder processing and effective aerosol performance (Staniforth, 1995). These properties include particle size, density, morphology and surface composition (including adsorbed moisture) (Edwards et al. 1997; Hickey et al. 1990; Staniforth et al. 1996).

1.5.1 Physical Properties of the Drug Particles

Drug particle size is the most important parameter governing the efficient and effective performance of DPI formulations (Staniforth, 1996). The particle size is a primary determinant not only of the fraction of aerosol deposited but also of the deposition site itself.

It is difficult to specify an ideal size for aerosol particles, partly because it is not certain where the particles should be deposited within the respiratory tract and partly because of the difficulty in predicting the aerodynamic behaviour of the inhaled particles. The deposition pattern can be complicated by hygroscopic growth (Byron et al. 1977), particle agglomeration and particle charge (Balachandran et al. 1991).

However, it is generally considered that to promote deposition within the deep lung, powders containing drug particles with an $D_{ae} \leq 5$ μm must be employed (Ganderton and Kassem, 1992). Studies using liquid aerosols (where aerodynamic and geometric diameters are comparable) have demonstrated that an D_{ae} window of 1-3 μm is optimal

for inhalation drug delivery (Adjei and Garren, 1990; Clay et al. 1986; Zanen et al. 1994 and 1995).

In two separate studies, Zanen et al. (1994 and 1995) found that monodisperse aerosols of salbutamol sulphate and ipratropium bromide with a particle size of 2.8 μm, produced greater bronchodilation than droplets of a larger size (5 μm). These findings were supported by Clay et al. (1986) who found that a terbutaline aerosol (D_{ae}: 1.8 μm) induced a stronger bronchodilation in asthmatics than aerosols containing droplets of a larger size (D_{ae}: 4.6 or 10.3 μm).

However, when considering DPI formulations, consideration must not only be given to the optimal particle size for deep lung penetration but also to the effects of the increased cohesive interactions acting between the fine drug particles (Byron, 1986). To date, few studies have investigated the optimal drug particle size <5 μm for dry powder systems in terms of the contribution of the various interparticle forces on the degree of particle deaggregation. It is considered that these interactions will be especially important when considering the deaggregation and aerosolisation of pure drug or high dose carrier based powder formulations. In these systems, drug-drug interparticle interactions would be expected to govern the aerosol performance of the formulation.

Persson and Wirén (1989) found that the bronchodilator response was increased when a greater mass of terbutaline particles <5 μm (D_{ae}) were delivered. Altounyan (1985) found that small particles of disodium cromoglycate (DSCG) (94% <10 μm) produced improved clinical effects compared with larger particles (99.5% >10 μm).

Curry et al. (1974) found a greater response to DSCG when administered in a size range around 2.0 μm compared with particles of a larger size (6.0 and 11.7 μm), findings supported by Godfrey et al. (1974). Similar observations have been made by Rees et al. (1982) who showed greater bronchodilation with terbutaline particles less than 5.0 μm compared with inhaled particles in the size range 5-10 μm or 10-15 μm.

However, Wong et al. (1995b) demonstrated a two-fold increase in the generation of potentially respirable nedocromil sodium trihydrate (NST) particles, formulated as a high dose powder system (50% $^{w}/_{w}$), when apex-milled drug particles (10.17 μm: VMD) as opposed to micronised drug particles (5.01 μm: VMD) were employed. The improvement in dispersion and subsequent fine particle deposition was attributed to a reduction in the cohesive interactions operating within the milled NST system.

Edwards et al. (1997) studied the *in-vivo* and *in-vitro* deposition of particles possessing low mass densities and consequently larger geometric particle size distributions such that the mean D_{ae} was still considered potentially respirable. The increased particle size resulted in a decreased tendency of the particles to aggregate which in combination with the low mass density, enabled a more efficient aerosolisation.

Drug Particle Shape and Surface Properties

The morphology of the interacting surfaces will have a significant effect on the interparticle interactions influencing the performance of agglomerated or carrier based systems. Drug particle shape is largely determined by the method used to prepare the powders, e.g. comminution, screening, spray drying, crystallisation etc. The interaction

between two spherical particles (a) would be expected to be less than between smooth flat particles (b) due to the decreased area of intimate contact (figure 1.3).

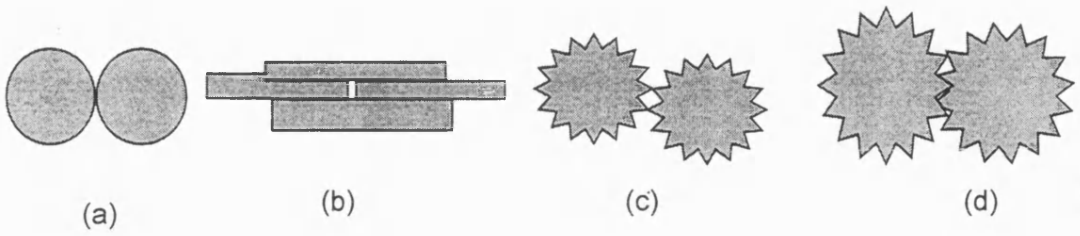

Figure 1.3 Diagrammatic representation of possible interparticle interactions.

Hiestand (1966) suggested that cohesive interactions between fine particles might vary due to differences in surface textures. Powders with smooth surfaces (figure 1.3a) would be expected to produce higher true areas of contact compared with irregular particles (figure 1.3c) therefore, display an increased cohesive interaction. However, it could also be envisaged that the size and distribution of the asperities might encourage maximum contact (figure 1.3d).

The influence of drug particle shape on the aerosol performance has not been fully evaluated however, it has been shown to alter the interparticle interactions in powder systems (Wong and Pilpel, 1988; Wong and Pilpel, 1990). When considering the adhesion of fine particles (calcium carbonate) onto the surface of a coarser carrier (lactose), it was demonstrated that the more irregular fine particles tended to adhere more strongly to lactose crystals than equivalent more regular particles (Wong and Pilpel, 1988). The practical significance of this is that by exercising control over the shapes of the fine particle, it should be possible to produce an ordered mix that is stable towards de-mixing and segregation.

The effects of drug particle shape on the aerosol performance of powder systems formulated for inhalation was investigated by Wong et al (1989) who found that the FPF of DSCG was not significantly altered by varying the drug particle shape.

Applications of spray drying to powder formulations for inhalation have appeared in several articles (Ampratwum et al. 1997; Chawla et al. 1994; Edwards et al. 1997; Vidgren et al. 1987b, 1988a, 1988b, 1989 and 1991). Vidgren et al. (1987b) concluded that spray dried DSCG deaggregated more completely to particles within an D_{ae} size range of 0.3-3.3 μm compared to micronised particles. Following physicochemical characterisation of the micronised and spray dried DSCG material, it was concluded that the more spherical spray dried particles experienced decreased cohesive interactions compared to the irregular particles of the mechanically micronised material (Vidgren et al. 1987b). However, the presented data revealed that there was no significant difference in the percentage of particles deaggregating to a size <7.1 μm. Due to the smaller particle size of the spray dried material, no conclusions can be drawn regarding the regeneration of discrete drug particles since the 3.3 μm cut-off would in theory restrict a proportion of the discrete micronised particles reaching the lower stage of the impactor. The improved *in-vitro* aerosol performance of the spray dried DSCG compared to the micronised DSCG (based on regeneration of discrete particles), can only be attributed to the spray dried material having a smaller particle size and not to any changes in the cohesive interactions suggested by the physical analysis of the materials.

Other techniques for the generation of powders for inhalation containing microfine particles include supercritical fluids processes (Phillips and Stella, 1993; York and Hanna 1996; York et al. 1998) and novel condensation technology (Hindle et al. 1998).

The effects on the deaggregation performance of DSCG particles surface treated with a series of saturated fatty acids has been investigated (Fults et al. 1997; Hickey et al. 1992). An increase in stage-2 drug deposition (D_{ae} <6.4 μm) was observed following lauric acid and stearic acid treatment (two and three fold respectively) when compared to non-treated DSCG. It was concluded that a change in particle morphology of the treated DSCG contributed to the improved deaggregation of the drug system (Fults et al. 1997).

1.5.2 Physical Properties of the Carrier Particles

The particle size and surface morphology of the carrier component influence the powder performance of carrier based systems during powder preparation, processing and following aerosolisation. A number of different carriers particles have been used (Braun et al. 1996; Mackin et al. 1997) although lactose is most frequently employed (Timsina et al. 1994).

Drug dispersion is dependent upon the size and shape (French et al. 1996; Robertson, 1997) and surface morphology (Kassem and Ganderton, 1989) of the carrier particles. The size of the carrier can influence both the entrainment of powders and the force required to liberate drug particles from surfaces (Akiyama and Tanijri, 1989; Kassem, 1990; Lord, 1993; Steckel and Müller, 1997b).

Because adhesion of particles is a surface phenomenon, the morphology of the surface will have a significant effect on the adhesion of drug particles (Staniforth et al. 1982). Staniforth (1981) concluded that rougher surfaces (associated with deeper energy traps) produced higher adhesion profiles than for the same adherent particle component blended with smoother carrier crystals. Figure 1.4a depicts particles that are lodged between the surface asperities, resulting in stronger adhesive interaction due a larger area of surface contact and a reduction in the interparticle separation distance. Therefore, carriers that possess a more porous surface may form stronger interparticle bonds due to the entrapment of the fine drug particles within surface clefts and indentations (Kawashima et al. 1998a).

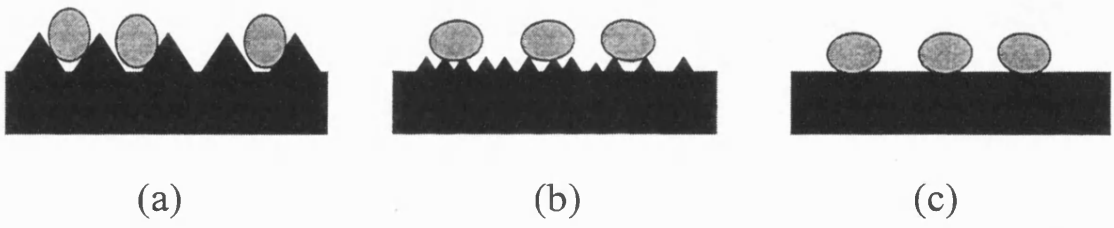

Figure 1.4 Diagrammatic representation of the possible effects of the carrier surface on the adhesion of finer drug particles.

The interparticle contacts depicted in figure 1.4b occur only at the tip of the carrier surface asperities. This may result in a decreased interparticle interaction due to a decrease in surface contact and an increase in the separation distance. Carrier particles with a low surface roughness (figure 1.4c) have been shown to facilitate a more effective re-dispersion of drug particles in an inhaled airstream (Kassem and Ganderton, 1989; Robertson, 1997; Kawashima et al. 1998a).

Ideally, the surface should be optimised, possessing sufficient adhesion so that ordered systems do not segregate in the handling and filling processes but release most of the drug substance upon patient inhalation.

1.5.3 Ternary Components

Manipulation of the particle interactions in a dry powder aerosol system can also be achieved by the addition of ternary components to the formulation (Lord and Staniforth, 1996). It has been demonstrated that the addition of fine particle lactose (FPL) (Lord 1993, Lucas, 1998a; Zeng et al. 1998), magnesium stearate (Kassem, 1990; Peart, 1996) and L-leucine (Peart, 1996; Staniforth, 1996) can improve the separation of the drug from the carrier, improving the aerosol performance of the formulation.

Mechanistically the action of fine particle excipients cannot be unequivocally explained. However, according to the ordered mixing theories of Hersey (1975), it is to be expected that upon blending, the FPL would occupy the most active binding sites on the carrier lactose surface (Staniforth, 1996). In this case, only more passive sites would remain available for adhesion of drug particles (Staniforth 1996).

It has also been shown that some drug particles can adhere to the FPL to form drug/FPL multiplets (Lucas et al. 1998a). It is considered that the formation of these multiplets improves the aerosol performance as liberation of drug or protein particles from the surface of FPL can occur more readily than from coarser particles (Lord, 1993; Ganderton, 1992). This would be expected since smaller particles have a lower degree of surface roughness that restricts opportunities for contacts at clefts and asperities on

the surface of the substrate. A proportion of the drug/FPL multiplets may also be potentially respirable.

1.6 Characterisation of Aerosol Performance

In-vivo methods for determining the efficiency of inhaled drug delivery along the respiratory tract include, monitoring clinical changes (Basran et al. 1984; Edwards and Chambers, 1989; Persson and Wiren, 1989; Vidgren et al. 1991) and the pharmacokinetic assessment of blood and/or urine drug concentrations (Altounyan, 1985; Hindle et al. 1995). Gamma scintigraphy and single photon emission computed tomography have also been used to assess *in-vivo* aerosol deposition (Biddiscombe et al. 1993; Newman and Wilding, 1998; Summers et al. 1996). Vidgren et al. (1987b, 1988a, 1988b, 1989 and 1990) has used gamma scintigraphy to characterise the *in-vivo* aerosol deposition of spray dried DSCG particles.

However, clinical studies are expensive and time consuming. Therefore, alternative methods have been developed to assess the potential aerosol performance of powder formulations for inhalation. Size measurements on impacted particles using optical microscopy have been conducted to characterise the properties of the aerosol cloud (Evans, 1993; Hallworth and Hamilton, 1976). However, these techniques do not take into account the anatomical structure of the human respiratory tract or the aerodynamic behaviour of the particles. Therefore, inertial separation techniques that determine the

size distribution of aerosol particles based on their mass and velocity are perhaps the most appropriate *in-vitro* methods to assess the potential *in-vivo* deposition.

However, although inertial impaction methods are based on the principle mechanism relevant to the fractionation of aerosols within the respiratory tract, *in-vitro* aerosol assessments can not directly predict the lung dose *in-vivo*. This is in part due to the primitive design of impactors compared with the anatomical complexity of the respiratory tract and the fact that many *in-vitro* deposition studies do not try to mimic temperature and humidity conditions within the lungs (Martin et al. 1988). The potentially respirable dose as determined by current particle impactors, almost always overestimates the actual amount of drug deposited in the lungs (Vidgren et al. 1988a). Vidgren et al. (1988a) found a greater *in-vitro* fine particle deposition (0.3-7.1 μm) of spray dried DSCG (39.4 ± 1.6%) compared with *in-vivo* results (16.4 ± 3.9%). Nevertheless, cascade impactors can provide a useful measure of the aerodynamic particle size distribution with which to compare devices and formulations.

1.6.1 Impactor Theory

Cascade impaction is based on the principle that a particle/droplet moving in an airstream will impact on a surface placed in its path, provided that the inertia of the particle/droplet is sufficient to overcome the drag force that tends to keep it in the airstream. By successively increasing the velocity of the airstream as it passes through the stages of the impactor, the particles are separated into various size fractions. The increase in velocity is accomplished by successively decreasing the jet size at each stage of the impactor. A pre-separator is often included to collect the larger particles whilst

the last stage is generally followed by a filter to capture all particles less than the final cut-off size.

1.6.2 Apparatus A (BP, 1998)

Apparatus A of the British Pharmacopoeia (1998) is an inertial aerosol classifier also referred to as the twin stage impinger (Hallworth and Westmoreland, 1987). The aerosol cloud deposits on three impaction surfaces. Following impaction on the back of the glass throat, the particles then pass through a liquid impinger (upper impinger) that has an effective cut-off diameter ($ECD_{50\%}$) of 6.4 μm at the prescribed flow rate of 60 ± 5 litres min^{-1} (Hallworth and Westmoreland, 1987). This has more recently been verified (Miller et al. 1992). The last impaction surface is in the lower impinger, which traps the remaining drug although Miller et al. (1992) report that a significant fraction of sub-micron material may escape this final stage. The throat and upper impinger are defined as stage-1; the lower impinger is defined as stage-2.

Apparatus A (BP, 1998) functions simultaneously as a particle sizing device and as a means of assessing total drug output. The disadvantage is that the total sample is divided into only two size categories and separation between the two fractions is not sharp (Hallworth and Westmoreland, 1987; Miller et al. 1992). Since the aerosol cloud is only segregated into two fractions, no information is provided on the distribution of particle sizes above and below the selected cut-off.

Apparatus A has been used extensively to characterise and compare aerosol systems formulated as MDIs and DPIs (Jashnani and Byron, 1996; Jashnani et al. 1993; Lucas et

al. 1998a and 1998b; Phillips et al. 1990). Various studies have compared its use with other inertial impaction techniques (Holzner and Müller, 1995; Olsson et al. 1996).

1.6.3 Cascade Impaction

Cascade impactors provide a useful aerodynamic measure of the particle size distribution, which can be used to compare devices and formulations. The impactors available vary in their complexity, particle size resolution capabilities and their collection efficiencies. The reliability of the impactor data can be influenced by factors such as inter-stage wall losses, particle bounce/blow-off, particle deagglomeration or break up and the nature of the collection surfaces (Hickey, 1990; Hindle et al. 1996; Nasr et al. 1997).

Three different impactors are to be included in the Pharmacopoeias for the evaluation of therapeutic aerosols, the Anderson Mk II impactor (ACI), the Marple-Miller Impactor (MMI) and the (5-stage) Multi-Stage Liquid Impinger (MSLI). However, none of the three impactors are ideal and future work is concentrating on further developing each impactor to improve their versatility (Olsson et al. 1998).

The performances of the MMI and ACI with regards the characterisation of therapeutic aerosols are discussed by Hindle et al. (1996), Marple et al. (1995) and Vaughan (1989).

(5-Stage) Multistage Liquid Impinger

The original, all glass, multistage liquid impinger was constructed by May (1966) and has since been modified, incorporating additional stages and modified to a metal/glass construction to more fully and reproducibly characterise the aerosol cloud (Asking and Olsson, 1997; Bell et al. 1973a; Ganderton, 1996).

The upper stage of the MSLI serves as a pre-separator, having a high capacity for powder retention (Olsson et al. 1998). The MSLI impinges the aerosol onto wetted glass sinters. The trapping liquid used on the impaction stages allows high drug loading with minimum risk of re-entrainment (Asking and Olsson, 1997). All the important surfaces are easily rinsed therefore, there is no significant wall losses (Asking and Olsson, 1997). However, the MSLI is particularly weak as a classifier of fine aerosols at low flow rates therefore, an additional liquid stage ($ECD_{50\%}$ of 0.7 μm at 60 litres min^{-1}) has been designed, calibrated and performance tested to be possibly incorporated into the existing 5-stage compendial model (Olsson et al. 1998).

1.7 Nedocromil Sodium

Nedocromil sodium (NS) (disodium 9-ethyl-4, 6-dioxo-10-propyl-4H, 6H-pyrano[3,2-g]quinoline-2, 8-dicarboxylate) (figure 1.5) is a hydrophilic drug (Khankari et al. 1998) used in the treatment of reversible obstructive airways diseases such as asthma (Cairns et al. 1985).

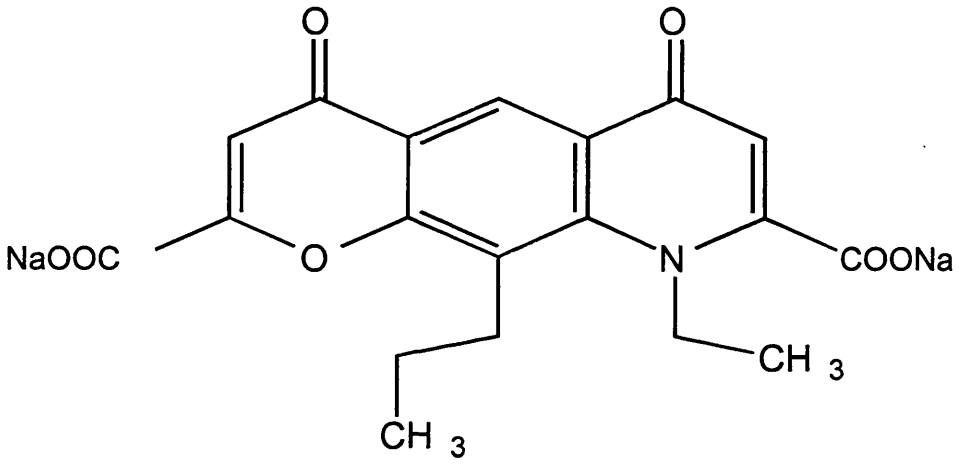

Figure 1.5 The Chemical Structure of Nedocromil Sodium

Preliminary work on the preparation and physicochemical properties of various nedocromil sodium hydrates of NS have been reported (Khankari et al. 1995 and 1998). NS has been found to exist in the following hydrate phases; the heptahemihydrate (NSHH), the trihydrate (NST), a monohydrate (NSM) and an amorphous phase which contains variable amounts of water (1.5 - 3 moles) (Khankari et al. 1998). The ranges of stability for the crystalline hydrate phases at 22°C are: NSM 0-6.4%; NST 6.4 to 79.5% and NSHH 80 to 92.9% RH (Khankari et al. 1998). At a RH of 92.9%, NS forms a saturated solution whereas at RH > 92.9%, NS forms an unsaturated solution (Khankari

et al. 1998). The optimum RH conditions for storage at 22°C are: 50% RH (ambient) for NST; 90% RH for NSHH and 0% RH for NSM (Khankari et al. 1998).

The monohydrate is the form used in the marketed MDI formulation (Tilade®). However, the monohydrate is extremely hygroscopic and rapidly converts to the trihydrate at RH ≥ 6.4% RH at 22°C (Khankari et al. 1998). The trihydrate has previously been investigated when considering the formulation of powder systems for inhalation (Wong et al. 1995a and 1995b).

NST converts to the heptahemihydrate at RH ≥ 80% therefore, when particles of NST are inhaled they have the potential to take up moisture in the RT and change their particle size and aerodynamic properties by hygroscopic growth (Byron et al. 1977).

The crystal structures of the trihydrate (Freer et al. 1987) and the heptahemihydrate (Khankari et al. 1995) of NS have been described but that of the monohydrate has not yet been reported (Khankari et al. 1988).

Different Salt Forms of Nedocromil

Mixing aqueous solutions of NS and water-soluble salts of bivalent metal cations produce nedocromil salts of lower solubility than NS (Zhu et al. 1997a). The crystal structures and physicochemical properties of various bivalent salts of nedocromil have been published; nedocromil zinc (Zhu et al. 1997a; Ojala et al. 1996), nedocromil magnesium (Ojala et al. 1996, Zhu et al. 1996) nedocromil calcium (Zhu et al. 1997b) and other metal ions (Macrae, 1992). These salts have a much lower solubility in water than the sodium salt therefore, rapid water uptake due to hygroscopicity and particle size

changes due to crystal growth would not be expected. Therefore, more predictable drug delivery to the RT may be achieved by selecting a suitable salt form. However, the toxicological profile of the salt may limit the usefulness of this approach (Zhu et al. 1997a). Both zinc and magnesium ions at low concentrations are acceptable for use in pharmaceutical applications not involving the lung whereas only the sodium ion is suitable in systems formulated for use in the lung (Ojala et al. 1996).

The free acid form of nedocromil has been prepared and the physicochemical (Chan and Gonda, 1995) and aerodynamic properties characterised (Chan and Gonda, 1993). The free acid of nedocromil shows practically no moisture uptake below 80% RH (<1 % $^{w}/_{w}$) and minimal uptake even at prolonged exposure of the particles to 99.2% RH at 37°C (3.5% $^{w}/_{w}$) (Chan and Gonda, 1995). The elongated particles of the free acid (D_{ae}~1 μm) may therefore offer advantages for increased pulmonary deposition (Chan and Gonda, 1993).

1.8 Aims of the Study

Nedocromil sodium is an anti-allergic drug administered in the prophylactic treatment of bronchial asthma. There is currently no marketed dry powder inhaler formulation for nedocromil sodium, which is due in part to a poor understanding of both the physicochemical properties of the micronised drug and the interparticle forces governing the aerosol performance of high dose inhalation systems.

Therefore, an attempt was made to formulate model DPI systems and assess the interparticle intercations governing the mixing behaviour and aerosol performance of these powder mixes.

A study was initiated to characterise the physical properties of the micronised drug particles, in particular the size and shape of the crystals, important parameters when considering the aerosol performance of powder systems.

Difficulties arise when characterising NST using conventional scanning electron microscopy (SEM) techniques, possibly due to the hydration state of the drug material. Therefore, it was considered essential to develop alternative microscopic techniques to fully characterise the particle size and shape of the micronised material. It was hoped that the techniques would enable characterisation of the drug particles' distribution within dry powder formulations.

By assessing the mixing and *in-vitro* aerosol behaviour of NST formulations, it was hoped that a more fundamental understanding of the interparticle forces governing the performance of this high dose powder system would be gained. By correlating the deaggregation and subsequent fine particle deposition of the powder systems following the various formulatory procedures, it was hoped that the contribution of cohesive (drug/drug) and adhesive (drug/carrier) interparticle interactions to the performance of nedocromil sodium as a high dose aerosol system could be established.

The cohesive interactions operating within the powder systems were assessed indirectly by measuring the deaggregation and subsequent fine particle generation using either a modified version of Apparatus A or a multistage liquid impinger.

It was hoped to characterise the effects of storage humidity on the physicochemical properties and *in-vitro* aerosol performance of nedocromil sodium to assess the contribution, if any, of adsorbed and absorbed moisture on the cohesive interactions operational within the pure drug system.

Finally, based on literature reports suggesting differences in the aerosol performance of milled and micronised NST (Wong et al. 1995b), studies to fully characterise the two materials (physicochemical and *in-vitro* aerosol properties) were initiated to increase understanding of the interactions governing the aerosol performance of the powder systems.

CHAPTER 2

MATERIALS AND GENERAL CHARACTERISATIONS

2.1 Materials

2.1.1 Analytical Materials

Methanol and cyclohexane were HPLC grade.

Water was freshly distilled (Fisons Scientific Equipment, Loughborough, U.K.). Hydrochloric acid (1.0 M) and lecithin were obtained from BDH Ltd., Poole, U.K.

Table 2.1 details the materials used to produce saturated salt solutions and table 2.2 details the materials used in the detection of fine particle lactose.

Salt	Supplier
Potassium chloride	BDH Laboratory Supplies, Poole, U.K.
Sodium chloride	BDH Laboratory Supplies, Poole, U.K..
Magnesium nitrate	BDH Laboratory Supplies, Poole, U.K.
Potassium acetate	BDH Laboratory Supplies, Poole, U.K.
Lithium chloride	Sigma Chemical Co., St. Louis, MO, U.S.A.

Table 2.1 Details of the salts used to produce the saturated salt solutions.

Material	Supplier
Glycine powder	Aldrich Chemical Company, Dorset, U.K.
Sodium hydroxide pellets	BDH Laboratory Supplies, Poole, U.K.
Methylamine (40% $^{w}/_{v}$ in water)	Aldrich Chemical Company, Dorset, U.K.
Sodium sulphite	BDH Laboratory Supplies, Poole, U.K.

Table 2.2 Details of the materials used for the detection of fine particle lactose.

2.1.2 Materials used in the Formulation of the Powder Systems

Table 2.3 details the formulation materials used in the study.

Classification	Material	Batch	Supplier
Coarse carrier lactose	α-lactose monohydrate	L6531	SpheroLac 100, Meggle GMBH, Wasserburg, Germany.
Fine particle lactose	α-lactose monohydrate	L7589	SorboLac 400, Meggle GMBH, Wasserburg, Germany.
Drugs	Micronised nedocromil sodium trihydrate	GMR 5019G	Rhône Poulenc Rorer, Cheshire, U.K.
	Milled nedocromil sodium trihydrate	3834E/A	Rhône Poulenc Rorer, Cheshire, U.K.
	Terbutaline sulphate	869-01	Astra Draco AB, Lund, Sweden

Table 2.3 Details of the materials used in the formulation of the powder systems.

2.2 General Methods

2.2.1 Preparation of Lactose Carrier Sieve Size Fractions

A vibratory sieve shaker (Fritsch 'Analysette', Christison, Gateshead, U.K.) with a set of standard brass test sieves (Endecotts, London, U.K.) was used for preparing sieve size fractions of α-lactose monohydrate. The sieves were assembled in ascending order of aperture diameter and approximately 20 g of the powder sample placed on the top sieve. The powders were vibrated for approximately 10 minutes, the contents of each sieve discharged and the sieve carefully brushed to unblock the mesh. The powder fractions were then returned to the sieves from which they were originally removed and vibrated for a further 10 minutes. The following sieve size fractions were produced: <45 and 63-90 μm.

The 63-90 μm sieve fraction was air-jet sieved (AJS) to try and remove adherent lactose fines from the coarse carrier surface. An Alpine air jet sieve (Augsburg, Germany) and a brass test sieve of 63 μm were used to remove the undersize fraction. Following 10 minutes of sieving, the sieve was cleaned in the manner described previously. The contents were then replaced on the sieve and the air jet sieve operated for a further 10 minutes.

2.2.2 The Control of Relative Humidity

Storage of the Drug and Excipient Powders

Environments of a fixed humidity were maintained within glass desiccators by preparing saturated salt solutions (table 2.4) from freshly distilled water. The desiccators were stored over the temperature range 20-25°C (Gallenkamp cooled incubator, U.K.) and the RH within the desiccators confirmed using a dial hygrometer.

Salt	Temperature °C			
	15	20	25	30
	Relative Humidity (%)			
Potassium chloride	87	86	85	84
Sodium chloride	76	76	75	75
Magnesium nitrate	56	55	53	52
Potassium acetate	23	23	22	22
Lithium chloride	13	12	12	12

Table 2.4 Saturated aqueous solutions of the salts (in contact with excess solute) in an enclosed system produce the humidities indicated. (Pharmaceutical Handbook, 1980)

Unless otherwise stated, all drug and excipient powders were stored in desiccators over a saturated solution of magnesium nitrate at 20-25°C (53-55% RH).

Experiments investigating the effects of humidity on the physicochemical (section 7.2) and *in-vitro* aerosol properties of NST (section 7.3) employed alternative saturated salts solutions to produce the desired RH conditions.

Formulation Procedures

Unless otherwise specified, all formulation procedures (powder screening, size classification and mixing) were conducted under ambient laboratory conditions. The humidity and temperature within the laboratory for the year 1998 were recorded and ranged from 19 to 63% RH and 16 to 29°C.

Following processing, the powder systems were stored at 53-55% RH and 20-25°C. All formulations were generally characterised (physicochemical and *in-vitro* aerosol investigations) within a month of preparation.

Storage of Hard Gelatin Capsules

The moisture content has a marked effect on the visco-elastic properties of gelatin capsules (Konty and Mulski, 1989). Konty and Mulski (1989) concluded that capsules stored < 40% RH exhibit brittleness at ambient temperature whereas at RH > 85% the gelatin sorbs considerable moisture causing swelling and altering the physical properties of the capsules.

Initial investigations, revealed that the mechanism of capsule piercing within the Cyclohaler® was an important factor influencing the deaggregation and dispersion of the powder system. Brittle fracture of the capsule allowed the powder formulation to "escape" from the capsule/device without being efficiently deaggregated by the shear forces generated upon aerosolisation of the powder system. Therefore, hard gelatin capsules (Davcaps®, Hertfordshire, U.K.) were stored in a desiccator at 53-55% RH for at least 24 hours before being used in the *in-vitro* aerosol investigations.

Several studies have reported on the transfer of moisture between gelatin capsules and the contents of the capsules including: Bell et al. (1973b) and Strickland and Moss, (1962). The transfer of moisture from the capsules to their contents may render the capsules brittle whereas moisture transfer to the capsules may cause capsule swelling and stickiness. The accumulation of moisture in an encapsulated powder may also lead to chemical decomposition, hydrate formation, moisture binding and cementing of the capsule contents.

Therefore, the capsules were removed from the desiccator (53-55% RH) and filled with the powder formulation immediately prior to *in-vitro* aerosol assessment. By filling capsules immediately before aerosol characterisation, it was hoped that any moisture transfer effects would be minimised. This was considered especially important when investigating the aerosol performance of powders stored at different humidities (section 7.3).

2.2.3 Mixing Techniques

Screening Stages

Metal meshes of defined aperture size (Endecotts sieves, London. U.K.) were used for all size classification and screening procedures. Fine particle material (NST, TS and FPL) was screened through a 355 μm aperture mesh prior to all formulation studies to remove any large agglomerates.

Hand Blending (HB)

Unless otherwise specified, HB was performed by mixing the powders for 15 minutes with a metal spatula in a glass mortar. A metal spatula was used in preference to a glass

pestle in an attempt to control the shear forces generated during the mixing process. The powders were screened (355 μm) at the mid-point of the mixing process to reduce/destroy any agglomerates and improve blend quality (Lord, 1993; Lucas et al. 1988a; Wong et al. 1995a).

Turbulent Tumbling Mixer (TTM)

Powders were mixed at 42 rev. min^{-1} in a glass container (250 ml) using the TTM (Turbula T2C, Bachofen, Basel, Switzerland). Studies that investigated the effects of extended mixing times and the introduction of additional screening stages on the drug content uniformity within the powder blends are described in section 4.2.1. The TTM was also used to further promote the aggregation of the NST/FPL powder systems (section 6.2).

Rotary Bladed Blender (RBB)

The powders were mixed in a RBB (Kenwood Mini Chopper, CH100, Kenwood Ltd., Havant, Hants, U.K.) at a constant blade speed. At intervals of 2 minutes, the blending process was stopped and the plastic mixing chamber emptied. Adhered powder was discharged from the wall using a soft powder brush. This procedure was adopted to minimise heat generation, by allowing the mixing chamber time to cool, and regularly re-introduce adhered powder (from the walls and metal blade of the mixing unit) back into the bulk powder bed.

2.2.4 Assessment of the Drug Content Uniformity

Unless otherwise specified, the drug content uniformity of the blends was assessed by removing ten powder samples (20 mg) from various parts of the powder bed using a

metal spatula. The samples were diluted with an appropriate volume of solvent using volumetric flasks. The size of the powder samples analysed and the dilution factor were dependent on the concentration of drug formulated and were chosen to allow accurate quantitative drug analysis. Details of the analytical techniques employed to detect the drug compounds are described in section 2.4.

2.3 Physical Characterisation of Materials

2.3.1 Particle Size Analysis

The particle size distribution of all materials used throughout the study was determined using the techniques of low angle laser light scattering (LALLS) and time-of-flight aerosol beam spectroscopy (TOFABS).

2.3.1.1 Low Angle Laser Light Scattering

Instruments operating on the principle of LALLS calculate the particle size distribution (by volume) from the pattern and intensity of scattered light from a cloud of droplets traversing a laser beam. The Mastersizer X (Malvern Instruments Ltd., Malvern, U.K.) employs a helium-neon laser beam (λ = 633 nm) which is shone through a cell in which the powder particles are suspended (Diffraction Training, 1993). The scattering of the particles is predicted by Mie theory and the information is used to calculate the particle size (Diffraction Training, 1993). The Mie scattering theory considers the optical properties of the material (Zhang and Xu, 1992) which is important when characterising particles <10 μm (Etzler and Sanderson, 1995; Nathier-Dufour et al. 1993). The

theoretical particle size, which most closely fits the experimental pattern, is presented by the instrument (Diffraction Training, 1993).

Materials and Methods

LALLS investigations were performed using the Malvern Mastersizer X in conjunction with either the dry powder feeder (DPF), the small volume stirred cell (SVC) or the large volume circulating cell (LVC).

Particle Size Characterisation of NST

The particle size distribution of micronised NST was determined using the SVC. The particle size distribution was measured using two dispersant solutions: a) cyclohexane and 0.1% $^{w}/_{v}$ lecithin and b) a saturated solution of NST dissolved in cyclohexane and 0.1% $^{w}/_{v}$ lecithin. Both solutions were filtered (Type A/E glass 76 mm diameter, Gelman Sciences, Michigan, U.S.A.) before use. The refractive properties of the two dispersant solutions were measured and an appropriate programme presentation selected.

The SVC was filled (15 ml) with one of the two dispersant solutions, the optics in the instrument aligned and the diffracted light measured with no sample present to establish a background reading. A small test tube was half-filled with one of the dispersant solutions and a small sample of NST added (approximately 1 mg). The tube was manually agitated to facilitate wetting and then placed in an ultrasonic water bath to disperse the solid particles. The temperature of the ultrasonic water bath was maintained between 20 and 25°C throughout the investigations by the addition of ice when required. Following a fixed sonication period, several drops of the suspension

were immediately added to the SVC until a suitable obscuration level was obtained (15-25%). The diffracted light was initially focused onto the photo detector array using a 100 mm lens (particle size range 0.5 to 120 μm). All solutions were prepared and analysed in duplicate.

Once the optimum conditions for deaggregation had been established, a 45 mm lens (particle size range 0.1 to 80 μm) was used to more accurately describe the particle size distribution of the micronised NST. The large volume circulating cell (LVC) (1 litre) was used in conjunction with the 45 mm lens.

Particle Size Distribution of the Lactose Size Fractions

The particle size distribution of the lactose size fractions was obtained either by suspending the particles in the SVC (<45 μm sieve fraction), the LVC (FPL) or by feeding the sample across the laser beam through the DPF (63-90 μm sieve fraction). The instrumental set-up is described in table 2.5.

Lactose Size Fraction	Presentation	Optical Lens (mm)	Measured Particle Size Range (μm)
63-90 μm	DPF	300	1.2 to 600
<45 μm	SVC	100	0.5 to 120
FPL	LVC	45	0.1 to 80

Table 2.5 Instrumental parameters for LALLS studies on the lactose size fractions.

The FPL and <45 μm size fraction were suspended in cyclohexane and 0.1% $^{w}/_{v}$ lecithin (saturated with the appropriate lactose sample and filtered). Sample preparation and

size measurements were as described for NST. The samples were examined following deaggregation for one minute in the ultrasonic water bath.

The coarse carrier sieve size fraction (63-90 μm) was measured using the DPF. A small mass of the lactose sieve fraction (2 to 3 mg) was drawn through the DPF using a vacuum cleaner (Electrolux Power System 1500W) at a flow rate of approximately 100 litres min^{-1} to aerosolise the powder samples.

Results and Discussion

Particle Size Distribution of NST

Tables 2.6 and figure 2.1 detail the particle size distribution of the NST after various time periods in the ultrasonic water bath. Table 2.6 and figure A1 (Appendix I) detail the particle size distribution of NST as measured with the 45 mm optic lens after optimum deaggregation (10 minutes) in the ultrasonic water bath. The values of d(0.1), d(0.5) and d(0.9) represent equivalent volume diameters with 10%, 50% and 90% of particles less than this value respectively.

Pre-sample preparation, in terms of the energy (sonication time) available for deaggregation of the drug agglomerates, would appear to be an important factor governing the measured particle size distribution of micronised NST. Sonication time was investigated over the range 1 to 30 minutes however, the particle size distribution appeared to remain constant after approximately 10 minutes (figure 2.1). The temperature of the ultrasonic water bath was maintained between 20 and 25°C to prevent/minimise the micronised powder sample dissolving in the dispersant medium.

Sonication Time (minutes)	Dispersant	d(0.1) (μm)		d(0.5) (μm)		D(0.9) (μm)	
		Run A	Run B	Run A	Run B	Run A	Run B
1	Non-saturated	0.64	0.61	5.21	1.36	10.15	5.48
3	Non-saturated	0.64	0.62	1.89	1.42	6.87	6.41
5	Non-saturated	0.62	0.62	1.34	1.34	3.86	5.17
10	Non-saturated	0.62	0.62	1.36	1.33	4.45	5.10
15	Non-saturated	0.61	0.62	1.31	1.41	4.70	4.55
30	Non-saturated	0.61	0.62	1.20	1.40	5.82	5.12
1	Saturated	0.67	0.64	2.89	2.50	15.89	12.12
3	Saturated	0.63	0.64	2.15	1.89	6.62	6.87
5	Saturated	0.64	0.62	1.80	1.34	4.76	3.86
10	Saturated	0.63	0.62	1.50	1.33	3.50	3.82
15	Saturated	0.63	0.62	1.57	1.38	4.13	4.62
30	Saturated	0.63	0.61	1.47	1.20	4.32	5.82
[a]10	Non-saturated	0.20	0.24	0.83	0.89	3.89	4.99

Table 2.6 The effects of sonication time, dispersant solution and focusing optics on the particle size distribution of micronised NST.
All investigations utilised a 100 mm lens in conjunction with a SVC except;
[a] A 45 mm lens was used in conjunction with a LVC.

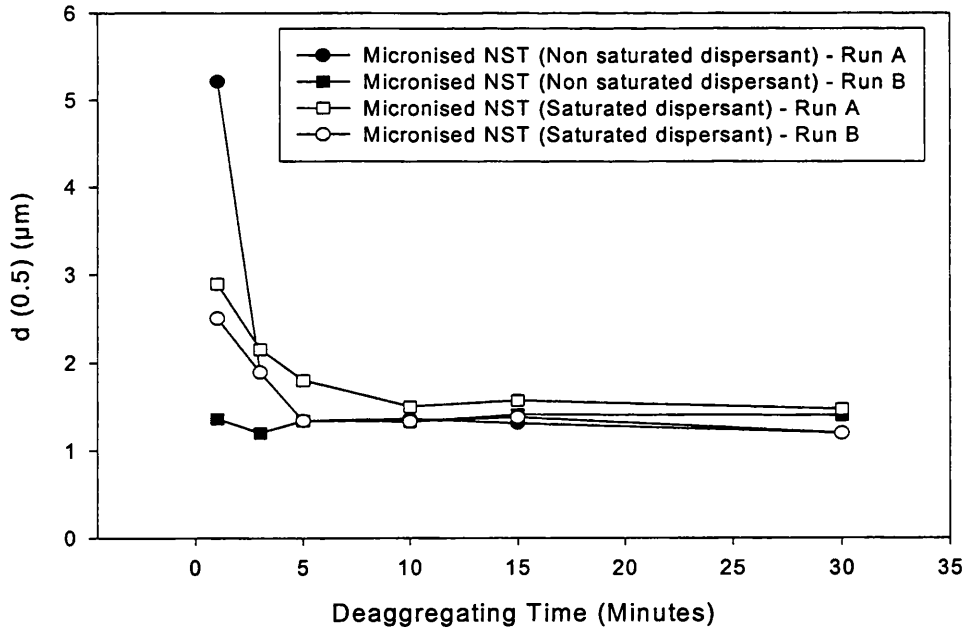

Figure 2.1 Effect of deaggregation time and dispersant solution on the particle size distribution of micronised NST.

Comparison of the particle size data obtained from the saturated and non-saturated dispersing solutions following fixed sonication times revealed no apparent differences in the particle size distribution. This would suggest that the decreasing particle size of the NST was a result of the deaggregation of the agglomerated drug system and not due to the drug dissolving in the suspending medium. The particle size distribution of the micronised NST after 10 minutes of sonication (LVC) revealed a VMD <0.9 μm with 90% of the particles having an equivalent volume diameter <5 μm.

Wong et al. (1995b) determined the VMD of micronised NST in liquid suspension (LALLS) as 5.01 μm with 67% of the material within the size range 0.5 and 7.0 μm. In the present study the particle size distribution of the micronised NST is considerably smaller than that determined by Wong et al. (1995b). Reasons for this could include the use of different batches of NST or differences in the preparation of the samples prior to particle size analysis.

Carrier Lactose Particles

Table 2.7 summarises the parameters that describe the particle size distribution of the lactose size fractions. The particle size distributions as determined by LALLS are shown in Appendix I (figures A3 to A5).

Lactose Size Fraction	d(0.1) μm		d(0.5) μm		d(0.9) μm	
	Mean	SD	Mean	SD	Mean	SD
63-90 μm AJS	64.9	3.0	96.5	1.7	140.3	5.6
<45 μm	1.3	0.3	23.0	5.1	47.9	6.1
FPL	1.2	0.1	5.8	0.2	19.3	1.0

Table 2.7 Particle size analysis of the size fractions of α-lactose monohydrate (n = 3).

For polydisperse systems analysed by LALLS, the diffraction pattern for each particle size overlaps with those of others in the powder system. Therefore, the mathematical algorithms and necessary assumptions required for calculation of the distribution are complex (Etzler and Sanderson, 1995). The sole use of unknown computer algorithms was considered scientifically unwise therefore, the measured particle size distribution was measured using alternative methods of particle sizing (TOFABS and SEM investigations).

2.3.1.2 Time of Flight Aerosol Beam Spectroscopy

The aerodynamic diameters of micronised NST and the lactose carrier size fractions were measured using the technique of TOFABS (Aerosizer® with Aerodisperser®, API, Hadley, MA). The Aerodisperser® is a computer controlled variable shear particle deaggregator designed to provide aerosolised dry powders to the sizing instrument. The Aerosizer® determines the aerodynamic particle size by accelerating particles in a sonic expansion flow and measuring their terminal velocity by transit time across two laser beams (Mitchell and Nagel, 1996).

The extent of powder deaggregation was electronically controlled by varying the pressure drop across the annular gap between the disperser pin and the pin bowl, which in turn produces a resultant shear force (Hindle and Byron, 1995a). Pressure drops in the range 0.5 psi to 5.0 psi (3.45 to 34.5 kPa) correspond to low and high shear forces, although the shear forces are neither determined nor displayed (Hindle and Byron, 1995a). The dispersing pin, which creates the pressure drop within the Aerodisperser®, was vibrated to reduce deposition of material on the disperser pin. The feed rate of powder to the sizing instrument was varied within an effective experimental range of 5000 to 10000 particles per second. To achieve this feed rate, the disperser automatically increases or decreases the strength and duration of the pulsed air supplied to the sample chamber (Hindle and Byron, 1995a).

The time of flight data collected by the instrument software is converted to either number or volume based frequency distributions and can be displayed as a function of the aerodynamic or geometric diameter. True powder densities (required by the sizing instrument for data processing) were determined by helium pycnometry (section 2.3.3).

Hindle and Byron (1995a) described their experiences with this instrument specifically as it relates to the particle size measurement of several sieve classifications of crystalline lactose and also micronised salbutamol sulphate (SS) and terbutaline sulphate (TS). Hindle and Byron (1995a) concluded that each compound, because of its inherent physical chemistry, required Aerodisperser® method optimisation.

Materials and Methods

Both the Aerosizer® and the Aerodisperser® were used as supplied. Niven (1993) describes the sizing instrument and the deaggregator is described by Hindle and Byron (1995a).

Micronised NST

The particle size characterisation of a micronised powder requires that the powder be dispersed into its constituent particles. The effects and interactions of the instrument variables on the deaggregation and resultant particle size distribution of NST were investigated. Operating variables were selected in an attempt to fully deaggregate NST (Hindle and Byron, 1995a). High and low shear forces (corresponding to pressure drops of 34.5 and 3.45 kPa) at high and low flow rates (5000 to 10000 particles per second) were investigated with a sample run time of between 60 and 300 seconds.

Lactose Size Fractions

Hindle and Byron (1995a) concluded that for lactose samples (sieve size fractions 0-63 μm, 63-120 μm and 120-200 μm), complete deaggregation occurred even at low shear forces. The particle size distribution of the lactose size fractions was not significantly altered as a function of run time (200-500 seconds). Particle size reduction even under high shear conditions did not occur (Hindle and Byron, 1995a).

The particle size distribution of the three size fractions of lactose (63-90 μm, <45 μm and FPL) were investigated using a high shear force (34.5 kPa) to deaggregate and disperse the powder samples and a high flow rate (10000 particles per second) to feed

the material into the sizing instrument. Samples were analysed for two minutes and three runs were performed for each lactose size fraction.

Results and Discussion

Figure 2.2 summarises the effects of varying the shear force and feed rate on the deaggregation and subsequent measured particle size distribution of the micronised NST.

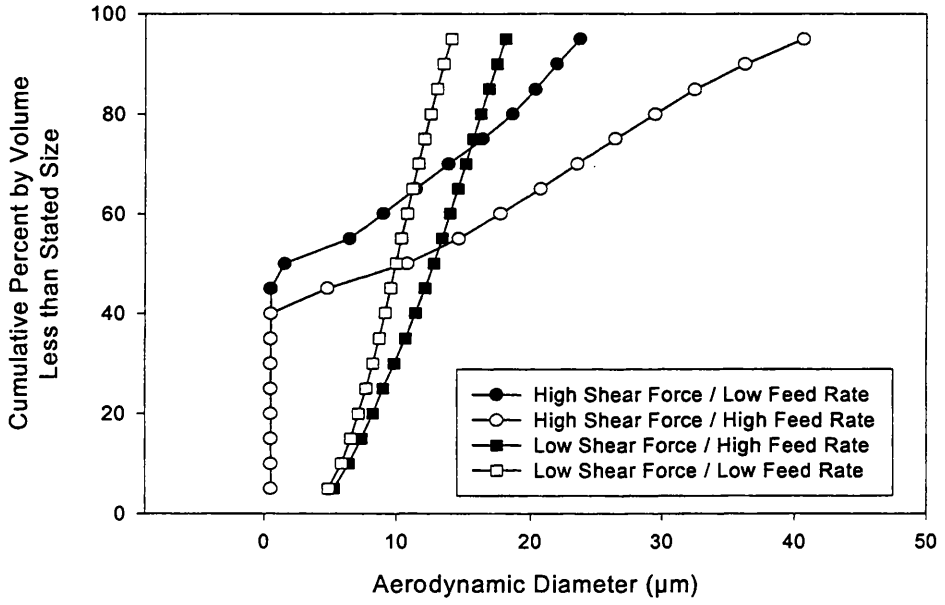

Figure 2.2 The effects of the deaggregating shear force and flow rate on the measured particle size of NST.

A high shear force and a low feed rate appear to produce the greatest degree of deaggregation however, even these "optimised" conditions fail to completely deaggregate the micronised powder system. Figure 2.2 is just a summary of part of the work conducted on trying to optimise the instruments variables (sample run time, shear forces, flow rate) in an attempt to fully deaggregate NST. NST failed to deaggregate

completely for any given set of experimental conditions, a finding also reported by Hindle and Byron (1995a) when analysing micronised TS. It would appear that either the shear forces generated with the deaggregator instrument are insufficient to completely break apart the particles of NST or that the pulsed air supply charges the powder particles within the metal sample chamber (tribolelectrification) causing re-agglomeration of NST particles.

However, Hindle and Byron (1995a) have successfully deaggregated micronised SS. Therefore, this technique could be used in future studies to assess the effects of physicochemical changes of the NST particles on the cohesive interactions governing the deaggregation and dispersion of the powder system (York and Hanna, 1996).

Table 2.8 summarises the parameters describing the particle size distributions of the lactose size fractions as measured by TOFABS, data which can be compared to information obtained from LALLS and SEM investigations.

Lactose size fraction	d(0.1)	d(0.5)	d(0.9)
63-90 μm (AJS)	55.2 ± 3.6	83.6 ± 2.9	109.1 ± 2.91
<45 μm	20.3 ± 2.4	36.1 ± 2.3	45.6 ± 1.6
FPL	6.9 ± 2.0	14.2 ± 1.3	23.4 ± 1.3

Table 2.8 The particle size distribution of the lactose carrier size fractions determined using TOFABS. Values are the mean ± SD of 3 determinations.

The data is a summary of a volume based frequency displayed as a function of the aerodynamic diameter.

2.3.2 Surface Area Measurements

Materials and Methods

Surface area determinations for the lactose size fractions (63-90 μm, <45 μm and FPL) and micronised NST were performed on the Gemini 2360 instrument (Micromeritics, Particle Technology Instruments, Georgia, U.S.A.). Nitrogen was used as the adsorbate gas and an empty balance tube of identical dimensions used to measure the pressure differential generated.

Fine materials (NST, FPL and the <45 μm lactose sieve fraction) were filled into the standard glass bulb (volume: 6.5 cm^3). The large glass bulb (volume: 12 cm^3) was used to characterise the 63-90 μm sieve size fraction of lactose.

Accurately weighed samples were loaded into the appropriate glass bulb and degassed at 50°C for 24 hours to try and remove pre-adsorbed gases and vapours from the surface of the solid (FlowPrep 060 Degasser, Micromeritics, Particle Technology Instruments, Georgia, U.S.A.). Increased temperatures were avoided to minimise dehydration of the samples. The samples were re-weighed following out-gassing and the values used for subsequent surface area determinations.

Results and Discussion

Table 2.9 details the specific surface area of the lactose size fractions and the micronised NST. Micromeritics claim that the Gemini 2360 instrument is able to measure specific surface areas as low as 0.01 $m^2 g^{-1}$ and total surface areas in the range 0.1 to 300 m^2.

Material	Run	Adsorption Parameters			Specific Surface Area ($m^2 g^{-1}$)
		C	Intercept	Correlation Coefficient	
Fine Particle Lactose	1	85	0.04	0.9998	1.2
	2	93	0.04	0.9999	1.2
	3	84	0.04	0.9986	1.2
<45 μm Lactose	1	38	0.21	0.9989	0.5
	2	36	0.27	0.9989	0.5
	3	38	0.25	0.9988	0.4
63-90 μm Lactose AJS	1	25	1.63	0.9997	0.1
	2	23	1.64	0.9998	0.1
	3	25	1.43	0.9998	0.1
Micronised NST GMR 5019G	1	61	0.01	0.9999	7.2
	2	60	0.01	0.9999	6.9
	3	59	0.01	0.9993	7.3

Table 2.9 Surface area determination of the lactose size fractions and NST.

When analysing the surface area data, a number of parameters should be checked to ensure the validity of the data. The correlation coefficient should be as close to 1 as possible, with a range of 0.999 to 1 being acceptable in most cases (Webb and Orr, 1997). The C constant is a measure of the affinity of the adsorbate for the material. For nitrogen, the C value can range from 3 to 1000 depending on the adsorption isotherm of the material (Webb and Orr, 1997).

As expected, decreasing the lactose size fraction increased the surface area of the material. The far greater specific surface area of the micronised NST when compared to the FPL (VMD = 5.8 μm) supported LALLS and LTSEM conclusions that the NST is an ultrafine powder. The results were used when: a) calculating the concentration of NST required for monolayer particle coverage on the coarse lactose size fraction (63-90 μm) (Appendix I) and b) comparing the milled and micronised forms of NST (section 8.3.4).

2.3.3 True Density Measurements

True density measurements for each sample were determined using a helium-air pycnometer (Type 1302 Micromeritics Instruments Corp., Norcross, USA).

Method

NST and the lactose size fractions were stored at 12% RH prior to measurements in an attempt to reduce/remove surface moisture. Nedocromil sodium is still stable as the trihydrate at this humidity (Khankari et al. 1998). Approximately 0.5 to 1 g of powder was accurately weighed into the small sample cell of a helium pycnometer. Each powder sample was purged with helium prior to collecting ten sequential density measurements and the mean density value determined. The mean value of three experimental runs, using different powder samples, was determined.

Results and Discussion

A summary of the density measurements is presented in table 2.10.

The values can be compared with data obtained by Wong et al. (1995a) who estimated the true density for micronised NST to be 1.60 g cm^{-3}. The values were used for the TOFABS investigations (section 2.3.1.2).

Material	True Density (g cm^{-3})
NST (micronised)	1.63 ± 0.0220
63-90 μm lactose	1.54 ± 0.0003
<45 μm lactose	1.54 ± 0
Fine particle lactose	1.54 ± 0

Table 2.10 True density values for the micronised NST and the carrier size fractions of lactose. Values are the mean ± SD of 3 determinations.

2.4 Analytical Techniques

2.4.1 UV Analysis of Nedocromil Sodium.

The British Pharmacopoeia (1998) does not include an official assay for the determination of NST therefore, the ultra violet/visible (UV/VIS) absorption spectrum was measured. Since NST has a chemical structure similar to DSCG (Suschitzky and Sheard, 1984) an assay was developed based on the assay for DSCG (BP, 1998). A 0.002 % $^{w}/_{v}$ solution of NST was prepared in distilled water and analysed over the range 230 to 800 nm using a scanning spectrophotometer (Perkin-lambda 3 UV/VIS, Spectrophotometer). The absorption spectrum of the 0.002% $^{w}/_{v}$ solution displayed four maxima: 245 nm, 280 nm, 340 nm and 375 nm. A wavelength of 375 nm was used for all future investigations.

Nedocromil sodium exists as the monohydrate at RH ≤ 6.4%, the trihydrate when equilibrated between the humidity range 6.4% ≤ RH ≤ 79.5% and the heptahemihydrate between 80% ≤ RH ≤ 90% (Khankari et al. 1998). The specific absorption coefficient ($E_{1cm}^{1\%}$) was determined for powder samples stored at humidities ranging from 12 to 76% RH (section 2.2.2) to investigate whether NST sorbs/desorbs significant amounts of moisture over the range of humidities likely to be encountered within the laboratory or during experimental investigations. The $E_{1cm}^{1\%}$ for the NSHH was determined by performing an assay on a sample of NST which had been stored at 86% RH/22°C for four weeks (section 2.2.2).

Equipment:

Hitachi UV spectrophotometer

Instrument settings: Detection λ: 375nm

1 cm path length cell

Solvent: distilled water

Method

Three stock solutions (0.1% $^{w}/_{v}$) were prepared from samples of NST stored at each of the following humidities (12, 22-23, 53-55 and 75-76% RH). Three sets of standard dilutions, covering the drug concentration range (0.001 to 0.005% $^{w}/_{v}$), were prepared from each of the three stock solutions. Each solution was assayed three times using the UV spectrophotometer and the mean absorbance recorded.

When determining a specific extinction coefficient for NSHH, two stock solutions were prepared (0.1% $^{w}/_{v}$) and two sets of dilutions from each stock solution produced, (covering the concentration range 0.001 to 0.005% $^{w}/_{v}$). Each solution was assayed three times using the UV spectrophotometer and the mean absorbance recorded.

Three stock solutions (for comparisons of $E_{1cm}^{1\%}$ for NST) and two stock solutions (for the determination of $E_{1cm}^{1\%}$ for NSHH) and then two series of dilutions for each stock solution, enabled the accuracy of the sample preparation to be confirmed and the effects of the storage conditions to be assessed.

Results and Discussion

Comparison of the $E_{1cm}^{1\%}$ for NST *Stored at Different Humidities*

Tables 2.11 to 2.14 and figure 2.3 summarise the linear regression data obtained from the calibration plots for solutions of NST prepared from powder samples stored at the four humidity levels. Linear regression was performed using MicroCal® Origin v2.94 (Microcal Software Inc., MA, U.S.A.).

% RH	Stock	Dilution	Slope ($E_{1cm}^{1\%}$)		Intercept		Correlation Coefficient
			Mean	SD	Mean	SD	
12	A	1	179.6	0.45	-0.00203	0.00154	0.99999
12	A	2	179.9	0.60	-0.00153	0.00208	0.99998
12	B	1	179.1	0.30	0.00180	0.00101	1.00000
12	B	2	178.7	0.40	0.00220	0.00133	0.99999
12	C	1	179.0	0.37	-0.00021	0.00125	0.99999
12	C	2	179.0	0.45	-0.00041	0.00150	0.99999

Table 2.11 Linear regression data for NST (0.001 to 0.005% $^{w}/_{v}$) analysed by UV spectrophotometry (stored at 12% RH).

% RH	Stock	Dilution	Slope ($E_{1cm}^{1\%}$)		Intercept		Correlation Coefficient
			Mean	SD	Mean	SD	
22-23	A	1	179.3	0.18	0.000046	0.00058	1.00000
22-23	A	2	179.5	0.26	-0.000354	0.00087	1.00000
22-23	B	1	178.8	0.46	-0.00135	0.00153	0.99999
22-23	B	2	179.2	0.16	-0.00255	0.00055	1.00000
22-23	C	1	179.1	0.50	-0.00033	0.00166	0.99999
22-23	C	2	179.1	0.56	-0.00013	0.00184	0.99999

Table 2.12 Linear regression data for NST (0.001 to 0.005% $^{w}/_{v}$) analysed by UV spectrophotometry (stored at 22-23% RH).

% RH	Stock	Dilution	Slope ($E^{1\%}_{1cm}$)		Intercept		Correlation Coefficient
			Mean	SD	Mean	SD	
53-55	A	1	178.7	0.50	0.00044	0.00167	0.99999
53-55	A	2	179.3	0.57	-0.00126	0.00190	0.99998
53-55	B	1	179.5	0.60	0.000036	0.00202	0.99998
53-55	B	2	179.7	0.55	-0.00036	0.00186	0.99999
53-55	C	1	179.5	0.53	0.00005	0.00178	0.99999
53-55	C	2	179.3	0.53	0.00105	0.00177	0.99999

Table 2.13 Linear regression data for NST (0.001 to 0.005% $^{w}/_{v}$) analysed by UV spectrophotometry (stored at 53-55% RH).

% RH	Stock	Dilution	Slope ($E^{1\%}_{1cm}$)		Intercept		Correlation Coefficient
			Mean	SD	Mean	SD	
75-76	A	1	179.1	0.29	-0.0012	0.0010	1.00000
75-76	A	2	178.9	0.24	0.0017	0.0008	1.00000
75-76	B	1	178.5	0.25	0.0034	0.0008	1.00000
75-76	B	2	178.7	0.29	0.0028	0.0010	1.00000
75-76	C	1	178.7	0.19	0.0020	0.0007	1.00000
75-76	C	2	178.7	0.12	0.0018	0.0004	1.00000

Table 2.14 Linear regression data for NST (0.001 to 0.005% $^{w}/_{v}$) analysed by UV spectrophotometry (stored at 75-76% RH).

The equality of the $E^{1\%}_{1cm}$ values obtained from each of the six regression plots (A1, A2, B1, B2, C1 and C2) for each humidity level were statistically compared using the Bartlett test (Appendix II). The Bartlett test indicated no significant difference between the values of $E^{1\%}_{1cm}$ obtained for powder samples stored within each of the four humidity levels: 12% ($\chi^2 = 4.81$, $p = 0.439$); 23-25% ($\chi^2 = 1.91$, $p = 0.861$); 53-55% ($\chi^2 = 2.12$, $p = 0.830$) and 75-76% ($\chi^2 = 2.36$, $p = 0.797$).

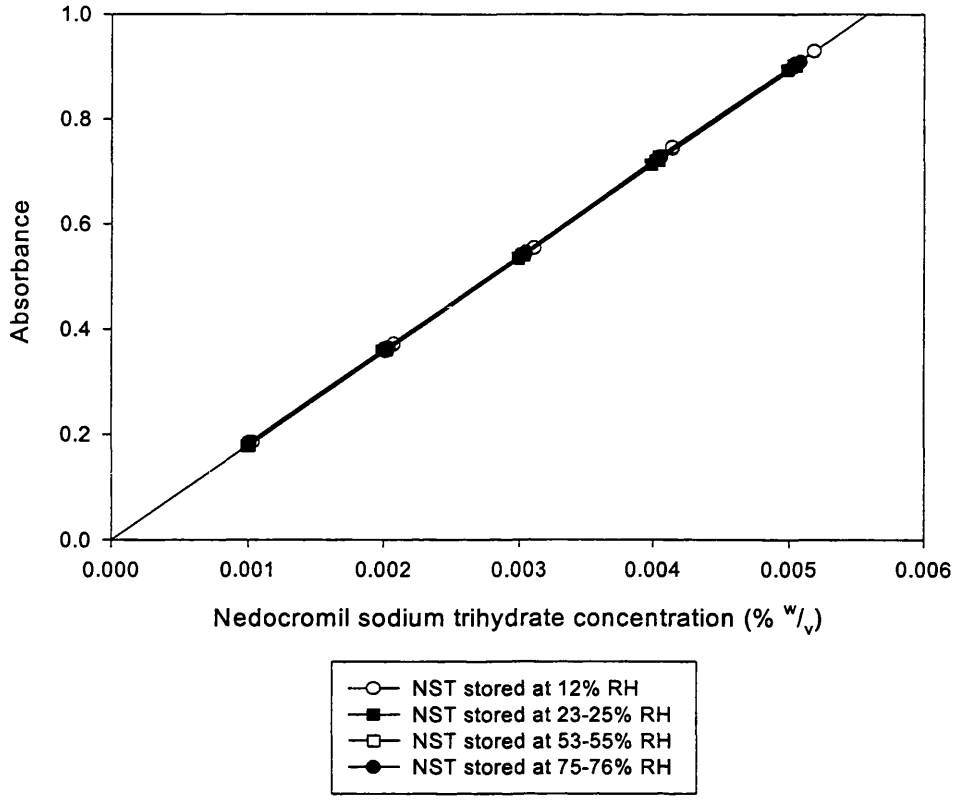

Figure 2.3 Calibration for NST (0.001 to 0.005% $^{w}/_{v}$) analysed by UV spectrophotometry.

The Bartlett test was then performed on the 24 calibration curves (six sets of data from each of the humidity environments) to assess any possible effects of the storage humidity on the $E_{1cm}^{1\%}$. The Bartlett test indicated no significant difference between the $E_{1cm}^{1\%}$ derived from the four humidity levels ($\chi^2 = 18.69$, $p = 0.719$). However, the data acquired for the NST stored at 76% RH appeared to provide $E_{1cm}^{1\%}$ values that are lower in value than the other three storage humidity. This was confirmed by one way analysis of variance (Minitab statistical software, Addison-Wesley Inc., MA) which revealed a statistical difference between the four sets of data ($F = 3.96$, $p = 0.023$). Fisher's pairwise comparisons revealed that the $E_{1cm}^{1\%}$ values derived for the powders stored at

75-76% were significantly lower than for powders stored at 12 to 55% RH. This may be due to adsorption/absorption of moisture by the NST samples.

Determination of the $E_{1cm}^{1\%}$ for NSHH

Table 2.15 and figure 2.4 summarise the linear regression data obtained from the calibration plots for NSHH.

% RH	Stock	Dilution	Slope ($E_{1cm}^{1\%}$)		Intercept		Correlation Coefficient
			Mean	SD	Mean	SD	
85-86	A	1	155.3	1.20	-0.0056	0.0039	0.99999
85-86	A	2	154.1	0.84	0.0000	0.0028	0.99999
85-86	B	1	154.5	0.25	0.0001	0.0008	1.00000
85-86	B	2	154.3	0.15	0.009	0.0005	1.00000

Table 2.15 Linear regression data for NSHH (0.001 to 0.005% $^{w}/_{v}$) analysed by UV sectrophotometry (stored at 85-86% RH).

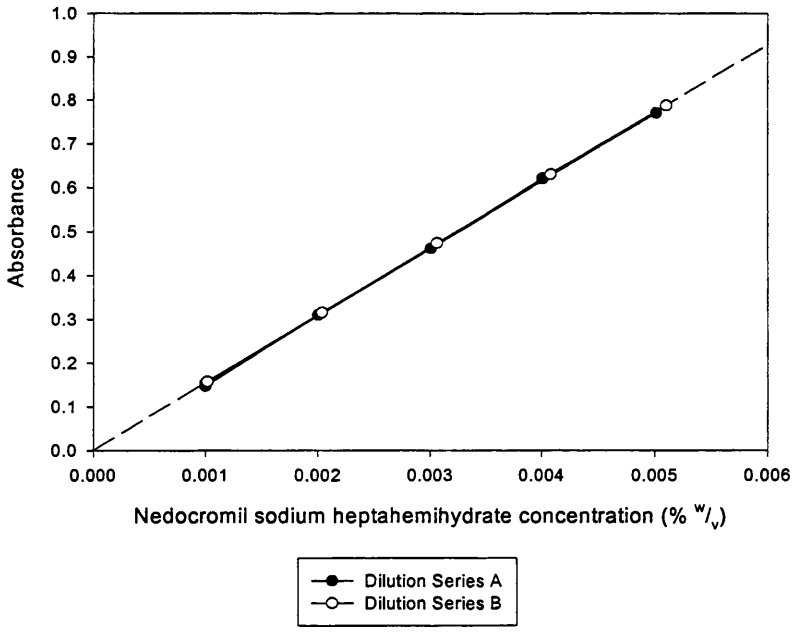

Figure 2.4 Calibration for NSHH (0.001 to 0.005% $^{w}/_{v}$) analysed by UV spectrophotometry.

The Bartlett test was used to statistically compare the $E_{1cm}^{1\%}$ values obtained for the powder samples stored at 86% RH (NSHH). No significant difference was observed between the values (χ^2 = 2.36, p = 0.797) therefore, the data was plotted as a single graph (figure 2.4) and regression values obtained for the NSHH (table 2.16). The conversion of NST to NSHH was confirmed by a stoicheiometric comparison of the extinction coefficients for both compounds.

General Discussion

Table 2.16 details the regression values used when calculating drug concentrations for future experimental procedures.

Experimental Procedure	Section	$E_{1cm}^{1\%}$	Intercept
Formulation of NST	Chapters 2,4,5,6,8	179.3	0.0003
Humidity Investigations			
NST stored between 12 and 55% RH	Chapter 7	179.3	0.0003
NST stored at 76% RH	Chapter 7	178.7	0.0017
NST stored at 86% RH (converted to NSHH)	Chapter 7	154.4	0.0004

Table 2.16 A summary of the regression values to be used in future experimental procedures.

For the general formulatory procedures, all powders/formulations were stored between 53 and 55% RH prior to all experimental investigations. All experimental procedures were carried out in an environment that ranged from 19 to 63% RH (section 2.2.2). Therefore, the regression data obtained for the powder sample stored at 53-55% RH was used. It has previously been demonstrated that the calibration data obtained is not significantly different from samples of NST stored at 12 and 23-25 % RH.

For the studies characterising the effects of storage humidity on the *in-vitro* aerosol performance of NST and NSHH, powders stored ≤55% RH were analysed using the calibration data obtained from powders sample stored at 53-55% RH. However, powders stored at 75-76 and 86% RH were analysed suing the calibration data obtained from powders samples stored at the respective humidities.

2.4.2 UV Analysis of Terbutaline Sulphate

Materials and Methods

Following the method outlined in the BP (1998), a 0.007 % $^{w}/_{v}$ solution of TS in aqueous hydrochloric acid (0.1 M) was prepared and then analysed over the absorbance range 240 to 340 nm. A λ_{max} of 278 nm was obtained and all subsequent measurements were made at this wavelength.

A validation was performed to ensure a linear relationship existed between the concentration of TS in the sample solution and the absorbance measured. Duplicate stock solutions containing approximately 0.1% $^{w}/_{v}$ (1 mg ml^{-1}) TS in 0.1M aqueous hydrochloric acid were prepared. Two sets of standard solutions were then prepared from each stock solution, covering the concentration range 0.002 to 0.010 % $^{w}/_{v}$ (0.02 to 0.10 mg ml^{-1}). Each solution was assayed using the UV spectrophotometer at a wavelength of 278 nm using a 1 cm cell. The mean of three absorbance readings for each standard solution was recorded.

Results and Discussion

Table 2.17 summarises the linear regression data obtained from the calibration plots (figure 2.5).

Stock solution	Dilution	No	Slope ($E_{1cm}^{1\%}$)		Intercept		Correlation Coefficient
			Mean	SD	Mean	SD	
A	1	5	69.3	0.12	-0.0007	0.0008	1.00000
A	2	5	69.2	0.14	0.0024	0.0009	0.99999
B	1	5	69.0	0.35	0.0009	0.0023	0.99996
B	2	5	68.9	0.24	0.0020	0.0016	0.99998
A+B	1+2	20	69.1	0.14	0.0011	0.0009	0.99996

Table 2.17 Linear regression data for terbutaline sulphate (0.002 to 0.010 % $^{w}/_{v}$) analysed by UV spectrophotometry.

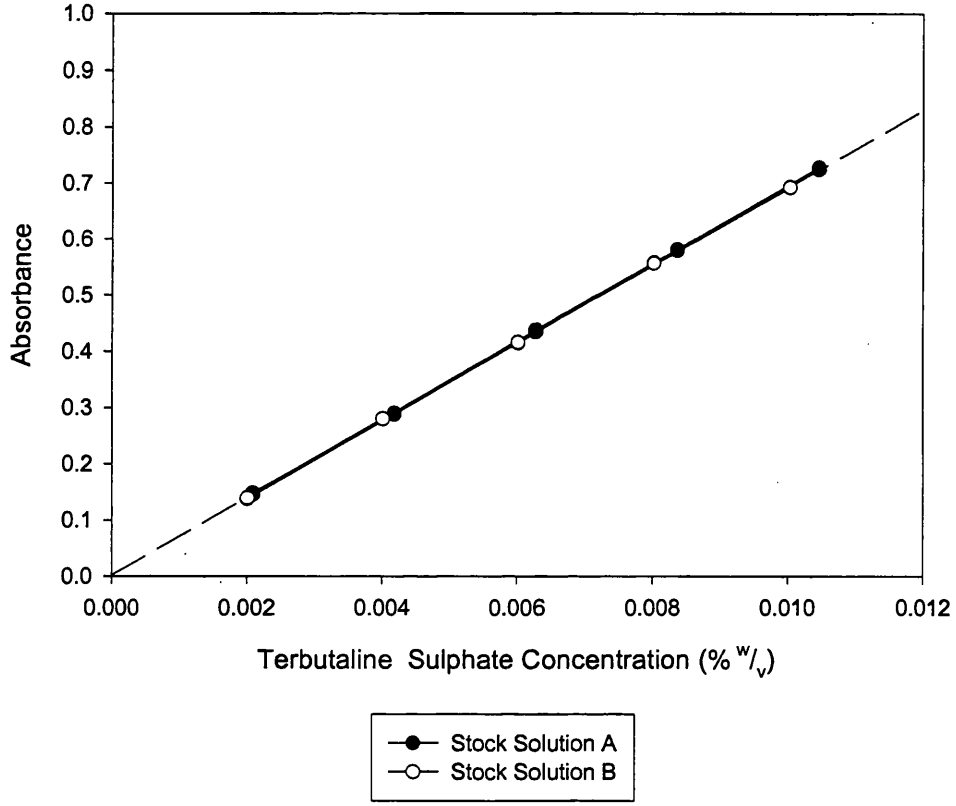

Figure 2.5 Calibration curves for TS analysed by UV spectrophotometry (0.002 to 0.010 % $^{w}/_{w}$).

The equality of the $E_{1cm}^{1\%}$ derived from the two sets of dilutions from each of the stock solutions (A and B) were statistically compared the Bartlett test (Appendix II).

There was no significant difference between the $E_{1cm}^{1\%}$ values obtained from each set of standard solutions ($\chi^2 = 0.83$, $p = 0.842$). Data from the four sets of standard solutions were combined; the $E_{1cm}^{1\%}$ value being 69.1 within the BP limits 65 to 70 (BP, 1998).

2.4.3 Colorimetric Estimation of Lactose

Lactose reacts with methylamine in hot alkaline solution to form a bright violet coloured compound with maximum absorbance at 540 nm (Nickerson et al. 1976). The reaction first described by Fearon (1942) is the basis for quantitative procedures developed by Narinesingh et al. (1992).

The first stage of the reaction is the opening of the glucose ring in the lactose by the action of the alkali, with the exposure of an aldehyde group, which then combines with the amine (Fearon, 1942). The pigment is liable to destruction by oxidation however, addition of a sulphite stabilises the pigment (Fearon, 1942).

Optimum Conditions for Colour Development

Conditions for development of the colour are critical, requiring careful control for consistent results. Heating temperature, heating time, pH of the aqueous lactose solution, concentration of reducing agent and time to analysis after cessation of the reaction must be optimised and then carefully controlled Nickerson et al. (1976).

A highly alkaline solution is needed for development of the red colour reaction. A pH within the range 12.7-12.8 (stabilised with a glycine-sodium hydroxide buffer) provided optimum colour development in studies performed by Nickerson et al. (1976).

Narinesingh et al. (1992) concluded that sodium sulfite should be used as the reducing agent and if low lactose concentrations are to be determined, concentrations close to the optimum (0.020 M) employed.

From his studies using the flow injection analysis apparatus, Narinsingh et al. (1992) concluded that the optimum reagent conditions were; 10 parts glycine-NaOH buffer, 1 part methylamine (5% $^{w}/_{v}$) and 1 part sodium sulfite (5% $^{w}/_{v}$).

Materials and Methods

The materials used for the experimental detection of lactose are tabulated in section 2.1.1, table 2.2.

Buffer Production

The buffer was prepared by adding 150 ml of a glycine solution (containing 0.033 moles of glycine (2.477 g) and 0.033 moles of sodium chloride (1.936 g)) to 850 ml of NaOH (0.385 M), adjusting the apparent pH to 12.7 with NaOH if necessary) (Corning pH meter 240).

Production of Methylamine Solution (5% $^{w}/_{v}$)

Methylamine solution (5% $^{w}/_{v}$) (100 ml) was produced from a concentrated source (40% $^{w}/_{v}$ methylamine in water) using distilled water. The solution was prepared daily and stored in the refrigerator.

Production of Sodium Sulfite Solution (5.0 % $^{w}/_{v}$)

Sodium sulfite (5.0 g) was dissolved in distilled water and diluted to 100 mls. The solution was prepared daily and stored in the refrigerator.

Temperature / Time Optimisation

Various investigators have used different temperature treatments to develop the violet colour (Nickerson et al. 1976). Pigments produced from aqueous lactose solution at higher temperatures (95°C for 5 minutes) were reported to be unstable however, at lower temperatures (55°C) an excessive reaction time (90 minutes) was required (Nickerson et al. 1976).

Following preliminary investigations assessing the extent and stability of colour development after various time periods at fixed temperatures, a reaction time of 40 minutes at 75°C was selected.

Linearity of Response

Preliminary studies were conducted to ensure a linear and reproducible response existed between the lactose concentration and the extent of the colour development. A 1 cm path length cell was initially employed to optimise the temperature and duration of time for optimum colour development (intensity and stability).

One stock solution containing approximately 2 mg ml^{-1} (0.2% $^{w}/_{v}$) of lactose (FPL) dissolved in the glycine-NaOH buffer was prepared. Three sets of standard dilutions were then prepared covering the lactose concentration range 0.2 to 1.6 mg ml^{-1} (0.02% to 0.16% $^{w}/_{v}$). Precise volumes of the lactose stock solution were added to 10 ml of methylamine (5% $^{w}/_{w}$) and sodium sulfite (5% $^{w}/_{w}$) solutions (1:1). The solutions were then made up to 50 ml using the glycine-NaOH buffer so that the ratio of components was; 8 parts glycine-NaOH buffer, 1 part methylamine (5% $^{w}/_{v}$) and 1 part sodium sulfite (5% $^{w}/_{v}$).

The dilutions were then transferred into 20 ml volumetric flasks and loaded at 1 minute intervals into the water bath (Gyrotory Water Bath Shaker, model 676, New Brunswick Scientific, N.J., U.S.A.), equilibrated at (75°C). After exactly 40 minutes, the samples were removed at 1 minute intervals from the water bath and analysed immediately using the UV spectrophotometer (Milton Roy Spectronic 601) (detection λ of 540 nm).

From figure 2.6, it can be seen that the colour development appears to be linearly related to the lactose concentration over the concentration range 0.06% to 0.18% $^{w}/_{v}$. Linear regression was conducted on the region of the plots between these two values and the results summarised in table 2.18. The final determination for stock A (dilution 1) (corresponding to a lactose concentration of approximately 0.17% $^{w}/_{v}$) did not appear to relate to all other determinations therefore the measurement was not included in the linear regression analysis.

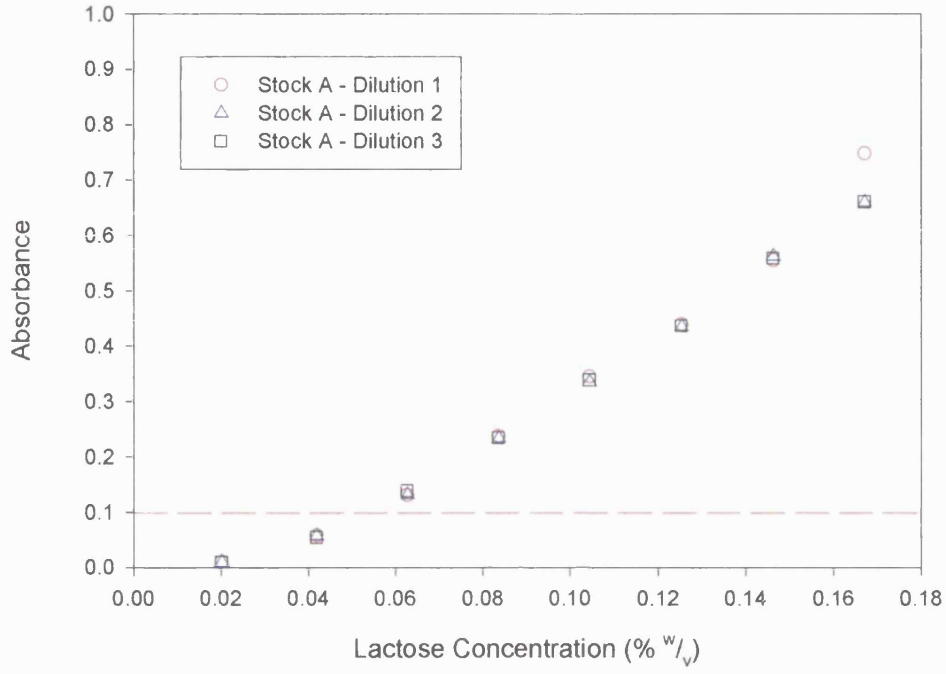

Figure 2.6 Calibration plot for the colorimetric determination of lactose (1 cm path length cell)

Parameter	*Dilution Series 1		Dilution Series 2		Dilution Series 3	
	Mean	SD	Mean	SD	Mean	SD
Slope	5.04	0.08	5.10	0.10	5.04	0.09
Intercept	-0.18	0.09	-0.19	0.10	-0.18	0.01
Correlation Coefficient	0.9996		0.9993		0.9994	

Table 2.18 Linear regression analysis for calorimetric determination of lactose (concentration range 0.06 to 0.18% $^{w}/_{v}$: 1cm path length cell) except *(concentration range 0.06 to 0.15% $^{w}/_{v}$: 1cm path length cell).

Using a 1 cm path length cell the minimum concentration detectable (i.e. above 0.1 absorbance units) was approximately 0.6 mg ml^{-1} (figure 2.6). However, the linear region of the calibration plot appears to extend below this region.

Therefore, a 4 cm path length cell was used to increase the sensitivity of the detection system. Following the procedures previously described, a series of dilutions were prepared covering the lactose concentration range 0.2 to 2.0 mg ml^{-1} (0.02 to 0.2% $^{w}/_{v}$). A 4 cm path length was chosen to increase the absorbance values at the lower end of the concentration range. The calibration curve appears to be linear over a lactose concentration range 0.3 to 0.6 mg ml^{-1} (figure 2.7). Therefore, a calibration plot was generated to more thoroughly cover this concentration range (figure 2.8).

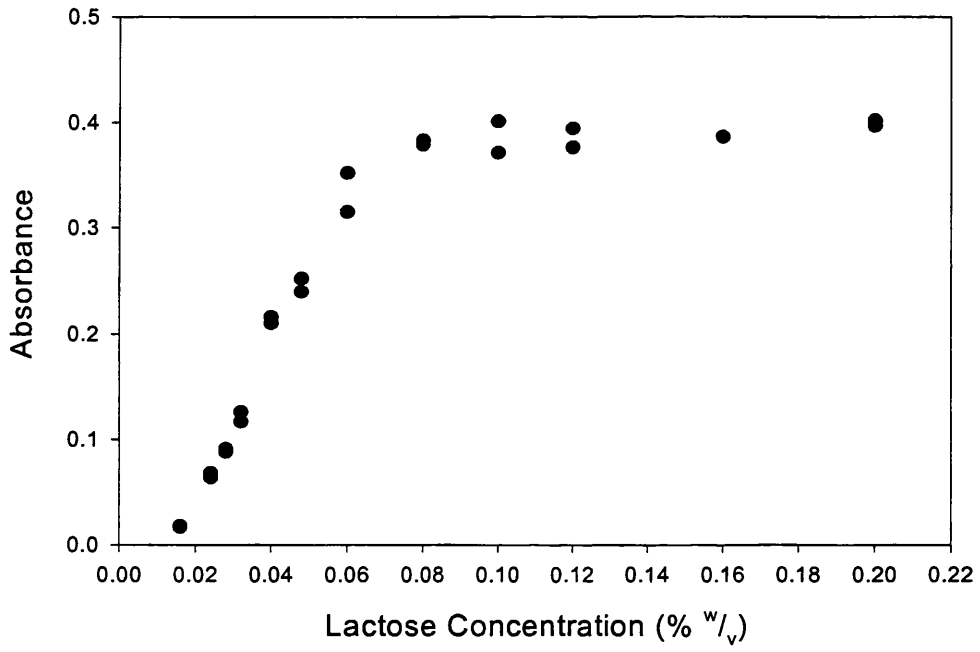

Figure 2.7 Calibration plot for colorimetric determination of lactose (concentration range 0.02 to 0.2 % $^{w}/_{v}$: 4cm path length cell).

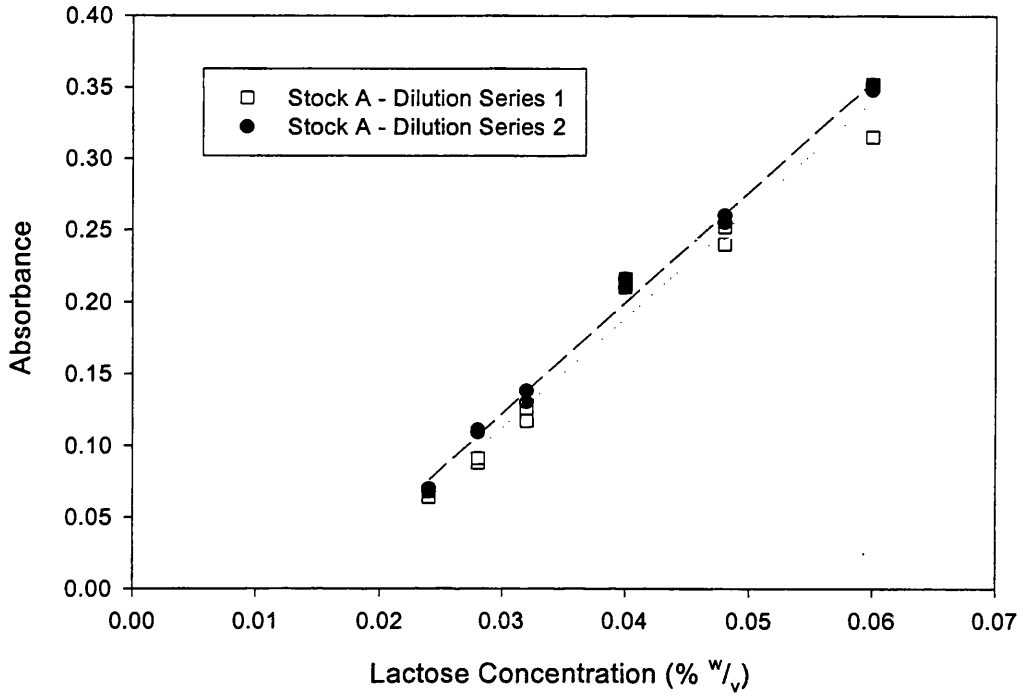

Figure 2.8 Calibration plot for colorimetric determination of lactose (concentration range 0.2 to 0.6 mg ml^{-1}: 4 cm path length cell).

Parameter	Dilution Series 1	Dilution Series 2
Slope (SD)	7.71 (0.19)	7.59 (0.36)
Intercept (SD)	-0.109 (0.01)	-0.115 (0.36)
Correlation Coefficient	0.99707	0.98907

Table 2.19 Linear regression results for colorimetric determination of lactose (concentration range 0.02 to 0.06 % $^{w}/_{v}$: 4 cm path length cell).

General Discussion

The limitations of the described technique are recognised however, the colorimetric reaction provides a semi-quantitative means of assessing the *in-vitro* aerosol deposition of FPL (section 5.2).

Alternative methods available for lactose determination include those based on high performance liquid chromatography using a refractive index detector (Srichana et al. 1998) and enzymology using β-galactosidase and glucose oxidase-peroxidase (Swindlehurst and Nieman, 1988). However, many of the above procedures are reported to be excessively time consuming, relatively insensitive and require either expensive equipment or involve complex sample pre-treatment (Narinesingh et al. 1992).

2.5 *In-vitro* Aerosol Characterisation

Device Selection

It was considered that the poor deaggregating capabilities of alternative capsule based devices (Rotahaler® and Spinhaler®) (Vidgren et al. 1988b) may cause problems when comparing the *in-vitro* aerosol performance of different powder systems. Therefore, a single dose capsule based device, the Cyclohaler®, was used to assess the *in-vitro* aerosol performance of the powder systems. Several studies have reported that when used optimally, the performance of the Cyclohaler® is comparable to that of other DPI devices (Pitcairn et al. 1997; Vidgren et al. 1988b; Zanen et al. 1992).

The majority of *in-vitro* aerosol investigations were performed using an airflow rate of 60 litres min^{-1}. However, it is now recognised that to more accurately relate to patient usage, the flow rates used in the *in-vitro* testing of DPIs should be adapted to the air flow resistance of the device. Clark and Hollingworth (1993a) and Olsson and Asking (1994) have reported on the air flow resistance of different DPI devices and the effects on the maximum inhaled flow rate (equation 2.1)

$$\sqrt{\Delta P} = Q_D . R_D \qquad \text{Equation 2.1}$$

ΔP = Pressure drop across the device

Q_D = Flow rate through the device

R_D = Device resistance

Available DPIs devices were categorised as being of low, medium or high resistance and then assessed at an appropriate flow rate (Hindle and Byron, 1995b). It is now generally accepted that the pressure drop across the DPI, achieved by adult patients with respiratory disease when inhaling through a DPI at peak inspiratory flow rate is typically in the region of 4 kPa. Therefore, international Pharmacopoeia harmonisation has concluded that drug delivery from DPIs should be determined at an air flow rate equivalent to a 4 kPa pressure drop across the device (Ganderton, 1996; Olsson et al. 1998).

Following methods described by the pharmacopoeias (EP and USP), a flow rate of 96 litres min^{-1} (corresponding to a pressure drop of 4 kPa across the device) would be necessary to assess the performance of the Cyclohaler®. Materials and methods used in the determination of the 4 kPa pressure drop are detailed in Appendix III. However, the present study used the two impingers (Apparatus A and MSLI) as a means of assessing

the interparticle interactions governing the aerosol performance of nedocromil sodium. It is considered that a reduced flow rate (60 as opposed to 100 litres min^{-1}) may be more appropriate for this type of investigation since the increased shear forces generated at higher flow rates may mask any beneficial formulatory changes.

2.5.1 Modified Apparatus A

The method used to assess the aerosol performance of the dry powder systems was based on that outlined in the British Pharmacopoeia 1998, Appendix XIIF (Figure 2.9).

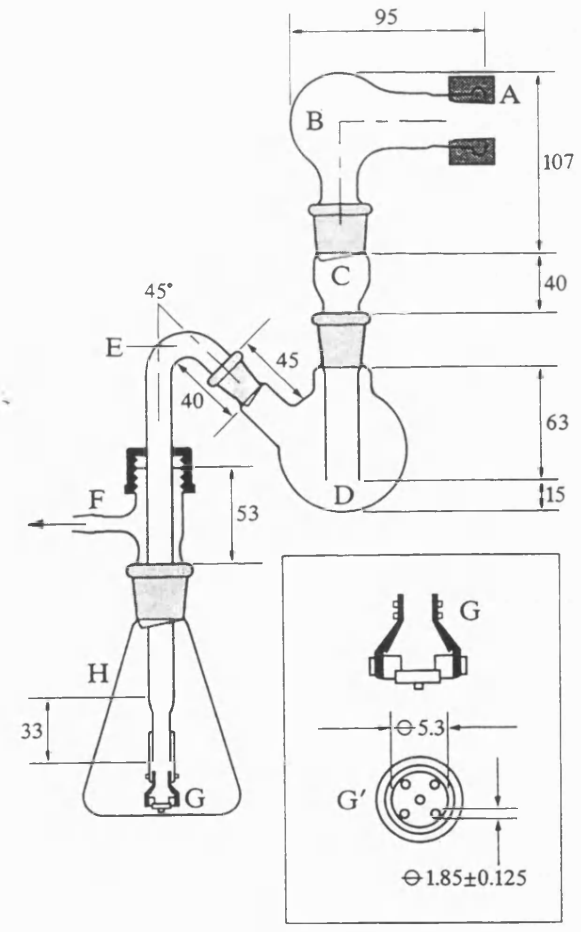

Figure 2.9 Apparatus A (BP, 1998). *Dimensions are in mm.*

Apparatus A has an $ECD_{50\%}$ of 6.4 μm at the prescribed flow rate of 60 ± 5.0 litres min^{-1} (Hallworth and Westmoreland, 1987). However, in the present study an $ECD_{50\%}$ of 5 μm was considered more representative of "potentially respirable" size fractions.

Impactor theory (Hinds, 1982) provides a relationship between the linear flow rate at the jet orifice, the jet diameter and the $ECD_{50\%}$ (equation 2.2).

$$ECD_{50\%} = \left[\frac{9 \cdot \eta \cdot W \cdot Stk_{50}}{C \cdot \rho \cdot U}\right]^{0.5} \qquad \text{Equation 2.2}$$

where,

η = viscosity of air

W = jet diameter

Stk_{50}=Stokes number for 50% collection efficiency

C = Cunningham slip factor (~1.0 for particles >1 μm)

ρ = density of reference particle (unit density, 1000 m^3 kg^{-1})

U = linear velocity of air

For the standard jet width (14 mm) and flow rate (60 litres min^{-1}) defined for Apparatus A, equation (2.2) reduces to equation (2.3) (Hallworth and Westmoreland, 1987).

$$ECD_{50\%} = X\left[\frac{W^3}{F}\right]^{0.5} \qquad \text{Equation 2.3}$$

When F, the volumetric flow rate at the jet orifice, is expressed as litres min^{-1} and W, the jet diameter is in mm, the Apparatus A constant X has a value of 0.95.

Although this has not been verified experimentally, Hallworth and Westmoreland (1987) claim this value should remain constant for alternative values of flow rate and jet diameter provided the stage-1 liquid vortex shape and jet orifice to liquid spacing are kept similar. However, Miller et al. (1992) state the latter is not a important parameter with respect to $ECD_{50\%}$.

The internal diameter of the stage-1 jet of Apparatus A was modified (University of Bath glass-blowing workshop, Bath, U.K.) to give a calculated $ECD_{50\%}$ of 4.80 μm at 60 litres min^{-1}. The upper section of the jet (between the throat cone joint and the stage-1 flask joint) retained the same standard dimensions and the length of the glass tube forming the jet was maintained as that specified for Apparatus A (BP, 1998) (figure 2.9).

Although no attempt was made to calibrate the modified Apparatus A, the proof of principle was confirmed by mono-sized sphere calibration of comparable jets. The $ECD_{50\%}$ of the modified stage-1 jet (11.6 mm) was measured as 5.3 ± 0.3 μm by AEA technology (Aerosol Science Centre, Oxfordshire, U.K.). The modified stage-1 jet (11.6 mm) was used throughout the study and the impinger subsequently referred to as modified Apparatus A.

When studying the effects of flow rate on the deaggregation properties of the powder systems (section 8.4), alternative stage-1 jets were manufactured, maintaining an $ECD_{50\%}$ of approximately 5 μm at the specified flow rate. The internal diameters of the stage-1 jets together with the theoretical and calculated $ECD_{50\%}$ are described further in section 8.4.

The majority of the studies utilising the modified Apparatus A, (chapters 2, 4, 5, 6 and 7) were performed at 60 litres min^{-1} as described in the BP (1998). Unless otherwise specified, the modified apparatus A was assembled and charged with 7 mls of solvent in stage-1 and 30 mls in stage-2. With the Cyclohaler® loaded with an empty capsule in position, the vacuum pump (Gast Manufacturing Inc., Michigan, U.S.A) was operated and the flow through the DPI was adjusted to 60 litres min^{-1} using a mass flow meter (Hastings Mass Flow Meter, HFM 201). Flow through the device was achieved by accommodating the device within a specially manufactured glass casing, which was fitted to the glass throat of the Apparatus A using an elastomeric adapter.

Capsules were removed from the storage environment (53-55% RH) and then filled with the powder formulation immediately before *in-vitro* aerosol assessment. If brittle fracture of the capsule occurred upon priming, the run was aborted and the capsule discarded.

The vacuum pump was operated at 60 litres min^{-1} for 4 seconds, sufficient time for 4 litres of air to pass through the device. The impinger was then dismantled and the capsule and Cyclohaler® contents, the throat and stage-1 combined, and stage-2 rinsed into appropriate volumetric flasks and adjusted to an appropriate volume with solvent.

2.5.2 (5-Stage) Multistage Liquid Impinger

The MSLI consists of impaction stages 1, 2, 3 and 4 and a final filter (Type A/E glass, 76 mm diameter, Gelman Sciences, Michigan, U.S.A.). At an airflow of 60 litres min^{-1}, the $ECD_{50\%}$ of stages 1 to 4 are 13.0, 6.8, 3.1 and 1.7 μm respectively. The after filter effectively retains aerosolised drug in the particle size range 0 to 1.7 μm.

The MSLI was assembled as described in the European Pharmacopoeia (1998) with twenty mls of distilled water filled into stages 1 to 4. The induction port used throughout the study was the Apparatus A glass throat (BP, 1998). However, it is recognised that the USP metal throat is now recommended (European Pharmacopoeia, 1998). The MSLI was connected to the vacuum pump and the flow through the impinger adjusted to 60 litres min^{-1} as described in section 2.5.1. The capsule was filled and then its contents discharged as described in section 2.5.1. Following powder discharge, the contents of the capsule and the Cyclohaler® were rinsed with distilled water and diluted quantitatively to an appropriate volume. The same procedure was adopted for the mouthpiece adapter and the glass induction port. The inside of the inlet jet tube (stage-1) was rinsed, allowing the solvent to flow into stage 1. The drug was rinsed from the inner walls and the collection plate into the solution in the respective stage by tilting and rotating the apparatus while ensuring that no liquid transfer occurred between the stages. The MSLI was then placed on a rotating platform (Bellydancer®, Stovall Life Science Inc., Greensboro, U.S.A.) for 10 minutes to promote further rinsing. Each stage was then thoroughly rinsed out and made up to an appropriate volume using distilled water.

2.5.3 Parameters Describing the *In-vitro* Aerosol Performance.

Emitted Dose

The drug emitted from the device was expressed as the total quantity of drug recovered from the sampling apparatus (MSLI or modified Apparatus A), as a mass (Emitted Dose or ED) and as a percentage of the recovered dose (Emitted Percent).

Fine Particle Component (Modified Apparatus A)

The fine particle component of the aerosol was expressed as the quantity of drug recovered in stage 2, as a mass (Fine Particle Dose or FPD) and as a percentage of the ED (Fine Particle Fraction or FPF).

Fine Particle Component (MSLI)

The fine particle component of the aerosol was defined as the quantity of drug recovered on stages 3 to 5 (filter) (MMAD: 0-6.8μm at 60 litres min^{-1}), expressed as a mass (FPD) or as a percentage of the ED (FPF).

The extra fine particle component of the aerosol was defined as the quantity of drug recovered on stages 4 and 5 (filter) (MMAD: 0-3.1 μm at 60 litres min^{-1}), expressed as a mass (Extra Fine Particle Dose) or as a percentage of the ED (Extra Fine Particle Fraction).

Approximately 8 mg (pure NST) or 20 mg (carrier based systems) were accurately weighed into hard gelatin capsules before *in-vitro* aerosol assessment. In order to accurately compare the ED and FPD, the two parameters were normalised with respect to either an 8 or 20 mg capsule fill weight. Capsules fill weights were maintained within ±10 % of the desired weight. It was considered that the minor differences in fill weights would not dramatically influence the aerosol performance of the formulation.

2.6 *In-Vitro* Aerosol Characterisation of NST

The *in-vitro* aerosol performance of the pure drug system was characterised to investigate the magnitude of the cohesive interactions; assessed by the degree of deaggregation and subsequent stage-2 deposition of NST (modified Apparatus A).

During the preparation of carrier lactose based formulations (chapters 4, 5 and 6), various blending procedures (HB, TTM and RBB) were employed to mix the powder systems. Screening procedures were introduced either as pre-blending stages or incorporated into the mixing protocol to improve the distribution of micronised drug particles upon the surface of the coarse lactose particles by increasing the deaggregation of the drug agglomerates (Lord, 1993; Peart, 1996; Robertson, 1997). With high dose drug systems these processing procedures may have a detrimental effect on drug deaggregation and subsequent dispersion upon aerosolisation. Therefore, the effects of the screening and blending procedures on the *in-vitro* aerosol performance of the pure drug powder was investigated.

2.6.1 Formulation Procedures

Table 2.20 summarises the experimental procedures performed on the drug powder prior to *in-vitro* aerosol characterisation. The procedures were designed to try and reproduce the shear forces the powder system may be subjected to during the formulation studies. Approximately 10 grams of micronised NST was used in each study. The three blending procedures have been described in detail in section 2.2.3.

Experimental Procedure	Method
Non sieved	NST used as received.
355 μm	NST passed through a 355 μm aperture sieve mesh using a soft powder brush.
250 μm	NST passed through a 250 μm aperture sieve mesh using a soft powder brush.
Hand Blended	NST passed through a 355 μm aperture sieve mesh using a soft powder brush. Hand blended for 30 minutes.
Rotary Bladed Blender	NST passed through a 355 μm aperture sieve mesh using a soft powder brush. Mixed for 2 minutes.
Turbulent Tumbling Mixer	NST passed through a 355 μm aperture sieve mesh using a soft powder brush. Tumbled for 10 minutes at 42 rev min^{-1}.

Table 2.20 Preparation of "processed" NST for *in-vitro* aerosol characterisation.

2.6.2 *In-vitro* Aerosol Characterisation of NST

Materials and Methods

The aerosol performance of micronised NST subjected to the formulation procedures outlined in table 2.20 was characterised using the modified Apparatus A. Approximately 8 mg of drug was accurately weighed (Mettler AT261 DeltaRange, Mettler Toledo, Switzerland) into a hard gelatin capsule and discharged from the Cyclohaler® at 60 litres min^{-1}. The 8 mg capsule fill weight was chosen in order to make comparisons with the ED and FPD of carrier based systems formulated in sections 4 and 5.

Results and Discussion

Table 2.21 and figures 2.10 and 2.11 summarise the *in-vitro* aerosol performance of the processed NST.

In-vitro Aerosol Characterisation						
Aerosol Parameter	No Screening Stage	Screening Stage 355 μm	Screening Stage 250 μm	Hand blended	Tumbling Action Mixer	Rotary Bladed Blender
% Capsule	19.2 ± 8.4	2.95 ± 0.31	2.88 ± 0.40	4.64 ± 0.86	4.02 ± 0.52	5.12 ± 1.1
% Device	20.3 ± 2.6	21.7 ± 1.7	22.5 ± 1.4	19.5 ± 2.3	19.0 ± 0.73	17.5 ± 3.3
% Stage One	50.3 ± 10	63.1 ± 2.4	59.9 ± 1.4	65.0 ± 3.5	66.2 ± 1.2	66.5 ± 5.1
% Stage Two	10.2 ± 0.65	12.3 ± 1.1	14.8 ± 0.65	10.9 ± 2.1	10.8 ± 0.74	10.8 ± 0.88
Emitted Dose (mg)	4.82 ± 0.75	6.05 ± 0.17	6.00 ± 0.10	6.13 ± 0.14	6.19 ± 0.09	6.27 ± 0.41
Emitted Percent (%)	60.5 ± 9.8	75.4 ± 1.6	74.6 ± 1.2	75.9 ± 1.8	77.0 ± 1.1	77.4 ± 4.4
Fine Particle Dose (mg)	0.811 ± 0.056	0.985 ± 0.083	1.19 ± 0.058	0.882 ± 0.18	0.869 ± 0.061	0.875 ± 0.062
Fine Particle Fraction (%)	17.3 ± 3.8	16.3 ± 1.7	19.8 ± 0.94	14.4 ± 3.0	14.1 ± 0.96	14.1 ± 1.9
Drug Recovered (%)	99.8 ± 1.1	100 ± 1.4	100 ± 1.1	101 ± 1.3	100 ± 2.1	101 ± 1.2

Table 2.21 The effects of various formulation procedures on the *in-vitro* aerosol performance of NST.

Values are the mean ± SD of 5 determinations.

ED and FPD were normalised with respect to an 8 mg capsule fill weight.

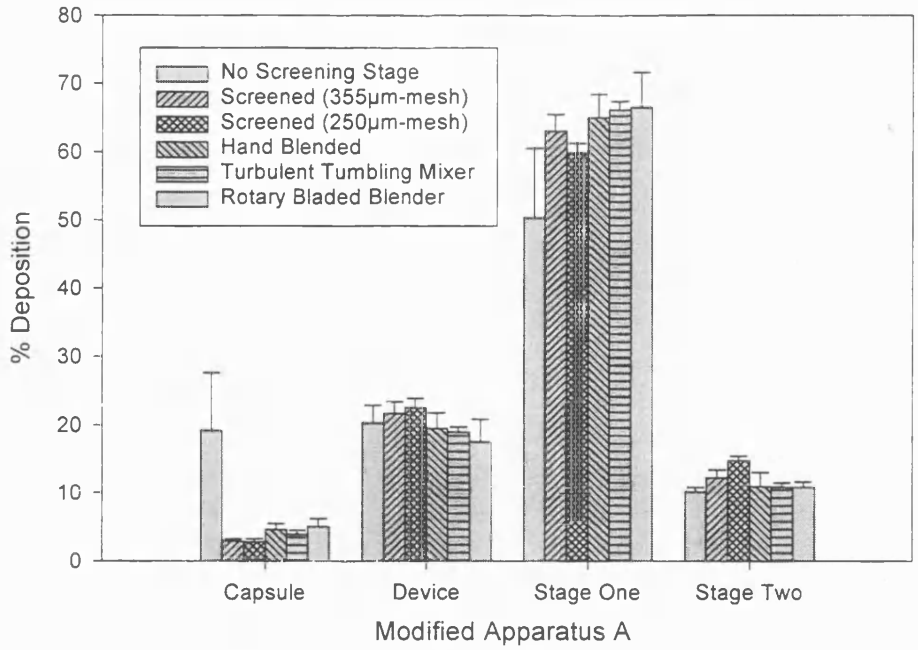

Figure 2.10 The effects of the formulation procedures on the *in-vitro* aerosol performance of NST.

Each column shows the mean of 5 determinations (bars represent SDs).

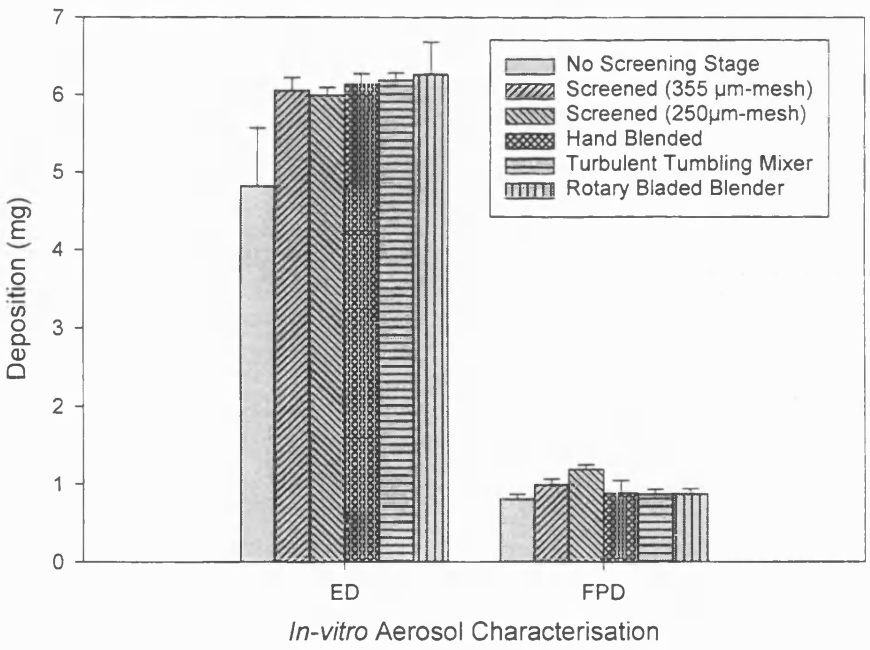

Figure 2.11 The effects of the formulation procedures on the *in-vitro* aerosol performance of NST.

Each column shows the mean of 5 determinations (bars represent SDs).

Incomplete capsule emptying was observed for the sample of NST which was used as received (not screened), e.g. 19.2 ± 8.4% of the nominal dose remained within the capsule compared with ≤5 % for the NST screened through a 355 μm aperture sieve mesh. Therefore, the use of a screening stage prior to all future formulation studies was considered essential to destroy/reduce agglomerates of pure drug, promoting both complete and reproducible capsule emptying.

One way analysis of variance revealed significant differences between the deaggregation (FPF) ($F = 4.91$, $p = 0.003$) and subsequent stage-2 deposition (FPD) ($F = 10.58$, $p < 0.001$) of NST samples subjected to the formulation procedures.

The introduction of a screening stage could be envisaged to affect the interparticle cohesive interactions in one of two ways. In the first, screening the powder sample through decreasing mesh apertures may force the constituent particles closer together, increasing the interparticle forces of attraction (Hickey et al. 1994). Alternatively, the screening stages may deaggregate the drug self-agglomerates providing an increased number of potentially respirable fine particles. Fisher's pairwise comparisons revealed that the introduction of a screening stage (355 μm) significantly increased the generation of fine particles (D_{ae}: 0.5 to 5.3 μm) when compared to the non-screened material. Fisher's pairwise comparisons also revealed that the use of the finer mesh (250 μm) further improved the generation of fine particles. However, due to difficulties/drug losses upon screening the powder samples through a 250 μm aperture mesh, all future formulations were prepared from NST pre-screened through a 355 μm aperture mesh.

Following the screening stage (355 μm), the blending procedures (TTM, RBB and HB) did not significantly affect the ED ($F = 0.73$, $p = 0.550$) the deaggregation (FPF) ($F = 1.40$, $p = 0.278$) nor the fine particle deposition of NST ($F = 1.32$, $p = 0.302$).

Based on the *in-vitro* aerosol characterisation of the pure drug systems following the various processing stages, it was hoped that changes affected by the formulatory procedures (chapters 4 and 5) could be interpreted more accurately in terms of changes in the interparticle interactions within the powder mixtures.

CHAPTER 3

SCANNING ELECTRON MICROSCOPY AND ENERGY DISPERSIVE X-RAY ANALYSIS

3.1 General Introduction

The particle size and shape of drugs commonly administered to the lung have previously been determined using conventional SEM. Pre-formulation changes to the morphology and particle size of these drug particles have also been characterised using conventional SEM. These studies include: determining the effects of micronisation and spray drying on compounds (Chawla et al. 1994; Vidgren et al. 1989), selection of alternative salts forms (Jashnani et al. 1995; Jashnani and Byron, 1996) and surface modification of the drug particles (Fults et al. 1997; Hickey et al. 1992). Studies on carrier based inhalation systems have provided information relating to the action of binary and ternary components within powder blends (Braun et al. 1996; Lucas et al. 1998a).

3.1.1 Conventional SEM

The technique of SEM involves the bombardment of a sample surface with a fine beam of electrons. Upon impact, secondary electrons from atoms in the sample surface are liberated and are subsequently detected to form an image. The SEM image typically contain wide ranges of contrast and depth of field (Jeffree and Read, 1991a). As a result, SEM can provide an excellent picture of the sample surface.

Conventional SEM ideally requires samples which are dry, mechanically stable, non-volatile and electrically conducting (Jeffree and Read, 1991a). Unfortunately, many pharmaceutical powders do not possess these characteristics. Due to the high electrical resistivity of the majority of pharmaceutical powders, samples must be coated with a thin layer of gold prior to imaging to prevent accumulation of beam electrons during electron irradiation.

When imaging hydrated powders such as NST using conventional SEM, the low pressures within the SEM chamber ($<10^{-3}$ Pa) may cause evaporation of adsorbed or loosely bound absorbed surface water. This may lead to a break up of the conducting gold coat with subsequent sample charging. The loss of water may also lead to dimensional changes within the sample (Beckett and Read, 1986).

LTSEM and ESEM were used as alternative techniques to image nedocromil sodium, alleviating the problems of sample charging and image distortion associated with conventional SEM investigations.

3.1.2 LTSEM

By freezing and thus stabilising the adsorbed and absorbed water, LTSEM enables powders and other delicate materials (Babic et al. 1996; Bastacky et al. 1987) to be analysed in their fully hydrated state (Jeffree and Read, 1991a). The benefits of analysing frozen-hydrated pharmaceutical samples are: (a) they retain most or all of their water (absorbed and adsorbed); (b) they display a reduced number of artefacts relating to dehydration (shrinkage and structural collapse) and (c) crystalline and surface water is rapidly immobilised by cryofixation hence the conducting coat remains intact, minimising charging effects.

For high resolution studies, attention must be paid to minimising the artefacts that may be associated with LTSEM, e.g. ice crystal formation, water vapour contamination and electron beam damage (Jeffree and Read, 1988). However, for most biological applications it has been well established that LTSEM can provide improved

preservation of sample fine structure compared with conventional SEM (Jeffree and Read, 1991b).

3.1.3 ESEM

Examination of hydrated compounds at increased pressures within the ESEM is another alternative to conventional SEM. The environmental SEM uses a differential pumping system to separate the high vacuum region of the electron gun and column from the specimen chamber (Danilatos, 1991). Pressures in the range of 0.13-2.7 kPa are maintained in the chamber by controlling the admittance of a water vapour (Danilatos, 1991). The water vapour in the specimen chamber also contributes to the amplification of the signal generated by the secondary electrons produced from the sample surface (Danilatos, 1991). Ionisation of the gas around the sample also suppresses charge accumulation on insulating specimens (Danilatos, 1991). Therefore, ESEM allows the sample surface to be imaged in its natural hydrated state without prior sample preparation that can include freeze drying and coating (D'Emanuele et al. 1998). However, there is an increased tendency for beam damage to occur due to the sample interacting with water (Jenkins and Donald, 1997).

The ESEM has been shown to be a useful tool in the examination of pharmaceutical formulations where it has been used to evaluate a range of hydrated and other materials (D'Emanuele and Gilpin, 1996).

3.1.4 EDAX

X-ray microanalysis is a technique that allows a chemical analysis to be performed on a material within a well defined region (1 μm^2) of the specimen (Goldstein et al. 1992). The energy of the X-ray released by an atom, excited by electron irradiation, is dependent upon the elemental atomic number (Goldstein et al. 1992). Elemental analysis can be performed on SEM samples since beam electrons also form X-rays by beam deceleration and interaction with the atoms of the solid. The technique known as energy dispersive X-ray analysis (EDAX) can give information regarding the location of an element within a sample.

3.2 Materials and Methods

3.2.1 Conventional SEM

Conventional SEM was carried out using the JEOL T330 scanning electron microscope (Japanese Electron Optics Ltd, Tokyo, Japan). Representative powder samples were mounted on aluminium specimen stubs using double-sided carbon coated adhesive tabs. Prior to examination and analysis the powders were gold coated for five minutes (Sputter Coater, Model S150B, Edwards High Vacuum, Sussex, U.K.). Carrier size fractions of lactose (63-90 μm, <45 μm and FPL) were analysed using conventional SEM. Initially, this technique was also used to analyse NST.

3.2.2 LTSEM

The preparation and analysis of frozen hydrated samples for LTSEM examination involves three main operational phases: (a) sample preparation and cryofixation, (b) coating and (c) examination and analysis (Jeffree and Read, 1991a) (figure 3.1).

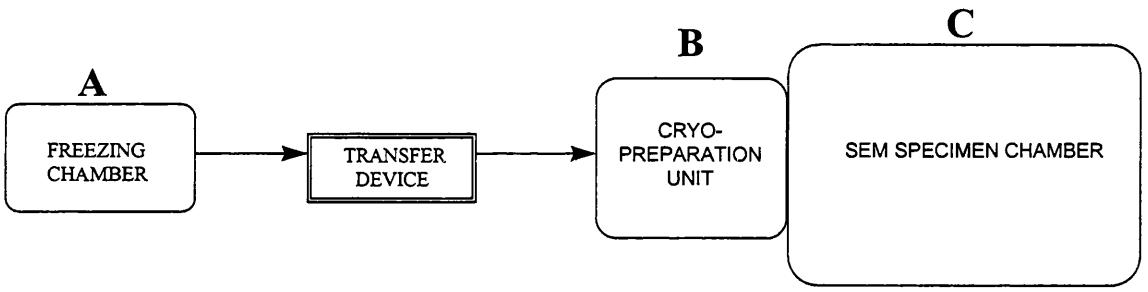

Figure 3.1 Flow diagram depicting the operational stages necessary for LTSEM sample preparation and analysis.

(a) Sample Preparation and Cryofixation

Samples for cryofixation were sprinkled onto adhesive carbon disks which were then attached to a metal stub using a mixture of a cryo-adhesive (Tissue-Tek O.C.T. Compound, Miles Laboratories Inc., Naperville, USA) and a conducting compound, colloidal carbon (Leit-C, Gerhard Neubauer, Munster, Germany). The cryo-adhesive formed a strong bonding, wax-like solid when frozen. Cryofixation was then achieved by immersing (plunge cooling) the powder sample into sub-cooled nitrogen at -210°C (nitrogen slush). This process instantly freezes the sample and should stabilise its physical structure. The sample was then transferred to a cryogenic unit (CT1500 Cryo-Trans system, Oxford Inst., U.K.) in an evacuated transfer device to avoid condensation of atmospheric moisture onto the cold sample surface. The sample was subsequently loaded into the SEM chamber via the cryo-preparation chamber. Sublimation of

superficial ice from the powder surface, in the form of contaminating frost, was achieved in the SEM chamber by increasing the stage temperature to -80°C for approximately 10 minutes. This process, termed partial freeze-drying (Jeffree and Read, 1991a), can be directly visualised in the SEM.

(b) Coating

The sample was then transferred from the SEM chamber to the cryogenic preparation chamber (-180°C) where it was sputter coated with gold in a low-pressure atmosphere of argon. The sample was coated at -180°C for three minutes. During coating a vacuum of 20 Pa was drawn and a current of 2 mA at 4V applied across the sample.

(c) Examination and Analysis

Examination of the powder samples was carried out at approximately -170°C using a low temperature SEM stage (SEM 6310, JEOL, U.K.). The stage was cooled using cooled nitrogen gas. Specimens of drug particles and powder blends were imaged at magnifications over the range x 100 to 25000. This provided information on the size and shape of individual drug crystals as well as the distribution of the drug particles within the powder systems.

3.2.3 ESEM

ESEM studies were performed on an Electroscan E3 (Philips ElectroScan, Wilmington, Mass., U.S.A.). The powder samples were sprinkled onto aluminium specimen stubs, mounted onto the peltier stage and allowed to cool to 4°C. The ESEM chamber was then pumped down to 0.53 kPa with water vapour introduced as the imaging gas. An accelerating voltage of 10 kV was used. The working distance used of 12 mm represents a gas path length of 1.5 mm. Manipulating the gas pressure within the ESEM

chamber controlled the humidity. The technique was used to investigate samples of the drug and powder formulations at magnifications up to x 1700.

3.2.4 EDAX

Sample Preparation

Sample preparation for EDAX was similar to that employed for studies using the techniques of LTSEM. Cryofixation, transfer to the cryogenic unit and sublimation of superficial ice was achieved as previously described in section 3.2.2. However, a thick gold coating would reduce the intensity of emitted X-rays therefore, the samples were carbon coated. Carbon has a low atomic number and does not interfere with the measurements of other elements (Goldstein et al. 1992). The samples were evaporatively coated with carbon in the cryogenic preparation chamber (-180°C) in a low-pressure atmosphere of argon. During coating a vacuum of 20 Pa was drawn and a current of 2 mA at 4 V applied across the sample.

Sample Analysis

EDAX analysis was carried out at approximately -170°C using a low temperature SEM stage. Samples were analysed for sodium, present as the salt of the nedocromil powder but not present in significant quantities in the other formulation components. The X-rays signals were analysed with an X-ray analyser (AN1000, Oxford Instruments, U.K.). An accelerating voltage of 15 kV was used and the powder irradiated for 100 to 200 seconds.

3.3 Results and Discussion

SEM images of the micronised NST and the lactose carrier size fractions (63-90 μm, <45 μm and FPL) are described in sections 3.3.1 to 3.3.3. The remaining electron micrographs, including conventional SEM, LTSEM and ESEM images of micronised TS (figure 6.10), milled NST (figures 8.2 and 8.3) and formulations containing NST blended with various lactose size fractions (chapters 4 and 5) are discussed in the relevant section of the study.

3.3.1 Conventional SEM

Table 3.1 details the drug and excipient powders imaged using conventional scanning electron microscopy.

Material	Figure
α-lactose monohydrate: 63-90 μm (AJS)	3.2 and 3.3
<45 μm	3.4
FPL	3.5
Micronised NST	3.6
	3.7

Table 3.1 Conventional scanning electron micrographs of the excipient and drug powders used in the study.

Lactose Size Fractions

Images of the carrier size fractions of α-lactose monohydrate (figures 3.2 to 3.5) support the particle size measurements obtained using the techniques of LALLS (section 2.3.1.1) and TOFABS (section 2.3.1.2). Conventional SEM investigations produced clear images with negligible charging effects.

Micronised NST

Figures 3.6 and 3.7 depict a binary powder blend containing NST (40% $^{w}/_{w}$) formulated with the 63-90 μm lactose size fraction, studied using conventional SEM.

NST is stable as the trihydrate under ambient conditions (55% RH and 20-25°C) (Khankari et al. 1998). Thermal analysis of the trihydrate revealed that two thirds of the absorbed moisture is loosely bound whilst one third is tightly bound (Khankari et al. 1995). The research conducted by Khankari and Grant is discussed further in section 7.2. However, it is considered that damage to the conductive gold coating, likely due to evaporation of water from the highly hydrated sample (loosely absorbed and adsorbed surface moisture), caused an accumulation of negative charge on the sample surface. Subsequent powder charging produced effects of over-brightness and image distortion making the resulting electron micrographs impossible to interpret.

In non-hygroscopic powders some of these problems can be overcome if samples for SEM are prepared by pre-storing the powders at low humidities or drying the samples under vacuum to remove any excess surface moisture. However, storage and/or drying of NST may convert the trihydrate to the monohydrate, which is very hygroscopic (Khankari et al. 1998). Initial investigations suggested that rapid re-uptake of water by the sample during powder transfer and sample mounting negated the effects of this pre-conditioning.

3.3.2 LTSEM

LTSEM electron micrographs of fully hydrated micronised NST particles are shown in figures 3.8 and 3.9. The uncharged nature of the specimen resulting from cryogenic

preparation can be seen from the resolution and clarity of the images compared with those obtained using conventional SEM (figures 3.6 and 3.7). Accelerating voltages of 15 kV at magnifications up to x 25000 (figure 3.9) were employed without any apparent build up of negative charge.

Imaging of the shape and particle size of NST revealed an ultrafine powder consisting of irregularly shaped particles (figure 3.8 and 3.9). From the samples analysed, the particle size would seem to correlate well with measurements obtained from the LALLS studies: VMD <1 μm with 90% of the particles having an equivalent volume diameter of <5 μm (section 2.3.1.1). The images also support the conclusions that the decrease in the measured particle size following fixed sonication periods was due to the deaggregation of larger drug agglomerates and not a result of the powder samples dissolving in the suspending medium. These images further support the suggestions that Wong et al. (1995b) and Clark and Hollingworth (1993b) may have measured agglomerates of NST and not discrete particles. It is concluded that LTSEM has provided important supporting evidence that the micronised NST provided is an ultrafine powder.

The technique of LTSEM was also employed to image the distribution of NST particles within lactose carrier based systems (chapters 4 and 5). Information derived from these images supported theories regarding the effects of formulation procedures on the interparticle forces governing the aerosol performance of the powder systems. The images are described further in the appropriate sections.

3.3.3 ESEM

ESEM images of the binary powder systems containing NST are displayed and described in detail in the appropriate section of the study (chapters 4 and 5). The electron micrographs provided important information as to the effects of various mixing procedures on the drug particle's distribution within powder blends formulated for inhalation.

3.3.4 EDAX

Table 3.2 details the drug and excipient powders investigated using EDAX. Spot analysis was initially performed on a sample of pure NST (no carrier) to ensure a satisfactory sodium peak was obtained (figure 3.10). Fine particle lactose (figure 3.11) and the adhesive carbon stubs (figure 3.12) were then analysed to confirm that no sodium signal was generated.

Material	Figure
NST	3.10
FPL	3.11
Carbon adhesive tab	3.12

Table 3.2 Materials analysed using the technique of EDAX

Powder blends containing NST and FPL were studied using EDAX (spot analysis) to support a theory relating to the intercalation of fine excipient particles within self-agglomerated drug systems. Section 5.1.2 summarises the results of this study and discusses the theory of intercalation.

3.4 General Discussion

ESEM analysis of binary powder blends containing 40% $^{w}/_{w}$ NST and a lactose carrier, produced lower resolution images (figures 4.7 to 4.9) than were achieved in the LTSEM studies (figures 4.5 and 4.6). However, the ESEM images still provided important information and confirmed that the preparation stages (cryo-fixation and gold coating) and the low pressures necessary for LTSEM investigations, do not appear to affect the drug particles' appearance or distribution within these binary systems.

LTSEM and ESEM are alternative techniques to conventional SEM for imaging hygroscopic hydrated pharmaceutical compounds when dehydration of the powder is either undesirable or impractical. Consideration must also be given to the effects of the low pressures ($<10^{-3}$ Pa), encountered within the conventional SEM chamber, on the distribution of drug particles within blends formulated for inhalation. Loosely adhered drug particles may be redistributed or removed from the carrier lactose system when subjected to the high vacuum within the conventional SEM sample chamber. This is undesirable when trying to image the drug particles' distribution within high and low dose DPI formulations. ESEM and LTSEM procedures may minimise this problem by analysing the powder samples at higher pressures (~0.5 kPa) or by freezing and thus stabilising the powder system. LTSEM has been used to study highly hydrated fragile biological specimens including frozen hydrated mouse lungs (Bastacky et al. 1987). The technique also proved essential in the imaging of highly hydrated polysaccharide macromolecules (Chenu and Tessier, 1995). However, the use of LTSEM to study pharmaceutical powder formulations prior to this study (Clarke et al. 1998) has not been reported.

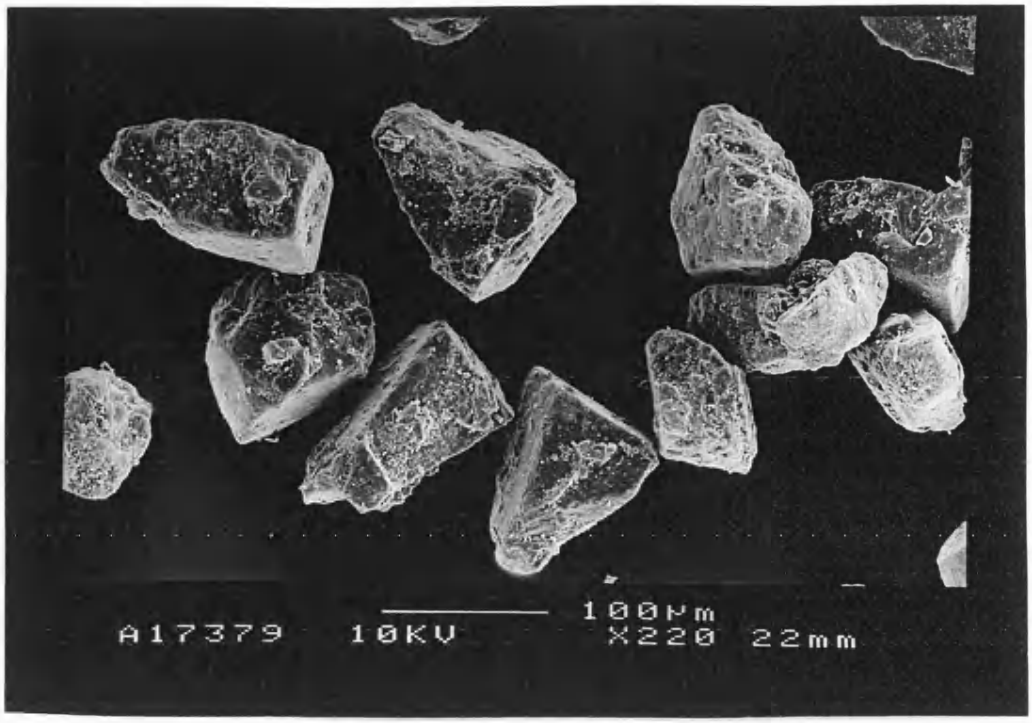

Figure 3.2 Conventional SEM electron micrograph of α-lactose monohydrate (63-90 µm carrier sieve fraction).

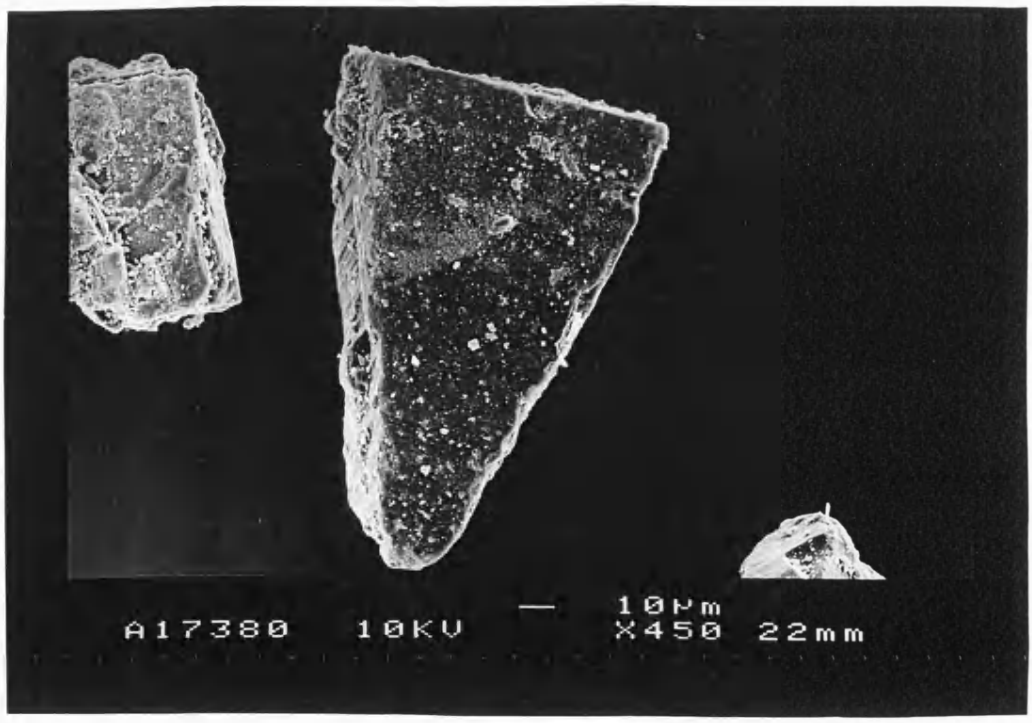

Figure 3.3 Conventional SEM electron micrograph of α-lactose monohydrate (63-90 µm carrier sieve fraction).

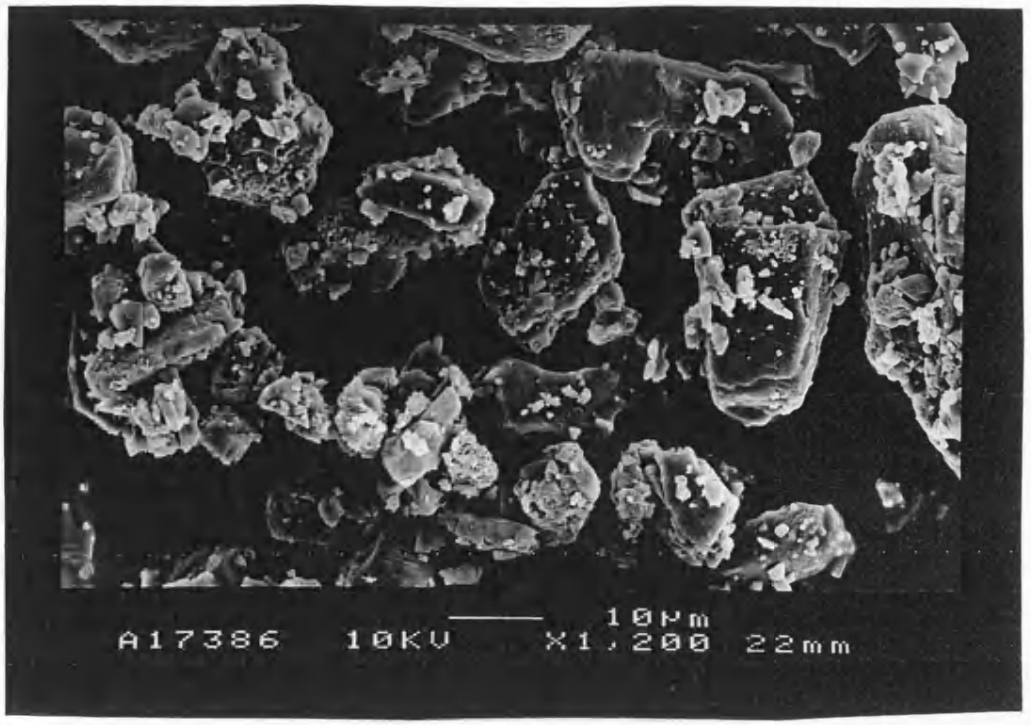

Figure 3.4 Conventional SEM electron micrograph of α-lactose monohydrate (<45µm carrier sieve fraction).

Figure 3.5 Conventional SEM electron micrograph of α-lactose monohydrate (Fine Particle Lactose).

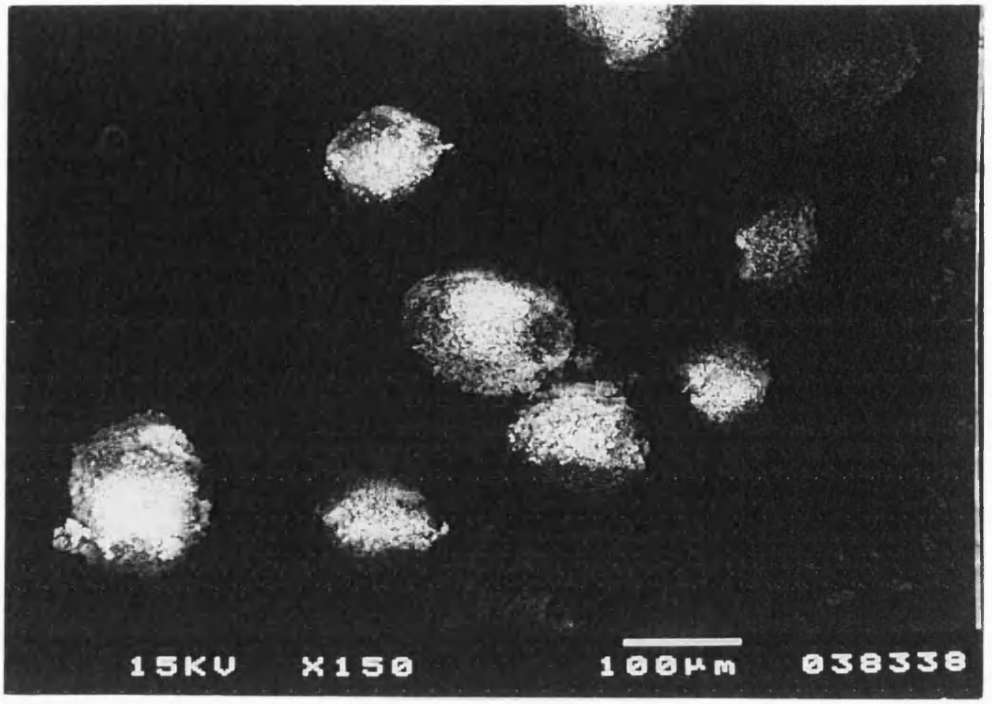

Figure 3.6 Conventional SEM electron micrograph of a binary powder blend containing NST (40% $^{w}/_{w}$) and a 63-90 µm lactose size fraction (60% $^{w}/_{w}$).

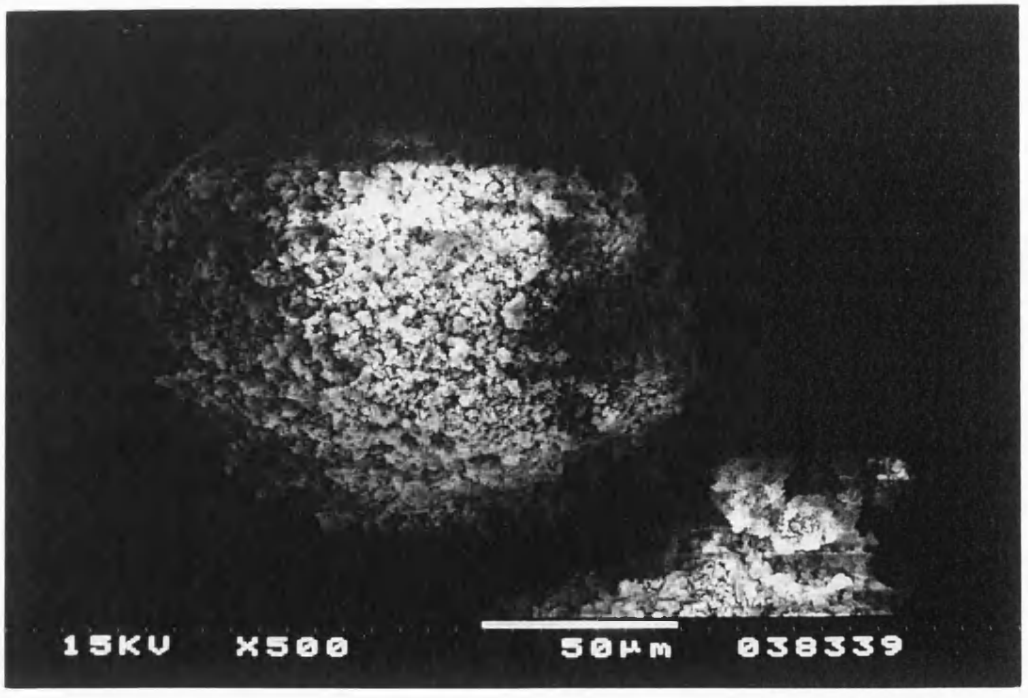

Figure 3.7 Conventional SEM electron micrograph of a binary powder blend containing NST (40% $^{w}/_{w}$) and a 63-90 µm lactose size fraction (60% $^{w}/_{w}$).

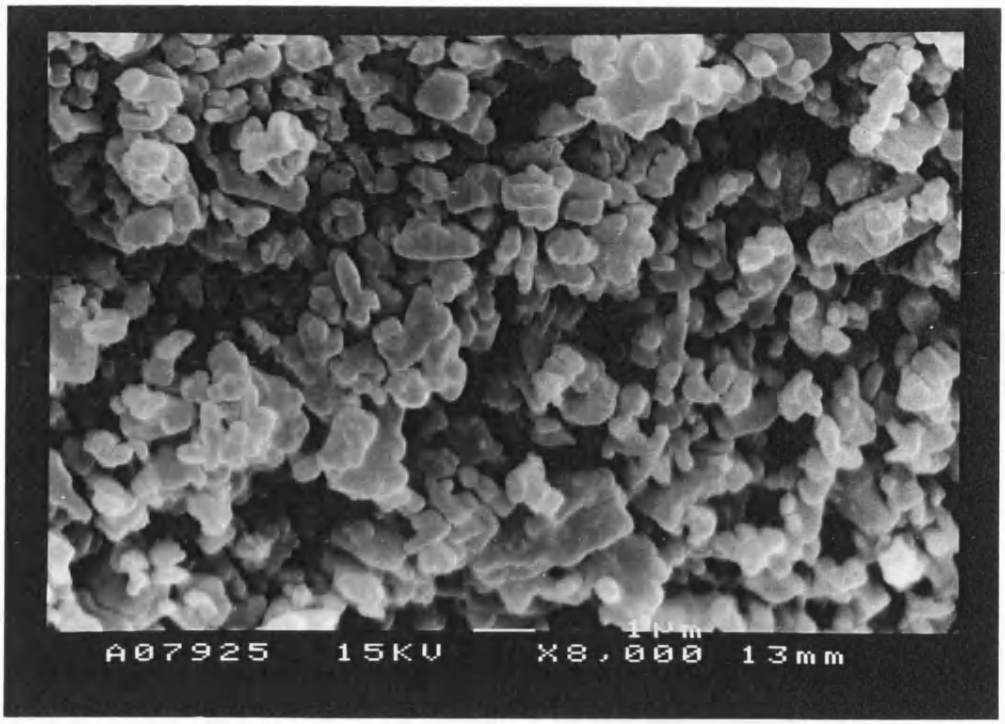

Figure 3.8 LTSEM electron micrograph of micronised NST.

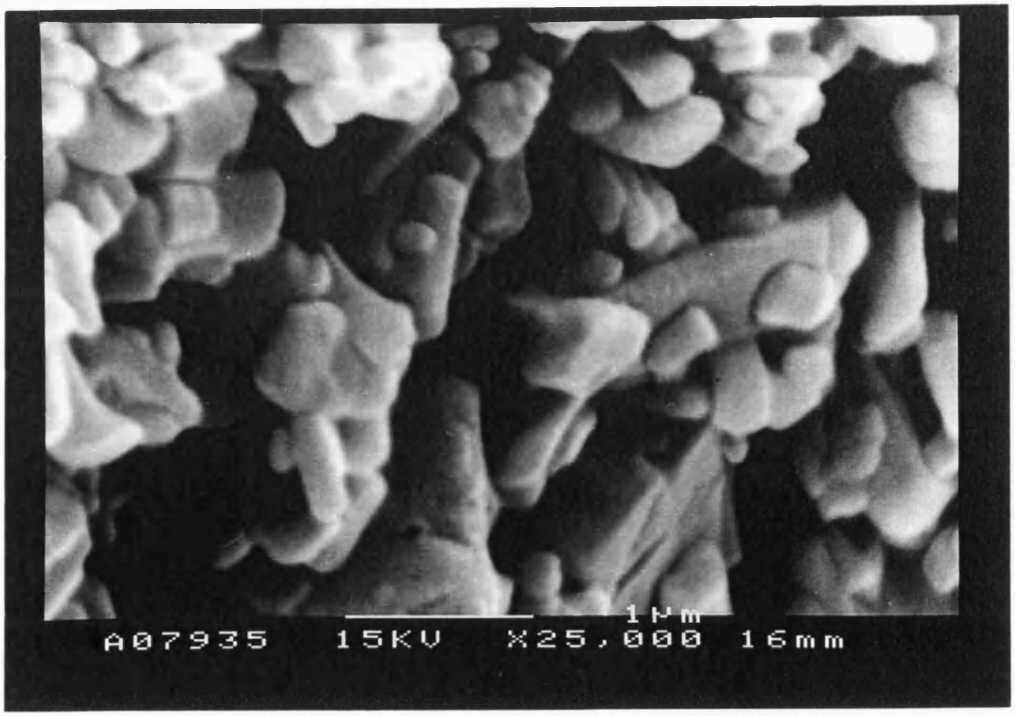

Figure 3.9 LTSEM electron micrograph of micronised NST.

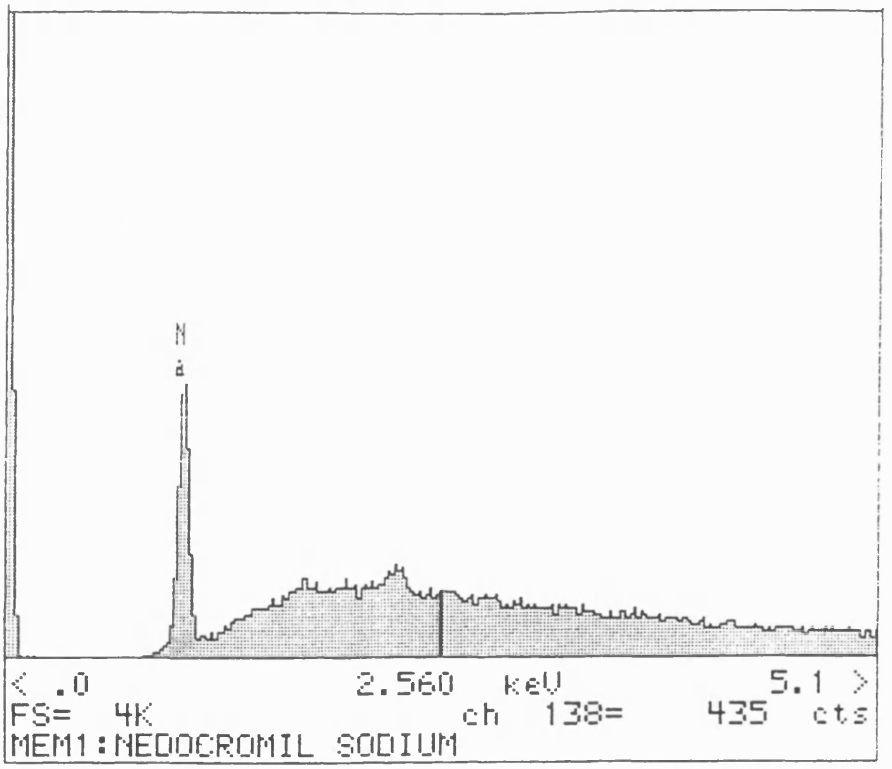

Figure 3.10 Energy dispersive X-ray spot analysis of NST.

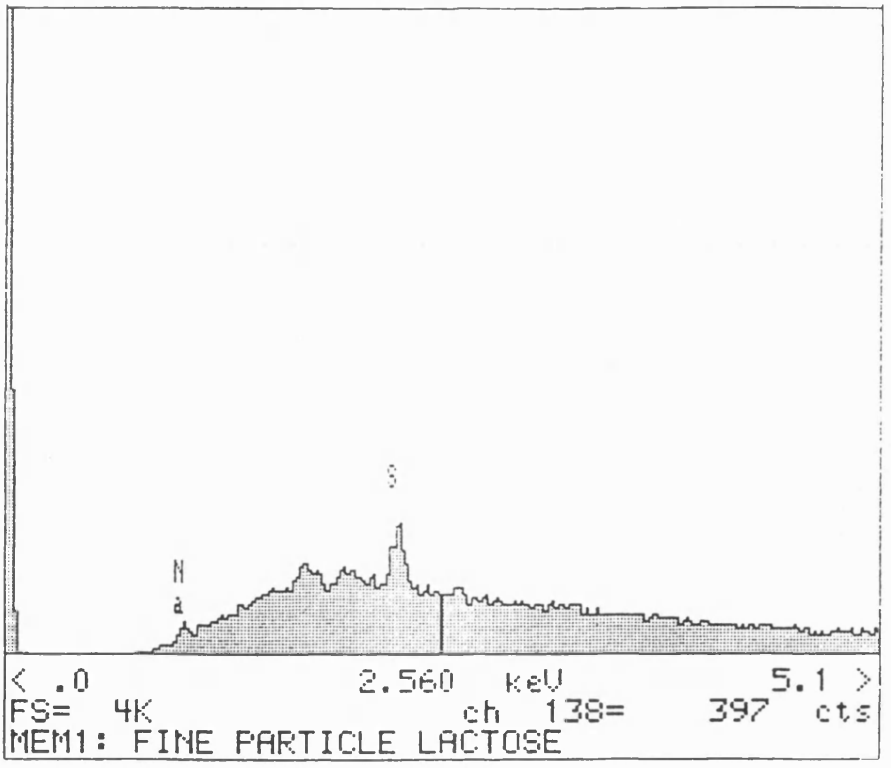

Figure 3.11 Energy dispersive X-ray spot analysis of FPL.

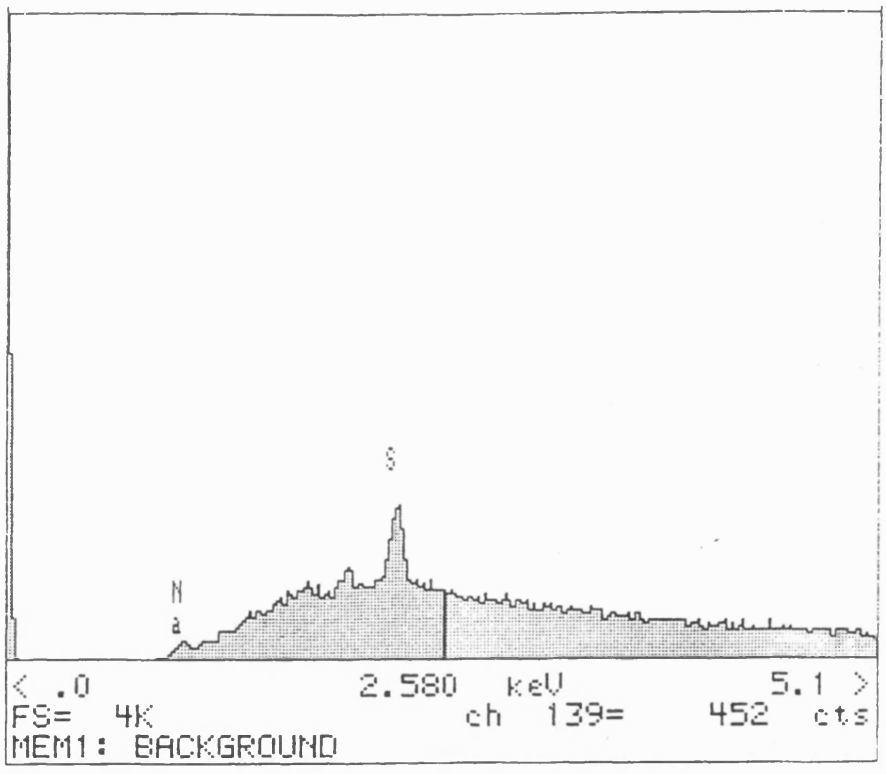

Figure 3.12 Energy Dispersive X-ray spot analysis of carbon adhesive tab.

CHAPTER 4

THE FORMULATION OF NEDOCROMIL SODIUM TRIHYDRATE AS A DRY POWDER FOR INHALATION

4.1 Introduction

The performance of carrier based and agglomerated dry powder aerosol formulations is predominantly influenced by the physicochemical characteristics of the constituent particles and the interparticle interactions operating within these systems (Hickey et al. 1994). The interparticle forces must be sufficient to withstand disruption by general processing techniques but should allow efficient regeneration of discrete particles or potentially respirable drug agglomerates upon aerosolisation.

To assess the interparticle forces that govern the aerosol performance of the high dose NST powder systems, various formulatory procedures were investigated. The effects of different lactose size fractions, alternative blending techniques and drug concentration on the deaggregation and subsequent fine particle deposition of NST were characterised.

Carrier-based formulations were initially prepared incorporating a high percentage of NST (40% $^{w}/_{w}$) with a 63-90 μm sieve size fraction of α-lactose monohydrate (AJS). 40% $^{w}/_{w}$ NST was selected based on the provision of an acceptable powder dose in light of existing formulations of a high dose anti-allergic compound DSCG, currently available in a DPI formulation as Intal®. The recommended adult dose for DSCG is 10 mg four times a day when administered as a MDI compared to 20 mg four times a day when administered as a DPI formulation (BNF, 1999). Despite the differences in drug concentration, the DPI and MDI formulations both display a similar therapeutic efficacy (Taburet and Schmit, 1994).

Nedocromil sodium is only available for the treatment of asthma in the U.K. as an MDI formulation (Tilade®), with a recommended dose of 4 mg four times a day (BNF, 1999). Therefore, 8 mg of NST was initially formulated with a lactose carrier for dry powder inhalation, double the MDI dose as for the DSCG. For a 20 mg capsule fill this corresponded to a concentration of 40% $^{w}/_{w}$ NST and was in the concentration range (10 to 50% $^{w}/_{w}$) of previous studies assessing the *in-vitro* aerosol performance of NST as a high dose inhalation system (Wong et al. 1995a and 1995b).

Unless otherwise stated, the drug content uniformity and *in-vitro* aerosol performance of all blends was investigated as described in section 2.2.4 and 2.5.1.

4.2 Mono-Component Coarse Lactose Carrier Systems

4.2.1 Formulations Prepared Using the Turbulent Tumbling Mixer

The term "mono-component lactose system" is defined as a carrier containing a single sieve size fraction of lactose (Lord, 1993).

The component powders were initially blended using a TTM, a mixing technique central to recent studies investigating the interparticle forces that influence the performance of DPI formulations (Lord, 1993; Lucas et al. 1998a and 1998b).

4.2.1.1 Mixing Investigations

Materials and Methods

Mixes were prepared (30 g) containing 40% $^{w}/_{w}$ NST and a carrier lactose sieve size fraction (63-90 μm; AJS) using the TTM (42 rev. min^{-1}). The two components were mixed in a 250 ml glass container with a plastic screw cap according to one of the following three blending procedures;

Mix A - The two components were mixed for 60 minutes.

Mix B - The two components were mixed for 5 minutes, the powder mix screened (355 μm) and then returned to the glass container for a further 55 minutes of mixing.

Mix C - The two components were mixed for 10 minutes, subjecting the powder mix to a two stage screening process after 5 minutes of mixing (355 μm and then a 250 μm aperture sieve mesh). Blends mixed following this procedure were prepared and analysed in duplicate.

Powder samples (20 mg) were removed from various parts of the powder bed after fixed time intervals for analysis of drug content (section 2.2.4). The distribution of NST particles within the coarse carrier based formulations was imaged using the techniques of LTSEM (section 3.2.2) and ESEM (3.2.3).

Results and Discussion

The drug content uniformity information and data for the three powder formulations are summarised in tables 4.1 (mix A and mix B) and 4.2 (mix C1 and C2) and in figures 4.1 (mix A), 4.2 (mix B) and 4.3 (mix C1 and C2).

Mixing Time (minutes)	Mix A Drug Content		Mix B Drug Content	
	Mean (mg)	CV (%)	Mean (mg)	CV (%)
1	7.43	7.33	7.45	5.82
2	7.61	6.06	7.42	4.37
3	7.62	8.09	7.79	4.14
4	7.46	5.42	7.64	3.18
5	7.88	4.12	7.51	4.20
	no screening stage		**355 µm screening stage**	
6	7.86	4.43	7.57	1.83
8	7.67	4.91	7.46	2.33
10	7.66	4.41	7.51	1.07
12	7.80	4.16	7.74	1.47
14	7.74	2.67	7.61	1.83
16	7.29	4.77	7.55	3.09
18	7.61	3.17	7.58	2.65
20	8.41	5.34	7.71	3.75
24	7.77	5.22	*No data acquired*	
28	7.50	4.04	*No data acquired*	
30	7.55	5.52	7.46	1.28
40	7.96	6.64	7.31	2.06
50	7.41	5.87	7.45	1.91
60	7.28	4.30	7.85	2.61

Table 4.1 Effects of the mixing time and the introduction of a screening stage on the drug content uniformity for mix A and B (n = 10 x 20 mg).

Mixing Time (minutes)	Drug Content Uniformity			
	Mix C1		Mix C2	
	Mean (mg)	CV (%)	Mean (mg)	CV (%)
1	7.78	6.46	7.95	4.13
2	7.79	3.83	8.31	5.31
3	7.84	2.00	7.83	1.47
4	7.95	2.71	8.05	1.33
5	8.07	6.31	7.90	2.27
	355 µm and 250 µm screening stage			
6	7.79	1.37	7.99	1.66
8	7.82	1.07	8.06	1.40
10	7.85	1.86	7.98	1.48

Table 4.2 Drug content uniformity data for mix C1 and C2 (n = 10 x 20 mg).

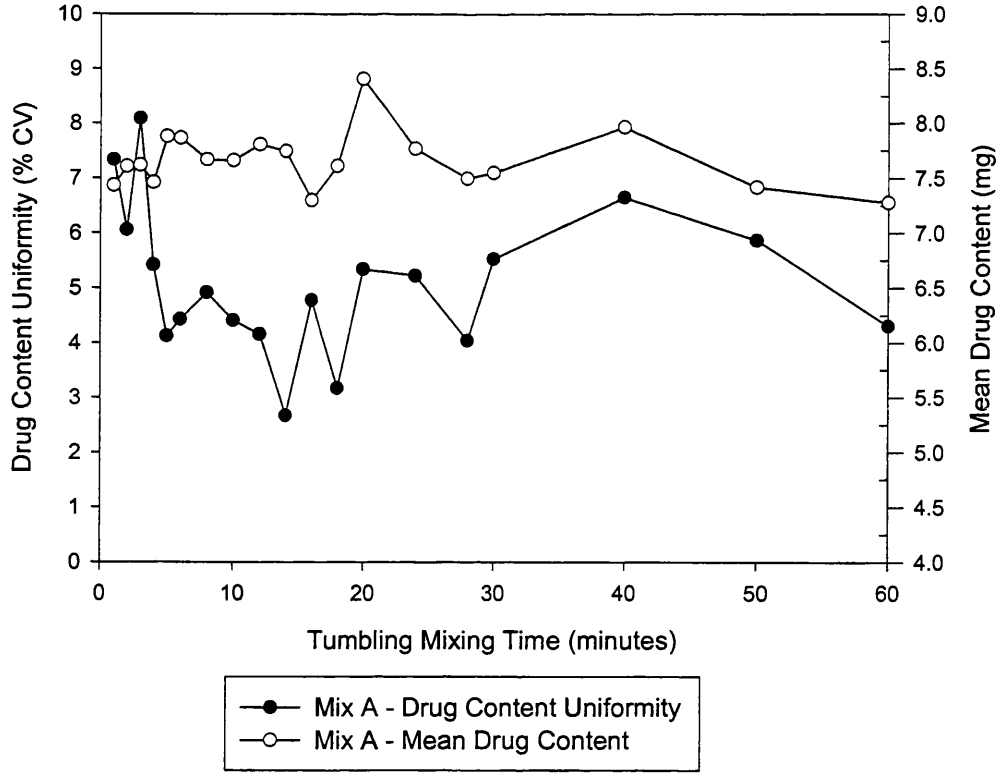

Figure 4.1 The effect of mixing time on the drug content uniformity of mix A.

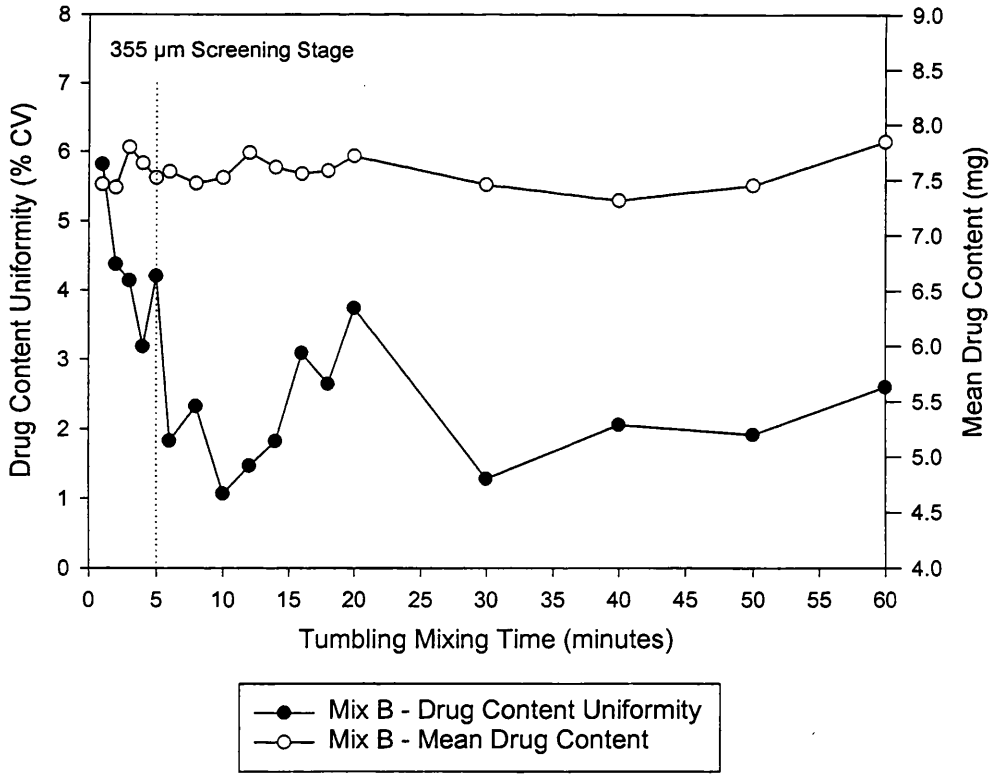

Figure 4.2 The effect of mixing time on the drug content uniformity of mix B.

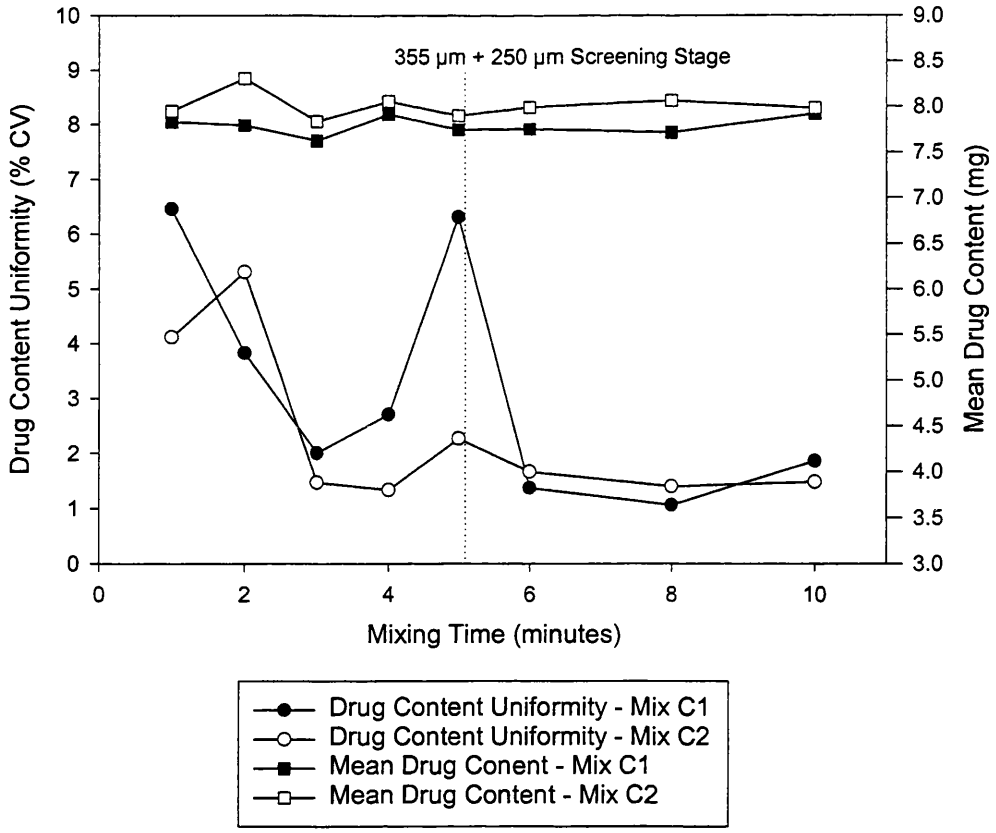

Figure 4.3 The effect of mixing time on the drug content uniformity data of mix C1 and C2.

A consideration of the mixing and segregation processes assumed to be operating within the powder mixture helps in the interpretation of the results (figure 4.4). Total mixing theory (Staniforth, 1981), asserts that particles may be mixed randomly, non-randomly, by ordering, by partial ordered randomisation or by any combination of these mechanisms occurring in dynamic equilibrium.

The situation would appear to be even more complex when considering a high dose micronised drug system (NST) and a coarse carrier component (63-90 µm lactose) (figure 4.4).

Ordered (cohesive and adhesive) interactions will exist between the drug/drug and drug/carrier particles (Hersey, 1975). During the process of mixing, a dynamic equilibrium will exist since some adhered drug particles may detach from the carrier surface whilst other unattached drug particles may subsequently adhere. These interactions are presumed to govern the mixing performance of low dose drug systems where the drug to carrier ratio is typically between 1:50 and 1:500 (Wong et al. 1995a).

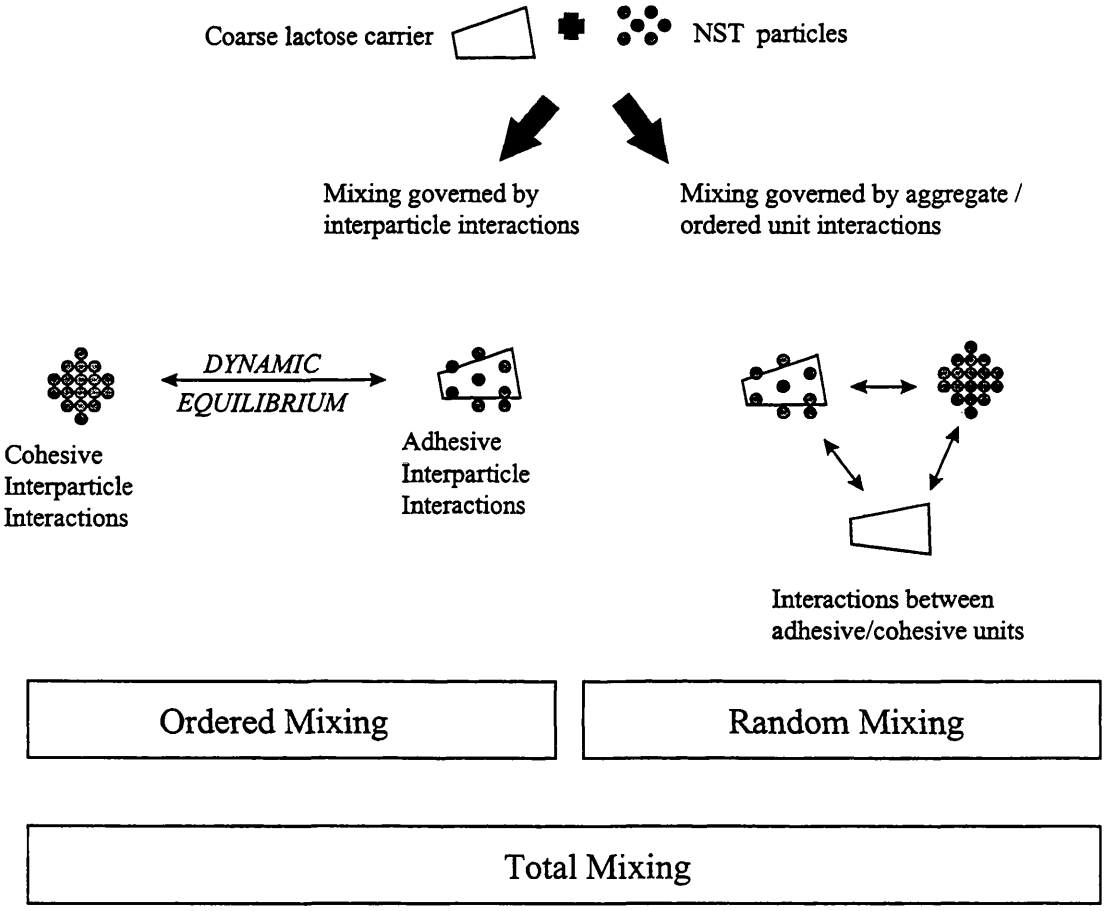

Figure 4.4 Diagrammatic representation of the interactions operating within the high dose powder system.

However, in high dose drug formulations, additional mechanisms are thought to be operational. It has previously been suggested that in high dose drug systems, drug

particles may adhere onto the carrier surface as multi-layers or exist as cohesive aggregates independent of the carrier component (French et al. 1996, Wong et al. 1995b). A percentage of the carrier particles may also exist practically devoid of adhered drug (Wong et al. 1995b).

Due to the high percentage of drug present within the system, it is considered that the quality of the mix will be governed by the interactions operating between the agglomerates of pure drug and the ordered units of NST and carrier (lactose particles with either minimal, mono- or multi-particle layer drug coverage).

Segregation of a powder is caused by differences in the physical and mechanical properties of the constituent particles and can be enhanced by the mode of mixing (Staniforth, 1982). The mechanisms of size segregation include percolation of fines through the gaps between larger particles and segregation due to vibration, causing large particles to move upwards through a mass of finer material (Williams and Shields, 1967).

Yip and Hersey (1977a) defined two distinct types of segregation occurring in ordered mixes, ordered–unit segregation and constituent segregation. Ordered unit segregation occurs when carrier particles of various sizes with different number of adherent particles move to different areas of the powder bed. Segregation occurs even though there is no change in the distribution of adherent particles on individual carrier particles. Ordered unit segregation can be minimised by using monosized carrier particles (Samyn and Murphy, 1974).

Therefore, it is suggested that when considering high dose formulations of NST, constituent segregation is mainly responsible for the increase in the % CV with an increase in mixing time. Constituent segregation occurs when the finer particles are dissociated from the coarse particles either by fine particles becoming dislodged as a result of weak interparticle forces or when a true ordered mix is not formed. The later system may occur when there are more fine particles in a mix than the carrier is able to carry (Bryan et al. 1979). Free particles within a mix have been shown to produce aggregates which exacerbate the segregation tendency (Yip and Hersey, 1977a).

Mixing Performance of Blend A

Visual inspection of mix A after the extended mixing time (60 minutes) revealed that agglomerates of pure NST appeared to be existing separately from the coarse lactose carrier. However, at some point during the mixing process, the pure drug agglomerates may be uniformly distributed throughout the powder system as suggested by the CV for mix A being less than 5% between the mixing times of 5 and 20 minutes.

The physical properties of the interacting particles may change throughout the mixing process. Electrical forces generated during the mixing process (triboelectrification) may contribute to the self-agglomeration of the micronised particles (Williams and Shields, 1967). Therefore, with an increased mixing time, the size and density of the pure drug agglomerates and/or drug coated lactose carrier may change, possibly promoting an increase in the segregation of the blends. Rippe et al. (1964) found that density differences alone had negligible effects on segregation but when combined with a particle size difference, a marked increase in segregation tendency occurred. This may

explain the decrease in drug homogeneity observed for mix A after 20 minutes (CV > 5%).

Alternatively, the aggregated drug particles (adsorbed multiparticle layers or self-agglomerates) may reach an optimum size after which, the gravitational forces acting on the aggregated drug system exceeds the van der Waals forces of attraction. Further mixing may cause the agglomerates to fracture, resulting in a proportion of the drug system existing within the powder system as smaller fragments and therefore more prone to segregation (Williams and Shields , 1967).

The material properties of the mixing vessel may also influence electrostatic charge and possibly the distribution of micronised drug particles within the carrier based system (Lord, 1993; Peart, 1996).

Further evidence of drug self-agglomerates existing within the powder systems was provided by the sieve size fractionation of mix A, to separate the agglomerated drug from the coarse carrier. Three sieve size fractions were collected (>212μm, 125-212 μm and <125 μm) by gently tapping the sieve stack for one minute. Vibration of the sieve stack and/or rolling of the powder across the metal mesh were avoided to reduce the possibility of promoting further agglomeration of the drug powder.

Table 4.3 summarises the drug content uniformity data for the three sieve size fractions (> 212 μm, 125-212 μm and < 125 μm).

Mixing Time (minutes)	Mix A Sieve Fraction (μm)	Drug Content	
		Mean (mg)	CV (%)
60	>212	19.59	1.18
60	125-212	5.32	2.28
60	<125	2.10	3.69

Table 4.3 Effect of sieve size classification on the drug content uniformity of mix A (n = 10 x 20 mg).

The finer aperture mesh (<125 μm) was selected to allow the majority of the lactose particles (63-90 μm) to pass through but prevent the passage of the larger agglomerates of pure drug. The <125 μm sieve fraction contained approximately 10 % $^{w}/_{w}$ NST whilst the >212 μm sieve fraction contained approximately 98% $^{w}/_{w}$ NST. Visual inspection of the >212 μm confirmed that excessive mixing within a TTM can lead to the formation of drug self-agglomerates which exist separately from the coarse carrier within the blend.

Mixing Performance of Blends B and C

The incorporation of screening stages in mixing procedures has been shown to significantly improve the drug particles distribution within carrier based formulations (Lord, 1993; Wong et al. 1995a). Therefore, the formulation procedure for blends B and C included a screening stage (250 μm mesh and/or 355 μm), introduced after 5 minutes in an attempt to destroy drug self-agglomerates and promote the redistribution of drug particles onto the surface of the lactose carrier (Lucas et al. 1998a). Screening the powder through a 355 μm aperture mesh was initially investigated (mix B) since the drug adhered to sieves with a smaller aperture size, making screening without drug losses difficult.

The screening procedure (mix B) reduced the % CV of the blend as shown in figure 4.2. However, the % CV again appeared to increase after approximately 10 minutes, presumably due to drug self-agglomeration and subsequent segregation. The blending procedure adopted for mix C incorporated a more stringent screening process in an attempt to more completely destroy the drug self agglomerates. The initial 355 μm screening stage enabled the second screening stage (250 μm) to be performed with greater ease. Following 10 minutes of mixing, the CV was < 2 % for both C1 and C2. The mixing procedure employed for the preparation of blends C1 and C2 was considered optimised for the TTM.

The effects of increased mixing times (TTM) on the physical properties and *in-vitro* aerosol performance of pure NST agglomerates are described in chapter 6.1.

LTSEM Investigations

LTSEM and ESEM analysis provided important information regarding the degree of mixing and the interparticle forces likely to influence the performance of the carrier based drug systems.

The existence of multi-layer particle adhesion was further supported by LTSEM (figures 4.5 and 4.6) and ESEM investigations (figures 4.7 to 4.9) of mix C. A large proportion of the NST appeared to be adhered onto the surface of the lactose carrier as multi-particle layers (figures 4.6 to 4.9).

The CV for the drug distribution within mix C was <2 %, again suggesting that the pure drug agglomerates may be evenly distributed throughout the powder mixture.

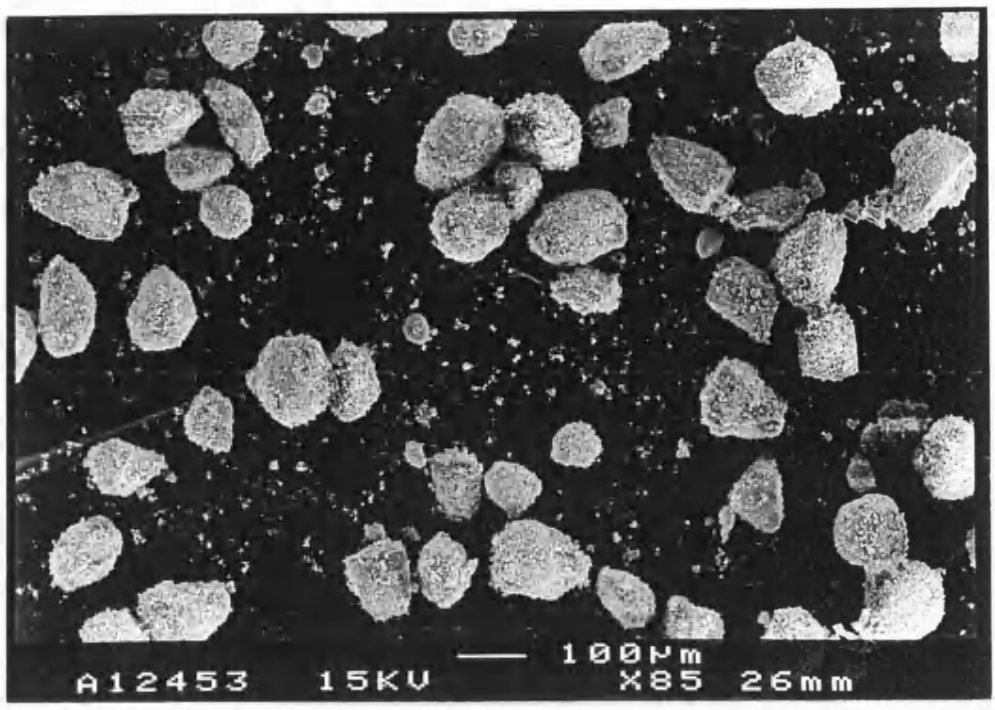

Figure 4.5 LTSEM electron micrograph of 40% $^{w}/_{w}$ NST blended (TTM) with 63-90 µm lactose (Mix C).

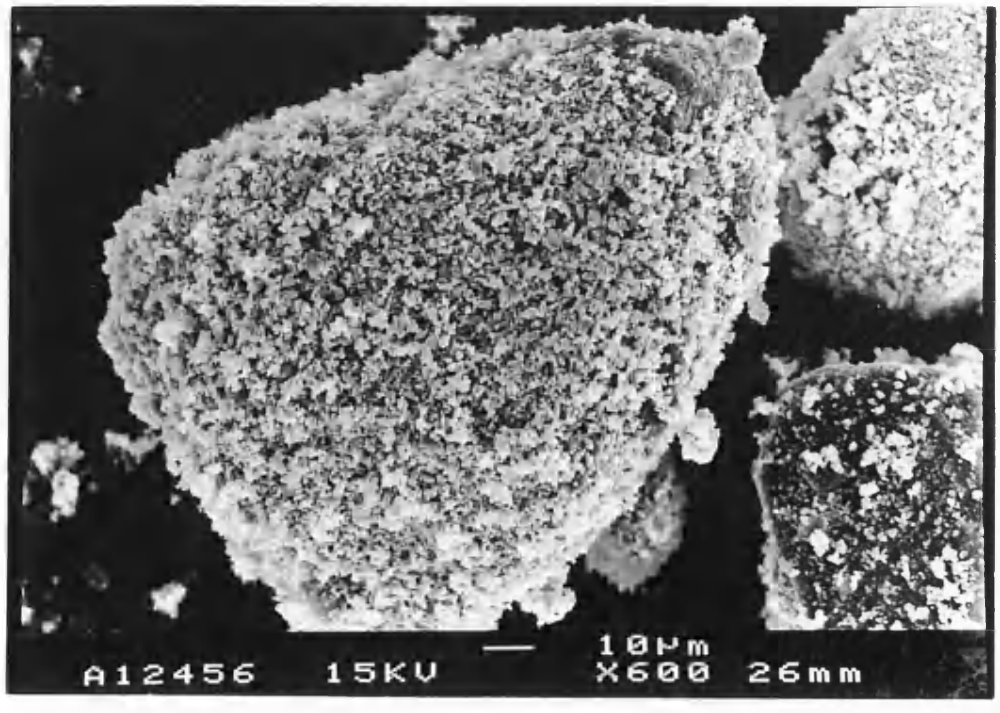

Figure 4.6 LTSEM electron micrograph of 40% $^{w}/_{w}$ NST blended (TTM) with 63-90 µm lactose (Mix C).

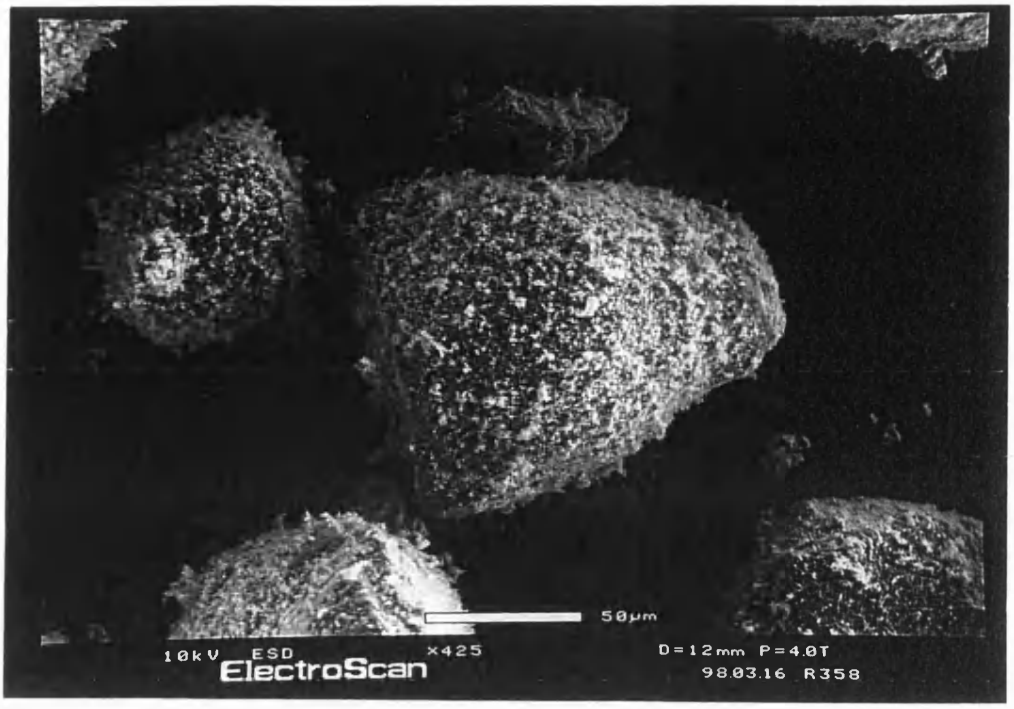

Figure 4.7 ESEM electron micrograph of 40% $^{w}/_{w}$ NST blended (TTM) with 63-90 µm lactose (Mix C).

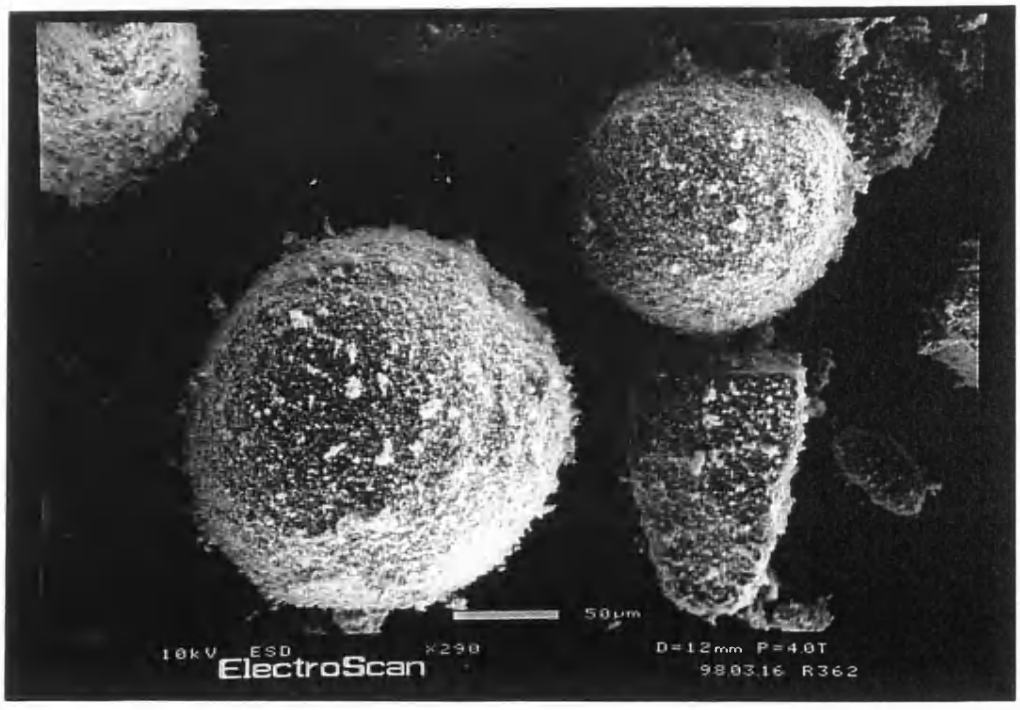

Figure 4.8 ESEM electron micrograph of 40% $^{w}/_{w}$ NST blended (TTM) with 63-90 µm lactose (Mix C).

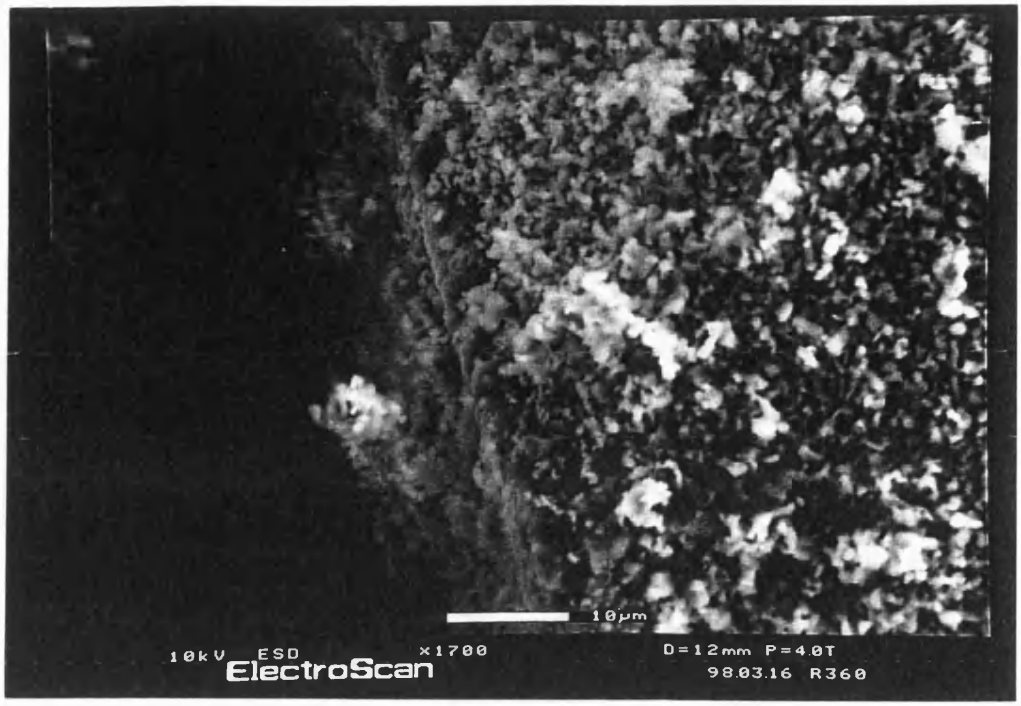

Figure 4.9 ESEM electron micrograph of 40% $^{w}/_{w}$ NST blended (TTM) with 63-90 μm lactose (Mix C).

Figure 4.8 also suggests the presence of self-agglomerates of drug existing within the mix even after a stringent screening stage and minimal mixing (Mix C).

The optimised mixing process detailed for the TTM is similar to the mixing technique described by Wong et al. (1995a). Wong et al. (1995a) concluded that provided the raw materials (carrier lactose and micronised NST) were pre-screened, a single 5 minute mixing stage (Turbula Mixer, 42 rev. min^{-1}) produced a satisfactory blend with the large drug agglomerates being removed/destroyed by the pre-screening technique. However, in the present study, inclusion of a screening stage both prior to and midway through the blending procedure although producing satisfactory drug content uniformity data failed to completely remove/destroy drug self-agglomerates within the system. A simple evaluation of drug content uniformity may disguise the presence of drug self

agglomerates in a high drug dose system since the drug aggregates themselves may be uniformly distributed throughout the powder sample.

4.2.1.2 In-vitro Aerosol Characterisation

Materials and Methods

Preliminary studies characterised the *in-vitro* aerosol performance of the formulations prepared using the optimised mixing procedure (blends C1 and C2). Optimisation of the binary system refers solely to the drug content uniformity of the powder mixture.

The aerosol performance of the formulation tumbled for 60 minutes (mix A), was subsequently characterised using the modified Apparatus A. Following 60 minutes of mixing, the NST had self-agglomerated with a large proportion of the drug existing separately from the lactose carrier system (4.2.1.1). Therefore, the mix was sieve classified and the *in-vitro* aerosol performance of the size fractions again characterised using the modified Apparatus A.

Results and Discussion

Data describing the *in-vitro* aerosol performance of the optimised formulations (mix C1 and C2) is summarised in table 4.4.

The *in-vitro* aerosol performance of mix *A* after 10, 30 and 60 minutes of mixing and following sieve fractionation is summarised in table 4.5 and figure 4.10.

In-vitro Aerosol Characterisation	Mix C1	Mix C2
% Capsule & Device	6.08 ± 1.6	5.69 ± 1.8
% Stage 1	86.6 ± 1.5	87.6 ± 2.1
% Stage 2	7.35 ± 0.72	6.72 ± 0.60
Emitted Percent (%)	93.9 ± 1.6	94.3 ± 1.8
Emitted Dose (mg)	7.20 ± 0.18	7.37 ± 0.17
Fine Particle Fraction (%)	7.83 ± 0.73	7.13 ± 0.68
Fine Particle Dose (mg)	0.59 ± 0.062	0.53 ± 0.053
Drug Recovery (%)	97.8 ± 1.0	99.1 ± 2.3

Table 4.4 The in *in-vitro* aerosol performance of mix C1 and C2.
Results are the mean ± SD of 5 determinations.
ED and FPD were normalised with respect to a 20 mg capsule fill weight.

The formulation of NST with the 63-90 μm lactose carrier size fraction of improved the percentage of drug emitted from the device/capsule system (>93%) when compared with the pure drug systems (<77%) (section 2.6.2). However, comparisons with the pure drug aerosol performance (section 2.6.2) suggest that the addition of the 63-90 μm coarse carrier or the selected blending procedure does not improve the deaggregation of the drug system upon aerosolisation.

A comparison of the aerosol performance of blends C1 and C2 with that of blend A (following 10 minute of mixing), suggest that the inclusion of a two stage screening process, in an attempt to more fully deaggregate the drug self-agglomerates, had no effect on the aerosol performance.

One way analysis of variance revealed no significant difference in the ED ($F = 0.10$; $p = 0.902$) following extended mixing times for blend A. However, there was a significant decrease in the deaggregation (FPF) ($F = 14.73$, $p < 0.001$) and subsequent stage-2 drug deposition (FPD) ($F = 4.87$, $p = 0.028$) of the powder systems following 60 minutes of

mixing (Fisher's pairwise comparisons). The extended mixing time has had a detrimental effect on the aerosol performance, presumably due to an increase in interactions between carrier/drug or drug/drug particles. Statistical analysis was performed on the aerosol performance of the powder system mixed for 60 minutes (TTM) before and after sieve size fractionation. One way analysis of variance indicated a significant difference in the deaggregation of the powder system (FPF) ($F = 14.73$; $p < 0.001$). Fisher's pairwise comparisons revealed that the lower dose sieve fraction (<125 μm) showed an improved deaggregation (FPF) compared with the higher dose powder sieve fractions (125-212 μm and >212 μm). However, the FPF is still > 10% $^{w}/_{w}$ for all systems.

TTM are recommended for producing ordered mixes when one coarse particle component is present (Yip and Hersey 1977b) and have been successfully employed when investigating coarse carrier systems containing a lower dose of drug (Lord, 1993; Lucas et al. 1998a). The TTM has also been used to formulate powder systems containing a high percentage (25 to 80% $^{w}/_{w}$) of drug, e.g. DSCG (Braun et al. 1996; Vidgren et al. 1987b, 1988a, 1988b, 1989, 1990) and NST (Wong et al. 1995a and 1995b). However, the shear forces generated in the TTM do not appear to be sufficient to promote the effective deaggregation and subsequent redistribution of the NST particles when formulated as a coarse carrier system. *In-vitro* aerosol characterisation of the formulations in conjunction with LTSEM and ESEM investigations, suggest that the drug particles exist mainly as self-agglomerates or as multi-particle layers adhered onto the lactose carrier surface. The TTM may even promote the self-agglomeration of the drug particles, which may have a detrimental effect on the mixing behaviour and aerosol performance of the system.

In-vitro Aerosol Characterisation						
	Mixing Time in the TTM (Minutes)					
	10	**30**	**60**	**60**	**60**	**60**
				>212µm	**212-125 µm**	**[A]<125µm**
% Capsule	1.97 ± 0.97	2.69 ± 0.57	2.76 ± 0.32	2.27 ± 0.65	3.0 ± 0.39	5.06 ± 0.39
% Device	5.02 ± 2.0	8.12 ± 2.4	5.62 ± 1.3	6.58 ± 1.2	5.1 ± 0.98	6.24 ± 0.34
% Stage One	86.3 ± 3.5	82.6 ± 4.0	86.4 ± 2.0	86.6 ± 1.7	87.0 ± 1.6	81.8 ± 0.70
% Stage Two	6.76 ± 0.72	6.64 ± 1.2	5.26 ± 0.82	4.59 ± 0.56	4.9 ± 0.68	6.91 ± 0.58
Emitted Dose (mg)	7.24 ± 0.23	7.35 ± 0.30	7.27 ± 0.50	17.8 ± 0.60	5.1 ± 0.19	1.84 ± 0.06
Emitted Fraction (%)	93.0 ± 2.8	89.2 ± 2.9	91.6 ± 1.3	91.2 ± 1.6	91.9 ± 1.3	88.7 ± 0.30
Fine Particle Dose (mg)	0.55 ± 0.051	0.60 ± 0.11	0.42 ± 0.062	0.90 ± 0.11	0.30 ± 0.047	0.14 ± 0.013
Fine Particle Fraction (%)	7.29 ± 0.97	7.48 ± 1.5	5.75 ± 0.97	5.04 ± 0.63	5.3 ± 0.76	7.79 ± 0.66
Drug Recovered (%)	102 ± 1.6	99.4 ± 2.1	99.4 ± 6.7	99.9 ± 1.8	103 ± 2.8	98.7 ± 2.8

Table 4.5 The *in-vitro* aerosol performance of mix A after extended mixing times (TTM) and following sieve fractionation.

Results are the mean ± SD of 5 determinations.

[A] Three 20 mg capsules were discharged into the modified Apparatus A for each determination.

ED and FPD were normalised with respect to a 20 mg capsule fill weight.

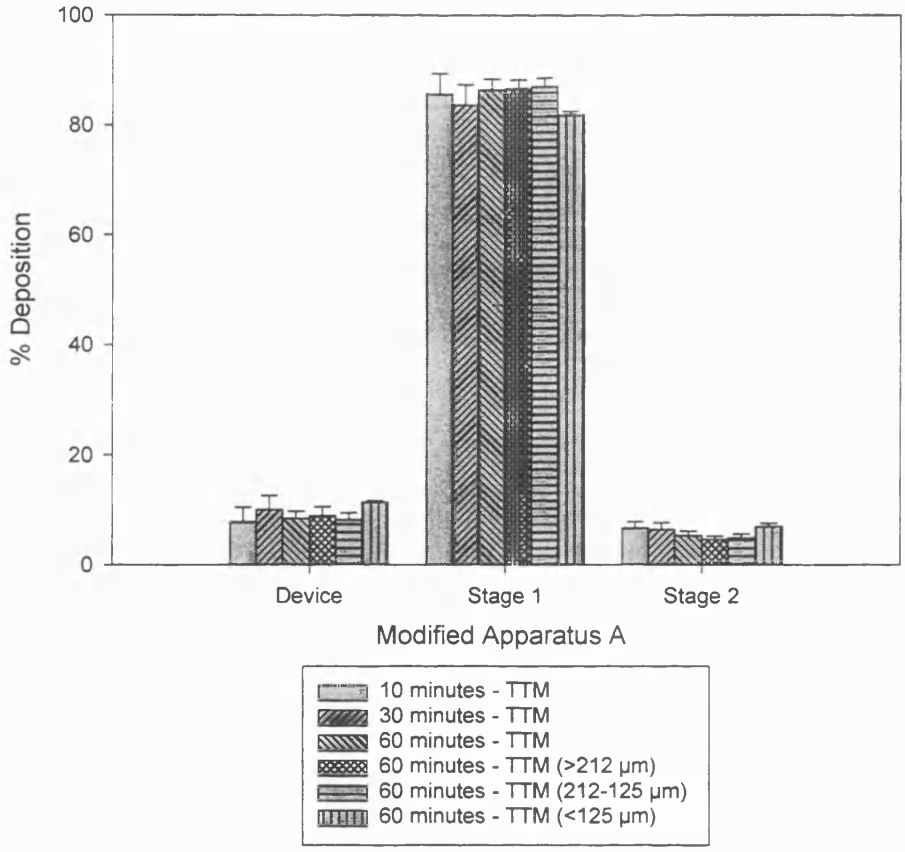

Figure 4.10 Effect of mixing time and size classification on the *in-vitro* aerosol performance of the binary powder system.
Each column shows the mean of 5 determinations (bars represent SDs).

Yip and Hersey (1977b) suggest that when an ordered mix of two fine particles is required, a mixer producing high shear forces is desirable. This suggestion may also be applicable to the formulation of high dose powder systems for inhalation.

4.2.2 Formulations Prepared Using Alternative Blending Techniques

Alternative blending techniques were employed in an attempt to improve the deaggregation of the NST self-agglomerates and promote the more complete redistribution of drug particles onto the lactose carrier surface.

4.2.2.1 Materials and Methods

The general mixing procedures are described in detail in section 2.2.3 with a brief description of the exact methods summarised below. All powder formulations were prepared and analysed in duplicate.

Turbulent Tumbling Mixer: Data obtained from the optimised blending procedure (mix C1 and C2) was selected. The blending procedure was discussed in detail in section 4.2.1.1.

Hand Blending: The blends (10 g) were hand mixed for 15 minutes as described in section 2.2.3.

Rotary Bladed Blender: The blends (10 g) were mixed for 4 minutes as described in section 2.2.3.

The drug content uniformity (section 2.2.4) and the aerosol performance (2.5.1) of the powder systems were assessed as previously described.

4.2.2.2 Results and Discussion

Table 4.6 summarises the drug content uniformity data for the formulations prepared using the different blending techniques.

Mixing Process	Content Uniformity			
	Run 1		Run 2	
	Mean (mg)	CV (%)	Mean (mg)	CV (%)
Turbulent Tumbling Mixer	7.85	1.86	7.98	1.48
Hand Blended	7.97	1.39	8.01	1.37
Rotary Bladed Blender	7.81	1.22	7.89	0.80

Table 4.6 Effect of the blending technique on the content uniformity of NST (40% $^{w}/_{w}$) formulated with a coarse carrier lactose (63-90 μm : AJS). n = 10 x 20 mg.

The results for all three mixing techniques indicate a similar degree of mixing in terms of drug content uniformity as indicated by CV < 2% for all blends. One way analysis of variance indicated a significant difference in the mean drug content for the formulation prepared using the three blending techniques ($F = 2.93$, $p = 0.026$) but Fisher's pairwise comparisons revealed no obvious trends. This would suggest that no significant drug losses have occurred when blending the powders using procedures capable of producing increased shear forces.

Table 4.7 and figures 4.11 and 4.12 summarise the *in-vitro* aerosol performance of the powder systems formulated using the three blending techniques.

In-vitro Aerosol characterisation	Turbulent Tumbling Mixer		Hand Blended		Rotary Bladed Blender	
	Run 1	Run 2	Run 1	Run 2	Run 1	Run 2
% Capsule & Device	6.08 ± 1.5	5.69 ± 1.8	14.9 ± 0.81	10.2 ± 1.7	18.8 ± 1.1	19.2 ± 4.7
% Stage 1	86.6 ± 1.5	87.6 ± 2.1	77.4 ± 1.2	83.1 ± 1.8	72.9 ± 0.82	72.1 ± 4.4
% Stage 2	7.35 ± 0.72	6.72 ± 0.60	7.70 ± 0.66	6.77 ± 0.14	8.25 ± 0.34	8.78 ± 4.4
Emitted Dose (%)	93.9 ± 1.5	94.3 ± 1.8	85.1 ± 0.81	89.8 ± 1.7	81.2 ± 1.0	80.9 ± 4.7
Emitted Dose (mg)	7.20 ± 0.18	7.37 ± 0.17	6.47 ± 0.20	7.01 ± 0.21	6.39 ± 0.079	6.37 ± 0.36
Fine Particle Fraction (%)	7.83 ± 0.73	7.13 ± 0.68	9.05 ± 0.79	7.54 ± 0.26	10.2 ± 0.33	10.9 ± 0.64
Fine Particle Dose (mg)	0.564 ± 0.056	0.525 ± 0.046	0.585 ± 0.053	0.529 ± 0.020	0.649 ± 0.024	0.692 ± 0.046
% Drug Recovery	97.8 ± 1.0	99.5 ± 2.3	96.8 ± 2.2	99.4 ± 2.0	100 ± 0.96	100 ± 1.7

Table 4.7 The *in-vitro* aerosol performance of NST (40% $^{w}/_{w}$) formulated with lactose (63-90 μm, AJS) using different blending techniques.

Results are the mean ± SD of 5 determinations.

ED and FPD were normalised with respect to a 20 mg capsule fill weight.

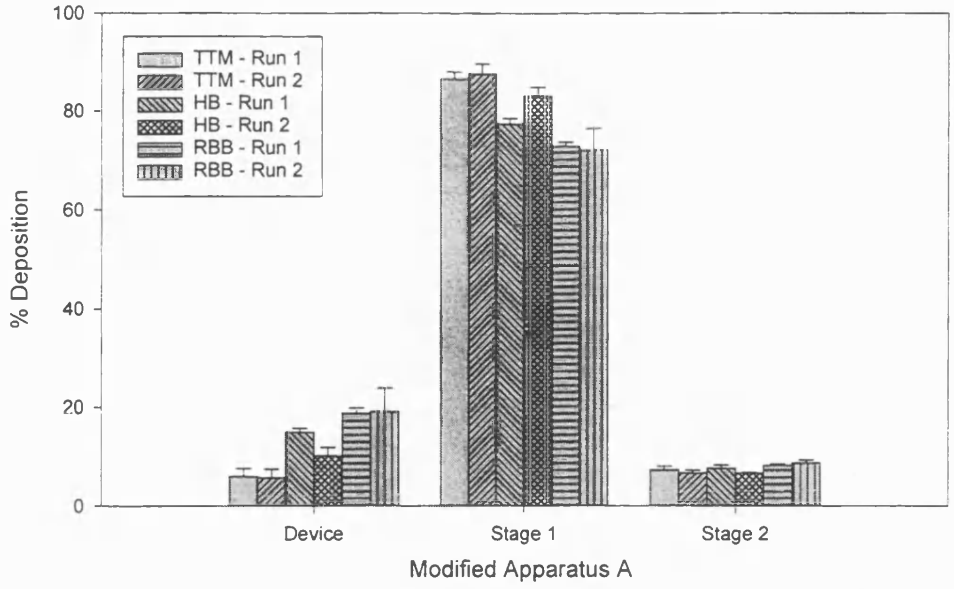

Figure 4.11 The *in-vitro* aerosol performance of NST (40% $^{w}/_{w}$) formulated with lactose (63-90 μm) using the three different blending techniques.
Each column shows the mean of 5 determinations (bars represent SDs).

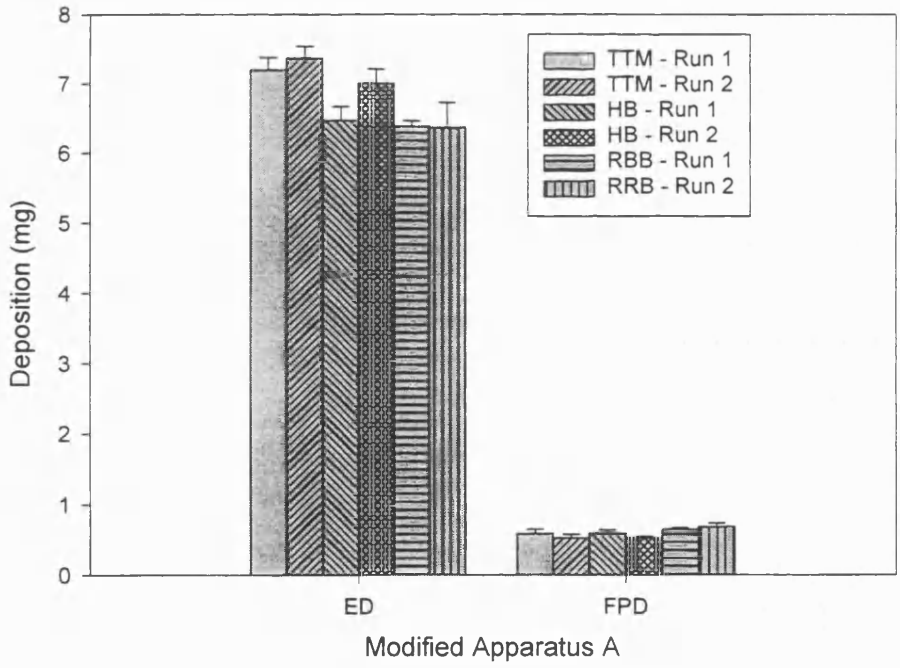

Figure 4.12 The *in-vitro* aerosol performance of NST (40% $^{w}/_{w}$) formulated with lactose (63-90 μm) using the three different blending techniques.
Each column shows the mean of 5 determinations (bars represent SDs).

One way analysis of variance in conjunction with Fisher's pairwise comparisons revealed a significant decrease in the ED ($F = 21.11$, $p < 0.001$) for the powder systems prepared using the RBB compared with the formulations mixed in the TMM. However, the formulations prepared using the RBB deaggregated more completely (FPF) ($F = 31.24$, $p < 0.001$) and generated a greater fine particle dose ($F = 12.13$, $p < 0.001$) compared with the formulations prepared by HB or using the TTM.

It is presumed that the slight increase in the deaggregation of the systems is caused by a greater disruption of the drug self-agglomerates with a subsequent redistribution of the drug particles onto the carrier surface. However, the aerosol performance of the systems is still considered poor and the adoption of mixing techniques capable of producing greater shear forces has not improved the aerosol performance compared with the pure drug systems (section 2.6.2).

4.2.2.3 Effect of the Blending Procedures on the Physical Properties of the Coarse Carrier Lactose

The particle size distribution of the coarse lactose sieve size fraction was investigated after subjecting the powder to shear conditions similar to those encountered in the HB and RBB mixing procedures.

Materials and Methods

The 63-90 μm (AJS) sieve size fraction of lactose (10 g) was HB for 30 minutes or mixed in the RBB for 10 minutes. The particle size distribution before and after the

blending procedures was characterised using the Malvern Mastersizer X in conjunction with the dry powder feeder (section 2.3.1.1).

SEM investigations were conducted to further characterise the particle size of the "processed" lactose. The methods used to prepare and analysis samples using conventional SEM were previously described (section 3.2.1).

Results and Discussion

Table 4.8 summarises the particle size distribution of the 63-90 μm carrier size fraction before and after processing. SEM electron micrographs of the carrier lactose before and after processing are shown in figures 4.13 and 4.14.

Material	Processing	d(0.1) μm	d(0.5) μm	D(0.9) μm
63-90 μm (AJS)	None	68.5 ± 0.68	94.3 ± 1.3	133.2 ± 3.5
63-90 μm (AJS)	HB	66.1 ± 1.6	94.1 ± 1.3	136.2 ± 5.7
63-90 μm (AJS)	RBB	67.9 ± 1.7	94.0 ± 0.91	130 ± 2.8

Table 4.8 Characterisation of the particle size distribution of the carrier lactose sieve size fraction (63-90 μm) before and after "processing".
Values are the mean ± 10 determinations.

LALLS in conjunction with conventional SEM investigations revealed that the particle size distribution of the lactose carrier fraction does not appear to change following processing (HB or RBB). Therefore, the slightly improved aerosol performance of the formulations prepared in the RBB is presumably due to the increased shear forces improving the re-distribution of NST onto the carrier surface.

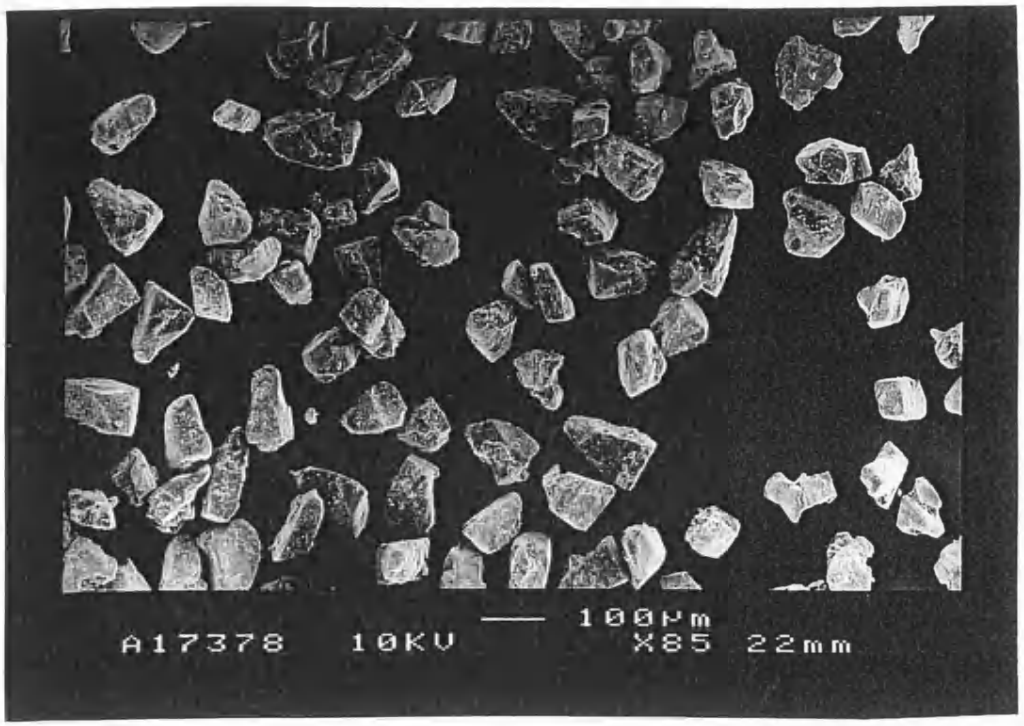

Figure 4.13 SEM electron micrograph of 63-90 µm (AJS) lactose hand blended for 30 minutes.

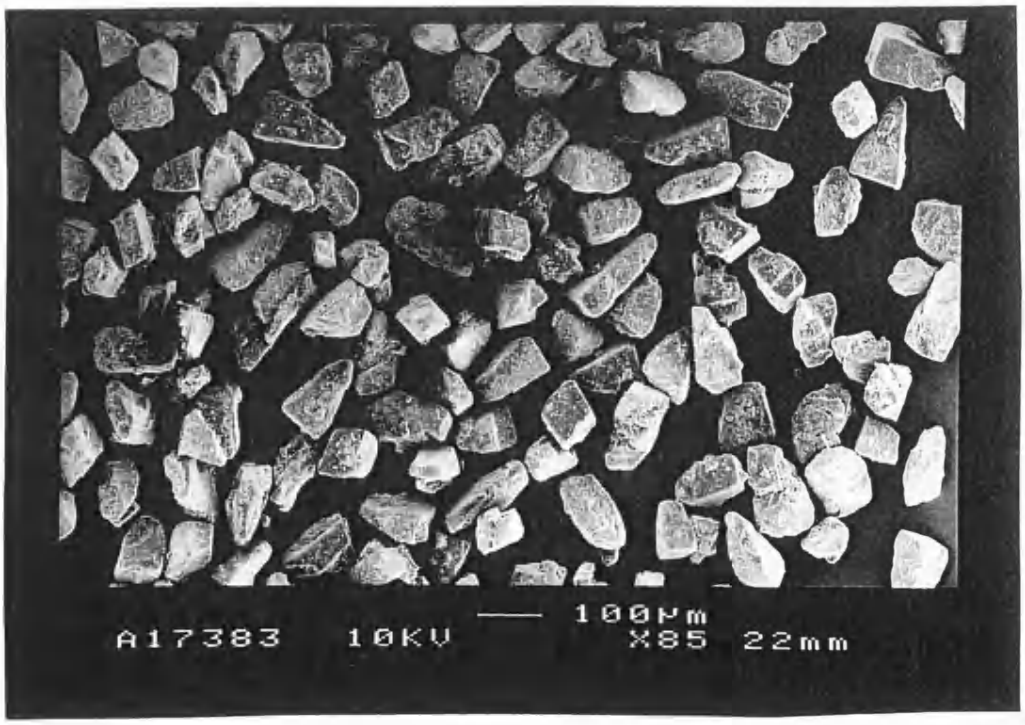

Figure 4.14 SEM electron micrograph of 63-90 µm (AJS) lactose blended (RBB) for 10 minutes.

4.2.3 Formulations Containing Different Concentrations of NST

The *in-vitro* aerosol performance of lower dose formulations containing NST and a carrier sieve size fraction of lactose (63-90 μm: AJS) were investigated. Assuming the formation of an ordered mix (Hersey, 1975) the theoretical estimation of the maximum NST concentration that could be adsorbed onto the coarse carrier surface was determined. Using true density and surface area measurements, calculated drug concentrations of 3.5 and 6.0 % were required for monolayer coverage (Appendix IV). To gain an increased understanding of the forces governing the aerosol performance of coarse carrier blends containing NST, formulations containing drug concentrations above and below this value were prepared and characterised.

4.2.3.1 Materials and Methods

Powder formulations (10 g) containing concentrations of NST ranging from 0.5 to 40 % $^{w}/_{w}$ were prepared by hand mixing the two components as previously described in section 2.2.3. HB was adopted to try and promote the redistribution of drug particles onto the carrier surface without encouraging drug aggregation, a problem that may arise with the use of the TTM (section 4.2.1).

Drug content uniformity was assessed by removing ten powder samples (of appropriate weight for quantitative drug analysis: 20 or 40 mg) from various parts of the powder bed (section 2.2.4). The *in-vitro* aerosol performance of the formulations was characterised using the modified Apparatus A (section 2.5.1). For accurate quantitative drug analysis, assessment of the *in-vitro* aerosol performance required the delivery of either ten capsules of 40 mg powder fill (NST = 0.5% $^{w}/_{w}$) or ten capsules of 20 mg powder fill (NST = 2.0% $^{w}/_{w}$) for each determination. For the formulations containing 10 to 40%

$^{w}/_{w}$ NST, one capsule (powder fill weight 20 mg) was fired for each determination. One powder formulation for each drug concentration was prepared and analysed.

4.2.3.2 Results and Discussion

Table 4.9 summarises the drug content uniformity for the formulations.

Drug Concentration ($\%$ $^{w}/_{w}$)	Drug Content Uniformity	
	Mean (mg)	CV (%)
[a] 0.5	0.22	4.16
[b] 2.0	0.41	0.80
[b] 10	1.96	1.18
[b] 20	3.99	2.13
[b] 30	6.06	0.54
[b] 40	7.97	1.39

Table 4.9 Drug content uniformity of the powder formulations containing various concentrations of NST blended with carrier lactose (63-90 μm: AJS). ([a]n = 10 x 40 mg; [b]n = 10 x 20 mg).

The drug content uniformity (CV) for all the powder systems was < 5%.

In-vitro Aerosol Characterisation

Table 4.10 and figures 4.15 and 4.16 summarise the *in-vitro* aerosol performance of the coarse carrier lactose formulations containing between 0.5 and 40% $^{w}/_{w}$ NST.

Data derived from the studies employing alternative blending techniques (run 1) (section 4.2.2) was incorporated into the statistical assessment.

In-vitro Aerosol Characterisation	NST Concentration (% $^{w}/_{w}$)					
	0.5[a]	2.0[b]	10[c]	20[c]	30[c]	40[c]
% Capsule & Device	6.02 ± 1.5	10.0 ± 1.1	12.2 ± 1.7	10.9 ± 0.95	12.9 ± 2.0	14.9 ± 0.81
% Stage 1	83.1 ± 1.9	79.3 ± 1.4	77.1 ± 2.4	82.2 ± 0.91	78.4 ± 2.1	77.4 ± 1.2
% Stage 2	10.9 ± 1.4	10.7 ± 0.81	10.7 ± 1.3	6.95 ± 0.15	8.75 ± 0.46	7.70 ± 0.66
Emitted Percent (%)	93.9 ± 1.5	90.0 ± 1.1	87.8 ± 1.7	89.1 ± 0.95	87.1 ± 2.0	85.1 ± 0.81
Emitted Dose (mg)	0.20 ± 0.004	0.37 ± 0.05	1.66 ± 0.05	3.55 ± 0.08	5.19 ± 0.19	6.47 ± 0.20
Fine Particle Fraction (%)	11.6 ± 1.5	11.9 ± 0.92	12.2 ± 1.6	7.79 ± 0.17	10.1 ± 0.62	9.05 ± 0.79
Fine Particle Dose (mg)	0.02 ± 0.003	0.04 ± 0.01	0.20 ± 0.02	0.28 ± 0.01	0.52 ± 0.04	0.59 ± 0.05
Drug Recovered (%)	96.3 ± 2.1	101 ± 1.1	100 ± 1.8	100 ± 1.3	102 ± 2.78	96.8 ± 2.2

Table 4.10 The effect of NST concentration on the *in-vitro* aerosol performance of the coarse carrier system.

[a]Capsule fill = 40 mg: *in-vitro* aerosol performance determined by firing ten capsules (40 mg) into the modified Apparatus A. ED and FPD were normalised with respect to a 40 mg capsule fill weight.

[b]Capsule fill = 20 mg: *in-vitro* aerosol performances determined by firing ten capsules (20 mg) into the modified Apparatus A. ED and FPD were normalised with respect to a 20 mg capsule fill weight.

[c]Capsule fill = 20 mg: *in-vitro* aerosol performance determined by firing one capsule (20 mg) into the modified Apparatus A. ED and FPD were normalised with respect to a 20 mg capsule fill weight.

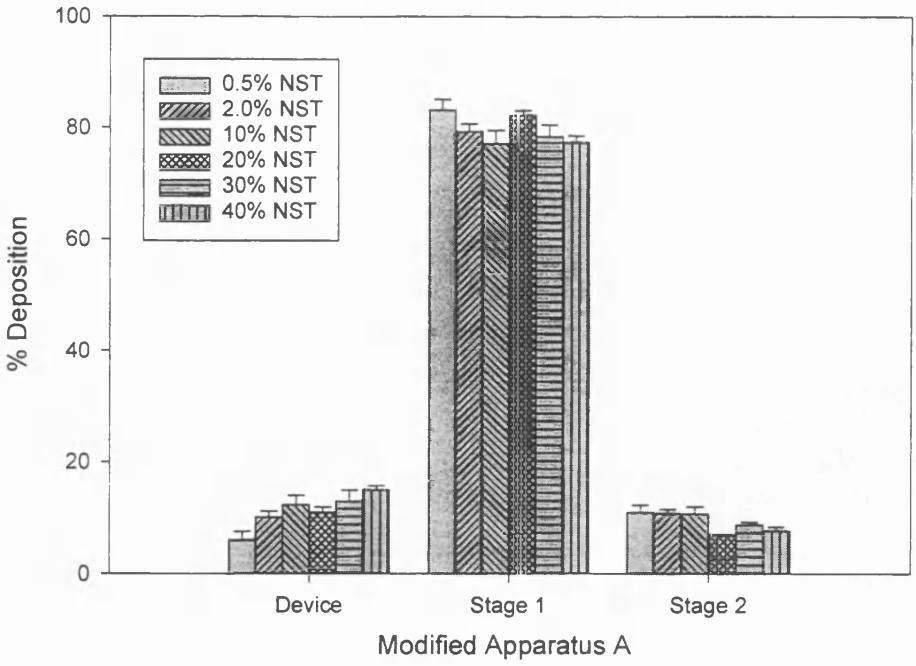

Figure 4.15 The effect of drug concentration on the *in-vitro* aerosol performance of coarse carrier system.

Each column shows the mean of 5 determinations (bars represent SDs).

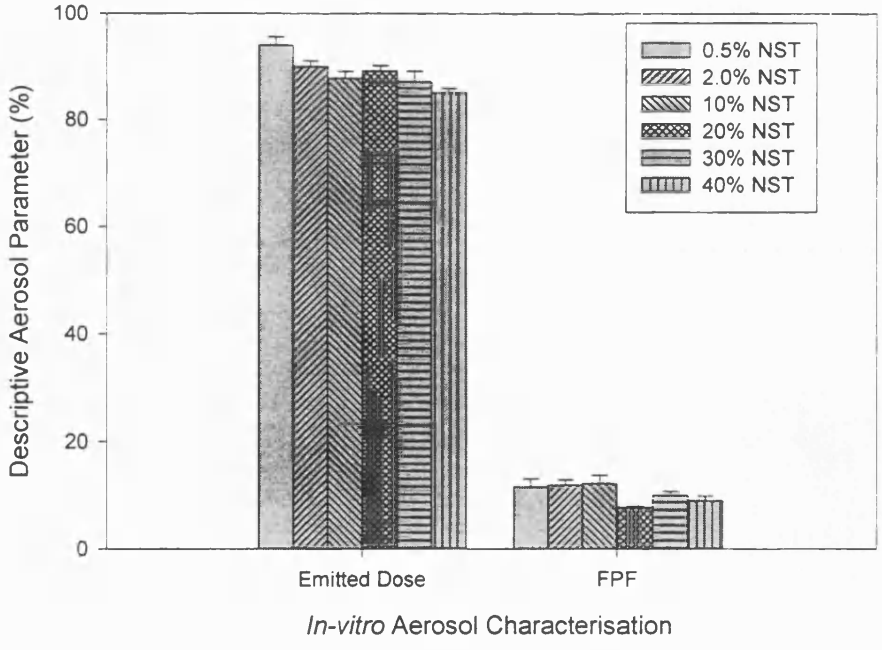

Figure 4.16 The effect of drug concentration on the *in-vitro* aerosol performance of coarse carrier system.

Each column shows the mean of 5 determinations (bars represent SDs).

Several studies have investigated the effects of drug concentration on the aerosolisation of carrier based powder systems by assessing the *in-vitro* (Braun et al. 1996; Kassem, 1990; Steckel and Müller, 1997b; Wong et al. 1995b) and *in-vivo* aerosol performance (Pitcairn et al. 1997) of blends for inhalation.

Kassem (1990) studied the aerosol behaviour of micronised SS blended with a coarse lactose carrier (63-90 μm) in the ratios of 1:135 to 1:1. The use of micronised drug without any carrier was also investigated. Kassem (1990) found that the addition of lactose to the formulation improved emptying of the inhaler therefore, more drug was made available for "inhalation". The work of Bell et al. (1971) demonstrated extensive coating of the Spinhaler® with DSCG in the absence of a coarse carrier supported the findings.

In the present study, one way analysis of variance also revealed a significant difference in the percentage of drug emitted for the formulations containing increasing concentrations (% $^{w}/_{w}$) of NST ($F = 23.15$, $p < 0.001$). However, Fisher's pairwise comparisons revealed that only the 0.5% $^{w}/_{w}$ NST formulation emitted a significantly greater percentage of drug compared with the other systems. Therefore, it would appear that for the higher dose formulations, the addition of a coarse carrier does not dramatically affect the mass of drug leaving the device.

Kassem (1990) also reported an increase in drug deposition on the lower stages of a MSLI as the proportion of lactose in the mixtures was decreased. It was therefore suggested that the FPF of a DPI formulation could be improved by increasing the concentration of drug in the system (Kassem, 1990). However, this suggestion assumes

that the interparticle forces dictating the aerosol performance of the powder system are the adhesive interactions acting between the drug and carrier particles.

The results of the present investigations suggest that this is not the case for micronised NST. One way analysis of variance on the FPF ($F = 14.35$, $p < 0.001$) and the subsequent stage-2 deposition (%) ($F = 18.06$, $p < 0.001$) indicated a significant decrease in both parameters when the concentration of NST increased. Fisher's pairwise comparisons revealed that the lower dose formulations (0.5 to 10 % $^{w}/_{w}$ NST) deaggregated more completely upon aerosolisation leading to a greater percentage of drug depositing in stage-2 of the modified Apparatus A. The formulations containing 20 to 40 % $^{w}/_{w}$ NST, showed a significant decrease in both parameters indicating that in this system, an increased concentration of NST does not improve the efficiency of the high dose formulations.

These findings were supported by Steckel and Müller (1997b) who found that increasing the concentration of micronised budesonide in a lactose carrier based system led to a continuous decrease in the FPF, agglomerates of pure drug building up which could not be re-dispersed. Wong et al. (1995a) studied the *in-vitro* aerosol performance of NST (10 to 50 % $^{w}/_{w}$) blended with a 45-63 μm sieve size fraction of lactose. The FPF (D_{ae} <6.5 μm) as determined by discharging the formulations from the Spinhaler® at 60 litres min^{-1} was approximately 15% and did not show any dramatic changes over the drug concentration range. This is presumably due to the choice of mixer (TTM) in combination with the coarser carrier system, not effectively deaggregating the drug systems. Even for the lower drug concentration formulations, the aerosol performance may be limited by the cohesive drug interactions.

The effects of powder concentration on the adhesion tendency and mechanical stability of interactive mixtures have been investigated by a sieving method (Malmqvist and Nystrom, 1982) and segregation tendency tests (Bryan et al. 1979; Staniforth et al. 1981; Staniforth and Rees, 1983). Centrifuge methods have also attempted to study the characteristics of drug adhesion in a model interactive system (Kulvanich and Stewart, 1987c).

These studies indicated a decrease in the adhesive properties of drug powder at increased concentrations. The reduction in adhesion tendency was explained by the limitation of active sites on the carrier capable of forming strong bonds with drug particles (Hersey, 1975; Staniforth et al. 1981). Excess drug particles formed weaker associations with the carrier or remained free in the bulk of the mixture. Multi-particle detachment in the form of particle layers or agglomerates may also occur (Kulvanich and Stewart, 1987c).

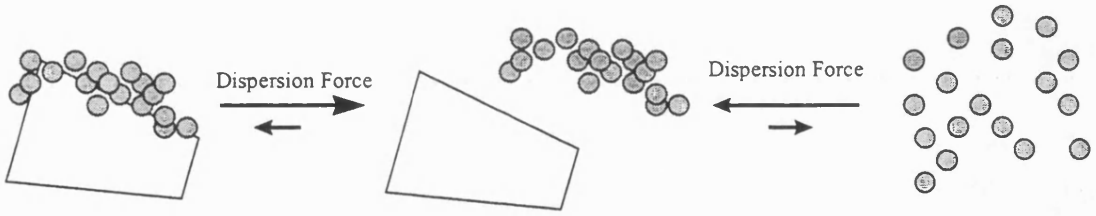

Figure 4.17 Diagrammatic representation of the interparticle forces presumed to be influencing the aerosol performance of the coarse carrier based systems

However, for an improved FPF and FPD, the dislodged drug particles need to deaggregate into potentially respirable aggregates/discrete particles (figure 4.17). This would appear to be the case for SS (Kassem, 1990) but not for micronised budesonide and NST (Steckel and Müller 1997b; Wong et al. 1995a).

Microscopic Investigations of the Coarse Carrier Based Systems

LTSEM images (figures 4.18 to 4.20) depict a hand blended carrier based formulation containing 10% $^{w}/_{w}$ NST. Multi-layers of drug particles are adhered onto the lactose carrier surface (figure 4.19). The drug particle's affinity for surface crevices and discontinuities on the carrier crystal's surface is also clearly visible (figure 4.20). It can be seen that fine powder is likely to fill up the carrier surface irregularities in agglomerates rather than cover the surface in a particulate manner.

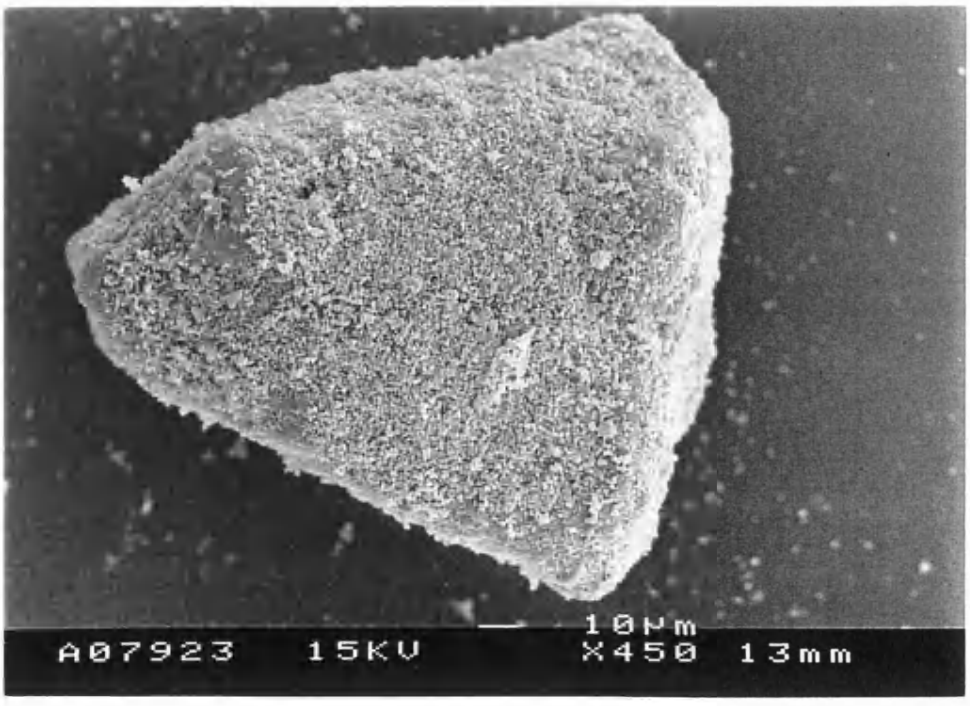

Figure 4.18 LTSEM electron micrograph of 10% $^{w}/_{w}$ NST blended (HB) with a coarse carrier (63-90) sieve fraction of lactose.

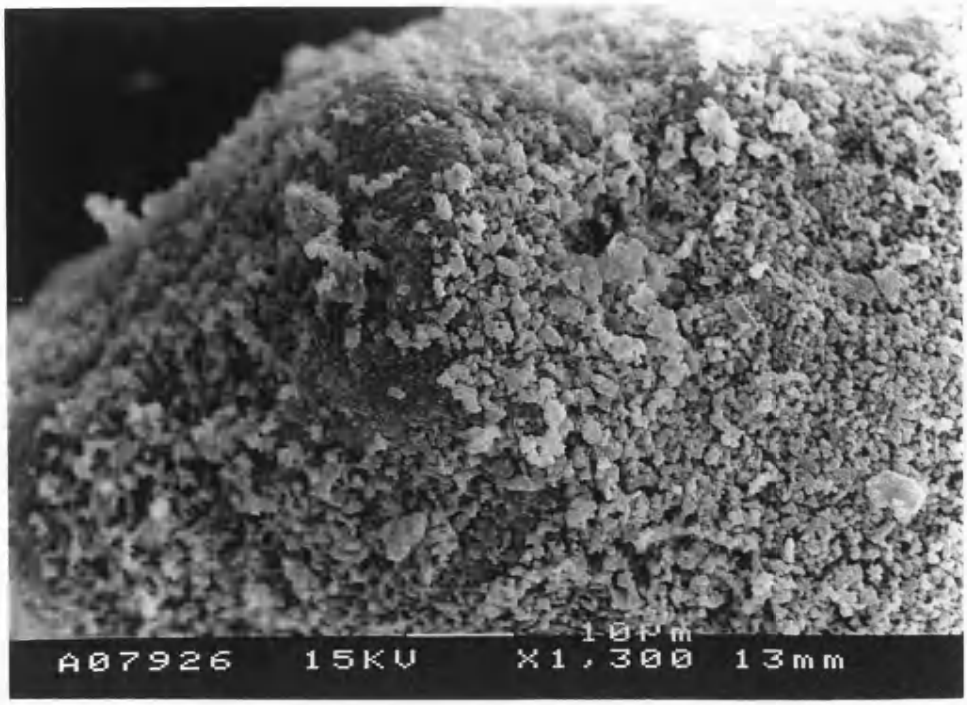

Figure 4.19 LTSEM electron micrograph of 10% $^{w}/_{w}$ NST blended (HB) with a coarse carrier (63-90) sieve fraction of lactose.

Figure 4.20 LTSEM electron micrograph of 10% $^{w}/_{w}$ NST blended (HB) with coarse carrier (63-90) sieve fraction of lactose.

4.2 Bi-Component Coarse Carrier Systems

4.3.1 The Addition of FPL to the Coarse Carrier System

Subsequent sections detail the use of "bi-component" lactose systems which are defined as carrier blends containing two size fractions of lactose (Lord, 1993). The effects of the addition of FPL on the drug content uniformity (as described in section 2.2.4) and the *in-vitro* aerosol performance of high dose (40% $^{w}/_{w}$ NST) carrier based systems (as described in section 2.5.1) were investigated.

4.3.1.1 Materials and Methods

40% $^{w}/_{w}$ NST was blended with a bi-component carrier system consisting of 63-90 μm (AJS) lactose and 5% $^{w}/_{w}$ FPL (% $^{w}/_{w}$ of carrier system). Three 10 g blends, containing NST (4 g), 63-90 μm lactose (5.7 g) and FPL (0.3 g) were prepared according to the following protocols.

Blend A - Ad-hoc: The three components were HB in one mixing stage for 15 minutes.

Blend B - FPL pre-mixed with the coarse carrier lactose: The lactose size fractions were initially HB for 15 minutes. After 15 minutes the carrier powder was screened (355 μm) and then mixed for a further 15 minutes. NST was then added to the binary carrier system and HB for 15 minutes.

Blend C - FPL pre-mixed with NST: NST and the FPL were HB for 15 minutes, introducing a 355 μm screening stage after 5 minutes. The coarse lactose carrier was then added to the NST/FPL binary system and the powder system mixed for a further 5 minutes.

Blend D - No FPL: The binary powder formulation prepared in section (4.2.2) containing 60 % $^{w}/_{w}$ carrier lactose and 40 % $^{w}/_{w}$ NST was defined as blend D. This blend was a control formulation, i.e. the formulation was prepared using a similar mixing procedure as for blends A to C however FPL was not incorporated into the system.

The blends were prepared and characterised in duplicate.

4.3.1.2 Results and Discussion

Table 4.11 summarises the drug content uniformity data for the three blending techniques.

Drug Content Uniformity	Blend A	Blend B	Blend C	Blend D	
				Run 1	Run 2
Mean (mg)	7.74	7.71	7.88	7.97	8.01
CV (%)	1.43	1.36	1.97	1.39	1.37

Table 4.11 Influence of mixing order on drug content uniformity. (n = 10 x 20 mg)

The CV for all formulations is <2 %, indicating a satisfactory distribution of NST within the powder systems. The addition of 5% $^{w}/_{w}$ FPL to the coarse carrier lactose system does not appear to have a detrimental effect on the drug content uniformity within the mixtures.

Table 4.12 and figures 4.21 and 4.22 summarise the *in-vitro* aerosol performance of the four formulations.

In-vitro Aerosol Characterisation	Blend A	Blend B	Blend C	Blend D	
				Run 1	Run 2
% Capsule & Device	12.8 ± 1.4	12.4 ± 1.4	12.1 ± 2.5	14.9 ± 0.81	10.2 ± 1.7
% Stage 1	79.6 ± 1.8	80.8 ± 1.7	80.9 ± 3.4	77.4 ± 1.2	83.1 ± 1.8
% Stage 2	7.57 ± 0.51	6.83 ± 0.41	6.88 ± 1.0	7.70 ± 0.66	6.77 ± 0.14
Emitted Dose (%)	87.2 ± 1.3	87.6 ± 1.4	87.8 ± 2.5	85.1 ± 0.81	89.8 ± 1.7
Emitted Dose (mg)	6.66 ± 0.16	6.60 ± 0.17	6.93 ± 0.24	6.47 ± 0.20	7.01 ± 0.21
Fine Particle Fraction (%)	8.69 ± 0.68	7.69 ± 0.55	7.87 ± 1.3	9.05 ± 0.79	7.54 ± 0.26
Fine Particle Dose (mg)	0.58 ± 0.03	0.51 ± 0.03	0.54 ± 0.08	0.59 ± 0.05	0.53 ± 0.02
% Drug Recovery	97.2 ± 1.5	98.2 ± 1.5	101 ± 3.0	96.8 ± 2.2	99.4 ± 2.0

Table 4.12 Influence of mixing order on the *in-vitro* aerosol performance of a NST blended with a binary lactose carrier system. Values are the mean ± SD of 5 determinations.

ED and FPD were normalised with respect to a 20 mg capsule fill weight.

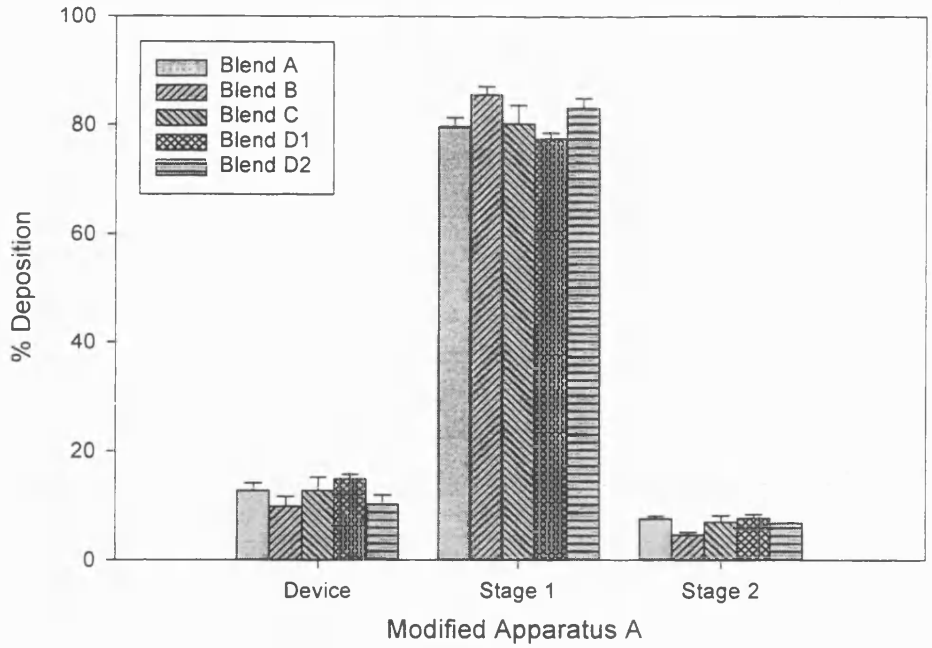

Figure 4.21 The effects of FPL and mixing order on the aerosol performance of NST. Each column shows the mean of 5 determinations (bars represent SDs).

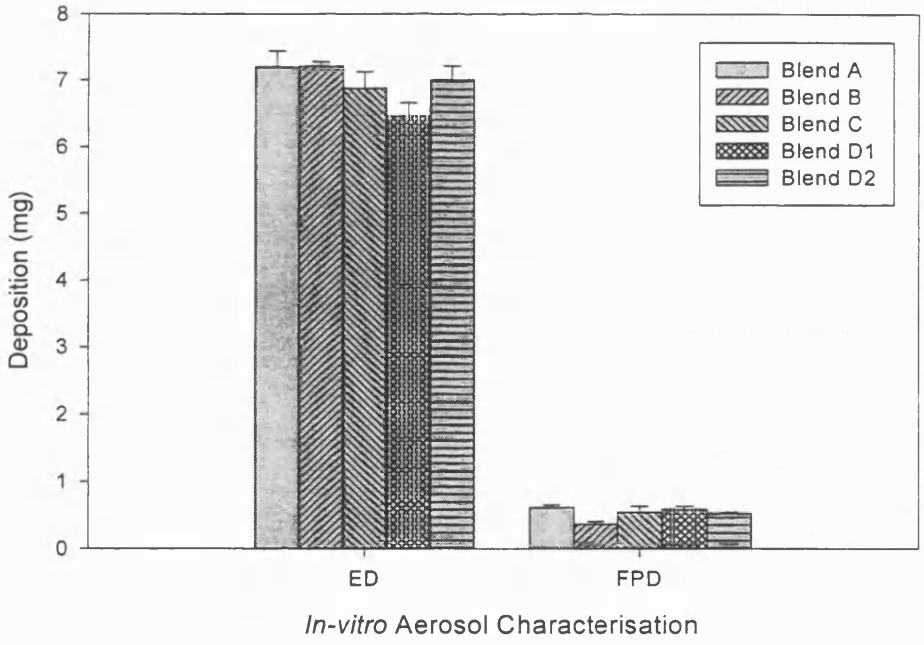

Figure 4.22 The effects of FPL and mixing order on the aerosol performance of NST. Each column shows the mean of 5 determinations (bars represent SDs). ED = Emitted Dose; FPD = Fine Particle Dose.

One way analysis of variance revealed that the addition of FPL had no significant effect on the ED ($F = 2.41$, $p = 0.083$). Similarly, no significant differences were observed in the deaggregation (FPF) ($F = 0.37$, $p = 0.70$) and subsequent stage-2 deposition (FPD) ($F = 2.32$, $p = 0.14$) on addition of 5 $\%^{w}/_{w}$ FPL, irrespective of the mixing sequence.

Zeng et al. (1996) reported that mixing order was important when considering the aerosol performance of formulations containing SS mixed with a coarse carrier lactose size fraction (63-90 μm) and FPL (0 to 9% $^{w}/_{w}$). Powder formulations, prepared by adding the drug to a pre-blend of the FPL and the coarse carrier component produced a significantly greater FPF of SS ($p < 0.05$) than formulations prepared using different orders of mixing. These findings supported the theories of Staniforth (1996) and Hersey (1975) regarding the saturation of the more active binding sites by the FPL.

However, the effects of mixing order were not shown to be significant when considering the aerosol performance of formulations containing SS and protein particles (Lucas et al. 1998a and 1998b).

Lucas et al. (1998a and 1998b) suggested that the incorporation of FPL into the powder system would cause a redistribution of drug/protein particles as previously demonstrated by Soebagyo and Stewart (1985), resulting in a hybrid ordered system containing drug/coarse lactose ordered units and drug/FPL multiplets. Improvements in the FPF of the active component were attributed to the improved liberation of drug/protein particles from the FPL. The aerosolised fraction depositing into the lower stage of Apparatus A (BP, 1998), may also have contained active/FPL multiplets, i.e. the drug particles are deposited without being redispersed (Lucas et al. 1998a and 1998b).

Reasons for these conflicting conclusions may include the use of different DPI devices, differing particle size distributions of SS and/or the influence of mixing procedures within each mixing stage. The findings reported by Zeng et al. (1996) were based on the deaggregation of SS (VMD = 6.6 μm) from the Rotahaler®. At both the experimentally employed flow rates (60 and 90 litres min^{-1}) a large percentage of the drug particles even if liberated from the carrier surface would not be able to penetrate to the lower stage of the Apparatus A (BP, 1998). Coupled with the poor deaggregating capabilities of the Rotahaler® (Vidgren, 1988b), Zeng's (1996) conclusions regarding the importance of mixing order are questionable.

Lucas et al. (1998b) used a sample of SS with a different particle size distribution (VMD 2.2 μm), assessed the *in-vitro* aerosol performance by discharging the formulations from the Diskhaler®.

The performance modifying effects of FPL are most likely due to a combination of the two mechanisms previously discussed.

Based on the theory proposed by Staniforth and Lord (1996), the liberation of drug particles from the carrier surface would be expected to be maximised for blend B. However, in the present study, the incorporation of FPL (5% $^{w}/_{w}$ of the coarse carrier system) irrespective of the mixing order had no significant effect on the aerosol performance of the powder systems. This again supports the theory that the interparticle forces dictating the aerosol performance of NST are the cohesive interactions binding the drug aggregates (existing independently from the carrier or as multi-particle layers) and not the adhesive interactions operating between the drug and carrier.

Blend D would in theory present the greatest opportunity to physically disrupt the drug/drug cohesive interactions. No significant differences were observed, presumably because the mixing procedure failed to efficiently deaggregate the drug agglomerates and/or the concentration of FPL was insufficient to produce a functional effect.

Therefore, based on the proposed requirement to physically disrupt the drug aggregates, alternative carrier systems were investigated in conjunction with mixing procedures considered to produce varying degrees of shear.

4.4 Alternative Lactose Carrier Systems

4.4.1 Materials and Methods

Mixtures were prepared by initially hand blending 40% $^{w}/_{w}$ NST with a 60% $^{w}/_{w}$ carrier system comprising different ratios of a coarse (63-90 μm) and a finer sieve size fraction (<45 μm) of lactose. All components were HB in one stage for 15 minutes according to the procedures described in section 2.2.3. Four blends (10 g) were prepared containing increasing concentrations of the <45 μm sieve size fraction of lactose (table 4.13). The first and final mixes in the series were binary blends containing 40% $^{w}/_{w}$ NST blended with either coarse carrier (63-90 μm) or fine carrier (<45 μm) lactose respectively.

A binary blend containing 60% $^{w}/_{w}$ FPL as the carrier system was then prepared using the same blending procedure.

The RBB and TTM were then used to prepare the binary blends (10 g) containing the 60 % $^{w}/_{w}$ FPL carrier system following the procedures described in section 2.2.3. The blends were mixed in the RBB for 2 minutes or the TTM for 10 minutes.

All blends were prepared and analysed in duplicate except the formulations containing 20 and 40 % $^{w}/_{w}$ of the <45 μm lactose sieve size fraction. Since the data appeared to be following a predictable trend, these formulations were prepared and analysed just the once.

4.4.2 Results and Discussion

Table 4.13 summarises the drug content uniformity data for the different lactose carrier systems blended as described in the previous section.

The drug homogeneity throughout the powder systems was satisfactory for all the formulation and blending procedures (CV ≤4.1%). The drug content uniformity data also suggests that the HB and RBB mixing procedures produce an improved distribution of NST within the powder systems (CV <2 %) compared with the TTM (CV >3%).

The Effects of Carrier Particle Size on the In-vitro Aerosol Performance of NST

Table 4.14 details the *in-vitro* aerosol performance of the 40% $^{w}/_{w}$ NST formulations blended with different carrier systems of 63-90 μm and <45μm sieve fractions.

One way analysis of variance in conjunction with Fisher's pairwise comparisons revealed that the hand blended formulations containing different lactose carrier sieve fractions (63-90 μm and <45 μm) showed a significant difference in their aerosol performance. There was a significant difference in the ED for the hand blended formulations ($F = 22.60$, $p < 0.001$). Fisher's pairwise comparisons revealed that increasing the concentration of the <45 μm sieve size fraction tended to reduce the mass of NST leaving the device/capsule system. These results are in agreement with Byron (1990) who concluded that a compromise must be made between coarse carriers that flow and empty efficiently and finer carriers that deliver an increased fraction of potentially respirable particles.

Lactose Carrier System (% $^{w}/_{w}$ of Total Powder System)			Blending Technique	Content Uniformity			
				Run 1		Run 2	
63-90 μm	<45 μm	FPL		Mean (mg)	CV (%)	Mean (mg)	CV (%)
60	0	0	HB	7.76	1.22	7.90	1.34
40	20	0	HB	7.87	1.04	Not Determined	
20	40	0	HB	7.63	1.13	Not Determined	
0	60	0	HB	7.69	1.12	7.92	1.28
0	0	60	HB	7.99	1.35	8.12	1.05
0	0	60	TTM	8.35	3.10	8.22	4.12
0	0	60	RBB	7.96	1.35	8.10	1.90

Table 4.13 Content uniformity data for NST (40% $^{w}/_{w}$) blended with different lactose carrier systems using various mixing techniques (n = 10 x 20 mg).

In-vitro Aerosol Characterisation	Lactose Carrier System					
	<45 μm (0%) 63-90 μm (60%)		<45 μm (20%) 63-90 μm (40%)	<45 μm (40%) 63-90 μm (20%)	<45 μm (60%) 63-90 μm (0%)	
	Formulation 1	Formulation 2	Formulation 1	Formulation 1	Formulation 1	Formulation 2
% Capsule & Device	14.9 ± 0.81	10.2 ± 1.7	16.8 ± 1.7	15.2 ± 1.5	21.0 ± 2.5	21.2 ± 1.6
% Stage 1	77.4 ± 1.2	83.1 ± 1.8	74.8 ± 2.4	69.2 ± 2.0	61.4 ± 2.6	62.8 ± 2.7
% Stage 2	7.70 ± 0.66	6.77 ± 0.14	8.38 ± 1.0	15.6 ± 1.6	17.6 ± 0.76	16.0 ± 1.8
Emitted Dose (%)	85.1 ± 0.81	89.8 ± 1.7	83.2 ± 1.7	84.8 ± 1.5	79.0 ± 2.5	78.8 ± 1.6
Emitted Dose (mg)	6.47 ± 0.20	7.01 ± 0.21	6.40 ± 0.08	6.31 ± 0.14	5.97 ± 0.22	6.05 ± 0.099
FPF (%)	9.05 ± 0.79	7.54 ± 0.26	10.1 ± 1.3	18.4 ± 1.9	22.3 ± 1.2	20.3 ± 2.4
Fine Particle Dose (mg)	0.585 ± 0.053	0.529 ± 0.020	0.645 ± 0.082	1.16 ± 0.11	1.38 ± 0.065	1.23 ± 0.13
% Drug Recovery	96.8 ± 2.2	99.4 ± 2.0	97.8 ± 0.95	97.5 ± 0.91	98.2 ± 0.88	97.0 ± 0.71

Table 4.14 *In-vitro* aerosol characterisation of NST (40% $^{w}/_{w}$) hand blended with different lactose carrier systems.

Values are the mean ± SD of 5 determinations.

The ED and FPD were normalised with respect to a 20 mg capsule fill weight.

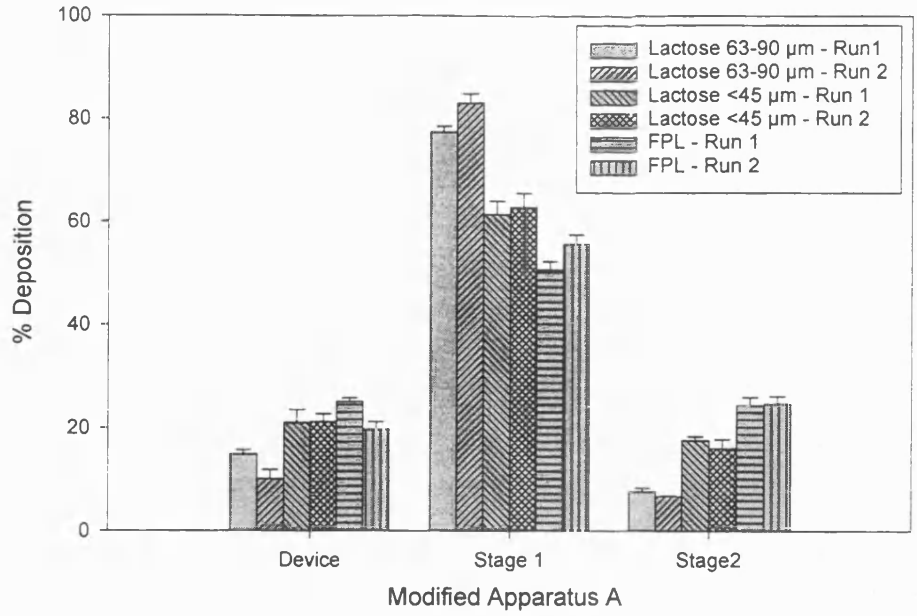

Figure 4.23 The effects of the carrier system on the in-vitro aerosol performance of NST (40% $^{w}/_{w}$).

Each column shows the mean of 5 determinations (bars represent SDs).

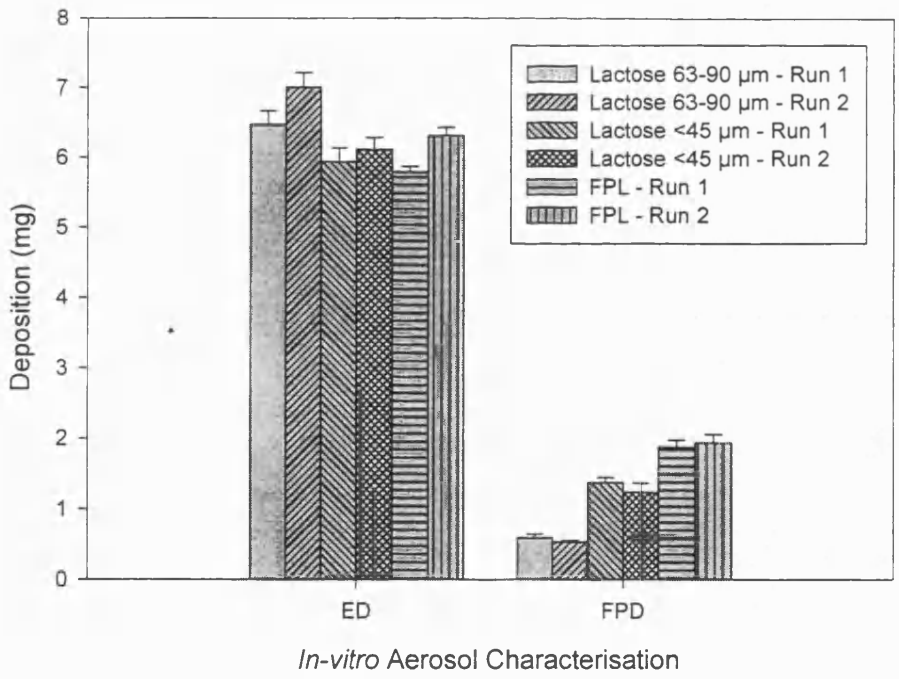

Figure 4.24 The effects of the carrier system on the *in-vitro* aerosol performance of NST (40% $^{w}/_{w}$).

Each column shows the mean of 5 determinations (bars represent SDs).

One way analysis of variance followed by Fisher's pairwise comparisons revealed that increasing the concentration (% $^{w}/_{w}$) of the <45 μm fraction significantly improved the deaggregation (FPF) ($F = 108.13$, $p < 0.001$) and subsequent stage-2 deposition of NST (FPD) ($F = 88.3$, $P < 0.001$). On addition of 40% $^{w}/_{w}$ of the <45 μm size fraction, there was a dramatic improvement in both the deaggregation and subsequent stage-2 drug deposition. The FPF of the systems containing the FPL displayed the greatest improvement in the deaggregation of emitted drug: >30% compared with <10% for the 63-90 μm carrier systems. This improved deaggregation for the FPL system, despite greater device retention, translated into an improved FPD: ≥ 1.89 mg compared with < 0.6 mg for the 63-90 μm carrier system.

The Effects of Blending Procedures on the In-vitro Aerosol Performance of NST

Table 4.15 and figures 4.25 and 4.26 summarise the *in-vitro* aerosol performance of the 40% $^{w}/_{w}$ NST / 60% $^{w}/_{w}$ FPL formulations prepared using the three different blending techniques.

One way analysis of variance revealed a significant difference in the ED for the powder systems prepared using the three different mixing procedures ($F = 56.73$, $p < 0.001$). Fisher's pairwise comparisons revealed that the powder systems prepared using the TTM displayed a greater ED compared with the blends prepared by HB or using the RBB. This may be due to: a) aggregation of the system or b) a decrease in the deaggregation of the formulation, with a subsequent decrease in the generation of discrete particles.

One way analysis of variance revealed a significant difference in the deaggregation (FPF) ($F = 43.69$, $p < 0.001$) and subsequent stage-2 deposition of NST (FPD) $F = 12.55$, $p < 0.001$). Fisher's pairwise comparisons revealed that there was a significant increase in the FPF following the order, RBB>HB>TTM. The mixing techniques were arbitrarily assigned as producing low, medium and high shear forces. Based on these assignments, it would appear that increasing the shear forces generated in the mixing process significantly improves drug particle deaggregation. However, the improved deaggregation of the NST only transfers into a significant improvement in the FPD for the systems prepared using the RBB since the more complete regeneration of fine particles of NST also increased the percentage of NST retained on the device walls, i.e. the formulations prepared by HB showed a decreased ED.

Lord (1993) investigated the performance modifying effects of multi-component lactose carrier systems with regards to the aerosol performance of SS. Although in the high dose NST investigations, the greatest improvement in the deaggregation of the drug system was achieved by reducing the particle size of the carrier material, further formulatory investigations could study the interactions/deaggregation mechanisms operating within alternative bi-component carrier systems. It is suggested that the addition of a far coarser carrier component (e.g. sieve size fraction > 355 μm) to the FPL/NST powder system may improve both the emptying and deaggregation of the powder system. The coarser carrier component may aid powder flow and fluidisation (Lord, 1993) and may even improve the deaggregation of the drug system by colliding with the NST/FPL fraction upon aerosolisation.

In-vitro Aerosol characterisation	Turbulent Tumbling Mixer		Hand Blended		Rotary Bladed Blender	
	Formulation 1	Formulation 2	Formulation 1	Formulation 2	Formulation 1	Formulation 2
% Capsule & Device	16.2 ± 1.1	17.9 ± 2.8	25.0 ± 0.76	19.7 ± 1.5	30.2 ± 2.5	24.9 ±. 1.3
% Stage 1	62.3 ± 3.1	61.5 ± 3.3	50.6 ± 1.7	55.7 ± 1.7	43.3 ± 1.9	45.7 ± 0.43
% Stage 2	21.6 ± 2.0	20.6 ± 1.1	24.3 ± 1.6	24.6 ± 1.5	26.6 ± 1.9	29.4 ± 1.4
Emitted Dose (%)	83.8 ± 1.1	82.1 ± 2.8	75.0 ± 0.76	80.3 ± 1.5	69.8 ± 2.5	75.1 ± 1.3
Emitted Dose (mg)	7.12 ± 0.068	6.92 ± 0.26	5.80 ± 0.067	6.35 ± 0.15	5.69 ± 0.30	5.87 ± 0.088
Fine Particle Fraction (%)	25.8 ± 2.7	25.1 ± 1.8	32.5 ± 2.1	30.6 ± 1.7	38.0 ± 2.1	39.1 ± 1.3
Fine Particle Dose (mg)	1.83 ± 0.19	1.73 ± 0.081	1.89 ± 0.12	1.95 ± 0.13	2.16 ± 0.16	2.30 ± 0.10
% Drug Recovery	102 ± 1.5	103 ± 1.13	97.3 ± 1.0	97.4 ± 1.5	97.5 ± 1.46	98.2 ± 1.7

Table 4.15 The *in-vitro* aerosol characterisation of NST (40% $^{w}/_{w}$) blended with a FPL carrier system using different blending techniques. Values are the mean ± SD of 5 determinations.

ED and FPD were normalised with respect to a 20 mg capsule fill weight.

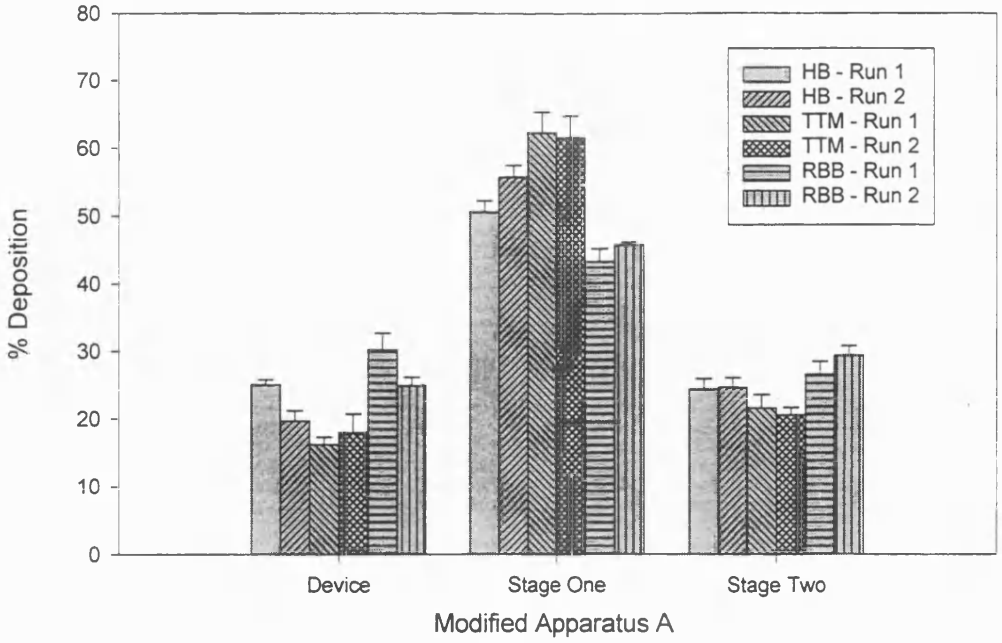

Figure 4.25 The effects of mixing technique on the in-vitro aerosol performance of a 40% $^{w}/_{w}$ / 60% $^{w}/_{w}$ FPL binary system.
Each column shows the mean of 5 determinations (bars represent SDs).

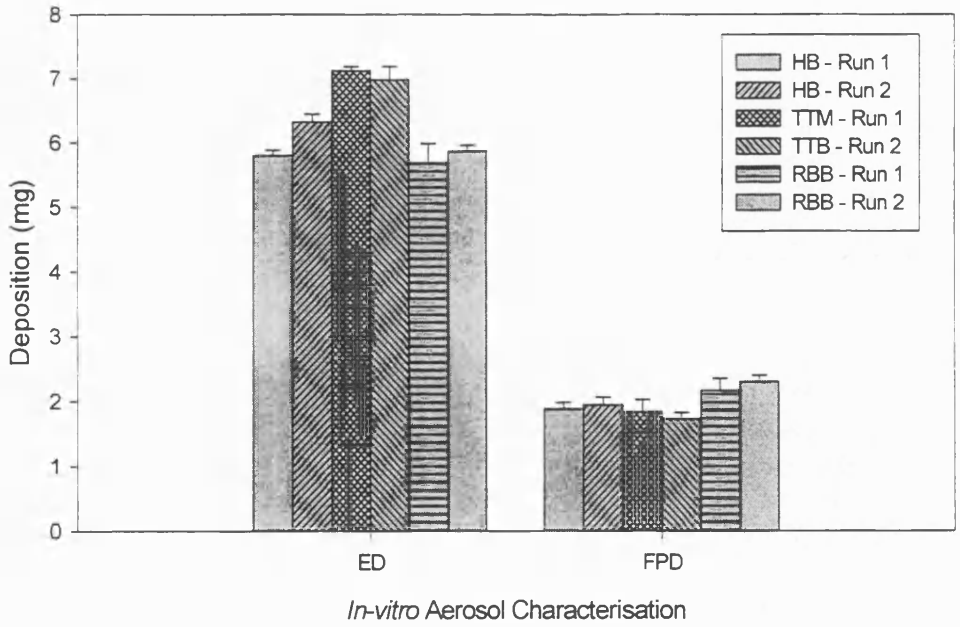

Figure 4.26 The effects of mixing technique on the *in-vitro* aerosol performance of a 40% $^{w}/_{w}$ NST / 60% $^{w}/_{w}$ FPL binary system.
Each column shows the mean of 5 determinations (bars represent SDs).

4.5 General Discussion

Unlike other systems (Kassem, 1990), it would appear that the interparticle forces governing the aerosol performance of high dose NST powder formulations are the cohesive interactions acting between the drug particles, a situation also reported for budesonide (Steckel and Muller, 1997b).

The dispersion of NST in high dose formulations is highly dependent on the particle size of the carrier material, a conclusion also reported by Braun et al. (1996) when investigating the aerosol performance of DSCG containing formulations discharged from the Microhaler®.

A reduction in the carrier particle size has also been reported to improve the *in-vitro* FPF of several low dose drug formulations including, SS from the Rotahaler® (Ganderton and Kassem, 1992; Lord 1993), budesonide from the Spinhaler®, (Steckel and Muller, 1997b). Kassem (1990) studied the *in-vitro* deposition of SS formulated with one of five sieve size fractions of lactose (<10 to 125-180 μm) at flow rates up to 200 litres min^{-1}. It was suggested that the improved FPF of SS was due to the smaller carrier particles being subjected to more intense perturbations in the turbulent airstream, dislodging drug particles more completely (Kassem and Ganderton, 1989). Another possible explanation is that the surface roughness is more pronounced in coarser carrier particles (Kassem and Ganderton, 1989).

The work of Lord (1993) also attributed the improved fine particle deposition of SS to the number of binding sites present on the lactose carrier surface. As the particle size

increases, the degree of surface roughness increases due to the greater number of crystal imperfections and inter-crystal porosity therefore, an increased number of strong binding sites (Lord, 1993).

However, with high dose NST systems, the interparticle interactions governing the aerosol performance of the powder formulation would appear to be the cohesive forces binding the drug particles. Therefore, it is suggested that the carrier particles are behaving as "spacers", exacting their performance modifying effects by physically disrupting the drug/drug interparticle interactions, reducing the number and strength of cohesive interactions.

By decreasing the excipient particle size and/or subjecting the powder systems to greater shear forces, the performance of NST as an aerosol system, in terms of more efficient regeneration of discrete drug particles can be improved. Both these formulatory strategies would be expected to increase the intercalation of FPL within the drug self- agglomerates (figure 4.27).

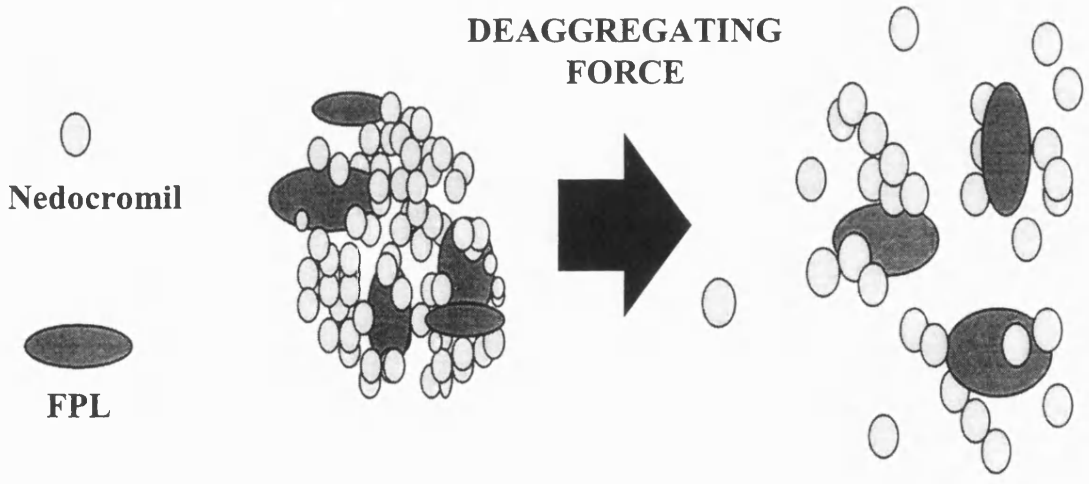

Figure 4.27 Intercalation of FPL within the self-agglomerated drug system.

CHAPTER 5

FINE PARTICLE LACTOSE CARRIER SYSTEMS

5.1 NST/FPL Powder Systems

The effect of an increased mixing time (RBB) on the *in-vitro* aerosol performance of the binary systems was initially investigated to provide further information on the performance modifying effects of FPL in high dose NST systems.

5.1.1 The Effects of an Increased Mixing Time (RBB) on the Aerosol Performance of the NST/FPL Powder Systems

Materials and Methods

The binary powder systems (40% $^{w}/_{w}$ NST / 60% $^{w}/_{w}$ FPL) (10 g) were mixed for fixed time periods as described in section 2.2.3, assessing the drug content uniformity (section 2.2.4) and *in-vitro* aerosol performance (section 2.5.1) of the formulations throughout the mixing process. The powder blends were prepared and analysed in duplicate.

Results and Discussion

Table 5.1 summarises the drug content uniformity information and data for the binary blends after fixed mixing times in the RBB.

After only 2 minutes of mixing, the mean drug content and uniformity of drug within the blend suggest that an acceptable mix has formed (CV <2 %). Increasing the mixing time does not appear to have any dramatic effect on the mean drug content nor the content uniformity.

Mixing Time in the RBB (minutes)	Drug Content Uniformity			
	Run 1		Run 2	
	Mean (mg)	CV (%)	Mean (mg)	CV (%)
2	7.81	0.47	7.96	1.33
4	8.04	0.62	7.89	0.40
8	7.97	0.49	7.90	1.33
16	8.05	1.00	8.14	0.58
24	8.14	2.22	8.07	2.98
32	7.95	0.52	7.88	1.73

Table 5.1 Effects of mixing time (RBB) on the drug content uniformity of the 40% $^{w}/_{w}$ NST and 60% $^{w}/_{w}$ FPL powder system (n = 10 x 20 mg).

Tables 5.2 and 5.3 and figures 5.1 and 5.2 summarise the *in-vitro* aerosol performance of the powder systems after fixed mixing times (RBB).

One way analysis of variance indicated a significant difference in the deaggregation (FPF) ($F = 34.56$, $p < 0.001$) and subsequent stage-2 drug deposition (FPD) ($F = 29.90$, $p < 0.001$) for the formulations blended (RBB) for increased time periods. Fisher's pairwise comparisons revealed that both the FPD and FPF increased significantly after each mixing stage up to 8 minutes mixing time. A further significant increase occurred following 24 minutes of mixing. However, after 32 minutes the powder formulations showed a decrease in drug deaggregation and lower stage deposition (Fisher's pairwise comparisons).

In-vitro Aerosol Characterisation	2 minutes		4 minutes		8 minutes	
	Formulation 1	Formulation 2	Formulation 1	Formulation 2	Formulation 1	Formulation 2
% Capsule & Device	24.5 ± 1.4	26.2 ± 1.8	24.9 ± 2.0	28.0 ± 2.9	20.2 ± 3.0	21.7 ± 2.0
% Stage 1	46.7 ± 2.0	46.7 ± 1.9	40.3 ± 2.8	40.6 ± 2.9	39.5 ± 2.7	38.7 ± 1.9
% Stage 2	28.8 ± 1.9	27.1 ± 1.5	34.8 ± 2.0	31.4 ± 3.2	40.3 ± 1.3	39.7 ± 1.8
Emitted Dose (%)	75.5 ± 1.4	73.8 ± 1.8	75.1 ± 2.0	72.0 ± 2.9	79.8 ± 3.0	78.4 ± 2.0
Emitted Dose (mg)	5.83 ± 0.063	5.64 ± 0.12	5.86 ± 0.22	5.63 ± 0.20	6.16 ± 0.18	6.01 ± 0.093
Fine Particle Fraction (%)	38.2 ± 2.3	36.7 ± 2.0	46.4 ± 2.9	43.6 ± 3.8	50.5 ± 1.8	50.7 ± 2.0
Fine particle Dose (mg)	2.23 ± 0.16	2.07 ± 0.12	2.71 ± 0.17	2.45 ± 0.24	3.11 ± 0.080	3.04 ± 0.14
% Drug Recovery	98.9 ± 1.4	97.8 ± 0.89	98.7 ± 1.8	97.3 ± 0.67	96.9 ± 0.84	97.1 ± 2.2

Table 5.2 Effect of mixing time on the *in-vitro* aerosol characterisation of NST (40% $^{w}/_{w}$) blended with FPL.

Values are mean ± SD of 5 determinations.

ED and FPD were normalised with respect to a 20 mg powder fill weight.

In-vitro Aerosol Characterisation	16 minutes		24 minutes		32 minutes	
	Formulation 1	Formulation 2	Formulation 1	Formulation 2	Formulation 1	Formulation 2
% Capsule & Device	18.8 ± 2.5	21.3 ± 1.5	20.5 ± 0.54	25.0 ± 2.6	27.1 ± 2.3	26.8 ± 3.5
% Stage 1	40.4 ± 2.7	36.4 ± 2.3	36.6 ± 2.5	33.3 ± 2.2	33.3 ± 0.79	34.2 ± 1.5
% Stage 2	40.8 ± 3.4	42.4 ± 3.1	42.9 ± 2.1	41.7 ± 2.0	39.7 ± 2.9	39.0 ± 3.8
Emitted Dose (%)	81.2 ± 2.5	78.8 ± 1.5	79.5 ± 0.54	75.0 ± 2.6	72.9 ± 2.3	73.2 ± 3.5
Emitted Dose (mg)	6.33 ± 0.13	6.15 ± 0.20	6.26 ± 0.13	5.86 ± 0.18	5.73 ± 0.24	5.60 ± 0.24
Fine Particle Fraction (%)	50.3 ± 3.6	53.7 ± 3.3	54.0 ± 2.9	55.6 ± 2.2	54.4 ± 2.3	53.2 ± 3.2
Fine Particle Dose (mg)	3.18 ± 0.25	3.31 ± 0.29	3.38 ± 0.12	3.26 ± 0.14	3.12 ± 0.26	2.98 ± 0.28
% Drug Recovery	96.7 ± 0.35	97.5 ± 0.90	97.4 ± 1.1	96.9 ± 1.7	98.8 ± 1.0	97.1 ± 1.1

Table 5.3 Effect of mixing time on the *in-vitro* aerosol characterisation of NST (40% $^{w}/_{w}$) blended with FPL.

Values are mean ± SD of 5 determinations.

ED and FPD were normalised with respect to a 20 mg powder fill weight.

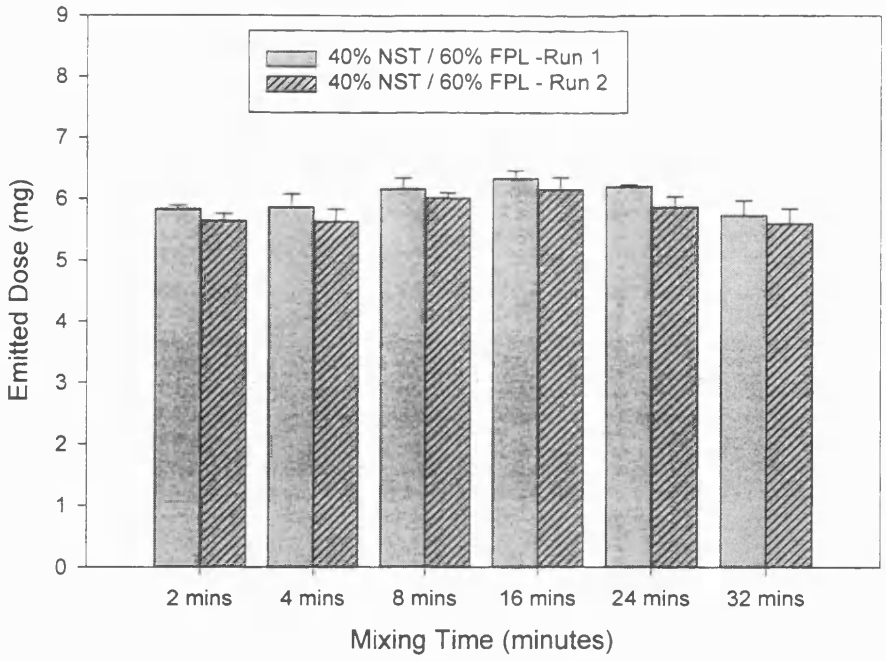

Figure 5.1 Effects of mixing time (RBB) on the emitted dose.
Bars represent the mean + SD of 5 determinations.

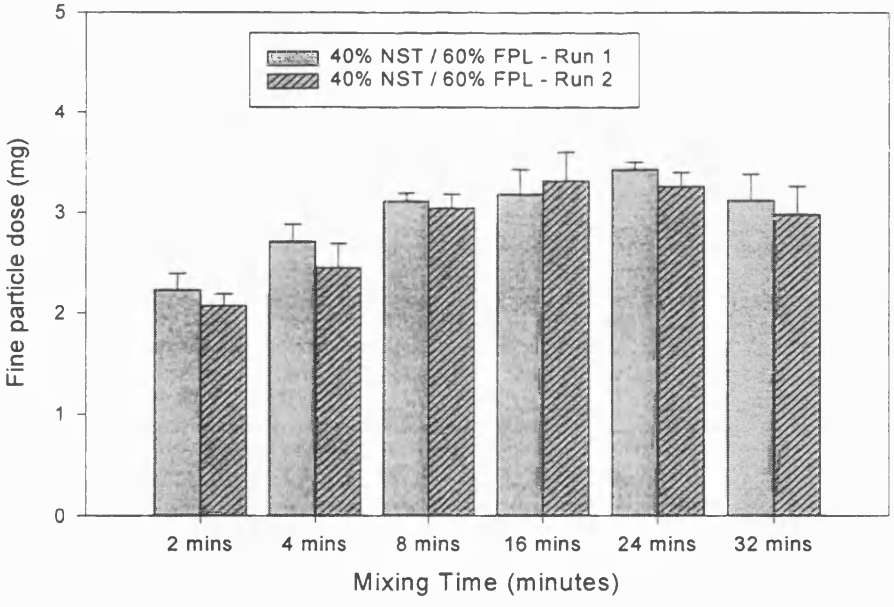

Figure 5.2 Effects of mixing time (RBB) on the fine particle dose.
Bars represent the mean +SD of 5 determinations.

Increasing the mixing time presumably increases the opportunity for intercalation of FPL within the drug self-agglomerates. The increased intercalation improves the deaggregation and subsequent *in-vitro* deposition of discrete or potentially respirable drug agglomerates as indicated by the increase in the FPF and FPD.

It is recognised that the assignment of shear forces to the three blending procedures was purely arbitrary. However, future experimental work may make use of the single vessel processor (SVP) developed by Kay et al. (1999) at the University of Bath. Comparable results have been obtained with the SVP under controlled operating conditions with respect to the drug homogeneity and aerosol performance of an optimised NST/FPL powder system (Kay et al. 1998). The FPF of NST (assessed as described in section 2.5.1) reached a maximum after a process time of 5 minutes. However, following extended mixing times, the FPF was again found to decrease. This may be due to particles of NST adhering to higher energy binding sites on the FPL.

The SVP was operated under controlled processing conditions however, by varying the pressure of the fluidising air, the SVP has the capability of controlling and quantifying the shear forces used to mix the binary powder systems (Kay et al. 1999).

5.1.2 LTSEM and EDAX Investigations

Materials and Methods

Representative samples of the FPL/NST powder system, mixed using the RBB for 8 minutes, were analysed using the technique of LTSEM (section 3.2.2). To distinguish between the two fine particle components, EDAX in conjunction with LTSEM was employed (section 3.2.4). Spot analysis of pure NST and FPL powder samples confirmed that the particles could be differentiated by the presence (NST) or absence (FPL) of a sodium signal (section 3.3.4).

Results and Discussion

LTSEM electron micrographs of the NST/FPL powder systems are depicted in figures 5.3 and 5.4. Figure 5.3 depicts a fine lactose particle (particle size ~5 μm) disrupting the NST self-agglomerates. The cracks and fissures present on the surface of the FPL particle are due to electron beam damage. Identification of the two component particles on a purely visual basis is scientifically unwise due to an overlap in their particle size distributions (section 2.3.1). Therefore, EDAX was employed in conjunction with LTSEM to chemically differentiate the particles. Spot analysis was used to focus on specific locations within the powder sample and ascertain whether or not a sodium signal was generated.

Figure 5.5 is an example of LTSEM characterisation with EDAX spot analysis of the binary powder system. The intercalation of FPL within the agglomerated drug system is supported by LTSEM and EDAX analysis.

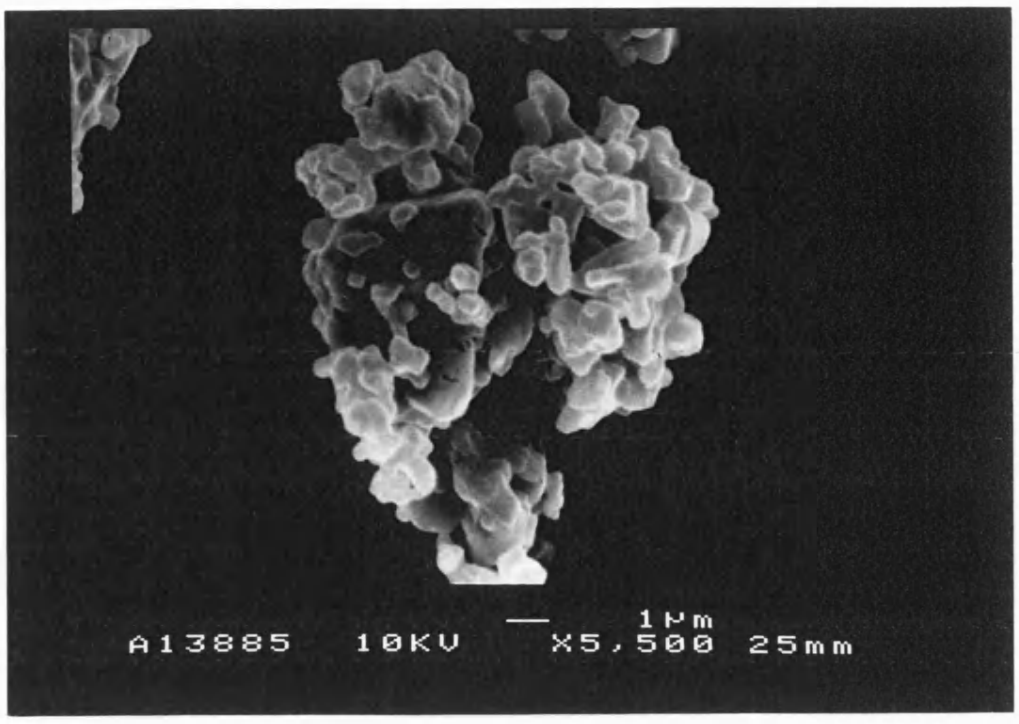

Figure 5.3 LTSEM electron micrograph of 40% $^{w}/_{w}$ NST blended with FPL in the RBB for 8 minutes.

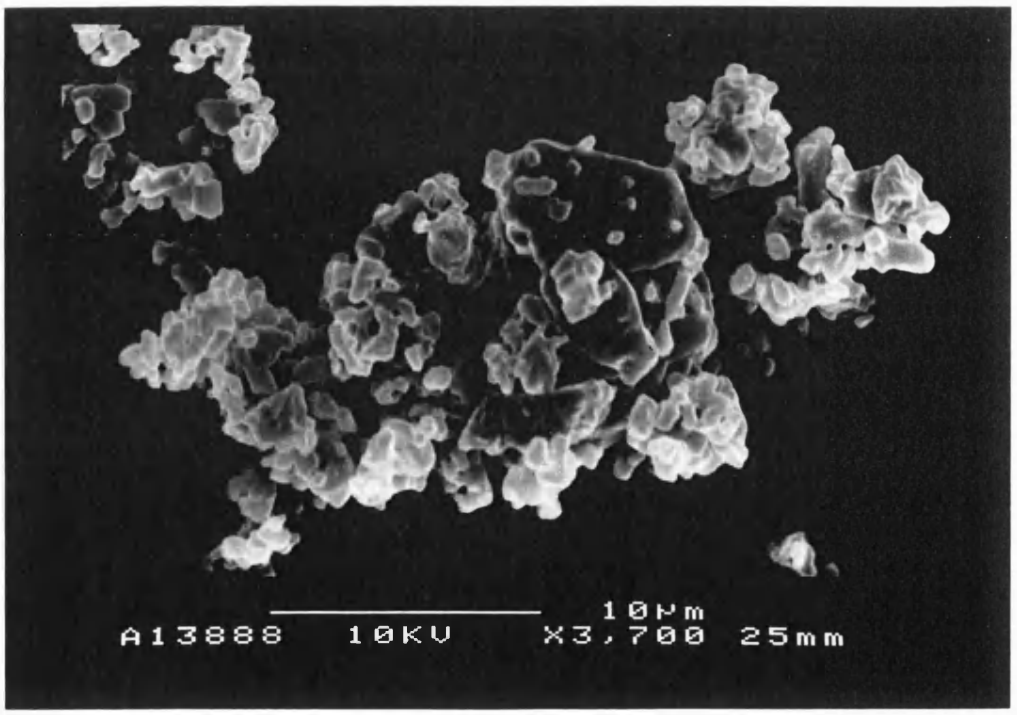

Figure 5.4 LTSEM electron micrograph of 40% $^{w}/_{w}$ NST blended with FPL in the RBB for 8 minutes.

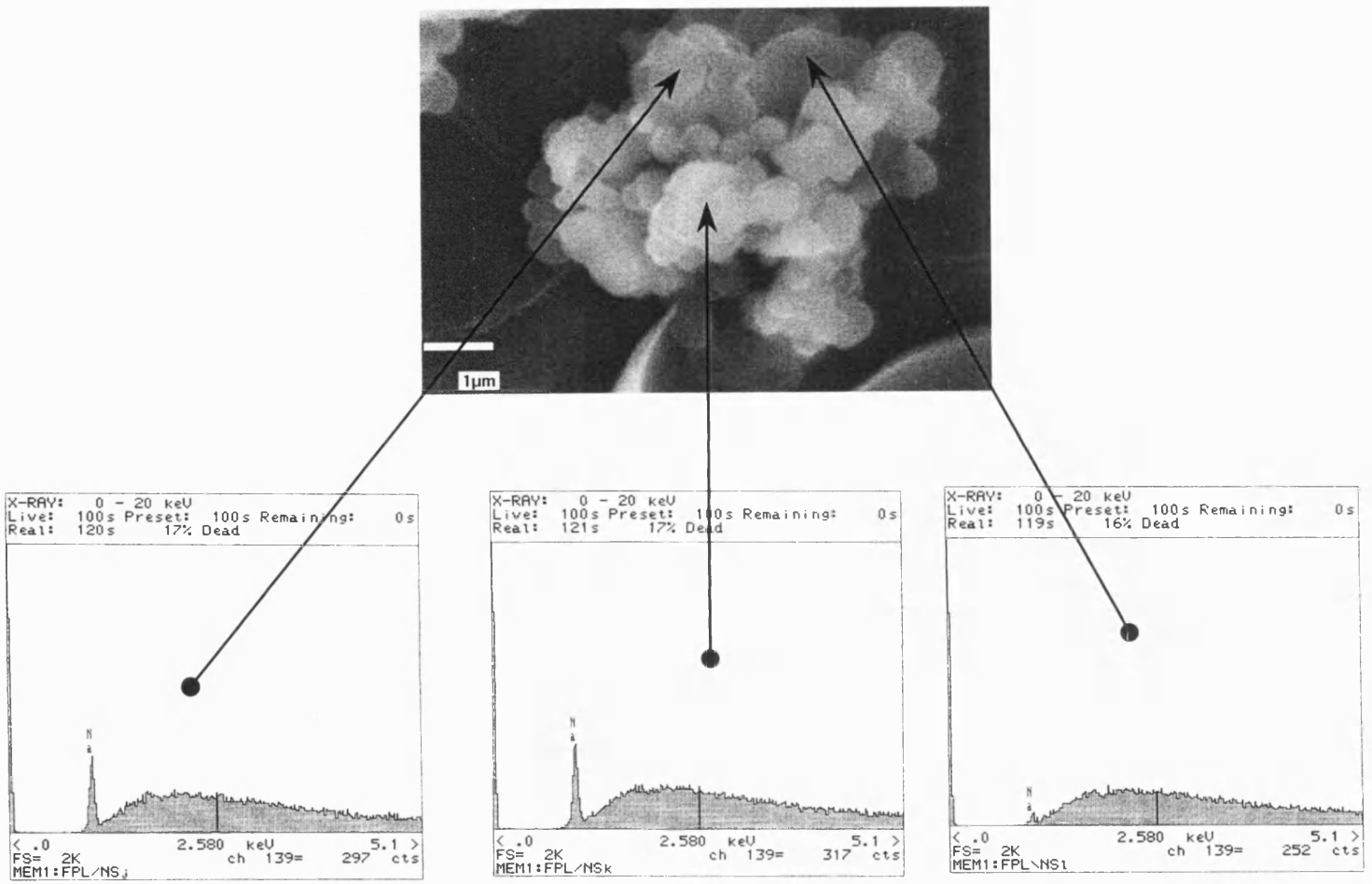

Figure 5.5 LTSEM and EDAX spot analysis of the 40% NST / 60% FPL binary powder system.

5.2 The *In-vitro* Aerosol Performance of FPL

Materials and Methods

The preparation and storage of the glycine-NaOH buffer, methylamine and sodium sulphite solutions were described in section 2.4.3.

Stage-1 of the modified Apparatus A was charged with 7 ml of glycine-NaOH buffer.

Stage-2 was charged with 5 ml of both methylamine (5% $^{w}/_{v}$) and sodium sulphite (5% $^{w}/_{v}$) and 15 mls of glycine-NaOH buffer.

Hard gelatin capsules (size 3) were filled with 20 mg of FPL immediately prior to aerosol characterisation and ten capsules subsequently fired into the modified Apparatus A (60 litres min^{-1}) for each determination.

The capsules and devices were rinsed with 40 ml of the glycine-NaOH buffer and then made up to volume (50 ml) with 5 ml of both methylamine (5% $^{w}/_{v}$) and sodium sulphite (5% $^{w}/_{v}$) solution.

The elastomeric throat-piece adapter, the throat and stage-1 were rinsed using the glycine-NaOH buffer into a 200 ml volumetric flask, and made up to volume (200ml) with the buffer. 100 ml of this solution was then added to 20 mls of both methylamine (5% $^{w}/_{w}$) and sodium sulphite (5% $^{w}/_{w}$) and then made up to volume (200 ml) with glycine-NaOH buffer. This procedure produced a 1 in 2 dilution of the stage-1 washing but maintained a buffer : methylamine : sodium sulphite ratio of 8:1:1.

The stage-2 contents were rinsed into a 50 ml volumetric flask using the buffer solution, and made up to volume (50ml). All solutions were then transferred to 25 ml volumetric flasks allowing analysis of FPL to be performed in duplicate for each set of washings.

The water bath was loaded with washings from two experimental runs and a series of standard solutions. Conditions and experimental procedures for colour development and FPL determination were as described in section 2.4.3. Six experimental runs were performed.

Results and Discussion

Table 5.4 and figure 5.6 summarise the *in-vitro* aerosol characterisation of FPL. It would appear that within the FPL carrier based system, approximately 12% of the carrier material would be potentially respirable. When considering the optimised 40% NST / 60% FPL system previously described this equates to approximately 1.4 mg of FPL for a 20 mg capsule fill weight.

Investigations studying the deposition of FPL when formulated with NST were unsuccessful due to the NST interfering with the colour development of the lactose/methylamine reaction.

Due to the extremely low specific absorption coefficient and the poor calibration results (section 2.4.3), the technique was considered only semi-quantitative. It is also recognised that the aerosol performance of FPL in NST/FPL formulations may be influenced either by: a) the NST particles binding to the FPL particles increasing the D_{ae} or b) the NST improving the deaggregation of the FPL.

In-vitro Aerosol Characterisation	Mean ± SD
Capsule + Device (%)	5.75 ± 0.45
Stage 1 (%)	82.7 ± 1.2
Stage 2 (%)	11.6 ± 1.2
Emitted Dose (mg)	18.9 ± 0.17
Emitted Dose (%)	94.3 ± 0.45
Fine Particle Dose (mg)	2.32 ± 0.25
Fine Particle Fraction (%)	12.3 ± 1.3
FPL Recovered (%)	100 ± 3.1

Table 5.4 The *in-vitro* aerosol characterisation of FPL determined by discharging 10 x 20 mg powder samples (n = 6). ED and FPD were normalised with respect to a 20 mg capsule fill weight.

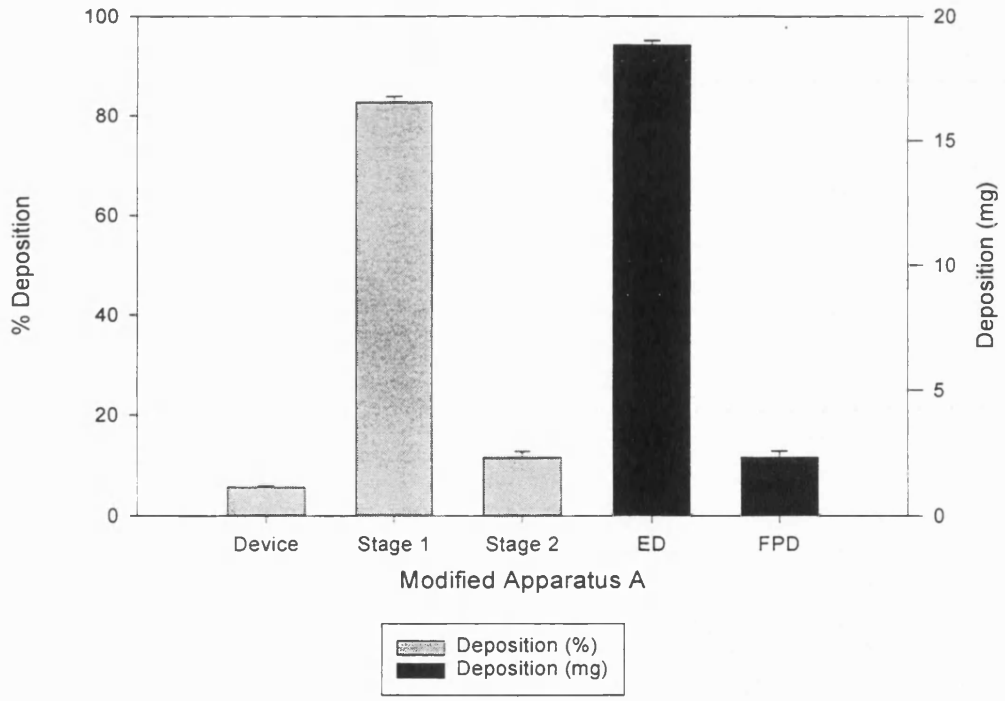

Figure 5.6 *In-vitro* aerosol characterisation of FPL.

Bars represent the mean + SD of 6 determinations.

ED and FPD were normalised with respect to a 20 mg capsule fill weight.

However, the results give an approximate estimation of the potential fine particle deposition of the FPL. Decreasing the particle size of the lactose carrier in the powder formulations is one strategy for improving the FPD of NST. However, this formulation approach will also increase the fraction of lactose likely to reach the lower RT.

5.3 General Discussion

It has been demonstrated that the introduction of FPL can improve the *in-vitro* aerosol performance of NST (section 4.4). By selecting the appropriate size fraction of lactose (FPL) together with an optimised blending protocol (RBB), the deaggregation of the NST (FPF) can be increased from approximately 15% for the pure drug system (section 2.6.2) to >50% for an optimised formulation (section 5.1.1).

It would appear that the excipient particles produce their optimal functional effects when a particle size distribution is selected in conjunction with an appropriate mixing process to promote optimal intercalation of the lactose particles within the drug/drug self agglomerates. Future policies for the formulation of high dose cohesive drug systems (small or large molecules) may include: a) further increasing the shear forces generated during the mixing process, possibly allowing the more complete intercalation of fine excipient material into the aggregated drug system or b) selection of an even finer excipient material.

Figure 5.7 is a diagrammatic representation of the possible interactive system that could be achieved by formulating the NST with an even finer excipient.

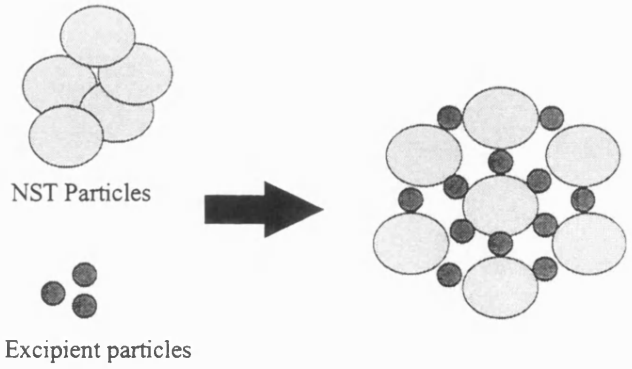

Figure 5.7 Theoretical consideration of a possible future formulation strategy to promote the more complete deaggregation of high dose drug systems.

The effect of these spacer particles would be to decrease the van der Waals attractive forces, forces thought to predominate when considering the interactions dictating the aggregation of the ultrafine NST powder. The fine excipient material may decrease the number of drug/drug contacts and increase the separation distance between neighbouring particles.

However, it is recognised that the excipient material itself would need to be efficiently deaggregated under the shear forces produced in the appropriate mixing process. Toxicological issues would also need addressing since the fine excipient material would be capable of depositing in the deep lung. However, it is conceivable that optimisation of the blending process together with selection of an appropriate "intercalating" material may reduce the required concentration of excipient. Provided that the excipient material selected was fully deaggregated into discrete particles, it is conceivable that a proportion of the material (D_{ae} <1 μm) may be too small to deposit in the deep lung and therefore be exhaled (Zanen et al. 1994).

Surface treatment of the drug particles is an alternative technique to decrease the cohesive interactions operating within a micronised powder system (Fults et al. 1997; Kawashima and Hino, 1996; Kawashima et al. 1998b).

Fults et al. (1997) reported that fatty acid surface-treated DSCG, differed from the non-treated DSCG in particle size, shape and dispersion properties. They concluded that treatment with the fatty acids could improve the FPF of the drug particles either by changing the morphology of the drug particles or altering the extent of interaction between drug particles.

Another possible strategy to reduce the cohesive drug interactions is to encapsulate the drug particles in microspheres, which may provide further benefit by resisting hygroscopic growth within the RT and/or showing sustained release characteristics (El-Basier et al. 1997). El-Basier et al. (1997) prepared and characterised (physicochemical studies) poly(L-lactic acid) microspheres containing either nedocromil sodium or budesonide. They concluded that whilst hydrophobic drugs (budesonide) could be effectively incorporated into the microspheres, hydrophilic drugs (nedocromil sodium) were difficult to entrap.

CHAPTER 6

AGGREGATED POWDER SYSTEMS

6.1 Aggregated NST Powder Systems

The inclusion of coarse carrier particles has been avoided in aerosol formulations of TS (Trofast and Falk, 1996; Wetterlin, 1988) and DSCG (Bell et al. 1971) by the controlled aggregation of fine drug particles into free flowing spheres. The energy driving agglomerate formation is the surface free energy of individual particles; formation of interparticle bonds reduces the exposed surface area and therefore the surface free energy of the system (Adjei and Gupta, 1997). NST exhibits spontaneous aggregation although it is possible to develop more uniform agglomerates by rolling the powder on a metal mesh (spheronisation).

6.1.1 Materials and Methods

The flow properties and *in-vitro* aerosol performance of the aggregated pure drug system were characterised and compared to the non-aggregated drug powder (section 2.6.2).

Approximately 10 grams of NST was screened through a metal sieve (1.4 mm aperture diameter) onto a finer sieve mesh (63 μm aperture) and spheronised by rolling the screened material across the finer mesh for three minutes. The spheres were then size classified by placing the loosely aggregated powder on top of a stack of metal process sieves and gently hand tapping the sieve stack for approximately 1 minute to fractionate the powder sample. More uniform aggregates were produced (visual inspection) by rolling the powder aggregates over the smaller sized mesh of each classification stage for a further five minutes. Four sieve size fractions of aggregates were collected: 212-355, 355-500, 500-710 and 710-1400 μm.

The aerosol performance of the aggregated micronised NST was characterised using the modified Apparatus A. Approximately 8 mg of drug was accurately weighed into a hard gelatin capsule and discharged from the Cyclohaler® at 60 litres min^{-1} (section 2.5.1).

6.1.2 Powder Flow Properties

Materials and Methods

The flow properties of the screened (355 μm) NST powder were compared to the four sieve size fractions of aggregates. The powder flow properties were investigated by evaluating bulk density and angle of repose measurements.

Bulk Density Measurements

Accurately weighed powder was filled into a 50 ml measuring cylinder using a glass funnel. The initial volume was recorded and the cylinder then placed on a jolting volumeter (Type STAV 2003, J Engelsmann GmbH, Ludwigshafen, Germany), which was operated at approximately 4 Hz. The cylinder was tapped until a constant volume was attained (1000 taps). Equations 6.1 and 6.2 were used to determine the Carr's index (CI) (Carr, 1965) and Hausner ratio (HR) (Hausner, 1967) respectively.

Equation 6.1 $$\text{Carr's Index (\%)} = \frac{\text{Tapped Density - Poured Density}}{\text{Tapped Density}} \times 100$$

Equation 6.2 $$\text{Hausner Ratio} = \frac{\text{Tapped Density}}{\text{Poured Density}}$$

The CI defines the type of powder flow as; 5-15% excellent, 12-16% good, 18-21% passable, 23-35% poor, 33-38% very poor and> 40% extremely poor. Values less than 1.25, as defined by the HR, indicate good flow properties whilst values greater than 1.25 suggest poor flow.

Angle of Repose

The "poured" angle of repose (AR) was determined using the method described by Jones and Pilpel (1966). A powder funnel was fixed using a retort stand so that the bottom of the funnel's orifice was 10 cm from the bench surface (covered with paper). The outlet was closed and the funnel carefully filled to the brim with the powder. The powder was then allowed to pour out and the AR determined. The AR defines the type of powder flow as; <25° excellent, 25-30° good, 30-40° passable and >40° very poor (Wells, 1993).

Results and Discussion

Table 6.1 summarises the powder flow measurements obtained by comparing the poured and tapped density and measuring the AR. Results for NST indicate that the micronised powder exhibits very poor flow properties (CI > 36% and AR ~ 40°).

One way analysis of variance followed by Fisher's pairwise comparisons revealed that the aggregated NST systems displayed significantly improved flow properties when compared to the non-aggregated NST ($F = 71.38$; $p < 0.001$). However, only the larger three fractions (≥355-500 μm) exhibit what would be defined as good/excellent flow (AR< 30°). The flow properties of the larger three fractions of aggregated NST are comparable to the coarse lactose sieve fraction (63-90 μm) which is generally added to

aerosol formulations to improve the flow properties of the micronised drug powder (Lucas et al. 1998b).

The CI for the aggregated and non-aggregated systems were in general agreement with AR determinations, indicating that the aggregated sieve fractions showed a significant improvement in flow compared with the non-aggregated powder (ANOVA: $F = 35.48$, $p < 0.001$). Fisher's pairwise comparisons revealed that the aggregated size fraction ≥355-500 μm showed a significant improvement in flow compared with the 212-355 μm fraction. However, the powder flow even for the three larger fractions of aggregates would still be defined as poor using the Carr's index definitions whereas the coarse lactose fraction would again be described as having good flow properties. This was due to the partial break-up of the aggregated system upon consolidation, leading to a greater volume reduction and subsequent greater measured tapped density than would otherwise be expected.

Material	Bulk Density (g cm^{-3})		Carr's Index (%)	Hausner Ratio	Angle of Repose (θ)
	Poured	Tapped			
[A] Micronised NST	0.16 (0.001)	0.25 (0.004)	36.9 (1.4)	1.58 (0.04)	38.1 (1.6)
[A] Aggregated NST (212-355 μm)	0.12 (0.002)	0.17 (0.001)	27.7 (0.60)	1.38 (0.01)	34.7 (2.0)
[A] Aggregated NST (355-500 μm)	0.14 (0.007)	0.17 (0.008)	21.3 (0.57)	1.27 (0.01)	23.6 (1.0)
[A] Aggregated NST (500-710 μm)	0.20 (0.02)	0.25 (0.013)	19.5 (3.9)	1.25 (0.06)	21.4 (1.8)
[A] Aggregated NST (710-1400 μm)	0.16 (0.01)	0.20 (0.003)	23.2 (1.8)	1.30 (0.03)	25.6 (0.04)
[B] Lactose (63-90 μm)	0.70 (0.007)	0.84 (0.000)	16.4 (0.82)	1.20 (0.01)	25.2 (0.76)
[B] Fine Particle Lactose	0.32 (0.006)	0.60 (0.013)	47.1 (0.86)	1.89 (0.03)	[c]test failed

Table 6.1 Powder flow characteristics of non-aggregated NST, aggregated NST and two lactose size fractions. Results are the mean (SD) of three determinations.
[A] Results were obtained using a 50 ml measuring cylinder.
[B] Results were obtained using a 250 ml measuring cylinder.
[c] Test failed: the fine particle lactose would not pour from the funnel.

6.1.3 *In-vitro* Aerosol Characterisation of the Aggregated NST Powder Systems

Table 6.2 and figures 6.1 and 6.2 summarise the *in-vitro* aerosol performance of the aggregated NST systems.

The aerosol performance of the non-aggregated NST sample screened through a 355 μm aperture mesh (section 2.6.2) was compared to that of the aggregated systems. One way analysis of variance revealed a significant difference in the ED ($F = 97.37$, $p < 0.01$), the deaggregation (FPF) ($F = 24.75$, $p < 0.001$) and subsequent stage-2 drug deposition (FPD) ($F = 16.51$, $p < 0.01$) between the aggregated and non-aggregated powder systems. Fisher's pairwise comparisons revealed that the two smaller sized aggregate fractions (212-355 and 355-500 μm) showed a significant improvement in the ED compared with the non-aggregated powder. This may be a result of the aggregated systems being entrained and then aerosolised more efficiently than the non-aggregated powder (Lord and Staniforth, 1996).

Alternatively, the aggregated system may not adhere to the device wall to the same extent as the non-aggregated powder, due to a reduction in the generation of fine particles upon powder aerosolisation. Fisher's pairwise comparisons also revealed that the two larger sieve fractions (500-710 μm and 710-1400 μm) showed a significant decrease in the ED compared with the non-aggregated system, due to incomplete capsule emptying.

The generation of fine particles from both the aggregated and non-aggregated powder systems is dependent on the strength of the interparticle cohesive interactions and the shear forces generated within the device upon aerosolisation (Lord and Staniforth,

1996). The process of spheronisation appeared to increase the cohesive interactions, presumably by decreasing the interparticle separation distance thereby increasing the strength of the van der Waals interactions (Hickey et al. 1994). This was reflected in the significant decrease in the deaggregation (FPF) of the smaller aggregate fractions (≤500 μm) compared with the non-aggregated powder (Fisher's pairwise comparisons).

The significant increase in the deaggregation of the larger aggregate fractions may result from the increased shear forces experienced by the larger systems upon aerosolisation. These increased shear forces may result from more frequent and intense collisions of the larger powder aggregates when delivered from the pierced gelatin capsule. However, the improved FPF of the largest aggregate fraction did not translate into an increase in the FPD since a greater percentage of the aggregate mass was retained within the capsule (~40% of the recovered drug).

An alternative method of assessing the strength of agglomerated powder systems was described by Boerefijn et al. (1998). They described an impact testing technique by which they assessed the strength of weak lactose agglomerates.

In-vitro Aerosol Characterisation	Sieve Size Fraction of NST Aggregates				
	212-355 µm	355-500 µm	500-710 µm	710-1400 µm	non-aggregated
% Capsule	4.18 ± 0.94	6.00 ± 2.4	10.1 ± 3.9	39.9 ± 5.3	2.95 ± 0.31
% Device	15.7 ± 2.9	13.6 ± 0.97	19.9 ± 2.0	15.8 ± 2.7	21.7 ± 1.7
% Stage One	70.3 ± 2.6	71.3 ± 3.0	57.6 ± 4.7	34.6 ± 5.0	63.1 ± 2.4
% Stage Two	9.87 ± 0.64	9.07 ± 0.90	12.5 ± 0.82	9.76 ± 0.90	12.3 ± 1.1
Emitted Dose (mg)	6.47 ± 0.18	6.49 ± 0.19	5.68 ± 0.33	3.54 ± 0.42	6.05 ± 0.17
Emitted Percent (%)	80.1 ± 2.4	80.4 ± 2.2	70.1 ± 4.4	44.3 ± 4.9	75.4 ± 1.6
Fine Particle Dose (mg)	0.796 ± 0.052	0.732 ± 0.072	1.01 ± 0.067	0.780 ± 0.074	0.985 ± 0.083
Fine Particle Fraction (%)	12.3 ± 0.97	11.3 ± 1.4	17.9 ± 1.9	22.2 ± 3.2	16.3 ± 1.7
Drug Recovered (%)	101 ± 2.0	101 ± 0.97	101 ± 0.98	99.9 ± 2.2	100 ± 1.3

Table 6.2 *In-vitro* aerosol characterisation of the non-aggregated (355 µm screened) and aggregated sieve size fractions of NST.
Values are the mean ± SD of 5 determinations
ED and FPD were normalised with respect to an 8 mg capsule fill weight.

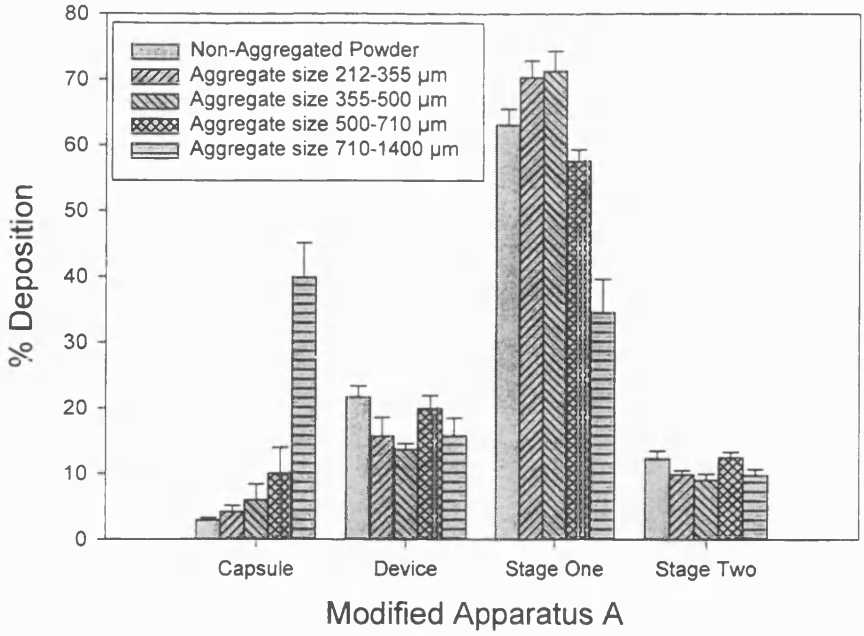

Figure 6.1 *In-vitro* aerosol performance of the size fractions of aggregated NST. Each column shows the mean of 5 determinations (bars represent SDs).

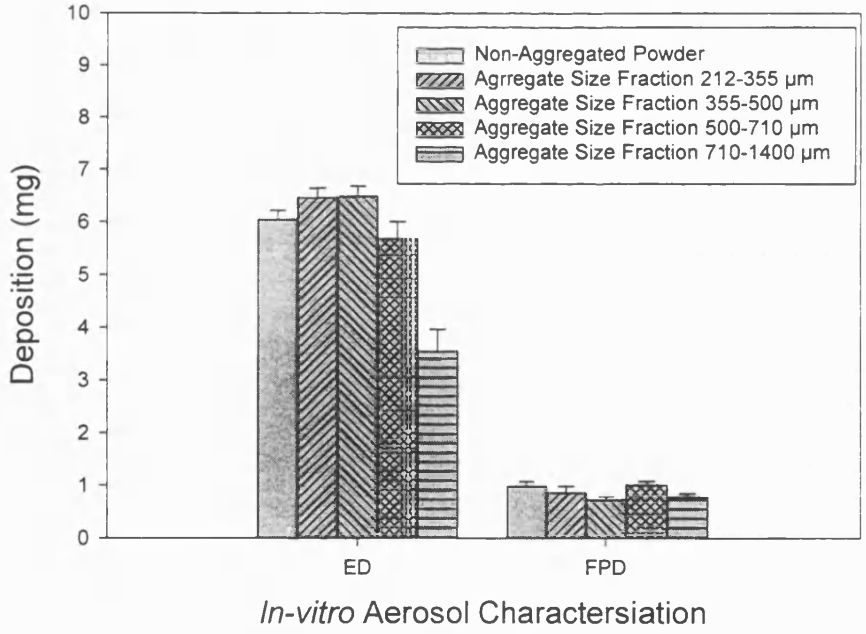

Figure 6.2 *In-vitro* aerosol performance of the size fractions of aggregated NST. Each column shows the mean of 5 determinations (bars represent SDs).

6.2 Aggregated NST/FPL Powder Systems

Although the NST/FPL powder systems (section 5.1.1) displayed improved deaggregation properties when compared to the pure NST (section 2.6.2) and the coarse carrier based systems (section 4.2), the flow properties of the formulations were considered poor (CI > 50%). Therefore, blends of NST and FPL were aggregated in a controlled manner to improve the flowability of the cohesive systems.

Improvements in the *in-vitro* aerosol performance of NST when formulated with FPL have been attributed to the ability of the FPL to intercalate within the NST self-agglomerates, reducing the number and/or strength of the drug/drug interparticle interactions. The process of spheronisation whereby the powder formulations are aggregated into free flowing systems has previously been shown to improve the flow properties of the powder systems (section 6.1). However, the process of aggregation may bring the drug particles into closer proximity, possibly increasing the strength of the cohesive interactions. Therefore, the effects of aggregation on the aerosol performance of the NST/FPL systems were investigated.

6.2.1 Materials and Methods

The binary formulation consisting of 40% $^{w}/_{w}$ NST and 60% $^{w}/_{w}$ FPL was prepared using an optimised mixing procedure (section 5.1.1), blending the two components in the RBB for 8 minutes. The blend was then aggregated as previously described for the pure drug system (section 6.1.1).

Studies were then performed to investigate the possibility of "over spheronising" the powder formulation. The aggregate sieve size fraction (500-710 μm) (10g) was placed in a glass jar with a plastic screw tap and tumbled in the TTM (42 rev. min^{-1}) for 10, 60 and 180 minutes. The TTM had previously been shown to promote self-agglomeration of NST (section 4.2). The 500-710 μm fraction was chosen after consideration of the aerosol performance of all the fractions and the ease of preparation of larger quantities of aggregates.

In-vitro Aerosol Characterisation of the Powder Systems

The content uniformity of the sieve size fractions and the powder systems subjected to the extended tumbling times was investigated (section 2.2.4). The *in-vitro* aerosol performance of the four sieve size fractions was investigated using the modified Apparatus A (section 2.5.1). Subsequent studies assessed the effects of increased aggregation time (TTM) on the aerosol performance of the 500-710 μm fraction.

Microscopic Investigations

The powder systems (aggregated and non-aggregated) were photographed (Photographic Unit, University of Bath, Bath, U.K.). The aggregated powder system was also imaged using the technique of ESEM (3.2.3).

6.2.2 Results and Discussion

In-vitro Aerosol Characterisation

Table 6.3 summarises the drug content uniformity data for the four different sieve size fractions of NST/FPL aggregates. All sieve size fractions displayed an acceptable degree of mixing (CV <1.2 %) and there was no dramatic difference between the mean

drug content for the four size fractions indicating that the aggregation process had not caused any major drug segregation.

Agglomerate Sieve Size Fraction	Drug Content Uniformity	
	Mean (mg)	RSD (%)
212-355 μm	8.07	1.14
355-500 μm	7.88	0.89
500-700 μm	7.88	1.00
710-1400 μm	7.93	1.06

Table 6.3 Content uniformity data for the different sieve size fractions of NST/FPL agglomerates (n = 10 x 20 mg).

Table 6.4 and figures 6.3 and 6.4 summarise the *in-vitro* aerosol performance of the aggregated NST/FPL powder systems.

To investigate the effects of aggregation on the aerosol performance of the NST/FPL powder mixtures, data from the non-aggregated powder formulation (section 5.1.1) was included in the statistical analysis. The Students *t-test* revealed that the repeat formulations (run 1 and 2) for the non-aggregated systems (RBB: 8 minutes) displayed statistical similar aerosol parameters: (ED) $t = 1.65$, $p = 0.14$; (FPD) $t = 0.89$, $p = 0.40$. Therefore, the data from run 1 was incorporated to assess the effects of aggregation.

One way analysis of variance followed by Fisher's pairwise comparisons revealed a significant increase in the ED for the spheronised systems compared with the non-spheronised powder ($F = 2.90$, $p = 0.048$). However, there was no significant difference in the ED for the four sieve size fractions of aggregates. This result is in contrast to data

obtained for the various sieve size fractions of pure drug aggregates where a significant decrease in the ED occurred for the larger size fractions (section 6.1.3). This decrease in ED was attributed to the increased capsule retention for the larger sized aggregates.

The intercalation of FPL within the drug agglomerates has presumably increased the deaggregation of the agglomerates therefore less drug is retained within the capsule.

One way analysis of variance revealed no significant difference in the deaggregation (FPF) ($F = 1.90$, $p = 0.15$) and stage-2 drug deposition (FPD) ($F = 0.80$, $p = 0.54$) for the aggregated and non-aggregated systems. This would suggest that loosely aggregating the NST/FPL formulation did not dramatically affect the cohesive interparticle interactions.

In-vitro Aerosol Characterisation	Non-aggregated (run 1)	Sieve Size Fraction (μm)			
		212-355	355-500	500-710	710-1400
Capsule (%)	Not recorded	1.87 ± 0.09	2.17 ± 0.48	1.94 ± 0.42	2.05 ± 0.31
Device (%)	Not recorded	13.8 ± 0.92	14.3 ± 1.7	15.5 ± 3.0	15.3 ± 2.8
Capsule + Device (%)	20.2 ± 3.0	15.7 ± 0.95	16.5 ± 2.0	17.4 ± 2.7	17.4 ± 3.0
Stage 1 (%)	39.5 ± 2.7	44.3 ± 1.7	42.2 ± 3.1	41.5 ± 1.2	42.7 ± 2.5
Stage 2 (%)	40.3 ± 1.3	40.1 ± 1.7	41.3 ± 1.5	41.1 ± 2.3	39.9 ± 1.2
Percentage Emitted (%)	79.8 ± 3.0	84.3 ± 0.95	83.5 ± 2.0	82.6 ± 2.7	82.6 ± 3.01
Emitted Dose (mg)	6.16 ± 0.18	6.62 ± 0.20	6.42 ± 0.27	6.48 ± 0.16	6.43 ± 0.25
Fine Particle Fraction (%)	50.5 ± 1.8	47.5 ± 2.0	49.5 ± 2.7	49.7 ± 1.5	48.3 ± 1.4
Fine Particle Dose (mg)	3.11 ± 0.08	3.15 ± 0.15	3.17 ± 0.076	3.22 ± 0.17	3.11 ± 0.089
% Drug Recovery	96.9 ± 0.84	97.4 ± 1.9	97.6 ± 1.9	99.6 ± 0.85	98.2 ± 1.7

Table 6.4 The effects of sieve size classification on the *in-vitro* aerosol performance of NST (40% $^{w}/_{w}$) blended with FPL (60% $^{w}/_{w}$) and loosely aggregated.

Results are the mean ± SD of five determinations.

ED and FPD were normalised with respect to a 20 mg capsule fill weight.

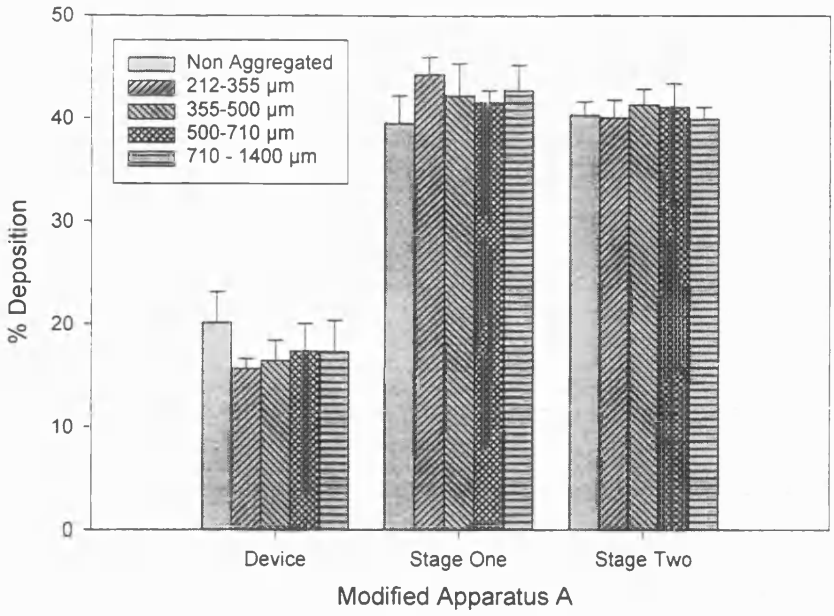

Figure 6.3 The *in-vitro* aerosol performance of the size fractions of the aggregated and non-aggregated NST/FPL systems.
Each column shows the mean of 5 determinations (bars represent SDs).

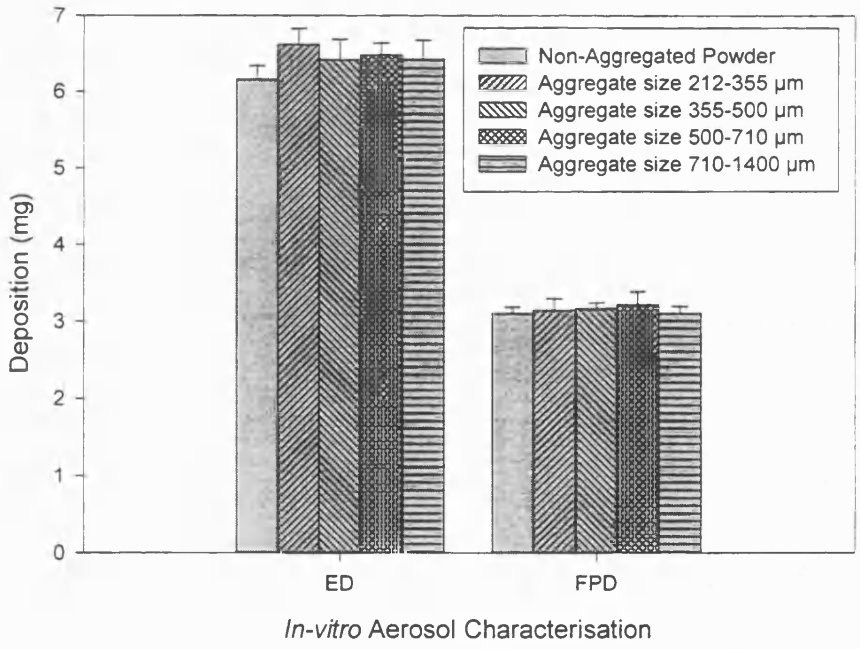

Figure 6.4 The *in-vitro* aerosol performance of the size fractions of the aggregated and non-aggregated NST/FPL systems.
Each column shows the mean of 5 determinations (bars represent SDs).

Increased Tumbling Times

The drug content uniformity data for the 500-710 μm aggregate sieve size fraction following extended tumbling times is summarised in table 6.5. Analysis of the drug content uniformity data revealed an acceptable drug distribution (CV <2 %) for all the powder systems.

The *in-vitro* aerosol performance of the 500-710 μm aggregate sieve size fraction following increased tumbling times is summarised in table 6.6 and figures 6.5 and 6.6.

One way analysis of variance revealed that increasing the tumbling time (TTM) (500-710 μm sieve fraction) had no significant effect on the ED ($F = 0.39$, $p = 0.76$). However, an increased tumbling time significantly decreased the deaggregation (FPF) and subsequent stage-2 drug deposition (FPD) ($F = 45.53$, $p < 0.001$). Fisher's pairwise comparisons revealed that tumbling the mixture for 10 minutes had no significant effect on the FPD however, a significant decrease in both FPF and the FPD occurred after 60 minutes. Since no significant difference is observed in the ED, the decrease in the FPD is a direct result of the decrease in the deaggregation of the powder system, which decreased from an initial value of 49.7 ± 1.5% to 27.1 ± 2.3% after 180 minutes of tumbling.

It is clear that when formulating powders for inhalation as aggregated systems, a compromise must be reached between the robustness of the aggregates and downstream deaggregation. The strength on the interparticle interactions should be such that the aggregates remain intact during down stream processing and device/capsule filling but are deaggregated into discrete particles upon patient inhalation.

Tumbling Time (minutes)	Drug Content Uniformity	
	Mean (mg)	CV (%)
0	7.88	1.00
10	8.01	1.22
60	8.04	0.90
180	8.16	1.86

Table 6.5 The effect of tumbling time on the drug content uniformity of the NST/FPL agglomerates (sieve size fraction = 500-710 μm).

In-vitro Aerosol Characterisation	Tumbling Time (minutes)			
	0	10	60	180
Capsule (%)	1.94 ± 0.42	2.97 ± 1.1	2.67 ± 0.29	5.31 ± 5.2
Device (%)	15.5 ± 3.0	14.2 ± 2.9	16.1 ± 4.4	13.5 ± 2.5
Stage 1 (%)	41.5 ± 1.2	44.6 ± 2.1	53.6 ± 7.9	59.1 ± 2.5
Stage 2 (%)	41.1 ± 2.3	38.2 ± 1.2	27.6 ± 3.8	22.1 ± 2.6
Emitted Dose (%)	82.6 ± 2.7	82.8 ± 2.5	81.3 ± 4.6	81.2 ± 4.0
Emitted Dose (mg)	6.48 ± 0.16	6.48 ± 0.28	6.54 ± 0.39	6.68 ± 0.41
FPF (%)	49.7 ± 1.5	46.2 ± 1.3	34.3 ± 6.3	27.1 ± 2.3
Fine particle Dose (mg)	3.22 ± 0.17	2.99 ± 0.12	2.22 ± 0.30	1.82 ± 0.24
Drug Recovered (%)	99.6 ± 0.85	97.7 ± 1.9	100 ± 0.68	101 ± 1.8

Table 6.6 The effects of extended tumbling times on the *in-vitro* aerosol behaviour of the NST/FPL (500-710 μm) sieve size fraction.
Results are the mean ± SD of five determinations.
ED and FPD were normalised with respect to a 20 mg capsule fill weight.

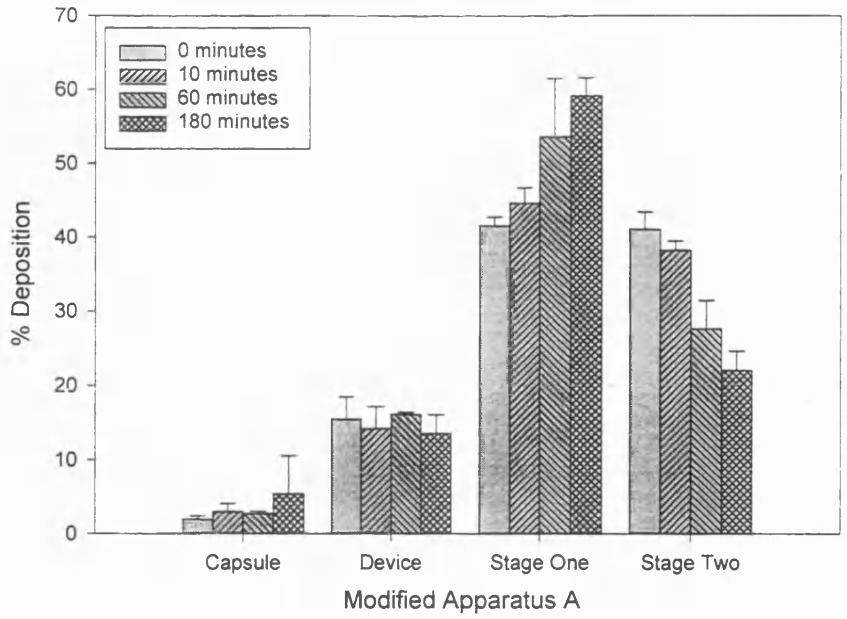

Figure 6.5 Effect of increased aggregation time on the *in vitro* aerosol performance of the 500-710 μm aggregated NST/FPL system.
Each column shows the mean of 5 determinations (bars represent SDs).

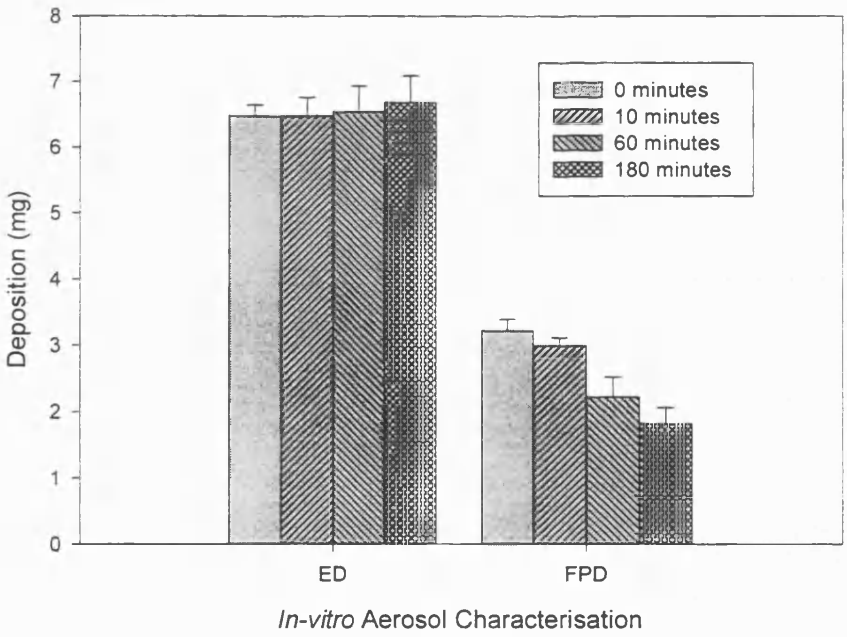

Figure 6.6 Effect of increased aggregation time on the *in vitro* aerosol performance of the 500-710 μm aggregated NST/FPL system.
Each column shows the mean of 5 determinations (bars represent SDs).

Any changes in the size of the aggregated NST/FPL systems during the extended mixing period would have little effect on the aerosol performance since the deaggregation and subsequent stage-2 deposition of the various aggregated sieve size fractions were not statistically different.

It is presumed that increasing the mixing time may increase the van der Waals forces of interaction by decreasing the interparticle distance, increasing the area of interparticle contact and/or causing a transient increase in the electrostatic forces of attraction.

Microscopic Analysis

Figures 6.7 and 6.8 are photographic images of the aggregated (pre size classification) and non-aggregated NST/FPL powder systems. The images indicate that the cohesive powder system readily aggregates into spherical agglomerates.

Figure 6.9 is an ESEM image of the surface of one of the aggregates (pre-size classification). The image shows that within the spherical agglomerate, larger particles of fine lactose can be seen physically disrupting the drug/drug cohesive interactions.

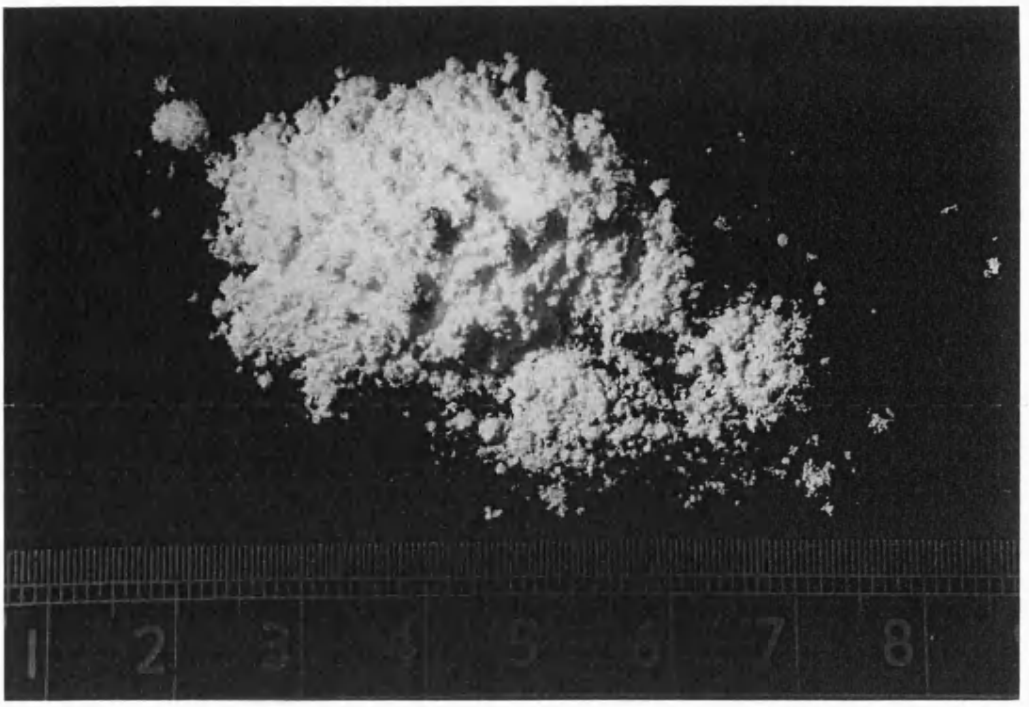

Figure 6.7 Photographic image of the non-aggregated NST/FPL powder system.

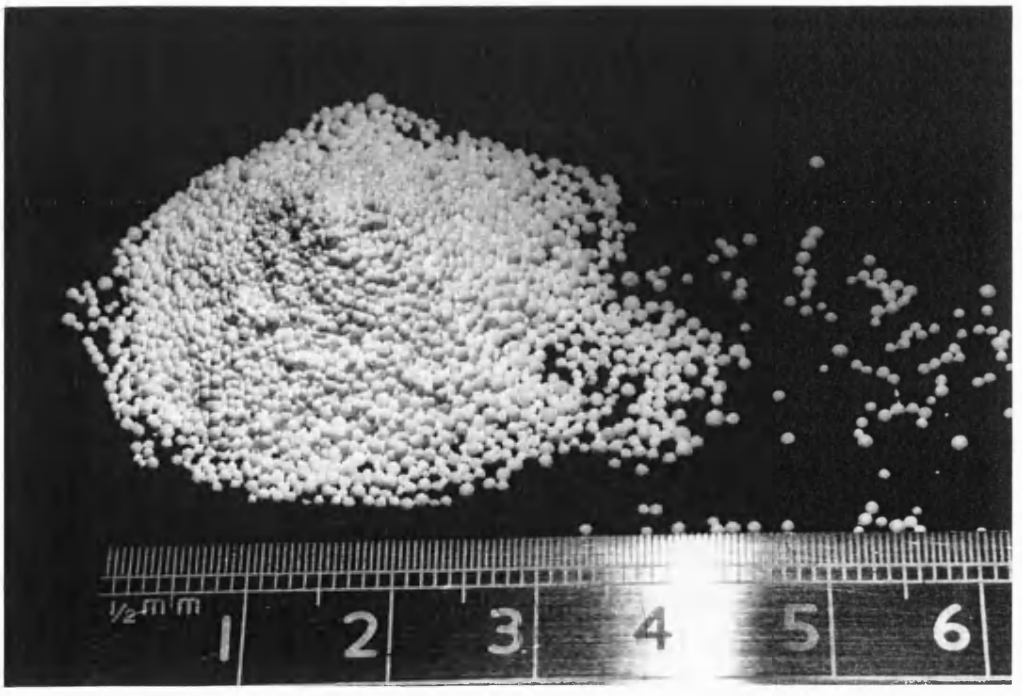

Figure 6.8 Photographic image of the aggregated NST/FPL powder system.

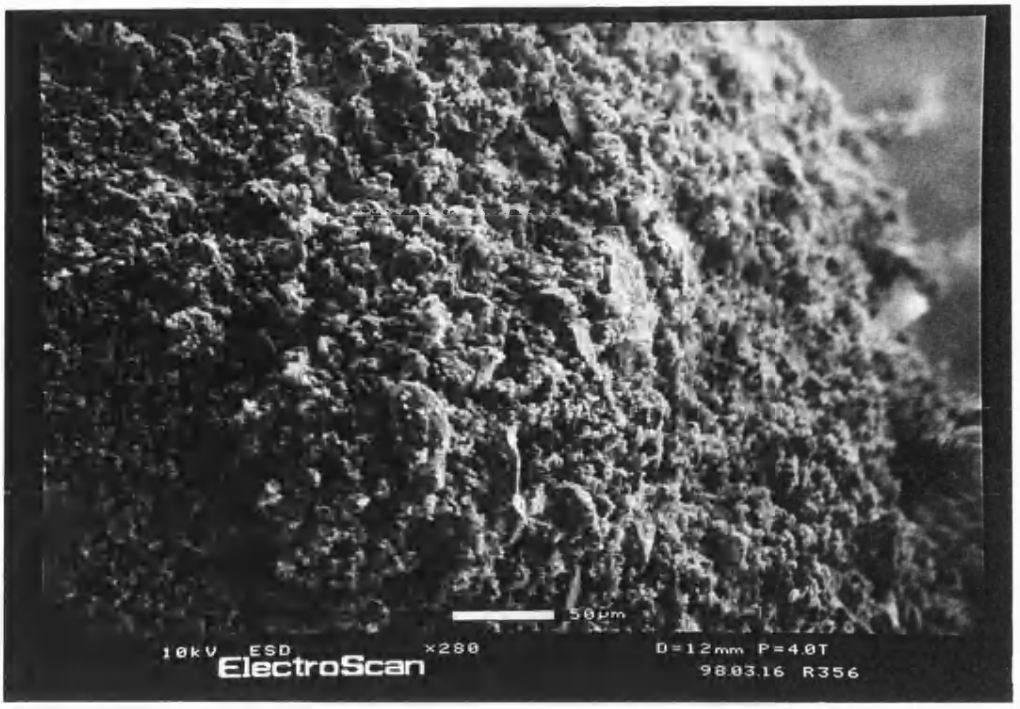

Figure 6.9 ESEM image of the aggregated NST/FPL powder system.

6.3 Aggregated TS/FPL Powder Systems

Micronised TS is formulated as a dry powder inhalation by Astra Pharmaceuticals, AB Draco, Sweden. The micronised drug is transformed by spheronisation into soft aggregates to improve powder processing and aerosolisation (Wetterlin, 1988).

The intercalation of FPL within the aggregated TS system was investigated to see if the improved deaggregation observed for NST was material dependent.

6.3.1 Materials and Methods

Particle Size Characterisation

The particle size of TS was measured using the technique of LALLS as described in section 2.3.1.1. The size distribution was determined using the SVC in conjunction with the 100 mm optical lens. Cyclohexane + 0.1% $^{w}/_{v}$ lecithin was used as the dispersant medium.

A sample of the TS powder was imaged using conventional SEM as described in section 3.2.1.

Formulation of the Powder Systems

Micronised TS aggregates were initially crushed in a weighing boat using a metal spatula to destroy the drug self-agglomerates. The TS was then hand blended for 15 minutes with an equal amount of FPL as described in section 2.2.3.

Both the TS/FPL mixture and the TS powder were screened through a metal sieve (1.4 mm aperture diameter) onto a finer sieve mesh (63 μm) and spheronised by rolling the screened material across the finer mesh for three minutes. The spheres were then size classified by placing the loosely aggregated powder on top of a stack of metal process sieves and gently hand tapping the sieve stack for approximately 1 minute to fractionate the powder sample. More uniform aggregates were produced (visual inspection) by rolling the powder aggregates over the smaller sized mesh of each classification stage for a further five minutes. Four sieve size fractions of aggregates were collected; < 125 μm, 125-500 μm, 500-710 μm and > 710 μm.

Using this procedure ensured that both the pure TS system and the TS/FPL formulation were aggregated following the same protocol. Therefore, any differences in the *in-vitro* aerosol performance of the systems could be related to the performance modifying effects of the FPL and not the methods of aggregation.

In-vitro Aerosol Characterisation

The *in-vitro* aerosol performance of the pure TS and the TS/FPL powder formulation was characterised using the modified Apparatus A (section 2.5.1). Capsules were filled with 10 mg of either pure TS or TS/FPL immediately before *in-vitro* aerosol assessment and discharged from the Cyclohaler® at 60 litres min^{-1}.

6.3.2 Results and Discussion

Particle Size Characterisation

The particle size distribution of TS is shown in Appendix I, figure A6. The VMD (±SD) was 1.8 ± 0.03 μm (n = 3). 90% of the particles had an equivalent volume diameter ≤ 5.3 ± 0.1 μm (n = 3).

Figure 6.10 is an electron micrograph of the TS particles, obtained using the technique of conventional SEM. The image revealed that the micronised TS powder consists of irregular shaped, plate-like crystals.

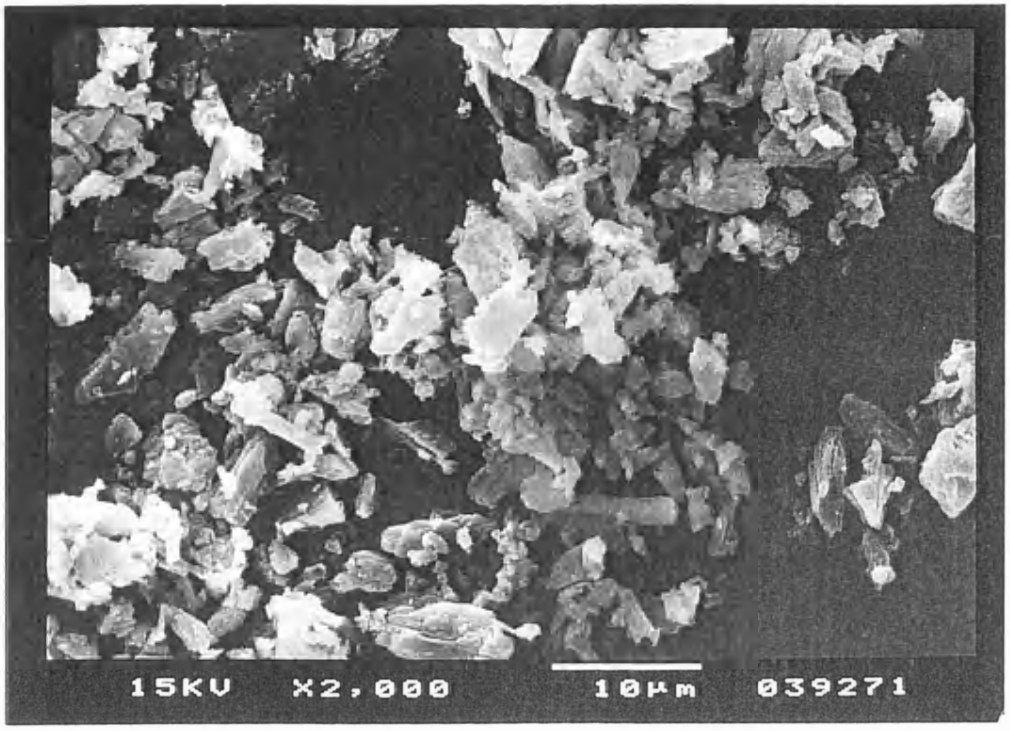

Figure 6.10 Conventional SEM electron micrograph of micronised TS.

In–vitro Aerosol Characterisation

Table 6.7 summarises the drug content uniformity data for the fractionated TS/FPL aggregated systems. The sieve fraction <125 µm did not appear to aggregate therefore was not investigated further. The two larger size fractions of spheres, 500-710 µm and >710 µm, showed acceptable drug content uniformity (CV <5 %).

Sieve Size Fraction (µm)	Content Uniformity	
	Mean (mg)	CV (%)
125-500 µm	4.40	8.57
500-710 µm	4.66	4.09
>710 µm	4.23	4.35

Table 6.7 Content uniformity data for TS blended with FPL (n = 10 x 10 mg).

The *in-vitro* aerosol performance of the 500-710 μm aggregated size fraction was characterised using the modified Apparatus A and compared to the aerosol behaviour of the pure (no carrier) TS (table 6.8).

In-vitro Aerosol Characterisation	Formulation (TS:FPL)	
	(100:0)	(50:50)
% Capsule	22.5 ± 3.0	15.4 ± 4.9
% Device	22.3 ± 3.6	17.6 ± 4.8
% Stage 1	22.3 ± 2.6	29.2 ± 3.3
% Stage 2	33.0 ± 3.4	37.8 ± 2.7
% Emitted	55.2 ± 2.1	67.1 ± 5.5
Fine Particle Fraction (%)	59.6 ± 5.0	56.5 ± 2.0
Drug Recovery (%)	99.7 ± 3.1	98.8 ± 3.6

Table 6.8 *In-vitro* aerosol characterisation of TS and TS/FPL powder systems. Values are the mean ± SD of 10 determinations.

The Students *t-test* revealed that the incorporation of FPL into the TS powder system significantly increased the percentage of drug emitted from the capsule/device ($t = 7.15$, $p < 0.001$). However, there was a significant decrease in the deaggregation (FPF) of the system ($t = 2.32$, $p = 0.03$) although the effects were not considered dramatic, i.e. TS = 59.6 ± 5.0% compared with TS/FPL = 56.5 ± 2.0%. The functional effects of FPL appear to be material dependent.

6.4 General Discussion

The formulation of agglomerated units of pure drug offers an alternative formulation strategy to carrier based systems when attempting to improve the flow, processing and entrainment properties of the fine drug particles (Bell et al. 1971; Wetterlin, 1988).

Under carefully controlled processing conditions, spherical agglomerates of NST possessing excellent flow characteristics can be formed. However, the *in-vitro* inhalation performance of NST in both the initial powder and the spheronised form is poor, presumably due to the strong cohesive interparticle interactions.

Controlled aggregation of the optimised NST/FPL powder systems results in agglomerates with excellent aerosol characteristics (deaggregation and subsequent fine dose deposition). However, it has also been demonstrated that increased aggregation periods can have a detrimental effect on the deaggregation of the systems following aerosolisation. Agglomerated powder systems must be sufficiently strong to withstand breakage during storage and transport but be weak enough to disintegrate upon patient inhalation. Therefore, there is a narrow window in which the agglomerates should be tailored (Boerefijn et al. 1998).

No significant clinical differences were observed between two formulations of DSCG, either a blend of DSCG (20 mg) plus lactose (20 mg) or a lactose-free pelletised formulation of DSCG (20 mg) (Edwards and Chambers, 1989). It is possible that the selection of carrier lactose and/or the mixing processes employed failed to deaggregate

the drug systems. The aerosol performance of both systems may therefore be limited by the cohesive drug interactions.

However, the pelletised formulation may have clinical value because it removes the possibility of any adverse effects due to lactose intolerance in lactase deficient patients and it also removes any possibility of allergenicity to protein contaminants in the lactose (Edwards and Chambers, 1989). Since there is half the amount of powder in a capsule of pelletised sodium cromoglycate (20 mg), compared to that of the blend formulation (40 mg), it is reasonable too expect that patients would require less inhalations to empty a pelletised capsule.

CHAPTER 7

THE EFFECTS OF RELATIVE HUMIDITY ON THE PHYSICAL PROPERTIES AND *IN-VITRO* AEROSOL BEHAVIOUR OF NEDOCROMIL SODIUM

7.1 Introduction

NST is stable over the RH range 6.4 to 79.5 % (Khankari et al. 1998). However, NST may sorb/desorb surface moisture over this humidity range. The sorption/desorption of surface moisture may affect both the electrostatic and capillary interactions at low and high humidities respectively. Therefore, samples of NST powder were stored near the extremes of this stability range (12 and 76% RH) to assess any possible effects on the total moisture content and aerosol performance of the system. NSHH was subsequently investigated (physicochemical properties and *in-vitro* aerosol behaviour) and compared to NST.

7.2 Effect of RH on the Physical Properties of Nedocromil Sodium

7.2.1 Preparation of Nedocromil Sodium Hydrates

Samples of nedocromil sodium were received as the trihydrate (Rhône Poulenc Rorer, U.K.). NSHH was obtained by equilibrating NST at 85-86% RH at 25°C for a four week period. Total conversion of NST to NSHH has been reported to occur within 10 days if stored at a RH of 90% (Khankari et al. 1998). The conversion was monitored visually since the colours of the hydrates are strikingly different, crystals of NST are pale yellow whereas those of NSHH show a more intense yellow colour (Khankari et al. 1998). It has been reported that the pale yellow monohydrate can be obtained by storing

the trihydrate over phosphorus pentoxide under vacuum (0 % RH) at 22°C for six months (Khankari et al. 1998). However, since the monohydrate is highly unstable, rapidly taking up moisture and converting to the trihydrate at RH >6 % (Khankari et al. 1998), this conversion and associated experimental investigations were not attempted.

The effects of storage humidity on the total water content of the powder samples and/or the conversion from the trihydrate to the heptahemihydrate were monitored using the following methods.

7.2.2 Gravimetric Investigations

Materials and Methods

The percentage weight change of NST samples stored at 12, 53-55 and 75-76 % RH was investigated. Samples of approximately 400 mg of NST (initially stored at 53-55% RH) were accurately weighed using a five figure balance (Mettler AT261 DeltaRange, Mettler Toledo, Switzerland) and then spread thinly over the inside of small plastic petri-dishes. The powder samples were then placed in an appropriate desiccator (section 2.2.2).

Changes in the total water content were monitored gravimetrically over a period of eight weeks by regularly removing the powder samples from the desiccators and recording any weight changes using the five figure balance. Investigations were performed in duplicate.

Results and Discussion

Table 7.1 summarises the percentage weight changes for the NST powder samples stored at the three humidity levels. Negligible weight changes occurred over the eight week period for all powder samples. The results suggest that not only is nedocromil sodium stable as the trihydrate but that NST does not appear to sorb or desorb large quantities of moisture over this humidity range.

% RH	% Weight Change	
	Run 1	Run 2
12	-0.0003	-0.0002
53-55	0.0001	0.0000
75-76	0.0093	0.0120

Table 7.1 Summary of the gravimetric study for NST stored over a range of humidities

7.2.3 Karl Fischer Analysis

Materials and Methods

The total water content of the NST powder samples stored at the three humidity levels and the NSHH was determined using the Karl Fischer (KF) method of analysis.

Materials and Methods

KF titrations were initially performed by adding a powder sample (5-10 mg) directly into the titration vessel (684 KF Coulometer, Metrohom with 728 Stirrer) using a glass capsule filler to ensure all the powder was delivered to the titration solution. The glass capsule was accurately weighed (Mettler AT261 DeltaRange, Mettler Toledo, Switzerland) before and after delivery of the powder sample to the titration vessel to

ensure an accurate determination of the delivered mass. Powder samples from the four defined storage humidities: 12 %; 53-55 %; 75-76 % and 85-86 % were analysed.

Due to concerns regarding adhesion of the cohesive powder to the glass titration vessel (near the port of entry), an alternative method of sample preparation and delivery was employed. Approximately 200 mg of powder was accurately weighed and made up to 50 ml in a volumetric flasks using methanol (water content 0.0024% $^{w}/_{w}$). An accurate volume of the solution (1 ml) was injected into the titration vessel using a Hamilton syringe (Hamilton Gastight 1700 Syringe, Hamilton Company, Nevada, U.S.A.). The source of methanol used in the preparation of the samples was used as a blank throughout all investigations. Due to the hygroscopic nature of methanol (Connors, 1988), a fresh source was obtained and dedicated to the study and its exposure to the atmosphere minimised.

Results and Discussion

Results for the KF analysis of the powder samples prepared using the two techniques are shown in table 7.2.

The water contents derived for the NST are in agreement with values previously reported of; 12 % $^{w}/_{w}$ (Wong et al. 1995b) and 11.72 % $^{w}/_{w}$ (Khankari et al. 1998). The method described by Khankari et al. (1998) is based on the addition of the sample as a dry powder. Therefore, similar concerns are expressed regarding the suitability of this method for such a cohesive material. Theoretical values based on molecular weights are: NSHH 24.5% $^{w}/_{w}$; NST 11.5 % $^{w}/_{w}$ and 4.2 % $^{w}/_{w}$ NSM (Khankari et al. 1998). However, these values only take into account water of hydration and not the presence of any adsorbed surface moisture.

Storage Condition (% RH)	Sample Presentation	Water content (% $^{w}/_{w}$)
12	dry powder	11.5 ± 0.13
53-55	dry powder	11.5 ± 0.10
75-76	dry powder	11.8 ± 0.25
85-86	dry powder	24.0 ± 0.51
12	powder in solution	12.6 ± 0.24
53-55	powder in solution	12.4 ± 0.13
75-76	powder in solution	12.9 ± 0.35
85-86	powder in solution	25.2 ± 0.88

Table 7.2 KF determination of the total water content of NS stored at different humidity levels. Results are the mean ± SD of 5 determinations.

a) Dry powder method - direct addition of the sample as a powder.

b) Powder in solution - addition of sample dissolved in methanol.

It would again appear that NST does not sorb/desorb large quantities of water over the range of humidities the trihydrate is stable.

7.2.4 Differential Scanning Calorimetry

In the DSC method, the sample and reference are maintained at the same temperature and the heat flow required to keep equality in temperature is measured. DSC thermograms are obtained as the differential rate of heating against temperature.

Materials and Methods

DSC thermal analysis of NST and NSHH powder samples was performed over the temperature range 40 to 350°C (Model 2910, TA Instruments Ltd, U.S.A.). Samples of powder (3 mg to 5 mg) were accurately weighed, enclosed in crimped aluminium pans and then heated at 10°C min^{-1}. An empty crimped aluminium pan was used as a

reference. The calorimeter furnace was continually purged with nitrogen gas at a flow rate of approximately 25 ml min^{-1}. The onset of melting of indium (156.6°C) and tin (231.9°C) were used to calibrate the calorimeter. Powder samples were prepared and analysed in duplicate.

Results and Discussion

Examples of the DSC thermograms for NST and NSHH are shown in figures 7.1 and 7.2. The peak temperatures and specific energies for the principle endotherms are summarised in table 7.3.

Material	Peak Temperature (°C)		ΔH of each endotherm (J g^{-1})	
	Run 1	Run 2	Run 1	Run 2
NST	129.8	130.7	266.2	266.5
	207.8	208.8	75.5	76.9
NSHH	70.5	67.3	76.2	82.8
	100.9	97.8	140.6	136.2
	124.4	125.1	142.4	147.4
	202.6	201.2	102.4	108.5

Table 7.3 Summary of the DSC analysis of NST and NSHH.

Nedocromil Sodium Trihydrate

The DSC thermogram for NST stored at 53-55% RH shows a sharp endotherm at approximately 130°C and a broad weak endotherm at approximately 208°C (figure 7.1). Khankari et al. (1995) correlated similar DSC data with information obtained from thermogravimetric analysis (TGA) and hot stage microscopy, confirming that the two endotherms relate to processes of dehydration. The first dehydration corresponds to the

loss of two thirds of the water (loosely bound) and the remaining one third is lost at about 208°C (tightly bound).

Nedocromil Sodium Heptahemihydrate

NSHH exhibits four endotherms, a very sharp narrow endotherm at approximately 70°C, followed by two broader endotherms at 100°C and 125°C and a still broader weaker endotherm at 200°C. The variation in the specific energies associated with the endotherms was considered a result of difficulties in integrating the peak areas since there is no obvious baseline. This degree of variability is also reflected in published data (DSC on NSHH) from two separate studies (Khankari et al. 1992; Khankari et al. 1995). The peak temperatures associated with each endotherm are in general agreement with Khankari et al. (1998) suggesting that the four week storage period was sufficient to cause complete conversion of NST to NSHH.

Initially it was reported that the dehydration of NSHH occurred in four steps, presumably due to four different binding environments available for the water molecules (Khankari et al. 1992). However, in crimped pan DSC and TGA, the relatively high water vapour pressures produced changes in the dehydration of NSHH. The NSHH melted at 75°C converting to NST, which on further heating converted to NSM and eventually the anhydrate (Khankari et al. 1998). More recent studies using techniques of open/closed pan DSC, TGA and hot stage microscopy revealed that the water molecules in NSHH are linked together to form continuous water channels. DSC and TGA of the NSHH in open pans revealed a single dehydration endotherm from 72 to 221°C corresponding to a single step dehydration (Khankari et al. 1998).

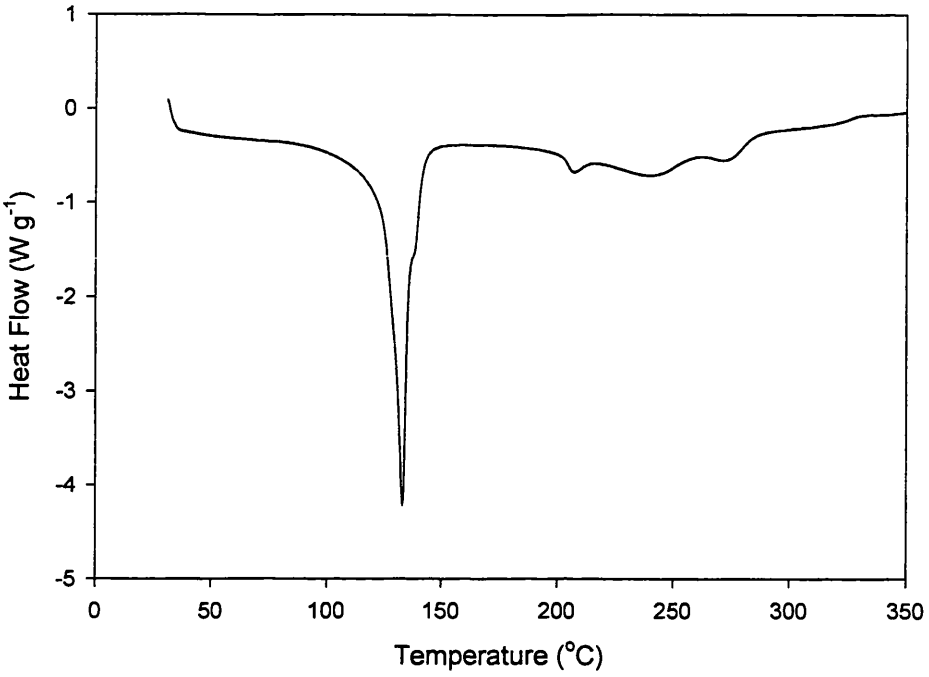

Figure 7.1 DSC thermogram for NST (stored at 53-55 % RH).

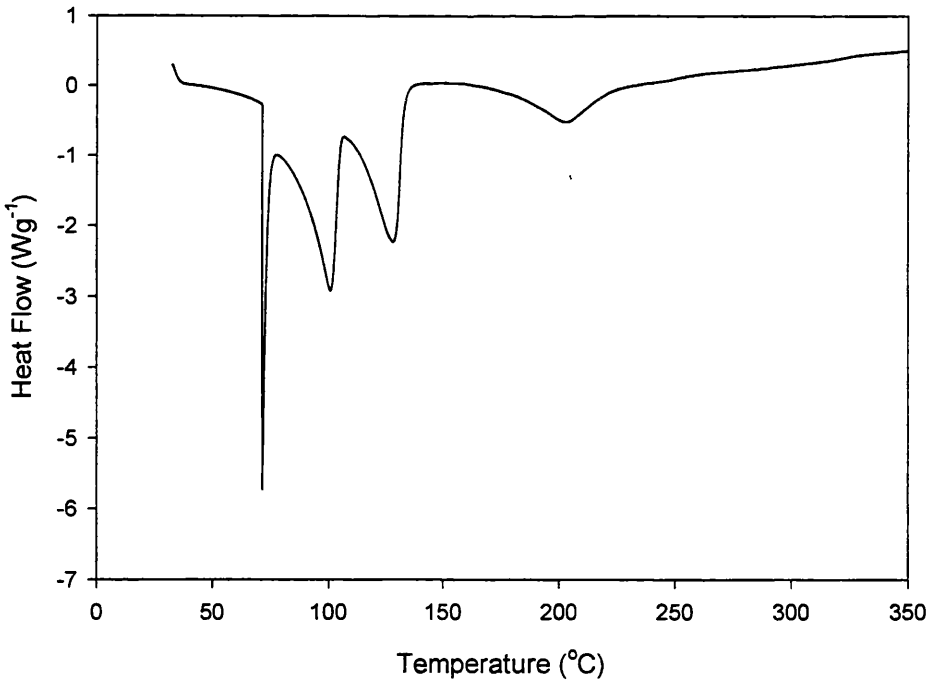

Figure 7.2 DSC thermogram for NSHH (stored at 85-86 % RH).

7.2.5 Microscopic Analysis

LTSEM electron micrographs of NST (figures 3.8 and 3.9) were described in section 3.3.2. LTSEM electron micrographs of NSHH are shown in figures 7.3 and 7.4. The techniques used to acquire the images are described in detail in section 3.2.2.

From figures 7.3 and 7.4, it would appear that solid/liquid bridges appear to have formed between the previously discrete drug particles, resulting in what can be envisaged as agglomerates with poor deaggregating capabilities. The uncharged nature of the sample, as seen from the resolution and clarity of the images, again reflects the usefulness of LTSEM for imaging highly hydrated pharmaceutical materials.

Ampratum et al. (1997) claim to have imaged both milled and spray dried NST using conventional SEM although the images were not presented. They concluded that on storage at 76 and 96 % RH, spray dried and milled NST particles appeared to fuse having no distinct shape and roughened surfaces. However, the imaging of such hydrated particles in the vacuum of a conventional SEM (SEM, Phillips XL20) without substantial damage to the conducting gold coating and subsequent sample charging is difficult to envisage.

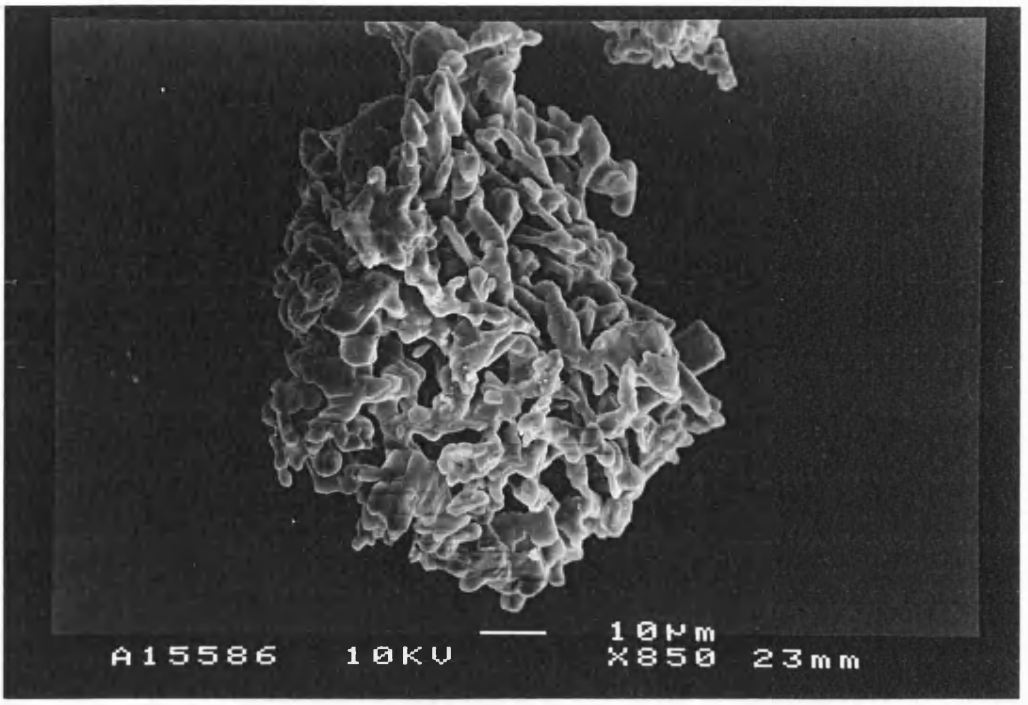

Figure 7.3 LTSEM electron micrograph of NSHH.

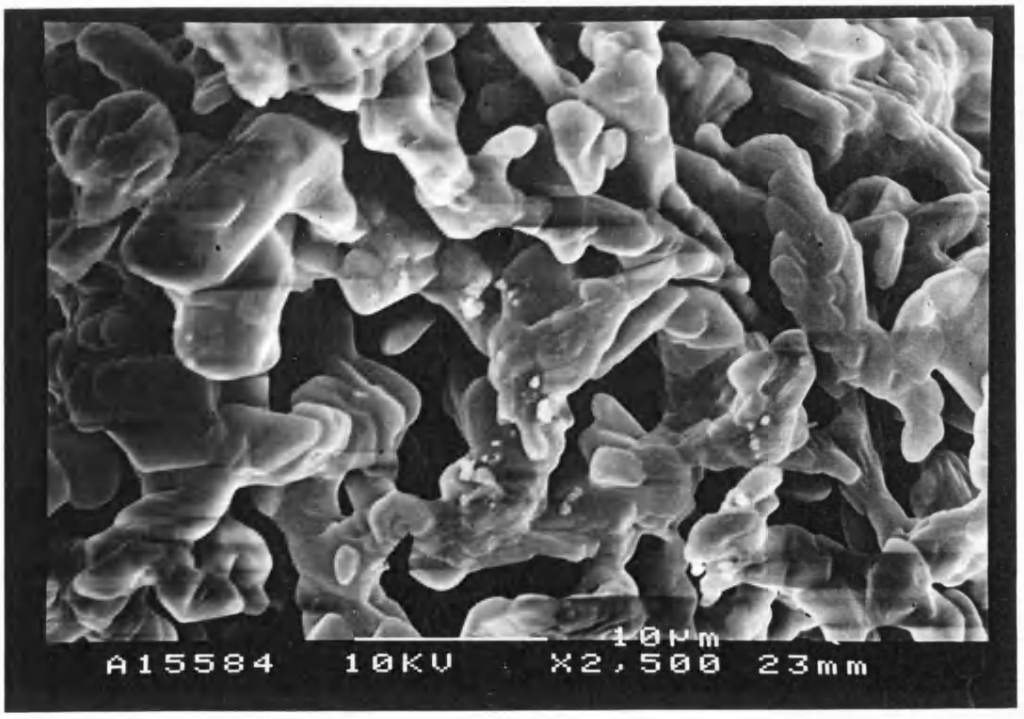

Figure 7.4 LTSEM electron micrograph of NSHH.

7.3 The Effects of Storage Humidity on the *In-vitro* Aerosol Performance of Nedocromil Sodium

The influence of the storage humidity on the interactive forces operating within the pure drug system was evaluated by measuring the deaggregation and subsequent fine particle deposition of the powder samples (modified Apparatus A and MSLI).

The *in-vitro* aerosol performance of NST stored over a range of humidities (12 to 76% RH) was characterised and compared to NSHH.

7.3.1 Materials and Methods

All powder samples were pre-screened through a 355 μm mesh before storage for four weeks at one of four humidities (12, 53-55, 75-76 and 85-86% RH). The conditions were chosen to represent a range of humidities throughout which NST is stable (12-76% RH) but where sorption/desorption of surface moisture may occur. The powder stored at 86% had converted to NSHH.

The modified Apparatus A was initially used to study the *in-vitro* aerosol properties of the drug powder. Data derived from these investigations was supplemented by MSLI investigations.

An 8 mg capsule powder fill weight was employed for the modified Apparatus A studies and a 20 mg fill weight investigated for the MSLI studies.

To minimise the effects of gelatin/powder moisture transfer (Bell et al. 1973b; Konty and Mulski, 1989) the powders were removed from the dessicators and filled into the gelatin capsule immediately before *in-vitro* aerosol assessment.

7.3.2 Results and Discussion

Table 7.4 and figures 7.5 and 7.6 summarise the *in-vitro* aerosol performance (modified Apparatus A) of NST stored under different humidity conditions.

The deaggregation of the pure drug system investigated immediately after screening (355 μm) (section 2.6.2) was compared to the aerosol performance of the sample stored at 53-55 % RH for four weeks. The Students *t-test* revealed no significant differences in the ED ($t = 1.22$, $p = 0.260$). However, there was a significant decrease in the deaggregation (FPF) ($t = 2.62$, $p = 0.030$) and subsequent stage-2 deposition of NST (FPD) ($t = 2.58$, $p = 0.033$).

The decrease in the deaggregation of the pure drug system following storage is presumably due to the screened material re-agglomerating. This would suggest that the aerosol performance of the optimised formulations (section 4 and 5) may decrease with time even if stored under ambient conditions (55% RH, 25°C).

In-vitro Aerosol Characterisation	Storage Humidity (% RH)				
	12	53-55[a]	53-55	75-76	85-86
% Capsule	5.41 ± 1.8	3.00 ± 0.31	4.02 ± 0.52	4.50 ± 0.69	16.5 ± 0.95
% Device	26.8 ± 3.0	21.7 ± 1.7	19.0 ± 0.73	21.3 ± 2.1	7.69 ± 0.62
% Stage 1	52.8 ± 4.3	63.1 ± 2.4	66.2 ± 1.3	62.5 ± 3.0	69.8 ± 0.44
% Stage 2	15.1 ± 1.4	12.3 ± 1.1	10.8 ± 0.74	11.7 ± 0.92	5.98 ± 0.77
Emitted Dose (%)	67.8 ± 4.1	75.4 ± 1.6	77.0 ± 1.1	74.2 ± 2.2	75.8 ± 1.2
Emitted Dose (mg)	5.46 ± 0.26	6.05 ± 0.17	6.16 ± 0.10	5.94 ± 0.19	6.09 ± 0.064
Fine Particle Fraction (%)	22.5 ± 2.2	16.3 ± 1.7	14.1 ± 0.96	15.7 ± 1.6	7.88 ± 0.89
Fine Particle Dose (mg)	1.21 ± 0.11	0.985 ± 0.083	0.865 ± 0.059	0.934 ± 0.087	0.479 ± 0.053
Drug Recovered (%)	101 ± 1.7	100 ± 1.4	100 ± 2.4	100 ± 2.43	100 ± 2.0

Table 7.4 *In-vitro* aerosol characterisation of NST stored under environments of different relative humidities. Discharged using ambient air as the carrier gas. Values are the mean ± SD of 5 determinations.

[a]Powder assessed immediately after screening (no 4 week storage period).

ED and FPD were normalised with respect to a 8 mg capsule fill weight.

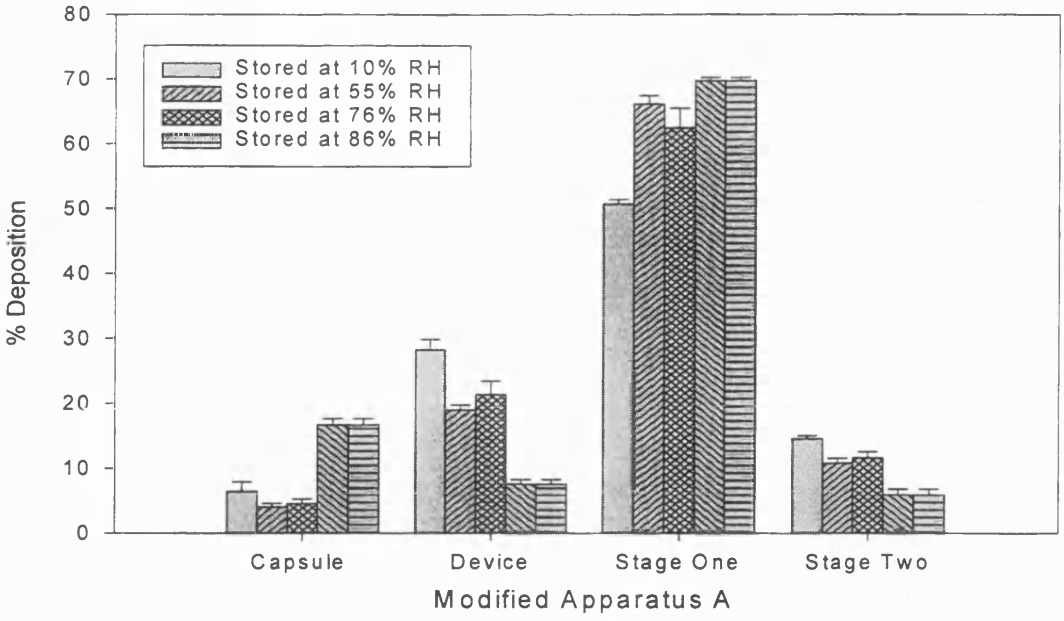

Figure 7.5 Effects of storage humidity on the *in-vitro* aerosol performance of NST and NSHH determined using the modified Apparatus A.
Each column shows the mean of 5 determinations (bars represent SDs).

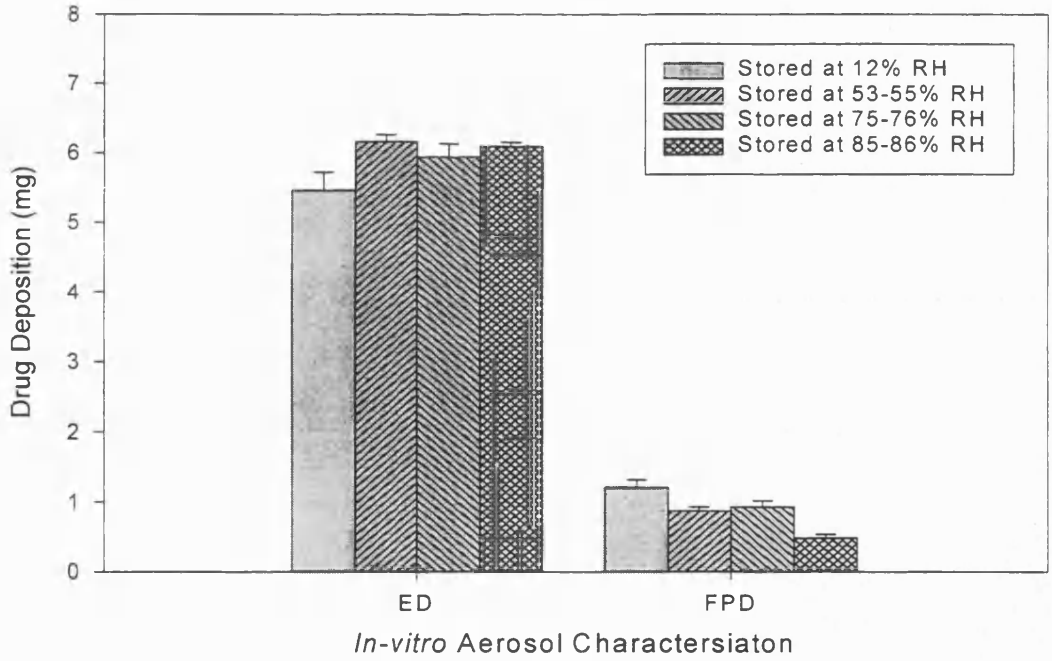

Figure 7.6 Effects of storage humidity on the *in-vitro* aerosol performance of NST and NSHH determined using the modified Apparatus A.
Each column shows the mean of 5 determinations (bars represent SDs).

One way analysis of variance indicated a significant difference in the ED ($F = 17.25$, $p < 0.001$) for the powder samples stored at the four different humidities. Fisher's pairwise comparisons revealed a significant decrease in the ED for the powder sample stored at 12% RH compared with the powder samples stored at the higher humidities (55-86%). This is presumably due to an increase in the adhesive interactions operating between NST and the device/capsule walls. The increase in adhesion may be a result of an increase in electrostatic interactions (Kulvanich and Stewart, 1988) and/or the more complete regeneration of fine particles of NST, possessing greater surface free energy.

As the powder sample is stored at progressively higher humidities, the percentage of drug adhered onto the device decreases (table 7.4). Braun et al. (1996) reported that micronised DSCG adhered to most surfaces at low moisture contents due to electrostatic interactions but when exposed to humid air, the micronised powder became more cohesive. A similar situation is observed with the NSHH where the percentage of NSHH adhered onto the device walls was <8% compared with ≥19% for samples of NST stored at 53-55% RH. However, the decrease in device adhesion did not translate into an increase in the ED since the percentage of NSHH retained in the capsule was greater (16.5 %) compared with the other powder samples (<6 %). All values were expressed as a percentage of the total drug recovered. The increased capsule retention is presumable due to a decrease in the deaggregation of the NSHH system upon aerosolisation possibly caused by an increase in capillary interactions or even the formation of solid bridges (figures 7.3 and 7.4).

The decreased deaggregation of NSHH (FPF) compared to the samples of NST was confirmed using Fisher's pairwise comparisons ($F = 72.9$, $p < 0.001$). However,

Fisher's pairwise comparisons also revealed a significant increase in the deaggregation (FPF) of the NST stored at 12% RH. The FPD followed the same trend ($F = 69.0$, $p < 0.001$), greatest for the powder sample stored at 12% RH (1.21 ± 0.11 mg) and lowest for the NSHH (0.48 ± 0.05 mg) (Fisher's pairwise comparisons). There was no significant difference in the aerosol performance, in terms of FPF and FPD for the samples of NST stored between 53 and 76% RH.

NST stored at lower humidities deaggregated more completely compared to the powder samples stored at 53-55 and 75-76% RH and NSHH. However, the improved deaggregation did not translate into a dramatic increase in the FPD since a greater percentage of the drug adhered to the device walls.

Multistage Liquid Impinger

Table 7.5 and figures 7.7 and 7.8 summarise the *in-vitro* aerosol characterisation of the powder samples measured using the MSLI. The capsule fill weights were increased to ensure adequate NST recovery for quantitative drug analysis using the selected analytical techniques. This was considered important for the quantification of drug deposition on the lower stages of the MSLI for the poorly deaggregating systems (NSHH). With the exception of the NSHH, a single actuation was sufficient to discharge the capsule contents; multiple actuations were required to empty the capsules containing NSHH.

When operated at a flow rate of 60 litres min^{-1}, the FPD determined using the MSLI (stage-2 to the filter) encompassed particles of a size 0-6.8 μm (D_{ae}); the modified-Apparatus A (stage-2) captured particles of a size 0.5-5.3 μm (D_{ae}).

In-vitro Aerosol Characterisation	12%	53-55%		75-76 %	85-86%	
	single shot	[a]single shot	single shot	Single shot	single shot	multiple shots
% Capsule	2.01 ± 0.27	6.88 ± 1.4	2.00 ± 0.25	1.79 ± 0.65	18.5 ± 4.9	1.87 ± 0.19
% Device	22.6 ± 0.83	16.4 ± 1.5	13.5 ± 2.2	9.35 ± 2.0	3.09 ± 0.41	3.24 ± 0.54
% Throat	43.5 ± 0.72	26.2 ± 2.1	39.5 ± 1.7	35.2 ± 11	25.7 ± 4.7	37.7 ± 8.9
% Stage 1	17.0 ± 1.8	36.8 ± 0.71	33.1 ± 3.4	40.1 ± 7.4	40.7 ± 1.7	46.8 ± 9.6
% Stage 2	2.82 ± 0.067	3.42 ± 0.42	2.12 ± 0.48	2.25 ± 0.56	5.23 ± 0.86	5.32 ± 0.24
% Stage 3	4.62 ± 1.1	4.98 ± 0.27	3.84 ± 0.30	4.05 ± 0.24	4.33 ± 0.23	3.42 ± 0.52
% Stage 4	5.81 ± 0.57	4.02 ± 0.44	4.64 ± 0.96	4.65 ± 0.31	1.40 ± 0.17	1.24 ± 0.23
% Filter	1.69 ± 0.094	1.37 ± 0.20	1.21 ± 0.27	1.69 ± 0.50	0.774 ± 0.52	0.417 ± 0.067
ED (%)	74.6 ± 1.8	78.2 ± 3.8	86.3 ± 2.9	89.1 ± 0.97	77.2 ± 4.3	95.9 ± 1.1
ED (mg)	14.9 ± 0.35	6.25 ± 0.30	17.3 ± 0.58	17.8 ± 0.19	15.4 ± 0.86	19.2 ± 0.22
*FPF (%)	16.1 ± 2.0	13.5 ± 0.44	11.5 ± 1.5	11.8 ± 1.1	8.31 ± 0.24	5.35 ± 0.68
*FPD (mg)	2.40 ± 0.35	0.845 ± 0.062	1.98 ± 0.29	2.16 ± 0.18	1.35 ± 0.071	1.01 ± 0.13
Extra FPF (%)	9.95 ± 0.55	7.01 ± 0.58	6.91 ± 1.3	7.23 ± 1.1	2.77 ± 0.50	1.75 ± 0.19
Extra FPD (mg)	1.48 ± 0.12	0.439 ± 0.058	1.20 ± 0.26	1.29 ± 0.19	0.438 ± 0.090	0.334 ± 0.032
% Drug Recovered	98.9 ± 1.6	102 ± 1.9	102 ± 0.80	100 ± 3.2	98.5 ± 1.0	101 ± 0.77

Table 7.5 *In-vitro* aerosol deposition data for NS stored at various humidities determined using a MSLI.

Capsule fill weight = 20 mg except [a]capsule fill weight = 8 mg.

Values are the mean ± SD of 3 determinations.

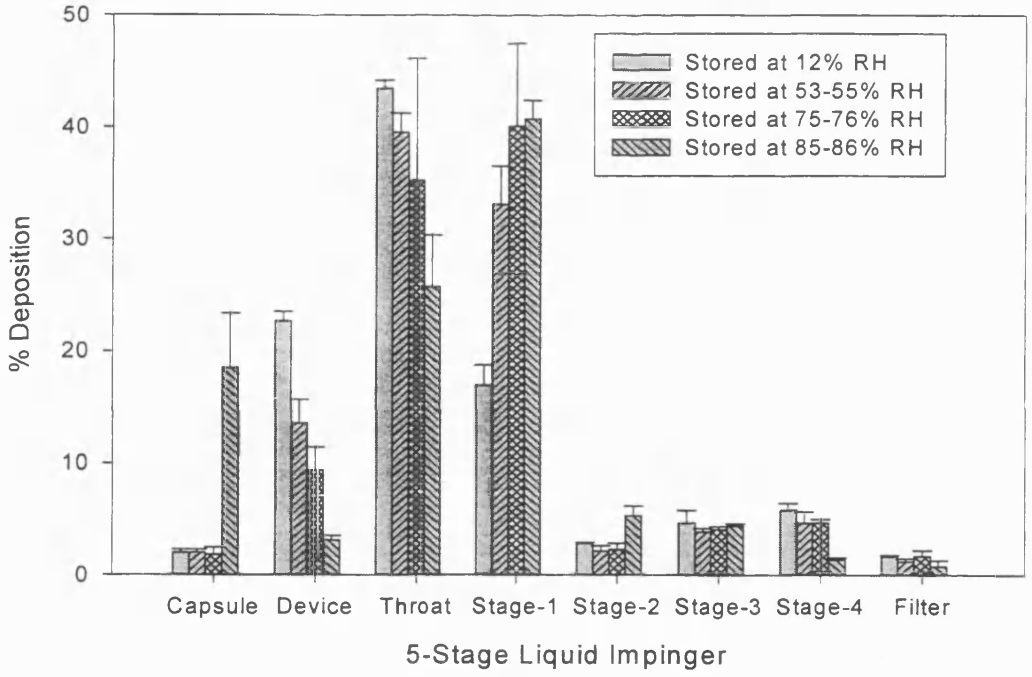

Figure 7.7 Deposition data for NS stored at various RH determined using a MSLI. Each column shows the mean of 3 determinations (bars represent SDs). Capsule fill weight = 20 mg.

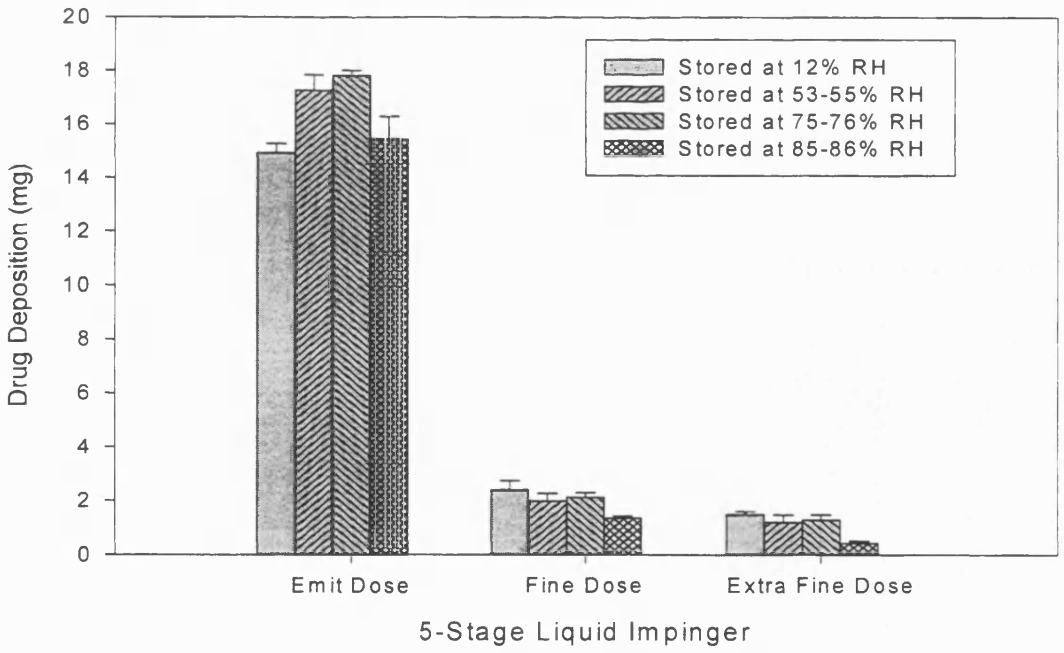

Figure 7.8 Deposition data for NS stored at various RH determined using a MSLI. Each column shows the mean of 3 determinations (bars represent SDs). Capsule fill weight = 20 mg.

Initially, the aerosol performance of the 8 mg capsule fill weight was assessed, comparing the modified Apparatus A data with that obtained from the MSLI investigations. The Students *t-test* revealed no significant differences between the ED ($t = 0.65$, $p = 0.54$), the deaggregation (FPF) ($t = 0.50$, $p = 0.63$) and subsequent stage-2 drug deposition (FPD) ($t = 0.92$, $p = 0.39$).

However, there was a significant decrease in the percentage of drug emitted (NST stored at 53-55% RH) for the 8 mg capsule fill weight (78.2 ± 3.8%) compared with the 20 mg capsule fill (86.3 ± 2.9%) ($t = 2.96$, $p = 0.04$). The reduced powder mass may experience increased shear forces upon aerosolisation, deaggregating the powder system into smaller sized aggregates. These smaller aggregates would have a greater surface area and therefore possess an increased surface free energy (Adjei and Gupta, 1997), causing them to adhere more readily to the device and capsule walls. However, the increased percentage of drug emitted from the 20 mg capsule fill weight did not translate into an increased percentage reaching the lower stages of the MSLI since the pre-separator collected a large percentage of the ED (table 7.5).

Generally the data obtained from the MSLI investigations supports the information derived from the modified Apparatus A studies in terms of the effects of storage humidity on the aerosol performance of NST and NSHH.

The MSLI studies again revealed significant differences in the aerosol performance of the NST compared with the NSHH samples. However, no dramatic effects on the aerosol performance were observed after storage of the NST at humidities ranging from 12 to 76% RH.

The results from the MSLI investigations suggest that the deaggregation of the pure drug systems does not result in discrete particle re-generation since <2 % of the recovered dose was collected on the final filter (D_{ae}: 0 to 1.7 μm).

From LALLS investigations, it was concluded that a large percentage of the NST particles had an equivalent volume diameter <1 μm. Miller et al. (1992) reported that consideration must be given to the possibility of a percentage of particles (D_{ae} <1 μm) penetrating stage-2 of Apparatus A. However, from the MSLI investigations the D_{ae} of the aerosolised aggregates would appear to be >1 μm therefore, penetration of the stage-2 liquid trap should be minimal.

Investigations into the aerosol performance of NSM were not performed since because the monohydrate is difficult to attain and is extremely hygroscopic, rapidly converting back to the trihydrate at RH ≥6.4% (Khankari et al. 1998).

7.4 General Discussion

It is recognised that the methods employed to determine the total water content of the powder system might only detect gross changes in the moisture content. Alternative methods may be employed in future studies to assess changes in the surface energetics of the interacting particles. These methods may include contact angle measurements (Chawla et al. 1993), isothermal microcalorimetry (Buckton, 1997) and inverse gas chromatography (Djordjevic et al. 1992; Dove et al. 1996; Ticehurst et al. 1994). Applications of inverse gas chromatography to pharmaceutical systems include a study on water adsorption by cyclosporin (Djordjevic et al. 1992) and of organic vapours by SS (Ticehurst et al. 1994) and xanthine bronchodilators (Dove et al. 1996).

Alternatively, the influence of storage humidity on the adhesion and cohesion drug/drug and drug/carrier could be studied using the centrifugal techniques (Podczeck et al. 1995, 1996 and 1997).

Numerous studies have investigated the effects of storage humidity on the *in-vitro* aerosol performance of dry powder systems formulated for inhalation (Braun et al. 1986; Genus et al. 1997; Jashnani and Byron, 1996; Vidgren et al. 1989).

Jashnani and Byron (1996) studied the aerosol performance of powders composed of three salts and the free base of salbutamol after storage at varying conditions of temperature and humidity. It was concluded that hydrophobic powders were less sensitive to high storage humidities than hydrophillic powders with respect to their *in-vitro* aerosol performance (Jashnani and Byron, 1996). This was in agreement with Padmadisastra et al. (1994a) who reported that the type of drug and carrier influenced

the degree of interaction; carriers with a higher capacity to adsorb water facilitated greater interaction by capillary and solid bridge formation.

For non-hydrating, crystalline solids, water is mainly adsorbed onto the particle surface at low humidities and as the RH is increased, multi-layer condensation of water vapour onto the particle surface may occur (Coelho and Harnby, 1978a).

However, for hydrating particles, condensation of water vapour onto the particle surface may not result in the formation of a multi layer. Instead, the sorbed water may be employed to convert the non-hydrated particle to the hydrated particles (Ahlneck and Zografi, 1990). Relatively large quantities of water vapour may penetrate or diffuse into the particles before any significant liquid bridges can be formed on the surface of the particle (Chan and Pilpel, 1983). In the case of NST, it is suggested that at increasing humidities, the majority of the sorbed moisture may be absorbed, converting the trihydrate to the heptahemihydrate. This may explain why NST samples stored at 76% RH, deaggregated as efficiently as the powder samples stored under ambient conditions (55% RH).

Investigations into the effects of storage humidity on the physical stability and *in-vitro* inhalation performance of micronised DSCG have been performed (Braun et al. 1986; Vidgren et al. 1989). Both studies assessed the influence of storage humidity on the mixture by measuring the *in-vitro* dispersibility of the systems after storage at fixed humidities.

Vidgren et al. (1989) found that the water content of mechanically micronised DSCG had no significant effect on the mechanical properties of the blend. Storing of the mixtures at elevated humidity affected neither the emptying of the capsules in the inhaler nor the liberation of micronised drug particles from the carrier particles. Chan and Pipel (1983), who reported no change in the binding properties of DSCG agglomerates with changing storage humidity supported these findings. DSCG was found to accommodate most of the absorbed moisture within its particles and only a small amount of water was adsorbed on to the particle surface (Chan and Pilpel, 1983).

These findings are in contrast to observations made by Braun et al. (1996) and Maggi et al. (1999). Braun et al. (1996) compared several formulations containing lactose or dextrose as a carrier and 20 mg of mechanically micronised DSCG. They found that the deaggregation (FPF) of DSCG increased markedly from 22.3 ± 1.86% to 34.4 ± 3.32% after storage at decreased humidities (33% compared to 55 % RH). Braun et al. (1996) explained the contradictory results by suggesting that the formation of soft agglomerates during their preparation process may change the binding properties acting between the powder particles. However, the mixing process employed by Vidgren et al. (1989) may also promote self-aggregation of the drug system (section 4.2.1) although this was not reported. It is believed that a consideration of the forces governing the aerosol performance of the interactive systems may provide a more feasible explanation as to the differing effects of humidity the aerosol performance of the DSCG formulations. Vidgren's work was based on the formulation of DSCG blended with an equal amount of coarse carrier lactose in a TTM, whereas Braun et al. (1996) and Maggi et al. (1999) employed a finer grade of lactose. Based on mixing experiences with NST (section 4.2.1) it is suggested that the aerosol performance of formulations prepared by Vidgren

et al. (1989) may be governed by the drug/drug interactions. However by the selection of a finer excipient (Braun et al. 1996; Maggi et al. 1999), the formulations may be influenced to a greater extent by the weaker drug/carrier adhesive interactions. The effects of humidity on the strong cohesive drug interactions may be minimal. However, adsorbed moisture may have a detrimental effect (in terms of subsequent deaggregation) on the weaker drug/carrier interactions. Future studies may assess the effects of storage humidity on the *in-vitro* aerosol performance of the optimised NST/FPL aggregated system (section 5.1).

Environmental chambers have also been used to assess the importance of carrier air temperature and/or humidity on the aerosol performance of powder systems (Byron et al. 1977; Hickey, 1988; Martin et al. 1988; Vidgren et al. 1992). The importance of both parameters was demonstrated by Bryon et al. (1977), who placed a cascade impactor in a climatic chamber at 37°C and monitored changes in the aerosol performance as a function of RH. Byron et al. (1977) found a large and significant decrease in the dose fraction of drug contained in particles below 5 μm when the RH was varied between 40 and 100 % for powder systems containing DSCG (Intal® Spincaps).

When considering dry powder systems, the decrease in the fine particle deposition can be attributed to; a) hygroscopic growth of the drug particles and/or b) a decrease in the deaggregation of the drug/carrier or drug/drug components (Jashnani and Byron, 1996; Vidgren et al. 1992).

CHAPTER 8

CHARACTERISATION OF DIFFERENT PHYSICAL FORMS OF NEDOCROMIL SODIUM.

8.1 Introduction

Fine powders for inhalation can be prepared either by particle size reduction (milling and micronisation) or by particle construction (condensation, evaporation or precipitation) (Chawla et al. 1994; Hickey et al. 1994; Hindle et al. 1998; York and Hanna 1996; York et al. 1998).

Hammer mills decrease the particle size by impacting the powder with rotating hammers. Clark and Hollingworth (1993b) claim to have used a hammer mill to manufacture potentially respirable particles of NST, although the majority of drug particles for inhalation are prepared using a jet mill in a process known as micronisation (Hallworth, 1987). In a jet mill, size reduction is obtained by interparticle collisions and attrition, producing particles with sizes ranging from 1-20 μm (Johnson, 1997).

It was considered that the strong cohesive interactions binding the NST particles within the pure powder system may be a result of the ultrafine nature of the micronised NST (LTSEM and LALLS analysis). Therefore, an alternative size distribution of NST (milled) was characterised and the aerosol performance of the pure drug system compared to that of the micronised NST.

8.2 Materials and Methods

Two batches of NST, micronised (Bn. GMR 5019G) and milled (Bn. 3834E/A), were supplied by Rhône Poulenc Rorer (Cheshire, U.K.) and used as received.

Re-crystallised nedocromil sodium was passed through a hammer mill (Model TBEP, Apex Construction Ltd, Dartford, U.K (Clark and Hollingworth, 1993b). This material is referred to as milled NST. The micronised material was prepared by fluid energy micronisation of the milled NST (Wong et al. 1995b). This material, referred to as micronised NST, has been investigated throughout the study.

8.3 Physicochemical Characterisation

The milling process has the potential to change more than just the particle size of the feed material. The heat generated during interparticle collisions can cause changes in the solid state properties of the material (Johnson, 1997). Therefore, the particle size and shape, the water content and the degree of crystallinity of the two samples was characterised in an attempt to correlate differences in the aerosol performance of the systems with the physicochemical properties of the powders.

8.3.1 Particle Size Analysis

Materials and Methods

The particle size distribution of milled NST was determined using the technique of LALLS and compared to measurements obtained for micronised NST (section 2.3.1.1). Section 2.3.1.1 details the methods and equipment used to prepare and then analyse NST by LALLS.

Results and Discussion

The effects of extended sonication periods and the use of a saturated or non-saturated dispersant on the particle size distribution of milled NST are summarised in tables 8.1 and 8.2 and figure 8.1. The particle size distribution of micronised NST, determined by LALLS investigations, was described in section 2.3.1.1 and is summarised in table 8.2. The particle size distributions for the two forms of NST are shown in Appendix I: micronised NST (figure A1) and milled NST (figure A2).

Clark and Hollingworth (1993b) and Wong et al. (1995b) have previously determined the particle size distribution of milled and micronised NST samples. Clark and Hollingworth (1993b) determined the VMD of a sample of milled NST to be 8 μm. Particle size determination was performed using LALLS (Malvern 2600, Malvern Instruments) with the sample suspended in propan-2-ol and the scattered light focused using a 63 mm lens. Prior to analysis, the sample was dispersed for 2 minutes using an ultrasonic water bath. Wong et al. (1995b) determined the VMD of milled and micronised NST in liquid suspension by LALLS to be 10.17 and 5.0 μm respectively. Details regarding the preparation of the samples prior to particle sizing were not provided.

Based on LALLS investigations, Wong et al. (1995) determined what they considered to be the potentially respirable fraction (0.5 to 7 μm, D_{ae}) of the milled and micronised NST to be 37.6 and 67 % respectively.

In the present study, the measured particle size distribution of both milled and micronised NST is smaller than that determined by Wong et al. (1995b) and Clark and Hollingworth (1993b). The milled and micronised NST samples have a VMD of approximately 1 μm with 90% of the milled material having an equivalent volume diameter <13 μm and 90% of the micronised NST having a diameter <5 μm. The measured difference may be due to the use of different batches of NST or a result of differences in the preparation of the samples prior to LALLS analysis. The present study has demonstrated the importance of optimising sample presentation prior to particle sizing. It is considered that the degree of deaggregation in both previous studies may have been insufficient to regenerate discrete NST particles and both Wong et al. (1995b) and Clark and Hollingworth (1993b) may have measured the particle size distribution of drug agglomerates.

Results obtained using the 45 mm lens to collate the scattered light suggest that the micronised and milled samples consist of a large proportion of sub-micron particles.

Sonication Time (minutes)	Dispersant	d(0.1) (μm)		d(0.5) (μm)		d(0.9) (μm)	
		Run 1	Run 2	Run 1	Run 2	Run 1	Run 2
1	Non-saturated	0.63	0.73	3.33	6.03	12.53	16.65
3	Non-saturated	0.63	0.69	3.23	5.52	12.06	12.35
5	Non-saturated	0.63	0.69	3.19	4.50	11.99	12.27
10	Non-saturated	0.62	0.64	3.06	3.59	11.28	9.28
15	Non-saturated	0.63	0.66	2.93	3.57	10.92	9.04
30	Non-saturated	0.62	0.63	2.80	2.72	10.34	7.81
1	Saturated	0.64	0.62	3.75	3.28	13.33	13.95
3	Saturated	0.63	0.62	3.46	3.18	11.66	13.04
5	Saturated	0.62	0.62	3.32	3.17	11.21	12.97
10	Saturated	0.62	0.62	3.24	3.19	10.88	12.48
15	Saturated	0.62	0.62	3.11	3.15	10.60	12.72
30	Saturated	0.62	0.62	2.97	3.10	10.62	10.07

Table 8.1 Particle size analysis of milled NST suspended in cyclohexane + 0.1% $^{w}/_{v}$ lecithin. Investigations were performed using the 100 mm lens in conjunction with a SVC.

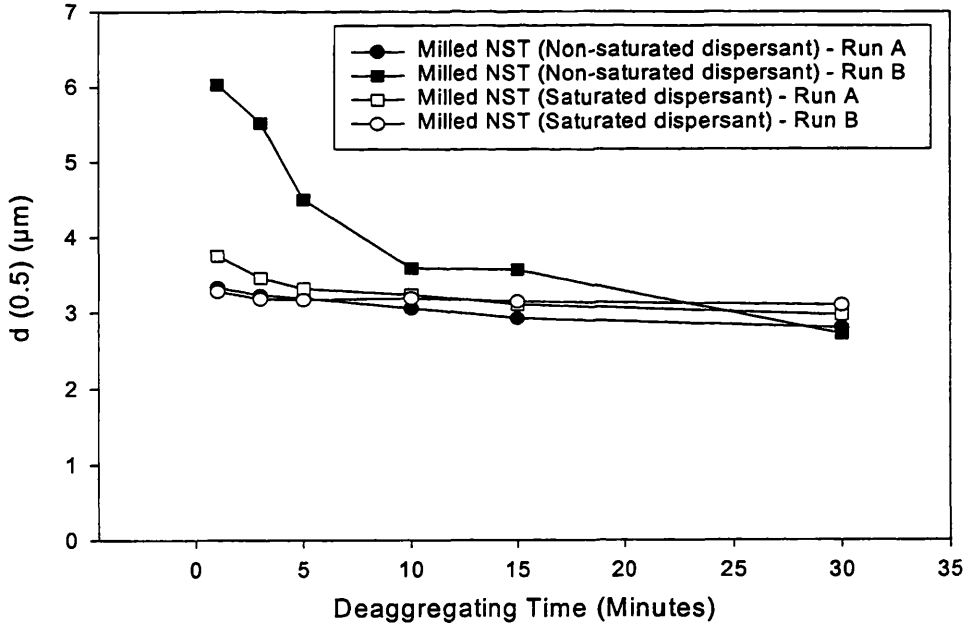

Figure 8.1 The effect of deaggregation time and suspending medium on the particle size distribution of milled NST.

NST	d (0.1) µm		d (0.5) µm		d (0.9) µm	
	Run 1	Run 2	Run 1	Run 2	Run 1	Run2
Micronised	0.20	0.24	0.83	0.89	3.89	4.99
Milled	0.22	0.23	0.86	1.08	12.84	20.34

Table 8.2 Particle size distribution of the milled and micronised NST.
The 45 mm lens was used in conjunction with the LVC.

8.3.2 Microscopic Investigations

Materials and Methods

Relying on particle size information from one method of analysis was again deemed scientifically unwise. Therefore, the particle size of the milled NST was studied using LTSEM and compared to previous images obtained for the micronised NST (figures 3.8 and 3.9). The techniques used to prepare and analyse the samples have previously been described in section 3.2.2.

Results and Discussion

LTSEM images of the milled NST are shown in figures 8.2 and 8.3.

From the samples analysed, the particle size would appear to correlate with particle size measurements obtained using the technique of LALLS. Visual assessment of the images, suggest that the particle size of the discrete particles of milled NST are of a similar size to the micronised particles. A large percentage of the milled and micronised particles appear to be approximately 1 µm with the majority of particles below 5 µm.

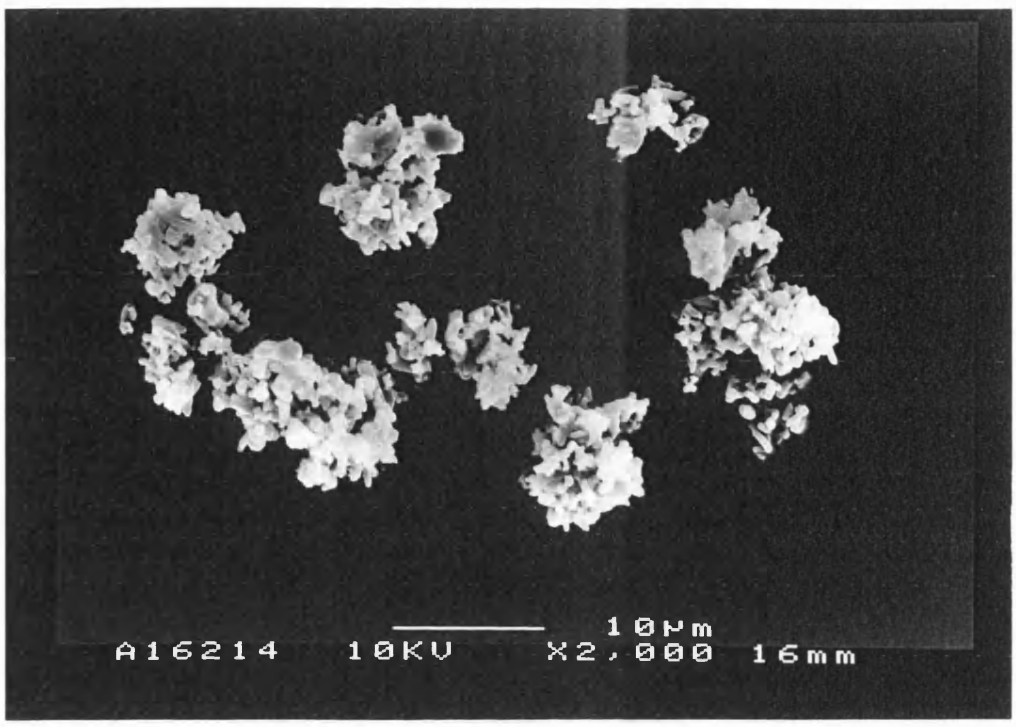

Figure 8.2 LTSEM electron micrograph of the milled NST.

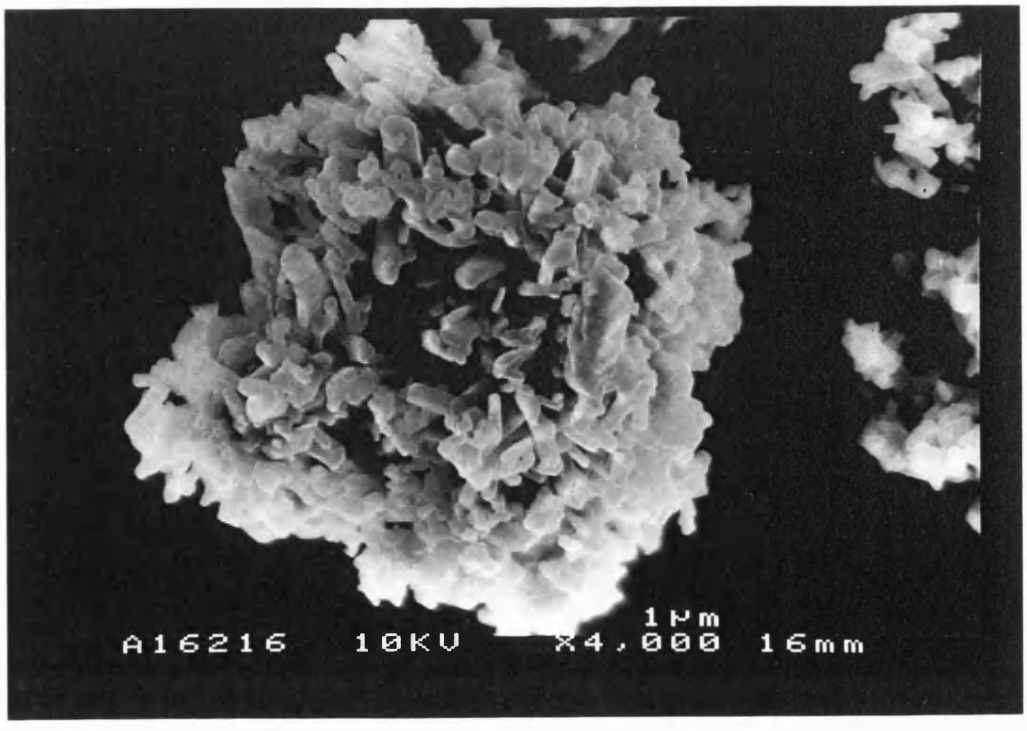

Figure 8.3 LTSEM electron micrograph of the milled NST.

As the particle size decreases, dispersion becomes increasingly difficult due mainly to an increase in van der Waals interparticle interactions (Hickey at al. 1994). The flat, irregular crystals of both materials may further increase the interparticle interactions operating within both systems due to an increase in contact area.

8.3.3 Characterisation of the Water Content

Materials and Methods

The water content of the milled NST was investigated using KF analysis and then compared to measurements obtained for the micronised NST (section 7.2.3). Methods for KF investigations have previously been described in section 7.2.3. Sample preparation involved dissolving the powder samples in methanol (section 7.2.3).

Results and Discussion

Data from KF analysis on the milled NST are summarised and compared with that of micronised NST in table 8.3.

Material	Mean	SD
Micronised nedocromil sodium	12.38	0.11
Milled nedocromil sodium	12.34	0.09

Table 8.3 Total water content of milled and micronised NST determined using KF analysis (n = 5).

The Students *t-test* revealed no significant difference between the total water content of the milled and micronised NST ($t = 0.73$, $p = 0.48$).

8.3.4 Surface Area Investigations

Materials and Methods

Methods for surface area investigations have previously been detailed in section 2.3.2.

Results and Discussion

Table 8.4 summarises the surface area measurements obtained for the milled and micronised NST. The Students *t-test* revealed that the specific surface area of the milled NST is significantly less than that measured for the micronised NST ($t = 8.56$, $p < 0.001$). This could be due to the constituent particles of the micronised NST having a smaller particle size. Alternatively, the constituent particles of the milled NST may be more firmly agglomerated, preventing the nitrogen permeating all the particle surfaces.

NST	Run	Adsorption Parameters			Specific Surface Area ($m^2 g^{-1}$)
		C	Intercept	Correlation Coefficient	
Micronised	1	61	0.01	0.9999	7.2
	2	60	0.01	0.9999	6.9
	3	59	0.01	0.9993	7.3
Milled	1	57	0.01	0.9999	5.6
	2	61	0.01	0.9999	5.5
	3	55	0.01	0.9999	5.9

Table 8.4 Surface area measurements for the milled and micronised NST.

8.3.5 X-Ray Powder Diffraction

Materials and Methods

X-ray powder diffraction (XRPD) was performed to assess the degree of crystallinity of both the milled NST and micronised material. The X-ray diffraction patterns were scanned between 5.00 and 59.62 in 0.02 degree steps.

Instrumentation

Philips PW 1730/00 4kW generator

Philips PW 2273/20 long fine focus 2kW copper target X-ray tube, operated at 40 kV, 25 mA.

Philips PW 1820/00 computer controlled vertical diffractometer goniometer.

Philips PW 1711/10 Xenon proportional counter with PW 1752/00 graphite monochromator and PW 1368/55 automatic divergence slit assembly.

Philips PW 1710/00 microprocessor diffractometer control Philips PW 1877 PC-APD, version 3.5b diffraction software.

Results and Discussion

Figure 8.4 shows the X-ray diffractogram for the milled NST superimposed on the X-ray information obtained for the micronised NST.

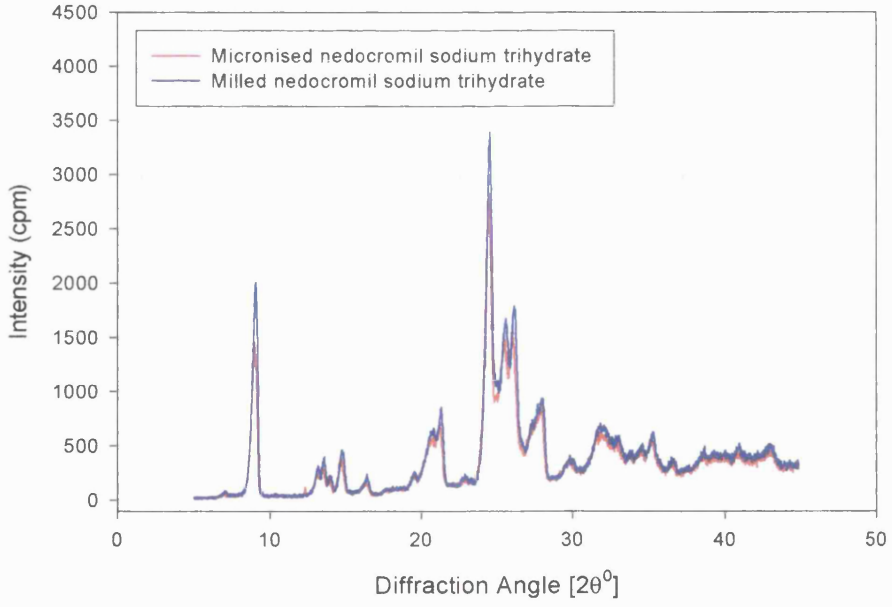

Figure 8.4 X-ray diffractograms for micronised and milled NST.

Figure 8.4 suggests that there is no difference in the degree of crystallinity between the milled and micronised NST.

The X-ray pattern of both materials show a series of sharp diffraction peaks indicating that these hydrates are crystalline.

8.4 *In-vitro* Aerosol Characterisation

Wong et al. (1995b) concluded that the *in-vitro* aerosol performance of milled NST was superior to that of the micronised NST. They reported that although the milled NST contained a smaller proportion of potentially respirable material when compared with the micronised material, a better *in-vitro* dispersion performance was obtained for blends containing the milled drug. The difference in dispersion was attributed to the cohesive interactions of the drug particles as a result of the differences in the particle size distributions. To more fully characterise the cohesive interactions governing the deaggregation and dispersion of milled and micronised samples of NST, a range of flow rates was employed to characterise the aerosol cloud.

8.4.1 Materials and Methods

The *in-vitro* aerosol performance of the milled and micronised NST was investigated using the modified Apparatus A at four different flow rates; 30, 60, 80 and 100 litres min^{-1}. Increasing the flow rate will reduce the $ECD_{50\%}$ for the stage-1 jet of Apparatus A (Hallworth and Westmoreland, 1987). Therefore, based on impactor theory (Hallworth and Westmoreland, 1987), modified stage-1 jets of known internal diameter were manufactured (section 2.5.1) and employed at the respective flow rate to maintain an $ECD_{50\%}$ of approximately 5 μm. Table 8.5 details the calculated and measured (if applicable) $ECD_{50\%}$ of the four stage-1 jets employed in the study. The modified stage-1 jet with an internal diameter of 14.2 mm was not calibrated.

Stage-1 Jet Internal Diameter (mm)	Calculated ($ECD_{50\%}$) (μm)	*Measured ($ECD_{50\%}$) (μm)
9.7	5.20 at 30 litres min^{-1}	6.6 (± 0.4)
11.6	4.80 at 60 litres min^{-1}	5.3 (± 0.3)
13.4	5.20 at 80 litres min^{-1}	5.4 (± 0.3)
14.2	5.08 at 100 litres min^{-1}	not measured

Table 8.5 Internal diameters for the stage-1 jets of the modified Apparatus A and the corresponding $ECD_{50\%}$ at the specified flow rate.
*Measured by AEA technology, Aerosol Science Centre, Oxfordshire, U.K.
±value in parenthesis is an estimate of precision (AEA data base).

8.4.2 Results and Discussion

For the 9.7 mm jet, the calibration value of 6.6 was higher than obtained from equation 2.3. Calculation of the Stokes number for the four jet sizes using equation 2.2 gives values of 0.115 – 0.118. However, for Reynold's numbers in the range 500-3000, the Stokes number for round impactor jets is quoted as 0.24 (Hinds, 1982). The calculated

Reynold's number for the 9.7 mm jet is 3500, which is not too far removed from the quoted range. Recalculation of the $ECD_{50\%}$ from equation 2.2 using a Stokes number of 0.24, gives a value of 7.3 μm. The measured value thus lies between the two estimates and can therefore be considered reasonable.

Capsules of fill weight 8 mg were discharged from the Cyclohaler® at the respective flow rate. Table 8.6 and figures 8.5 to 8.7 detail the aerosol performance of the milled and micronised NST at various flow rates.

One way analysis of variance revealed that increasing the flow rate produced a significant increase in the ED for the milled NST ($F = 98.4$, $p < 0.001$) but a significant decrease in the ED for the micronised NST ($F = 144.01$, $p < 0.001$). Fisher's pairwise comparisons revealed that the significant difference for both systems occurred when the flow rate was increased from 30 to 60 litres min^{-1}, with no significant differences in the ED observed thereafter. For both materials the capsule emptied efficiently and reproducibly (≤ 4% of the recovered drug retained) at all flow rates. However, when the flow rate was increased from 30 to 60 litres min^{-1}, there was a large increase in the percentage of micronised NST adhering to the device (5.04 ± 0.84% to 20.8 ± 2.2 % of the recovered drug).

It has been shown that increasing the flow rate generally increases the ED for carrier based DPI systems (Hindle and Byron, 1995b; Zanen et al. 1992). However, increasing the flow rate can also improve the deaggregation of the powder system leading to an increased generation of fine particle material (Newman et al. 1991a; Pitcairn et al. 1997). The increased surface area and hence surface free energy of the deaggregated systems may cause an increase in drug adhesion onto the device wall.

In-vitro Aerosol Characterisation			
Parameter	**Flow Rate (litres min^{-1})**	**Micronised NST**	**Milled NST**
% Capsule	30	2.09 ± 0.70	2.87 ± 0.49
% Device	30	5.04 ± 0.84	13.3 ± 2.0
% Stage 1	30	90.2 ± 1.4	69.5 ± 2.0
% Stage 2	30	2.66 ± 0.31	14.3 ± 0.89
Emitted Dose (mg)	30	7.53 ± 0.19	6.79 ± 0.18
Emitted Dose (%)	30	92.9 ± 1.4	83.8 ± 1.9
Fine Particle Dose (mg)	30	0.22 ± 0.024	1.16 ± 0.07
Fine Particle Fraction (%)	30	2.87 ± 0.34	17.1 ± 1.1
Drug Recovery (%)	30	101 ± 1.2	101 ± 1.2
% Capsule	60	3.73 ± 1.0	2.45 ± 0.20
% Device	60	20.8 ± 2.2	9.84 ± 2.6
% Stage 1	60	63.6 ± 3.7	66.2 ± 2.9
% Stage 2	60	11.9 ± 1.5	21.5 ± 2.6
Emitted Dose (mg)	60	6.06 ± 0.19	7.10 ± 0.26
Emitted Dose (%)	60	75.5 ± 2.4	87.7 ± 2.7
Fine Particle Dose (mg)	60	0.95 ± 0.12	1.85 ± 0.27
Fine Particle Fraction (%)	60	15.8 ± 2.5	24.5 ± 2.84
Drug Recovery (%)	60	100 ± 1.7	101 ± 0.96
% Capsule	80	3.42 ± 0.65	2.25 ± 0.39
% Device	80	19.3 ± 1.7	6.70 ± 0.75
% Stage 1	80	58.6 ± 2.4	67.9 ± 0.96
% Stage 2	80	18.7 ± 1.3	23.2 ± 0.72
Emitted Dose (mg)	80	6.28 ± 0.17	7.40 ± 0.12
Emitted Dose (%)	80	77.3 ± 1.7	91.1 ± 1.01
Fine Particle Dose (mg)	80	1.52 ± 0.10	1.88 ± 0.064
Fine Particle Fraction (%)	80	24.2 ± 1.9	25.5 ± 0.72
Drug Recovery (%)	80	102 ± 1.1	101 ± 1.27
% Capsule	100	3.65 ± 0.68	2.67 ± 0.33
% Device	100	19.3 ± 1.5	8.03 ± 0.95
% Stage 1	100	55.4 ± 2.8	67.1 ± 3.2
% Stage 2	100	21.6 ± 1.3	22.3 ± 2.2
Emitted Dose (mg)	100	6.23 ± 0.14	7.29 ± 0.18
Emitted Dose (%)	100	77.1 ± 1.8	89.3 ± 1.25
Fine Particle Dose (mg)	100	1.75 ± 0.10	1.82 ± 0.18
Fine Particle Fraction (%)	100	28.1 ± 2.1	24.9 ± 2.8
Drug Recovery (%)	100	101 ± 0.61	102 ± 1.7

Table 8.6 *In-vitro* aerosol characterisation of the milled and micronised NST at various flow rates. Values are the mean ± SD of ten determinations. ED and FPD were normalised with respect to an 8 mg fill weight.

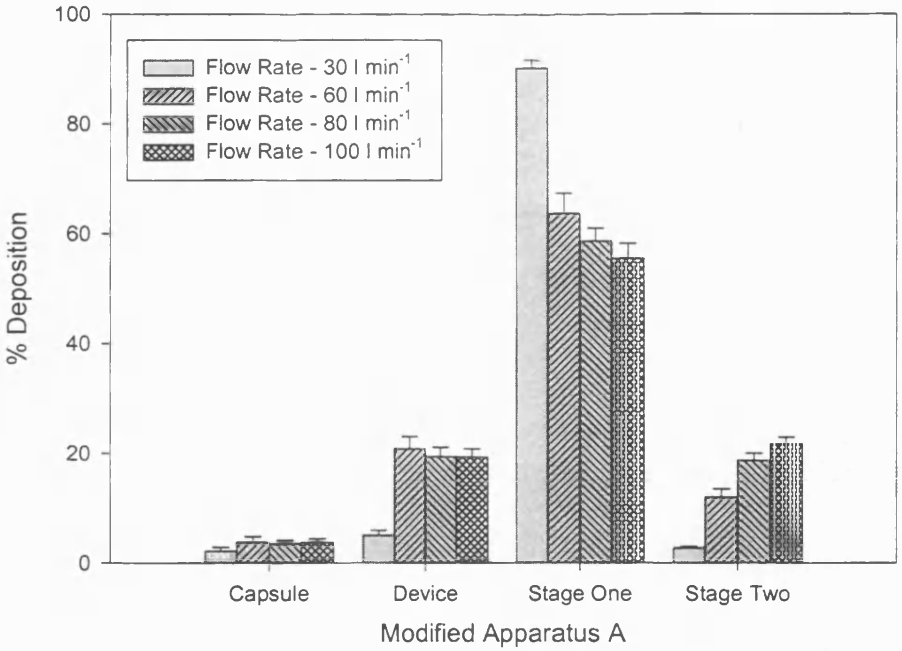

Figure 8.5 The effects of flow rate on the *in-vitro* aerosol performance of micronised NST.

Each column shows the mean of 10 determinations (bars represent SDs).

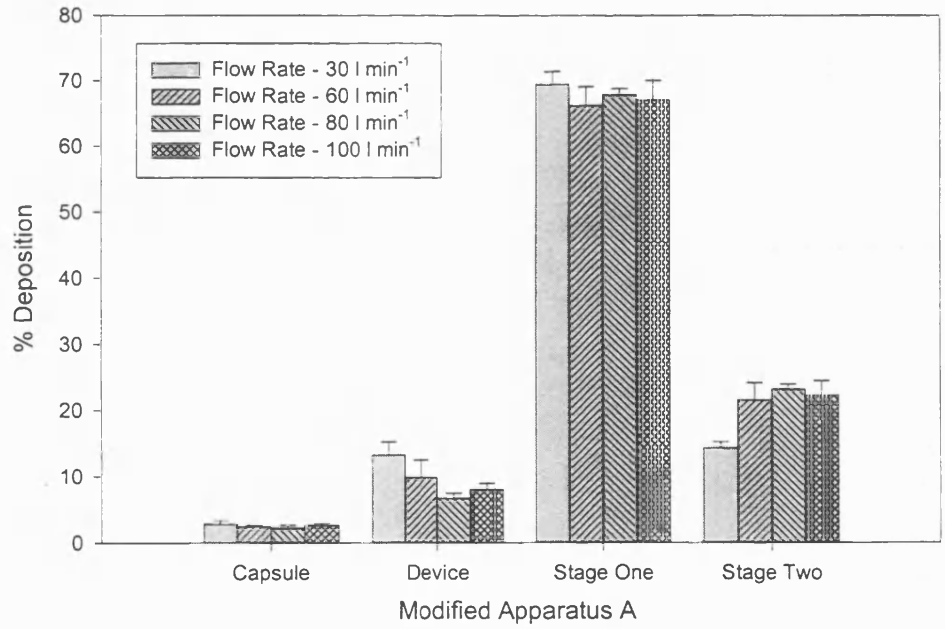

Figure 8.6 The effects of flow rate on the *in-vitro* aerosol performance of milled NST.

Each column shows the mean of 10 determinations (bars represent SDs).

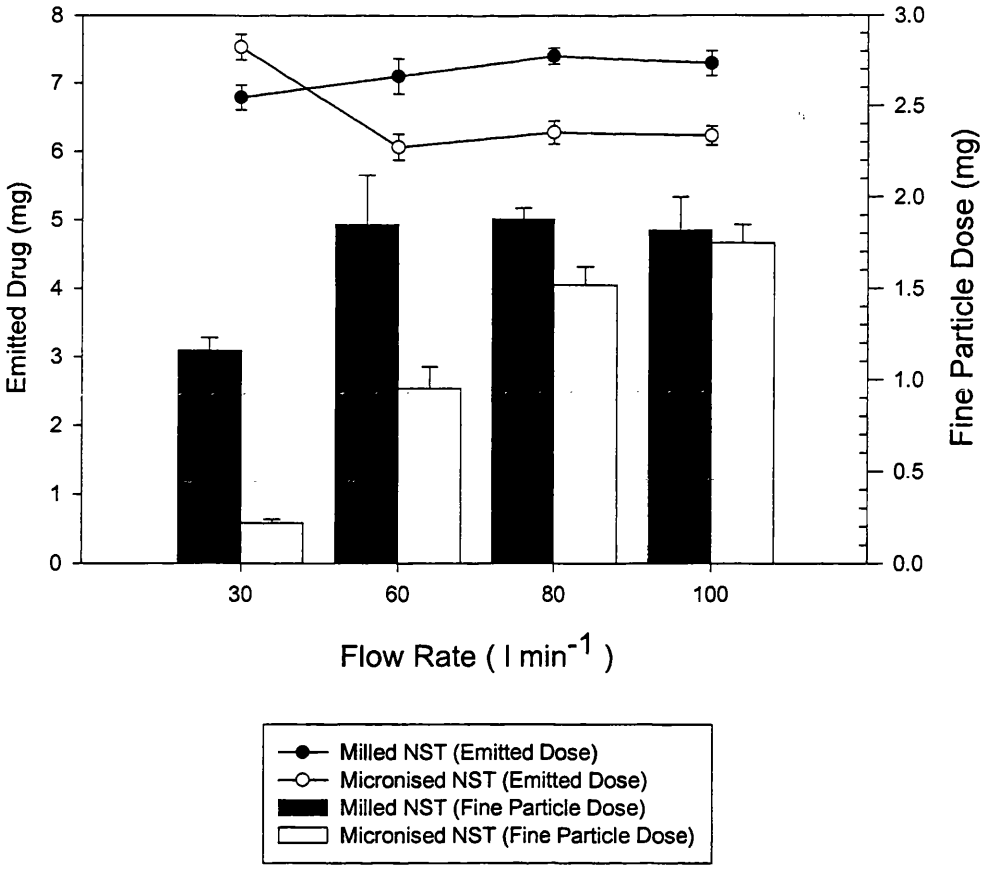

Figure 8.7 The effects of flow rate on the *in-vitro* aerosol performance of milled and micronised NST.
ED values are the mean ± SD of ten determinations.
FPD values are the mean + SD of ten determinations.

At flow rates ≥60 litres min^{-1}, the milled NST showed a decreased tendency to adhere to the device wall. This suggested that the deaggregation of the milled NST did not result in the regeneration of discrete particles. Instead, the milled powder system may deagglomerate into aggregates of milled NST with a larger effective size and therefore, a decreased surface free energy.

Fine Particle Drug Deposition

The deaggregation (FPF) and subsequent stage-2 deposition (FPD) of the pure drug systems was characterised over the range of flow rates. The micronised NST displayed

a continual increase in both the FPF and FPD with increasing flow rates. However, one way analysis of variance in conjunction with Fisher's pairwise comparisons, revealed that the milled NST only showed an increase in drug deaggregation (FPF) when the flow rate was increased from 30 to 60 litres min^{-1} ($F = 34.72$, $p < 0.001$). However, the milled system showed no significant increase in the deaggregation of the system thereafter.

The Students *t-test* revealed that the milled NST is deaggregated more completely (FPF) into discrete particles and/or potentially respirable aggregates (≤5 μm, D_{ae}) at flow rates of 30 litres min^{-1} ($t = 40.59$, $p < 0.001$) and 60 litres min^{-1} ($t = 7.24$, $p < 0.001$) when compared with the micronised NST. However, there is no significant difference between the FPF of the micronised or milled NST when the systems are deaggregated at 80 litres min^{-1} ($t = 2.06$, $p = 0.055$) and at 100 litres min^{-1}, the deaggregation of the emitted drug is significantly greater for the micronised material ($t = 2.17$, $p = 0.044$).

The results suggest that the cohesive interactions operating within the micronised NST powder system are greater than those operating within the milled NST system. However, from both LTSEM and LALLS studies, the particle size distributions of the two materials do not appear to differ dramatically.

It is proposed that the milling and micronisation stages, employed in the manufacture of the fine particle NST (Clark and Hollingworth, 1993b), are not in fact size reduction stages but instead deaggregation stages. The VMD of both materials is approximately 1 μm however, the micronised NST requires a greater input of energy (increased flow rate) to achieve the same degree of deaggregation. The initial process of crystallisation

produce particles with a VMD of approximately 1 μm, which due to their large surface area and excess surface free energy experience strong cohesive interactions (Adjei and Gupta, 1997). It is considered that the cohesive interactions operating within this system would not be overcome by the shear forces generated upon aerosolisation of the powder system from a DPI device.

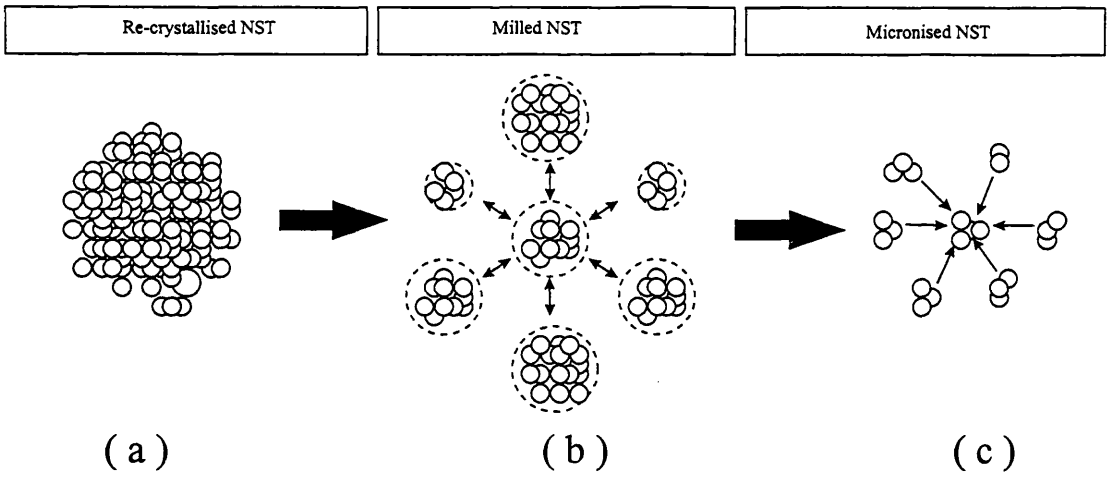

Figure 8.8 Diagrammatic representation of the cohesive interactions thought to be operational in the initial crystallised material and the milled and micronised NST systems.

The milling process may partially deaggregate the system into smaller sized agglomerates, of which a fraction may be potentially respirable (figure 8.8b). The cohesive interactions operating between agglomerates are considered to be reduced due to their larger effective size. However, the constituent particles within these milled agglomerates are still considered bound by strong cohesive interactions. Therefore, upon aerosolisation the system can be partially deaggregated (at relatively low shear forces) into the smaller agglomerates, some of which possess an $D_{ae} \leq 5$ μm. However, deaggregation will not be complete since the shear forces generated will only be sufficient to overcome the forces binding the agglomerates and not to deaggregate the

system into its constituent particles. Since only a fraction of the agglomerates have an $D_{ae} \leq 5$ μm, the efficiency of the system is compromised.

The air jet milling employed to produce the micronised NST may further deaggregate the milled NST. The micronised system (figure 8.8c) is considered to consist of a greater percentage of discrete particles together with smaller sized, potentially respirable agglomerates. Due to the increased surface area and surface free energy, the cohesive interactions binding the micronised NST particles/agglomerates are considered to be greater than the forces binding the agglomerates produced by milling. However, due to the deaggregation stages, the interparticle interactions are less than those acting within; a) the original crystallised material or b) the agglomerates of the milled system.

Therefore, a greater force is required to regenerate potentially respirable particles from the micronised system but there is an increased potential for fine particle deposition compared with the milled material; an optimum FPD is not attained even at 100 litres min^{-1} for the micronised NST. The increased regeneration of discrete NST particles is possibly reflected by the increase in adhesive interactions at the higher flow rates (increased device deposition).

At 100 litres min^{-1}, the micronised NST shows a significant improvement in the FPF compared with the milled material ($t = 2.17$, $p = 0.044$). However, this improved deaggregation does not translate into a significant improvement in the FPD ($t = 1.25$, $p = 0.23$) due to the increased adhesion of the micronised NST particles onto the device walls. The flow rate corresponding to a pressure drop of 4 kPa was measured (section

2.5) at 96 litres min^{-1}. Therefore, the difference in deaggregation properties of the two samples may not transfer into any improved performance in clinical practice.

Unfortunately, the unprocessed NST could not be obtained for characterisation.

8.5 General Discussion

It is recognised that the techniques employed to assess the total water content (KF and DSC) and the degree of crystallinity (XRPD) may not be sensitive enough to detect surface changes that may influence the physical properties of the two power samples. XRPD has been shown to only be able to detect 10% or more of amorphous material in powders (Saleki-Gerhardt et al. 1994). Stresses induced during processing may result in considerably less than 10% of the material becoming amorphous (Buckton, 1995). Furthermore, the disruption will not be distributed uniformly throughout the powder mass but will predominate at the surfaces that have been subjected to the processing stress (Elamin et al. 1994). Therefore, small quantities of amorphous material may be very significant with respect to surface interactions. Future experimental work may utilise techniques that can obtain a thermodynamic assessment of the powder surface properties of the milled and micronised NST (Buckton, 1997; Feeley et al. 1998; Ticehurst et al. 1994).

The cohesive interactions governing the aerosol performance of NST powder formulations would appear to result from the ultrafine nature of the constituent particles. The importance of formulating systems for inhalation, containing drug particles with an

D_{ae} ≤5 μm is widely recognised. However, the cohesive interactions operating within systems containing particles at the lower end of this particle size range may be too great for the efficient deaggregation and regeneration of discrete particles.

In agreement with Wong et al. (1995b), the milled NST demonstrates improved aerosol characteristics (increased ED and FPD) at lower flow rates (≤60 litres min^{-1}). However, the potential for complete deaggregation from a DPI formulation/device system at attainable flow rates would appear unattainable due to the strong interparticle forces acting within the aggregates.

It is considered, based on the aerosol performance of the milled and micronised NST, that to improve the performance of the micronised NST, the crystallisation of the original material needs optimising to produce potentially respirable particles but with a larger particle size. This may lead to a decrease in the surface free energy of the system and therefore, the more efficient regeneration of discrete particles upon aerosolisation.

CHAPTER 9

GENERAL DISCUSSION

The interparticle interactions governing the mixing and aerosol properties of powder systems containing a high mass of NST were investigated. By correlating the deaggregation of the powder system following various formulatory procedures, it was hoped that the contributions of cohesive (drug/drug) and adhesive (drug/carrier) interparticle interactions to the performance of NST as a high mass aerosol system could be established. To supplement these formulation studies, LTSEM and ESEM investigations were performed on the powder formulations since NST was not amenable to characterisation by conventional SEM techniques.

Optimisation of particle sizing procedures (LALLS), revealed that the micronised NST was an ultrafine powder with a VMD of approximately 1 μm and with 90% of the particles having an equivalent volume diameter <5 μm. LTSEM, a novel technique for studying hydrated pharmaceutical material, confirmed this particle size distribution.

Preliminary investigations studied the deaggregation and subsequent stage-2 deposition (modified Apparatus A) of pure NST (no carrier) to assess the extent of the cohesive interactions governing the aerosol performance of the system. Generally, the deaggregation and subsequent stage-2 deposition were considered to be poor; FPF <15 % and FPD <1 mg when an 8 mg capsule fill weight was discharged from the Cyclohaler® at 60 litres min^{-1}.

Therefore, the aerosol performance of NST formulated with lactose as a high mass drug system was assessed. Information regarding the interparticle forces of adhesion and cohesion governing the aerosol performance of high mass carrier based formulations of NST was inferred from these studies.

It has previously been reported that the TTM can be used to prepare carrier based systems for inhalation containing a high mass of both NST and DSCG (Braun et al. 1996; Vidgren et al. 1987b, 1988a, 1988b, 1989 and 1990; Wong et al. 1995a and 1995). Therefore, coarse carrier lactose based formulations (63-90 μm) were initially assessed, blending the drug and excipient materials for various time periods in the TTM with and without the inclusion of screening stages.

An acceptable homogeneity of drug within the blend (CV <5 %) was achieved by careful control of the mixing time and the inclusion of screening stages. However, it was considered that due to the high percentage of NST present within the formulation, the quality of the mix was governed by interactions operating between the ordered units of NST and the carrier component (lactose particles with either minimal, mono- or multi-particle layer coverage) and the agglomerates of pure drug. Formulations produced using the TTM with a 63-90 μm coarse carrier sieve fraction of lactose did not improve the deaggregation or subsequent fine particle deposition of NST when formulated as a high mass (40 % $^{w}/_{w}$) drug system. Although an acceptable drug content uniformity was obtained it was considered that the selection of the coarse carrier fraction and/or the mixing technique employed, failed to effectively deaggregate the pure drug agglomerates and promote the subsequent distribution of NST onto the carrier. Despite its extensive use in previous studies investigating high mass drug systems, the TTM is considered inappropriate for the formulation of high mass NST powder systems (and possibly other high dose compounds) when formulated as a coarse carrier based system. It was considered that despite the inclusion of a coarse carrier component, the aerosol performance of the powder systems was still governed by the cohesive drug/drug interactions.

Attempts were made to improve the aerosol performance of the coarse carrier formulations by blending the components using alternative mixing techniques, capable of producing increased shear forces (HB and RBB). However, the aerosol performance of the systems was still considered to be poor; FPF <11 % and FPD <0.7 mg.

Therefore, the use of alternative lactose size fractions was investigated. The addition of 5% $^{w}/_{w}$ FPL to the carrier component, a procedure which has previously been shown to improve the aerosol performance of low dose powder systems (Lucas et al. 1998a and 1998b) failed to improve the aerosol performance of the high mass NST systems. It was considered that although the FPL may promote drug liberation from the carrier surface (Hersey, 1975; Lucas et al. 1998a), the interparticle forces governing the aerosol performance of NST are the cohesive drug/drug interactions.

By decreasing the particle size of the carrier (<45 μm sieve size fraction or the use of FPL), the deaggregation and subsequent fine particle drug deposition was improved dramatically. Further improvements were made by selecting and then optimising high shear mixing procedures (RBB), resulting in efficient drug deaggregation FPF >50 % which translated into an improved FPD >3 mg. It was concluded, based on these findings together with the evidence from LTSEM and EDAX images, that the FPL is producing its functional effects by intercalating within the drug self-agglomerates and physically disrupting the cohesive drug/drug interactions. The use of a smaller sized lactose size fraction in conjunction with a blending procedure capable of disrupting the drug self-agglomerates allowed the optimum intercalation of the excipient material within the self agglomerates. It was concluded that the adhesive NST/FPL interactions were weak compared to the cohesive NST/NST particle interactions; cohesive

interactions that would normally govern the aerosol performance of high mass NST powder systems.

The optimised formulation was aggregated into free flowing spheres, which displayed the same improved aerosol properties as the non-aggregated system. However, it was demonstrated that a compromise must be attained between the robustness of the sphere and the efficient regeneration of discrete particles or potentially respirable drug aggregates upon aerosolisation.

The intercalation of FPL within systems containing TS failed to produce an improvement in the deaggregation of the powder system upon aerosolisation, suggesting that the functional effects of the FPL are material dependent.

It was subsequently decided to investigate possible causes of the strong cohesive interactions operating within the pure NST drug system. Since NST is a highly hydrated compound, the effects of storage humidity on the extent of water sorption and its subsequent effects on the aerosol performance of the drug system were assessed.

Nedocromil sodium is stable as the trihydrate over the relative humidity range 6.4 to 79.5% (Khankari et al. 1998). Over the humidity range 12% to 76% RH, no dramatic effects on the deaggregation and fine particle deposition were observed for the NST powder system. Particles stored at 12% RH showed an improved deaggregation (FPF ~20%) however, this did not translate into a dramatic improvement in the FPD (<1.2 mg) due to the increased adhesion of the system causing a greater device retention. However, conversion to the heptahemihydrate dramatically decreased the deaggregation (FPF < 8%) and subsequent fine particle deposition (FPD < 0.5mg). Liquid and/or solid

bridge formation, as suggested by LTSEM investigations, were believed to be the cause of the difficulty in deaggregating the NSHH system.

It was considered that the fine nature of the material might be responsible for the strong cohesive interactions governing the aerosol performance of NST containing systems. Therefore, based on reports in the literature (Wong et al. 1995b), a sample of milled NST was extensively characterised and its physicochemical and aerosol properties compared to the micronised material.

Both LTSEM and LALLS suggested that the particle size distributions of the two materials did not differ dramatically. However, the *in-vitro* aerosol characterisation of both materials suggested that the cohesive interactions operating within the micronised NST powder system were greater than those operating within the milled NST system.

It is suggested that the milling and micronisation stages, employed in the manufacture of the fine particle NST, are not in fact size reduction stages but instead deaggregation stages. Due to the increased surface area and surface free energy, the cohesive interactions binding the micronised NST particles/agglomerates are considered to be greater than the forces binding the agglomerates produced by milling.

The cohesive interactions governing the aerosol performance of NST powder formulations would appear to result from the ultrafine nature of the constituent particles. It is considered, based on the aerosol performance of the milled and micronised NST, that to improve the performance of the micronised NST the crystallisation of the original material needs optimising to produce potentially respirable particles but with a larger particle size. This may lead to a decrease in the surface free energy of the system and therefore, the more efficient regeneration of discrete particles upon aerosolisation.

The importance of formulating systems for inhalation containing drug particles with an $D_{ae} \leq 5$ μm is widely recognised. However, the cohesive interactions operating within systems containing particles at the lower end of this particle size range may be too great for the efficient deaggregation and regeneration of discrete particles.

CHAPTER 10

CONCLUSIONS

Conclusions

By assessing the mixing behavior and the *in-vitro* aerosol performance of high dose NST powder systems, information regarding the interparticle interactions governing the powders' properties was gained.

LTSEM, a technique considered novel to the characterisation of pharmaceutical particles, was developed. By freezing and thus stabilising sorbed moisture, LTSEM enabled the micronised and milled samples of NST and NSHH to be imaged. LTSEM and ESEM were both used to characterise the drug particles' distribution within powder systems containing coarse and/or fine lactose material.

The re-generation of potentially respirable NST particles from carrier based and self-agglomerated drug systems was considered poor due to the strong cohesive interactions operating within the drug system. Formulation studies revealed that the inclusion of a coarse lactose carrier in high dose drug systems containing NST, had no significant effect in disrupting the drug/drug cohesive interactions. It was also concluded that the use of tumbling action mixers should be avoided when formulating NST and possibly other fine material due to the increased chance of self-aggregation of the drug system.

An improved deaggregation of the pure drug system was achieved by selecting fine excipient material in conjunction with a mixing procedure capable of producing increased shear forces. The two formulatory procedures initially enabled the physical disruption of the cohesive drug interactions, which subsequently allowed the finer excipient particles to intercalate within the drug self-aggregates. By physically disrupting the drug/drug

interparticle interactions, more complete deaggregation of the drug system was achieved with a subsequent three-fold increase in the fine particle deposition of NST.

LTSEM in conjunction with EDAX confirmed the intercalation of FPL within the cohesive drug system. This combination of techniques is considered novel to the analysis of pharmaceutical particle systems.

The inclusion of the fine excipient material did not adversely affect the tendency of NST to self-agglomerate, a property considered useful when trying to formulate a powder for inhalation with acceptable flow properties.

Storage humidity does not have a dramatic effect on the deaggregation and subsequent fine particle deposition of NST.

LALLS and LTSEM characterisation of the milled and micronised NST revealed that both materials are ultrafine powders. The cohesive interactions dictating the performance of NST powder systems were considered to result from the ultrafine nature of the material. In this system, producing drug particles of too small a particle size compromised the DPI formulations without improving the fine particle dose.

Alternative methods of producing potentially respirable drug particles, e.g. supercritical fluid technology or spray drying, may result in the generation of fine particles with reduced surface energies. These particles may deaggregate more completely upon aerosolisation due to a reduction in the cohesive interactions operating within the system.

CHAPTER 11

FURTHER WORK

Further Work

Particles size within the D_{ae} range 1-5 μm needs to be investigated especially when considering high dose drug systems where cohesive interactions may govern the mixing and aerosol performance of the powder system.

Future work should concentrate on assessing the surface energetics of NST particles in discrete size channels between 1 and 5 μm. The atomic force microscope (AFM) may provide an ideal tool with which to further these investigations (Bowen et al. 1998). Additionally, the effects of triboelectrification on the deaggregation of the powder system should be assessed and correlated with electrostatic measurements on the bulk powder system (Peart, 1996). Assessment of the surface energetics of the milled and micronised NST as well as powder systems stored at various humidities might also provide useful information.

Optimisation of the aggregated drug systems by the inclusion of an even finer excipient material may also provide new formulation strategies with which to formulate high dose drug systems.

CHAPTER 12

REFERENCES

Adjei, A. and Garren, J. (1990). Pulmonary Delivery of Peptide Drugs: Effect of Particle Size on Bioavailability of Leuprolide Acetate in Healthy Male Volunteers. *Pharmaceutical Research,* **7(6)**, 565-569.

Adjei, A.L. and Gupta, P.K. (1997). Dry Powder Inhalation Aerosols. In. A.L. Adjei and P.K. Gupta (eds.), Inhalation Delivery of Therapeutic Peptides and Proteins, Marcel Dekker, New York, 625-665.

Ahlneck, C. and Zografi, G. (1990). The Molecular Basis of Moisture Effects on the Physical and Chemical Stability of Drugs in the Solid State. *International Journal of Pharmaceutics*, **62**, 87-95.

Akiyama, T. and Tanijri, Y. (1989). Criterion for Re-entrainment of Particles. *Powder Technology*, **57**, 21-26.

Altounyan, R.E.C. (1985). Sodium Cromoglycate More Effective in Small-Particle Inhalations. *The Practitioner*, **229**, 396-397.

Ampratwum, E.Y., Taylor, K.M.G., Buckton, G., Wong, D.Y.T. and Chippendale, K. (1997). The Effect of Relative Humidity on Milled and Spray Dried Nedocromil Sodium. *Journal of Pharmacy and Pharmacology*, **49(4)**, 48.

Asking, L. and Olsson, B. (1997). Calibration at Different Flow Rates of a Multistage Liquid Impinger. *Aerosol Science and Technology*, **27**, 39-49.

Auty, R.M., Brown, K., Neale, M.G. and Snashall, P.D. (1987). Respiratory Tract Deposition of Sodium Cromoglycate is Highly Dependent upon Technique of Inhalation Using the Spinhaler. *British Journal of Diseases of the Chest*, **88**, 371-378.

Babic, I., Roy, S., Watada, A.E. and Wergin, W.P. (1996).
Changes in Microbial Populations on Fresh Cut Spinach.
International Journal of Food Microbiology, **31**, 107-119.

Bailey, A.G. (1984). Electrostatic Phenomena During Powder Handling.
Powder Technology, **37**, 71-85.

Balachandran, W., Ahmad, C.N. and Barton, S.A. (1991). Deposition of Electrically Charged Drug Aerosols in Lungs. *Institute of Physics Conference Series*, **118**, 57-62.

Basran, G.S., Darbyshire, J.H., Nunn, A.J. and Turner-Warwick, M. (1984).
Inhaled Lactose Free Powder in the Treatment of Recurrent Asthma.
British Journal of Diseases of the Chest, **78**, 254-260.

Bastacky, J., Hook, G.R., Finch, G.L., Goerke, J. and Hayes, T.L. (1987).
Low Temperature Scanning Electron Microscopy of Frozen Hydrated Mouse Lung. *Scanning*, **9**, 57-70.

Beckett, A. and Read, N.D. (1986). Low Temperature Scanning Electron Microscopy. In: Aldrich, H.C. and Todd, W.J. (eds.), Ultrastructural Techniques for Micro-organisms. Plenum, New York, U.S.A., 45-86.

Bell, J.H., Hartley, P.S. and Cox, J.S.G. (1971). Dry Powder Aerosols. I. A New Powder Inhalation Device. *Journal of Pharmaceutical Sciences*, **60(10)**, 1559-1564.

Bell, J.H., Brown, K. and Glasby, J. (1973a). Variation in Delivery of Isoprenaline From Various Pressurised Inhalers.
Journal of Pharmacy and Pharmacology, **25(suppl.)**, 32P-36P.

Bell, J.H., Stevenson, N.A. and Taylor, J.E., (1973b). A Moisture Transfer Effect in Hard Gelatin Capsules of Sodium Cromoglycate.
Journal of Pharmacy and Pharmacology, **25(suppl.)**, 96P-103P.

Berressem, P. (1999). The Birth of New Delivery Systems.
Chemistry in Britain, 29-32.

Biddiscombe, M.F., Melchor, R., Mak, V.H.F., Marriott, R.J., Taylor, A.J., Short, M.D. and Spiro, S.G. (1993). The Lung Deposition of Salbutamol, Directly Labelled With Technetium-99m, Delivered By Pressurised Metered Dose and Dry Powder Inhalers.
International Journal of Pharmaceutics, **91**, 111-121.

Boerefijn, R., Ning, Z. and Ghadiri, M. (1998). Disintegration of Weak Lactose Agglomerates for Inhalation Applications.
International Journal of Pharmaceutics, **172**, 199-209.

Bowen, R.W., Hilal, N., Lovitt, R.W. and Wright, C.J. (1998). A New Technique for Membrane Characterisation: Direct Measurement of the Force of a Adhesion of a Single Particle Using an Atomic Force Microscope.
Journal of Membrane Science, **139**, 269-274.

Braun, M.A., Oschmann, R. and Schmidt, P.C. (1996). Influence of Excipients and Storage Humidity on the Deposition of Disodium Cromoglycate (DSCG) in the Twin Impinger. *International Journal of Pharmaceutics,* **135**, 53-62.

Brindley, A., Sumby, B.S., Smith, I.J., Prime, D., Haywood, P.A. and Grant, A.C. (1995). Design, Manufacture and Dose Consistency of the Serevent Diskus Inhaler. *Pharmaceutical Technology*, **1**, 22-32.

Brittain, H.G., Bugay, D.E., Bogdanowich, S.J. and DeVincentis, J. (1988).
Spectral Methods for Determination of Water.
Drug Development and Industrial Pharmacy, **14(14)**, 2029-2046.

British National Formulary. (1999). HMSO: London.

British Pharmacopoeia. (1998). HMSO: London.

Bryan, L., Runvejhavuttivittaya, Y., Stewart, P. (1979). Mixing and Demixing of Microdose Quantities of Sodium Salicylate in a Direct Compression Vehicle.
Journal of Powder Technology, **22**, 147-151.

Byron, P.R. (1986). Some Future Perspectives for Unit Dose Inhalation Aerosols. *Drug Development and Industrial Pharmacy*, **12(7)**, 993-1015.

Byron, P.R. (1990). "Aerosol Formulation, Generation and Delivery Using Nonmetered Systems". In: Byron, P.R. (ed.), Respiratory Drug Delivery, (CRC Press, Boca Raton, FL.), 144-165.

Byron, P.R., Davis, S.S., Bubb, M.D. and Cooper, P. (1977). Pharmaceutical Implications of Particle Growth at High Relative Humidities. *Pesticide Science*, **8**, 521-526.

Buckton, G. (1995). Surface Characterisation: Understanding Sources of Variability in the Production and use of Pharmaceuticals. *Journal of Pharmacy and Pharmacology*, **47**, 265-275.

Buckton, G. (1997). Characterisation of Small Changes in the Physical Properties of Powders of Significance for Dry Powder Inhaler Formulations. *Advanced Drug Delivery Reviews*, **26**, 17-27.

Cairns, H., Cox, D., Gould, K.J., Ingall, A.H. and Suschitzky, J.L. (1985). New Anti-Allergic Pyrano[3,2-g]Quinoline-2,8,-Dicarboxylic Acids with Potential for the Topical Treatment of Asthma. *Journal of Medicinal Chemistry*, **28**, 1832-1842.

Carr, R.L. (1965). Evaluating Flow Properties of Solids. *Chemical Engineering*, **18**, 163-168.

Chan, H-K. and Gonda, I. (1993). Preparation of Radiolabelled Materials for Studies of Deposition of Fibers in the Human Respiratory Tract.
Journal of Aerosol Medicine, **6**, 241-249.

Chan, H-K. and Gonda, I. (1995). Physicochemical Characterisation of a New Respirable Form of Nedocromil.
Journal of Pharmaceutical Sciences, **84(6)**, 692-696.

Chan, S.Y. and Pilpel, N. (1983). Absorption of Moisture by Sodium Cromoglycate and Mixtures of Sodium Cromoglycate and Lactose.
Journal of Pharmacy and Pharmacology, **35**, 477-781.

Chawla, A., Buckton, G., Taylor, K.M.G., Newton, J.M. and Johnson, M.C.R. (1993). Surface Energy Determinations of Powders for use in Dry Powder Aerosol Formulations. *Journal of Pharmacy and Pharmacology*, **44**, 1069.

Chawla, A., Taylor, K.M.G., Newton, J.M. and Johnson, M.C.R. (1994). Production of Spray Dried Salbutamol Sulphate for use in Dry Powder Aerosol Formulation. *International Journal of Pharmaceutics,* **108**, 233-240.

Chenu, C. and Tessier, D. (1995). Low Temperature Scanning Electron Microscopy of Clay and Organic Constituents and their Relevance to Soil Microstructure.
Scanning Microscopy, **9(4)**, 989-1010.

Clark, A.R. and Hollingworth, A.M. (1993a). The Relationship Between Powder Inhaler Resistance and Peak Inspiratory Conditions in Healthy Volunteers - Implications for *In-vitro* Testing. *Journal of Aerosol Medicine*, **6(2)**, 99-110.

Clark, A.R. and Hollingworth, A.M. (1993b). Pharmaceutical Composition. US Patent 5198221.

Clarke, M.J., Potter, U.J., Gilpin, C., Tobyn, M.J. and Staniforth, J.N. (1998). Imaging of Hygroscopic Ultrafine Pharmaceutical Powders Using Low Temperature and Environmental Scanning Electron Microscopy. *Pharmacy and Pharmacology Communications*, **4**, 419-425.

Clay, M.M., Pavia, D. and Clarke, S.W. (1986). Effect of Aerosol Particle Size on Bronchodilation with Nebulised Terbutaline in Asthmatic Subjects. *Thorax*, **41**, 364-368.

Coelho, M.C. and Harnby, N. (1978a). Moisture Binding in Powders. *Powder Technology*, **20**, 201-205.

Coelho, M.C. and Harnby, N. (1978b). The Effect of Humidity on the Form of Water Retention in a Powder. *Powder Technology*, **20**, 197-200.

Concessio, N.M., Van Oort, M.M. and Hickey, A.J. (1998). Impact Force Separation Measurements-Their Relevance In Powder Aerosol Formulation. In: Byron, P.R., Dalby, R.N. and Farr, S.J. (eds.), *Respiratory Drug Delivery VI*, Interpharm Press, Buffalo Grove, IL, 251-258.

Connors, K.A. (1988). The Karl Fischer Titration of Water.
Drug Development and Industrial Pharmacy, **14(14)**, 1891-1903.

Corn, M. (1966). Adhesion of Particles. In: C.N. Davies (ed.), Aerosol Science, Academic Press, N.Y., 359-392.

Crompton, G.K. (1982). Problems Patients have Using Pressurised Aerosol Inhalers.
European Journal of Respiratory Diseases, **63(suppl 119)**, 101-104.

Curry, S.H., Taylor, A.J., Evans, S., Godfrey, S. and Zeidifard, E. (1974).
Disposition of Disodium Cromoglycate Administered in Three Particle Sizes.
Journal of Pharmacy and Pharmacology, **26(Suppl.)**, 79P.

Danilatos, G.D. (1991). Review and Outline of Environmental SEM at Present.
Journal of Microscopy, **162(3)**, 391-402.

D'Emanuele, A. and Gilpin, C. (1996). Applications of the Environmental Scanning Electron Microscope to the Analysis of Pharmaceutical Formulations.
Scanning, **18**, 522-527.

D'Emanuele, A., Dennis, A., McCann, D. and Muir, I. (1998). The imaging of a Contolled-Release Pellet Formulation Using Scanning Electron Microscopy-Potential for Artefact Generation. *Pharmaceutical Development and Technology*, **3(1)**, 135-139.

Diffraction Training: Windows Diffraction Training Manual. (1993).
Malvern Instruments Ltd., U.K.

Djordjevic, N.M, Rohr, G., Hinterleitner, M. and Schreiber, B. (1992).
Adsorption of Water on Cyclosporin A, from Zero to Finite Surface Coverage.
International Journal of Pharmaceutics, **81**, 21-29.

Dove, J.W., Buckton, G. and Doherty, C. (1996). A Comparison of Two Contact Angle Measurement Methods and Inverse Gas Chromatography to Assess the Surface Energies of Theophylline and Caffeine.
International Journal of Pharmaceutics, **138**, 199-206.

Edwards, A.M. and Chambers, A. (1989). Comparison of a Lactose-Free Formulation of Sodium Cromoglycate and Sodium Cromogylcate plus Lactose in the Treatment of Asthma. *Current Medical Research and Opinion*, **11(5)**, 283-292.

Edwards, D.A., Hanes, J., Caponetti, G., Hrkach, J., Ben-Jebria, A., Eskew, M.L., Mintzes, J., Deaver, D., Lotan, N. and Langer, R. (1997). Large Porous Particles for Pulmonary Drug Delivery. *Science*, **276**, 1868-1871.

Elamin, A.A., Ahlneck, C., Alderborn, G. and Nystrom, L. (1994). Increased Metastable Solubility of Milled Griseofulvin Depending on the Formation of a Disordered Surface Structure. *International Journal of Pharmaceutics*, **111**, 159-170.

El-Basier, M.M., Phipps, M.A. and Kellaway, I.W. (1997). Preparation and Subsequent Degradation of Poly(L-lactic acid) Microspheres Suitable for Aerosolisation: A Physico-chemical Study.
International Journal of Pharmaceutics, **151**, 145-153.

Etzler, F.M. and Sanderson, M.S. (1995). Particle Size Analysis: A Comparative Study of Various Methods. *Particle and Particle System Characterization*, **12**, 217-224.

European Pharmacopeia (1998). Third Edition, Supplement, Strasbourg.

Evans, R. (1993). Determination of Drug Particle Size and Morphology Using Optical Microscopy. *Pharmaceutical Technology,* **March**, 146-152.

Fearon, W.R. (1942). The Detection of Lactose and Maltose by Means of Methylamine. *Analyst*, **67**, 130-132.

Feeley, J.C., York, P., Sumby, B. S. and Dicks, H. (1998). Determination of Surface Properties and Flow Characteristics of Salbutamol Sulphate, Before and After Micronisation. *International Journal of Pharmaceutics,* **172**, 89-96.

Freer, A.A., Payling, D.W., Suschitzky, J.L. (1987). Structure of Nedocromil Sodium: A Novel Anti-Asthmatic Agent. *Acta Crystallography*, **C43**, 1900-1905.

French, D.L., Edwards, D.A. and Niven, R.W. (1996). The Influence of Formulation on Emission, Deaggregation and Deposition of Dry Powders for Inhalation. *Journal of Aerosol Science*, **27(5)**, 769-783.

Fults, K.A., Miller, I.F. and Hickey, A.J. (1997). Effect of Particle Morphology on Emitted Dose of Fatty Acid-Treated Disodium Cromoglycate Powder Aerosols. *Pharmaceutical Development and Technology*, **2(1)**, 67-79.

Ganderton, D. (1992). The Generation of Respirable Clouds From Coarse Powder Aggregates. *Journal of Biopharmaceutical Sciences*, **3(1/2)**, 101-105.

Ganderton, D. and Kassem, N.M. (1992). Dry Powder Inhalers. In: Ganderton, D. and Jones, T. (eds.), Advances in Pharmaceutical Sciences, Vol 6, Academic Press, London 165-191

Ganderton, D. (1996). International Harmonisation: The Revision of the "Inhalanda" Monograph of the European Pharmacopoeia. *Pharmeuropa*, **8**, 245-258.

Genus, E.R.M., Toren, J.S., Barends, D.M. and Bult, A. (1997). Decrease of the Stage-2 Deposition in the Twin Impinger During Storage of Beclomethasone Dipropionate Dry Powder Inhalers in Controlled and Uncontrolled Humidities. *European Journal of Pharmaceutics and Biopharmaceutics*, **44**, 187-194.

Gerrity, T.R. (1990). Pathophysiological and Disease Constraints on Aerosol Delivery. In Byron, P.R., (ed.), Respiratory Drug Delivery, CRC Press Inc, Florida, 1-38.

Godfrey, S., Zeidifard, E., Brown, K. and Bell, J.H. (1974). The Possible Site of Action of Sodium Cromoglycate Assessed by Exercise Challenge. *Clinical Science of Molecular Medicine*, **46**, 265-272.

Goldstein, J.I., Newbury, D.E., Echlin, P., Joy, D.C., Fiori, C., and Lifshin, E. (1992). Scanning Electron Microscopy and X-ray Microanalysis. Plenum Press, New York, U.S.A.

Gonda, I. (1988). Therapeutic Aerosols. In: Aulton, M.E. (ed.), Pharmaceutics: The Science of Dosage Form Design. Churchill Livingstone, Edinburgh, 341-358.

Gonda, I. (1992). Targeting by Deposition. In: A.J. Hickey (ed.), Pharmaceutical Inhalation Technology. Marcel Dekker, New York, 61-82.

Hallworth, G.W. (1987). The Formulation and Evaluation of Pressurised-Metered Dose Inhalers. In: D. Ganderton and T.M. Jones. (eds.), Drug Delivery to the Respiratory Tract. Horwood, Chichester, England, 87-118.

Hallworth, G.W. and Hamilton, R.R. (1976). Size Analysis of Metered Suspension Pressurised Aerosols with the Quantimet 720. *Journal of Pharmacy and Pharmacology*, **28**, 890-897.

Hallworth, G.W. and Westmoreland, D.G. (1987). The Twin Impinger; A Simple Device for Assessing the Delivery of Drugs from Metered Dose Pressurised Aerosol Inhalers. *Journal of Pharmacy and Pharmacology*, **39**, 966-972.

Hausner, H.H. (1967). Friction Conditions in a Mass of Metal Powder. *International Journal of Powder Metallurgy*, **3**, 7-13.

Hersey J.A. (1975). Ordered Mixing: A New Concept in Powder Mixing Practice. *Powder Technology*, **11**, 41-44.

Hickey, A.J. (1988). Practical Aspects of Aerosol Characterisation in an Environment of Controlled Temperature and Relative Humidity. *Drug Development and Industrial Pharmacy,* **14(2&3)**, 337-352.

Hickey, A.J. (1990). Factors Influencing Aerosol Deposition in Inertial Impactors and their Effect on Particle Size Characterisation. *Pharmaceutical Technology,* **September**, 118-130.

Hickey, A.J., Gonda, I., Irwin, W.J. and Fildes, F.J.T. (1990). Factors Influencing the Dispersion of Dry Powders as Aerosols. *Journal Pharmaceutical Sciences*, **79**, 1009-1014.

Hickey, A.J., Fults, K.A., Pillai, R.S. (1992). Use of Particle Morphology to Influence the Delivery of Drugs from Dry Powder Aerosols. *Journal of Biopharmaceutical Sciences*, **3(1/2)**, 107-113.

Hickey, A.J., Concessio, N.M., Van Oort, M.M., and Platz, R.M. (1994). Factors Influencing the Dispersion of Dry Powders as Aerosols. *Pharmaceutical Technology*, **August**, 58-82.

Hickey, A.J. and Dunbar, C.A. (1997). A New Millennium for Inhaler Technology. *Pharmaceutical Technology*, **June**, 116-125.

Hiestand, E.N. (1966). Powders: Particle-Particle Interactions. *Journal of Pharmaceutical Science*, **55(12)**, 1325-1344.

Hindle, M. and Byron, P.R. (1995a). Size Distribution Control of Raw Material for Dry-Powder Inhalers Using the Aerosizer with the Aero-Disperser. *Pharmaceutical Technology*, **June**, 64-72.

Hindle, M. and Byron, P.R. (1995b). Dose Emissions from Marketed Dry Powder Inhalers. *International Journal of Pharmaceutics*, **116**, 169-177.

Hindle, M., Newton, D.A.G. and Chrystyn, H. (1995). Dry Powder Inhalers are Bioequivalent to Metered-Dose Inhalers: A Study Using a New Urinary Albuterol (Salbutamol) Assay Technique. *Chest*, **107(3)**, 629-633.

Hindle, M., Byron, P.R. and Miller, N.C. (1996). Cascade Impaction Methods for Dry Powder Inhalers Using the High Flow Rate Marple-Miller Impactor. *International Journal of Pharmaceutics*, **134**, 137-146.

Hindle, M., Byron, P.R., Jashnani, R.N., Howell, T.M. and Cox, K.A. (1998). High Efficiency Fine Particle Generation Using Novel Condensation Technology. In: Byron, P.R., Dalby, R.N. and Farr, S.J. (eds.), *Respiratory Drug Delivery VI*, Interpharm Press, Buffalo Grove, IL., 97-102.

Hinds, W.C. (1982). Aerosol Technology: Properties, Behaviour and Measurement of Airborne Particles. Wiley Interscience: New York

Holgate, S.J. (1996). The Efficacy and Therapeutic Position of Nedocromil Sodium. *Respiratory Medicine*, **90**, 391-394.

Holzner, P.M. and Müller, B.M. (1994). An *In-vitro* Evaluation of Various Spacer Devices for Metered-Dose Inhalers Using the Twin Impinger. *International Journal of Pharmaceutics*, **106**, 69-75.

Holzner, P.M. and Müller, B.M. (1995). Particle Size Determination of Metered Dose Inhalers with Inertial Separation Methods: Apparatus A and B (BP), Four Stage Impinger and Anderson Mark II Cascade Impactor. *International Journal of Pharmaceutics,* **116**, 11-18.

Jashnani, R.N., Byron, P.R. and Dalby, R.N. (1995). Testing of Dry Powder Aerosol Formulations in Different Environmental Conditions. *International Journal of Pharmaceutics*, **113**, 123-130.

Jashnani, R.N. and Byron, P.R. (1996). Dry Powder Aerosol Generation in Different Environments: Performance Comparisons of Albuterol, Albuterol Sulfate, Albuterol Adipate and Albuterol Stearate. *International Journal of Pharmaceutics*, **130**, 13-24.

Jashnani, R.N., Byron, P.R. and Dalby, R.N. (1993). Dry Powder Inhaler Performance in Different Environments. *Pharmaceutical Research,* **10**, S196, PDD7088.

Jeffree, C.E. and Read, N.D. (1988). Common Artefacts Associated with Biological Material Examined by Low-Temperature Scanning Electron Microscopy.
In: Dickinson, H.G. and Goodhew, P.J. (eds.),
Institute of Physics Conference Series, **93(3)**, 17-18.

Jeffree, C.E. and Read, N.D. (1991a). Ambient and Low Temperature Scanning Electron Microscopy. In: Hall, J.L. and Hawes, C. (eds.), Electron Microscopy of Plant Cells. Academic Press, London, 313-413.

Jeffree, C.E. and Read, N.D. (1991b). Low Temperature Scanning Electron Microscopy in Biology. *Journal of Microscopy,* **161(1)**, 59-72.

Jenkins, L.M. and Donald, A.M. (1997). Use of the Environmental Scanning Electron Microscope for the Observation of the Swelling Behaviour of Cellulosic Fibres.
Scanning, **19**, 92-97.

Johnson, K.A. (1997). Preparation of Peptide and Protein Powders for Inhalation. *Advanced Drug Delivery Reviews*, **26**, 3-15.

Jones, T.M. and Pilpel, N. (1966). Some Angular Properties of Magnesia and their Relevance to Material Handling.

Journal of Pharmacy and Pharmacology, **18(suppl)**, 182T.

Kassem, N.M. (1990). Generation of Deeply Inspirable Clouds from Dry Powder Mixtures. Ph.D. Thesis, King's College, University of London, London, U.K.

Kassem, N. M. and Ganderton, D. (1989). The Influence of Carrier Surface on the Characteristics of Inspirable Powder Aerosols.

Journal of Pharmacy and Pharmacology, **42(suppl.)**, 11P.

Kawashima, Y. and Hino, T. (1996). Design of Inhalation Dry Composite Powders by Surface Modification of Drug Particles.

Proceedings of International Symposium on Dry Powder Inhalers. Tokyo, Japan, 9-16.

Kawashima, Y., Serigano, T., Hino, T., Yamamoto, H. and Takeuchi, H. (1998a). Effect of Surface Morphology of Carrier Lactose on Dry Powder Inhalation Properties of Prankulast Hydrate. *International Journal of Pharmaceutics*, **172**,179-188.

Kawashima, Y., Serigano, T., Hino, T., Yamamoto, H. and Takeuchi, H. (1998b). A New Powder Design Method to Improve Inhalation Efficiency of Prankulast Hydrate Dry Powder Aerosols by Surface Modification with Hydroxypropyl Methylcellulose Pthalate Nanospheres. *Pharmaceutical Research*, **(15)11**, 1748-1752.

Kay, G.R., Staniforth, J.N., Tobyn, M.J., MacGregor, S.A., Newnes, L.B., Li, M., Horrill, M.D., Lamming, R.C. and Hajee, D.W. (1998). Relationship Between Dry Powder Inhaler (DPI) Performance and Single Vessel Processor (SVP) Blending Time. *PharmSci,* **1(1) suppl**, S161, PDTT 2080.

Kay, G.R., Staniforth, J.N., Tobyn, M.J., Horrill, M.D., Newnes, L.B., MacGregor, S.A., Atherton, G., Lamming, R.C. and Hajee,D.W. (1999).
Design of a Fluid Energy Single Vessel Processor for Pharmaceutical Use.
International Journal of Pharmaceutics, **181(2)**, 243-254.

Khankari, R.K., Law, D. and Grant, D.J.W. (1992).
Determination of Water Content in Pharmaceutical Hydrates by Differential Scanning Calorimetry. *International Journal of Pharmaceutics*, **82**, 117-127.

Khankari, R.K. and Grant, D.J.W. (1995). Pharmaceutical Hydrates.
Thermochimica Acta, **248**, 61-79.

Khankari, R.K., Ojala, W.H., Gleason, W.B. and Grant, D.J.W. (1995).
Crystal Structure of Nedocromil Sodium Heptahemihydrate and its Comparison with that of Nedocromil Sodium Trihydrate.
Journal of Chemical Crystallography, **25(12)**, 863-870.

Khankari, R., Chen, L. and Grant, D.J.W. (1998). Physical Characterisation of Nedocromil Sodium Hydrates. *Journal of Pharmaceutical Sciences,* **87(9)**, 1052-1061.

Kontny, M.J. (1988). Distribution of Water in Solid Pharmaceutical Systems. *Drug Development and Industrial Pharmacy*, **14(14)**, 1991-2027.

Kontny, M.J. and Mulski, C.A. (1989). Gelatin Capsule Brittleness as a Function of Relative Humidity at Room Temperature. *International Journal of Pharmaceutics*, **54**, 79-85.

Kulvanich, P. and Stewart, P.J. (1987a). An Evaluation of the Airstream Faraday Cage in the Electrostatic Charge Measurement of Interactive Drug Systems. *International Journal of Pharmaceutics*, **36**, 243-252.

Kulvanich, P. and Stewart, P.J. (1987b). Fundamental Considerations in the Measurement of Adhesional Forces Between Particles Using the Centrifuge Method. *International Journal of Pharmaceutics*, **35**, 111-120.

Kulvanich, P. and Stewart, P.J. (1987c). The Effect of Particle Size and Concentration on the Adhesive Characteristics of a Model Drug-Carrier Interactive System. *Journal of Pharmacy and Pharmacology*, **39**, 673-678.

Kulvanich, P. and Stewart, P.J. (1988). Influence of Relative Humidity on the Adhesive Properties of a Model Interactive System. *Journal of Pharmacy and Pharmacology*, **40**, 453-458.

Leach, C.L. (1995). Approaches and Challenges to the Use of Freon Propellants Replacements. *Aerosol Science and Technology*, **22(4)**, 328-334.

Leach, C. (1999). Site Directed Aerosol Delivery of HFA-Beclomethasone to the Lungs. *Drug Delivery to the Lungs IX*, The Aerosol Society, London, U.K., 7-11.

Lord, J.D. (1993). Particle Interactions in Dry Powder Inhalations. Ph.D. Thesis, University of Bath, Bath, U.K.

Lord, J.D. and Staniforth, J.N. (1996). Particle Size Effects on Packing and Dispersion of Powders. In: Byron, P.R., Dalby, R.N. and Farr, S.J. (eds.), *Respiratory Drug Delivery V*, Interpharm Press, Buffalo Grove, IL., 75-84.

Lucas, P., Anderson, K. and Staniforth, J.N. (1998a). Protein Deposition from Dry Powder Inhalers: Fine Particle Multiplets as Performance Modifiers. *Pharmaceutical Research*, **15(4)**, 560-567.

Lucas, P., Clarke, M.J., Anderson, K., Tobyn, M.J., and Staniforth, J.N. (1998b). The Role of Fine Particle Excipients in Pharmaceutical Dry Powder Aerosols. In: Byron, P.R., Dalby, R.N. and Farr, S.J. (eds.), *Respiratory Drug Delivery VI*, Interpharm Press, Buffalo Grove, IL., 243-250.

Macrae, R.J. (1992). *In-vitro* Evaluation of Chemically Modified Nedocromil. PhD Thesis, University of Strathclyde, Strathclyde, U.K.

Mackin, L.A., Rowley, G., Fletcher, E.J. and Marriott, R.J. (1993). An Investigation of the Role of Moisture on the Charging Tendencies of Pharmaceutical Excipients. *Proceedings Pharmaceutical Technology Conference*, **12(2)**, 300-316.

Mackin, L.A., Rowley, G. and Fletcher, E.J. (1997). An Investigation of Carrier Particle Type, Electrostatic Charge and Relative Humidity on *In-vitro* Drug Deposition from Dry Powder Inhaler Formulations. *Pharmaceutical Sciences*, **3**, 583-586.

Maggi, L., Bruni, R. and Conte, U. (1999). Influence of Moisture on the Performance of a New Dry Powder Inhaler. *International Journal of Pharmaceutics*, **177**, 83-91.

Malmqvist, K. and Nystrom, C. (1982). Sieve Methods for the Characterisation of the Adhesion Tendency in Ordered Mixing. *Acta. Pharm. Suec.*, **19**, 437-445.

Marple, V.A., Olsson, B.A. and Miller, N.C. (1995). A Low-Loss Cascade Impactor Stage collection Cups: Calibration and Pharmaceutical Inhaler Applications. *Aerosol Science and Technology*, **22**, 124-134.

Martin, G.P., Bell, A.E. and Marriott, C. (1988). An *In-vitro* Method for Assessing Particle Deposition from Metered Pressurised Aerosols and Dry Powder Inhalers. *International Journal of Pharmaceutics*, **44**, 57-63.

May, K.R. (1966). Multistage Liquid Impinger. *Bacteriological Review*, **30**, 559-570.

Miller, N.C, Marple, V.A., Schultz, R.K. and Poon, W.S. (1992). Assessment of the Twin Impinger for Size Measurement of Metered Dose Inhaler Sprays. *Pharmaceutical Research,* **9(9)**, 1123-1127.

Mitchell, J.P. and Nagel, M.W. (1996). An Assessment of the API Aerosizer for the Real-Time Measurement of Medical Aerosols from Pressurised Metered-Dose Inhaler (pMDI) Systems. *Aerosol Science and Technology*, **25**, 411-423.

Mizes, H.A. (1994). Adhesion of Small Particles in Electric Fields. *Journal of Adhesion Science and Technology*, **8(8)**, 937-951.

Moren, F. (1992). Towards Satisfactory *In-vitro* Testing Requirements for Single and Multi-Dose Powder Inhalers. *Journal of Pharmaceutical Science,* **(1/2)**, 123-129.

Narinesingh, D., Stoute, V.A., Davis, G., Persad, D. (1992). Improved Spectrophotometric Determination of Lactose in Milk Using Flow-Injection Analysis. *Analytica Chimica Acta*, **258**, 141-149.

Nasr, M.M., Ross, D.L. and Miller, N.C. (1997). Effect of Drug Load and Plate Coating on the Particle size Distribution of a Commercial Albuterol Metered Dose Inhaler (MDI) determined using the Andersen and Marple Miller Cascade impactor. *Pharmaceutical Research*, **14(10)**, 1437-1443.

Nathier-Dufour, N., Bougeard, L., Devaux, M-F., Bertrand, D. and Le Deschault de Monredon, F. (1993). Comparisons of Sieving and Laser Diffraction for the Particle Size Measurements of Raw Materials used in Foodstuff. *Powder Technology*, **76**, 191-200.

Newman, S.P. and Clarke, S.W. (1983).

Therapeutic Aerosol I - Physical and Practical Considerations. *Thorax,* 38, 881-886.

Newman, S.P., Weisz, W., Talaee, N. and Clarke, S.W. (1991a).

Improvement of Drug Delivery with a Breath Actuated Pressurised Aerosol for Patients with Poor Inhaler Technique. *Thorax*, **46**, 712-716.

Newman, S.P., Morén, F., Trofast, E., Talaee, N. and Clarke, S.W. (1991b). Terbutaline Sulphate Turbohaler: Effect of Inhaled Flow Rate on Drug Deposition and Efficacy. *International Journal of Pharmaceutics,* **74**, 209-213.

Newman, S.P. and Wilding, I.R. (1998). Gamma Scintigraphy: An *In-vivo* Technique for Assessing the Equivalence of Inhaled Products.

International Journal of Pharmaceutics, **170**, 1-9.

Nickerson, T.A., Vujicic, I.F., Lin, Y.A. (1976). Colorimetric Estimation of Lactose and its Hydrolytic Products. *Journal of Dairy Science*, **59(3)**, 386-390.

Niven, R.W. (1993). Aerodynamic Particle Size Testing Using a Time-of-Flight Aerosol Beam Spectrometer. *Pharmaceutical Technology*, **January**, 72-78.

Niven, R.W. (1995). Delivery of Biotherapeutics by Inhalation Aerosol.

Critical Reviews in Therapeutic Drug Carrier Systems, **12(2&3)**, 151-231.

Ojala, W.H., Khankari, R.K., Grant, D.J.W. and Gleason, W.B. (1996).
Crystal Structures and Physical and Chemical Properties of Nedocromil Zinc Heptahydrate and Nedocromil Magnesium Pentahydrate.
Journal of Chemical Crystallography, **26(3)**, 167-178.

Olsson, B. and Asking, L. (1994). A Model for the Effect of Inhalation Device Flow Rate Resistance on the Peak Inspiratory Flow Rate and its Application in Pharmaceutical Testing. *Journal of Aerosol Medicine*, **7**, 201-204.

Olsson, B., Aiache, J.M., Bull, H., Ganderton, D., Haywood, P., Meakin, B.J., Schorn., P.J. and Wright, P. (1996). The Use of Inertial Impactors to Measure the Fine Particle Dose Generated by Inhalers. *Pharmeuropa*, **8(2)**, 291-298.

Olsson, B., Asking, L., Johansson, M. (1998). Choosing a Cascade Impactor. In: Byron, P.R., Dalby, R.N. and Farr, S.J. (eds.), *Respiratory Drug Delivery VI*, Interpharm Press, Buffalo Grove, IL., 133-138.

Padmadisastra, Y., Kennedy, R.A. and Stewart, P.J. (1994a).
Influence of Carrier Moisture Adsorption Capacity on the Degree of Adhesion of Interactive Mixtures. *International Journal of Pharmaceutics*, **104**, R1-R4.

Padmadisastra, Y., Kennedy, R.A. and Stewart, P.J. (1994b).
Solid Bridge Formation in Sulphonamide-Emdex Interactive Systems.
International Journal of Pharmaceutics, **112**, 55-63.

Patton, J.S. (1996). Mechanisms of Macromolecule Absorption by the Lungs. *Advanced Drug Delivery Reviews*, **19**, 3-36.

Peart, J. (1996). Electrostatic Charge Interactions in Pharmaceutical Dry Powder Aerosols. Ph.D. Thesis, University of Bath, Bath, U.K.

Persson, G. and Wirén, J.E. (1989). The Bronchodilator Response from Inhaled Terbutaline is Influenced by the Mass of Small Particles: A Study on a Dry Powder Inhaler (Turbuhaler®). *European Respiratory Journal*, **2**, 253-256.

Pharmaceutical Handbook (1980). 19th Edition, The Pharmaceutical Press, London.

Phillips, E.M., Byron, P.R., Fults, K. and Hickey, A.J. (1990). Optimised Inhalation Aerosols II. Inertial Testing Methods for Particle Size Analysis of Pressurised Inhalers. *Pharmaceutical Research,* **7(12)**, 1228-1233.

Phillips, E.M. and Stella, V.J. (1993).
Rapid Expansion from Supercritical Solutions: Application to Pharmaceutical Processes. *International Journal of Pharmaceutics*, **94**, 1-10.

Pitcairn, G.R., Hooper, G., Luria, X., Rivero, X. and Newman, S.P. (1997).
A Scintigraphic Study to Evaluate the Deposition Patterns of a Novel Anti-Asthma Drug Inhaled from the Cyclohaler Dry Powder Inhaler.
Advanced Drug Delivery Reviews, **26**, 59-67.

Podczeck, F., Newton, J.M. and James, M.B. (1995). Assessment of Adhesion and Autoadhesion Forces Between Particles and Surfaces. Part II. The Investigation of Adhesion Phenomena of Salmeterol Xinafoate and Lactose Monohydrate Particles in Particle-On-Particle and Particle-On-Surface Contact.
Journal of Adhesion Science and Technology, **9(4)**, 475-486.

Podczeck, F., Newton, M.J., James, M.B. (1996). The Influence of Constant and Changing Relative Humidity of the Air on the Autoadhesion Force Between Pharmaceutical Powder Particles.
International Journal of Pharmaceutics, **145**, 221-229.

Podczeck, F., Newton, J.M, James, M.B. (1997). Variations in the Adhesion Force Between a Drug and Carrier Particles as a Result of Changes in the Relative Humidity of the Air. *International Journal of Pharmaceutics,* **149**, 151-160.

Rees, P.J., Clark, T.J.H. and Moren, F. (1982).
The Importance of Particle Size in Response to Inhaled Bronchodilators.
*European Journal of Respiratory Dis*eases, **63**, 73-78.

Rippie, E.G., Olsen, J.L. and Faiman, M.D. (1964). Segregation Kinetics of Particulate Solids. *Journal of Pharmaceutical Science*, **53**, 1360-1363.

Robertson, D.L.N. (1997). The Effect of Carrier Shape and Texture on Drug Availability of Aerosolised Particles. Ph.D. Thesis, University of Bath, Bath, U.K.

Saleki-Gerhart, A., Ahlneck, C. and Zografi, G. (1994). Assessment of Disorder in Crystalline Solids. *International Journal of Pharmaceutics*, **101**, 237-247.

Samyn, J.C. and Murphy, K.S. (1974). Experiments in Powder Blending and Unblending. *Journal of Pharmaceutical Sciences*, **63**, 370-375.

Smith, P.L. (1997). Peptide Delivery via the Pulmonary Route: A Valid Approach for Local and Systemic Delivery. *Journal of Controlled Release,* **46**, 90-106.

Smith, S.J. and Bernstein, J.A. (1996). Therapeutic Uses of Lung Aerosols. In Hickey, A.J. (ed.), Inhalation Aerosols: Physical and Biological Basis for Therapy. Marcel Dekker, Inc., New York, U.S.A., 234-269.

Soebagyo, S.S. and Stewart, P.J. (1985). The Effect of Cohesive and Non-Cohesive Ternary Components on the Homogeneity and Stability of a Prednisolone Interactive Mixture. *International Journal of Pharmaceutics*, **25**, 225-236.

Srichana, T., Martin, G.P. and Marriott, C. (1998). On the Relationship Between Drug and Carrier Deposition from Dry Powder Inhalers *In-Vitro*.
International Journal of Pharmaceutics, **167**, 13-23.

Staniforth, J.N. (1981). Total Mixing. *International Journal of Pharmaceutical Technology and Product Manufacture*, **2(1)**, 7-12.

Staniforth, J.N., Rees, J.E., Lai, F.K. and Hersey, J.A. (1981). Determination of Interparticulate Forces in Ordered Powder Mixes. *Journal of Pharmacy and Pharmacology*, **33,** 485-490.

Staniforth, J.N. (1982). Advances in Powder Mixing and Segregation in Relation to Pharmaceutical Processing. *International Journal of Pharmaceutical Technology and Product Manufacture*, **3(suppl.)**, 1-12.

Staniforth, J.N. and Rees, J.E. (1982). Electrostatic Charge Interactions in Ordered Powder Mixes. *Journal of Pharmacy and Pharmacology*, **34**, 69-76.

Staniforth, J.N. and Rees, J.E. (1983). Segregation of Vibrated Powder Mixes Containing Different Concentrations of Fine Potassium Chloride and Tablet Excipients. *Journal of Pharmacy and Pharmacology*, **35**, 549-554.

Staniforth, J.N. (1984). Relationship Between Sine Random Vibrations, Resonance and Drug Content Uniformity. *Journal of Pharmacy and Pharmacology*, **36**, 258-260.

Staniforth, J.N. (1987). Order Out of Chaos. *Journal of Pharmacy and Pharmacology*, **39**, 329-334.

Staniforth, J.N. (1995). Performance-Modifying Influences in Dry Powder Inhalation Systems. *Aerosol Science and Technology*, **22**, 346-353.

Staniforth, J.N. (1996). Pre-formulation Aspects of Dry Powder Aerosols. In: Byron, P.R., Dalby, R.N. and Farr, S.J. (eds.), *Respiratory Drug Delivery V*, Interpharm Press, Buffalo Grove, IL., 65-73.

Steckel, H. and Müller, B.W. (1997a). *In vitro* Evaluation of Dry Powder Inhalers I: Drug Deposition of Commonly Used Devices.
International Journal of Pharmaceutics, **154**, 19-29.

Steckel, H. and Müller, B.W. (1997b). *In-vitro* Evaluation of Dry Powder Inhalers II: Influence of Carrier Particle Size and Concentration on *In-vitro* Deposition.
International Journal of Pharmaceutics, **154**, 31-37.

Stewart, P.J. (1986). Particle Interactions in Pharmaceutical Systems.
Pharmacy International. **7**, 146-149.

Strickland, W.A. and Moss, M. (1962). Water Vapour Sorption and Diffusion Through Hard Gelatin Capsules. *Journal of Pharmaceutical Sciences*, **51**, 1002-1005.

Summers, Q.A., Fleming, J.S., Dai, Y., Perring, S., Honeywell, R., Gough, K.J., Renwick, A.G., Clark, A.R., Nassim, M.A. and Holgate, S.T. (1996). The Pulmonary Deposition of Two Aerosol Preparations of Nedocromil Sodium Delivered by MDI Assessed by Single Photon Emission Computed Tomography.
Journal of Aerosol Medicine, **9(1)**, S93-S109.

Suschitzky, J.L. and Sheard, P. (1984). The Search for Antillaergic Drugs for the Treatment of Asthma - Problems in Finding a Successor to Sodium Cromoglycate. In: Ellis, G.P. and West, G.B. (eds.), *Progress in Medicinal Chemistry,* Elsevier Science Publishers, B.V., **21**, 1-61.

Swindlehurst, C.A. and Nieman, T.A. (1988). Flow-Injection Determination of Sugars with Immobilised Enzyme Reactors and Chemiluminescence Detection. *Analytica Chimica Acta*, **205**, 195-205.

Taburet, A-M and Schmit, B. (1994). Pharmacokinetic Optimisation of Asthma Treatment. *Clinical Pharmacokinetics*, **26(5)**, 396-418.

Tansey, I.P. (1997). Changing to CFC-Free Inhalers: The Technical and Clinical Challenges. *The Pharmaceutical Journal*, **259**, 896-898.

Ticehurst, M.D., Rowe, R.C. and York, P. (1994). Determination of the Surface Properties of Two batches of Salbutamol Sulphate by Inverse Gas Chromatography. *International Journal of Pharmaceutics*, **111**, 214-249.

Timsina, M.P., Martin, G.P., Marriott, C., Ganderton, D. and Yianneskis, M. (1994). Drug Delivery to the Respiratory Tract Using Dry Powder Inhalers. *International Journal of Pharmaceutics*, **101**, 1-13.

Travers, D.N. and White, R,C. (1971).

The Mixing of Micronised Sodium Bicarbonate with Sucrose Crystals.

Journal of Pharmacy and Pharmacology, **23**, 260S-261S.

Trofast, E.A.C. and Falk, E.J. (1996).

Agglomeration of Finely Divided Powders. U.S. Patent No. 5551489.

Vaughan, N.P. (1989). The Andersen Impactor: Calibration, Wall Losses and Numerical Simulation. *Journal of Aerosol Science*, **20(1)**, 67-90.

Vidgren, M.T., Paronen, T.P., Kärkkäinen, A. and Karjalainen, P. (1987a). Effect of Extension Devices on the Drug Deposition from Inhalation Aerosols.

International Journal of Pharmaceutics, **39**, 107-112.

Vidgren, M.T., Vidgren, P.A. and Paronen, T.P. (1987b). Comparison of Physical and Inhalation Properties of Spray Dried and Mechanically Micronised Disodium Cromoglycate. *International Journal of Pharmaceutics*, **35**, 139-144.

Vidgren, M. Kärkkäinen, A., Karjalainen, P., Nuutinen, J. and Paronen, P. (1988a). *In-vitro* and *In-vivo* Deposition of Drug Particles Inhaled from Pressurised Aerosol and Dry Powder Inhaler.

Drug Development and Industrial Pharmacy, **14(15-17)**, 2649-2665.

Vidgren, M., Kärkkäinen, A., Karjalainen, P., Paronen, P. and Nuutinen, J. (1988b). Effect of Powder Inhaler Design on Drug Deposition in the Respiratory Tract. *International Journal of Pharmaceutics*, **42**, 211-216.

Vidgren, P., Vidgren, M. and Paronen, P. (1989). Physical Stability and Inhalation Behaviour of Mechanically Micronised and Spray Dried Sodium Cromoglycate in Different Humidities. *Acta Pharmaceutica Fennica*, **98**, 71-78.

Vidgren, M., Paronen, P., Vidgren, P., Vainio, P. and Nuutinen, J. (1990). *In-vivo* Evaluation of the New Multiple Dose Powder Inhaler and the Rotahaler Using the Gamma Scintigraphy. *Acta Pharmaceutica Nordica*, **1(2)**, 3-10.

Vidgren, M., Silvasti, M., Vidgren, P., Laurikainen, K., Lehti, H. and Paronen, P. (1991). Physical Properties and Clinical Efficacy of Two Sodium Cromoglycate Inhalation Aerosol Preparations. *Acta Pharmaceutica Nordica*, **3(1)**, 1-4.

Vidgren, M., Vidgren, P., Laine, E., Pirttimäki, J., Arppe, J. and Paronen, P. (1992). Effect of Humidity on the Behaviour of Inhaled Disodium Cromoglycate Particles. *Proceedings to the Pharmaceutical Technology Conference*, **15**, 414-424.

Vidgren, M. (1994). Factors Influencing Lung Deposition of Inhaled Aerosols. *European Respiratory Reviews,* **4(18)**, 68-70.

Visser, J. (1989). Van der Waals and Other Cohesive Forces Affecting Powder Fluidisation. *Powder Technology*, **58**, 1-10.

Webb, P.A. and Orr, C. (1997). Analytical Methods in Fine Technology. Micromeritics Instruments Corporation, Norcross, G.A., U.S.A.

Wetterlin, K. (1988). Turbohaler: A New Powder Inhaler for Administration of Drugs to the Airways. *Pharmaceutical Research*, **5(8)**, 506-508.

Williams, J.C., and Shields, G. (1967). The Segregation of Granules in a Vibrated Bed. *Powder Technology*, **1**, 134-142.

Wong, L.W. and Pilpel, N. (1988). The Effect of the Shape of Fine Particles on the Formation of Ordered Mixtures.
Journal of Pharmacy and Pharmacology, **40**, 567-568.

Wong, L.W., Kassem, N.M and Ganderton, D. (1989). The Effect of the Shape of Fine Particles on the Inhalation Properties of Powder Mixtures.
Journal of Pharmacy and Pharmacology, **41(suppl)**, 24P.

Wong, L.W. and Pilpel, N. (1990). Effect of Particle Shape on the Mixing of Powders. *Journal of Pharmacy and Pharmacology*, **42**, 1-6.

Wong, D.Y.T., Wright, P. and Aulton, M.E. (1995a). Effect of Drug/Carrier Ratio on the Mixing and Dispersion of Dry Powder Inhalations of Nedocromil Sodium. Proceedings 1st World Meeting on Pharmaceutics, Biopharmaceutics and Pharmaceutical Technology, Budapest, 767-768.

Wong, D.Y.T, Wright, P. and Aulton, M.E. (1995b). Influence of Drug Particle Size on the Performance of Dry Powder Inhalers. 14th Pharmaceutical Technology Conference, Barcelona, Spain, 86-97.

Yeung, C.C. and Hersey, J.A. (1979). Ordered Powder Mixing of Coarse and Fine Particulate Systems. *Powder Technology*, **22**, 127-131.

Yip, C.W., and Hersey, J.A. (1977a). Perfect Powder Mixtures. *Powder Technology*, **16**, 149-150.

Yip, C.W. and Hersey, J.A. (1977b). Ordered or Random Mixing: Choice of Ssystem and Mixer. *Drug Development and Industrial Pharmacy*, **3**, 429-438.

York, P. and Hanna, M. (1996). Particle Engineering by Supercritical Fluid Technologies for Powder Inhalation Drug Delivery. In: Byron, P.R., Dalby, R.N. and Farr, S.J. (eds.), *Respiratory Drug Delivery V*, Interpharm Press, Buffalo Grove, IL., U.S.A., 251-259.

York, P., Hanna, M., Yu-Shekunov, B. and Humphreys, G.O. (1998). Microfine Particle Formation by SEDS (Solution Enhanced Dispersion by Supercritical Fluids): Scale Up by Design. In: Byron, P.R., Dalby, R.N. and Farr, S.J. (eds.), *Respiratory Drug Delivery VI*, Interpharm Press, Buffalo Grove, IL., U.S.A., 169-175.

Zanen, P., van Spiegel, P.I., van der Kolk, H., Tushuizen, E. and Enthoven, R. (1992). The Effect of the Inhalation Flow on the Performance of a Dry Powder Inhalation System. *International Journal of Pharmaceutics*, **81**, 199-203.

Zanen, P., Go, L.T. and Lamers, J-W., J. (1994). The Optimal Particle Size for β-Adrenergic Aerosols in Mild Asthmatics.
International Journal of Pharmaceutics, **107**, 211-217.

Zanen, P., Go, L.T. and Lammers, J-W, J. (1995). The Optimal Particle Size for Parasympathicolytic Aerosols in Mild Asthmatics.
International Journal of Pharmaceutics, **114**, 11-115.

Zeng, X.M., Tee, S.K., Martin, G.P. and Marriott, C. (1996). Effects of Mixing Procedure and Particle Size Distribution of Carrier Particles on the Deposition of Salbutamol Sulphate from Dry Powder Inhaler Formulations.
Drug Delivery to the Lungs VII, The Aerosol Society, London, U.K., 188-191.

Zeng, X.M., Martin, G.P., Tee, S-K and Marriott, C. (1998). The Role of Fine Particle Lactose on the Dispersion and Deaggregation of Salbutamol Sulphate in an Air Stream *In-vitro*. *International Journal of Pharmaceutics*, **176**, 99-110.

Zhang, H-J. and Xu, G-D. (1992). The Effect of Particle Refractive Index on Size Measurement. *Powder Technology*, **70**, 189-192.

Zhu, H., Khankari, R.K., Padden, B.E., Munson, E.J., Gleason, W.B., Grant, D.J.W. (1996). Physicochemical Characterisation of Nedocromil Bivalent Metal Salt Hydrates. 1. Nedocromil Magnesium. *Journal of Pharmaceutical Sciences*, **85**, 1026-1034.

Zhu, H., Padden, B.E., Munson, E.J. and Grant, D.J.W. (1997a). Physicochemical Characterisation of Nedocromil Bivalent Metal Salt Hydrates: 2. Nedocromil Zinc. *Journal of Pharmaceutical Sciences,* **86(4)**, 418-429.

Zhu, H., Halfen, J.A., Young, Jr., V.G., Padden, B.E., Munson, E.J., Menon, V., Grant, D.J.W. (1997b). Physicochemical Characterisation of Nedocromil Bivalent Metal Salt Hydrates: 3. Nedocromil Calcium. *Journal of Pharmaceutical Sciences*, **86**, 1439-1447.

Zografi, G. (1988). States of Water Associated with Solids. *Drug Development and Industrial Pharmacy,* **14(14)**, 1905-1926.

APPENDICES

Appendix I Particle Size Analysis

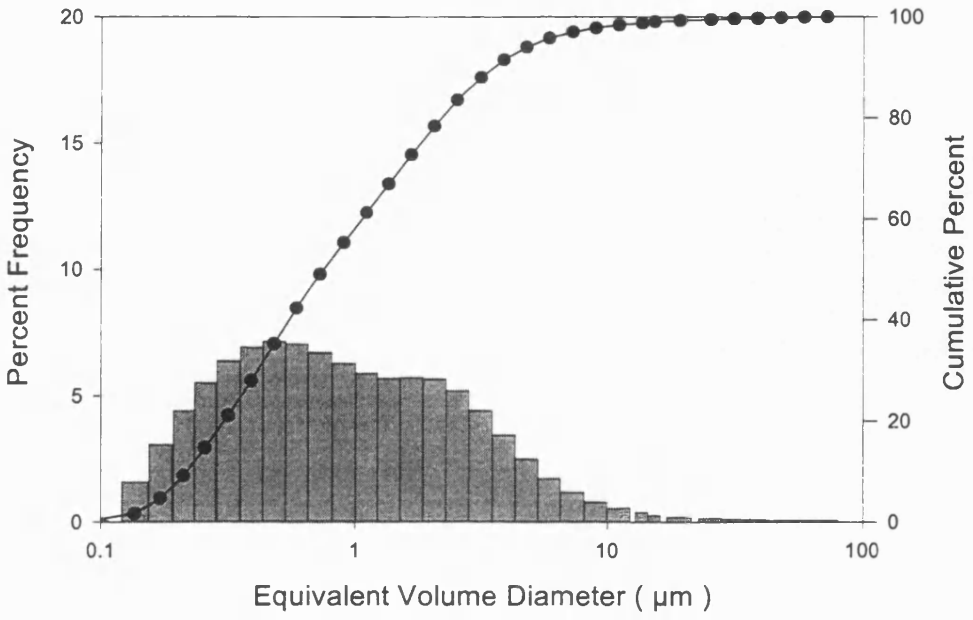

A1 Particle size distribution of micronised NST (LVC / 45 mm lens)

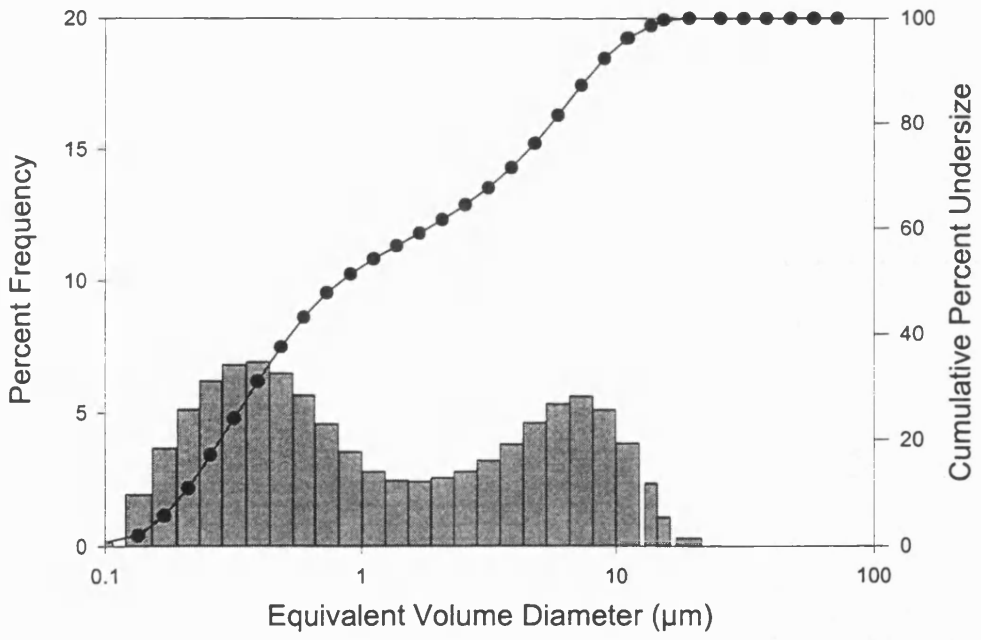

A2 Particle size distribution of milled NST (LVCC / 45 mm lens)

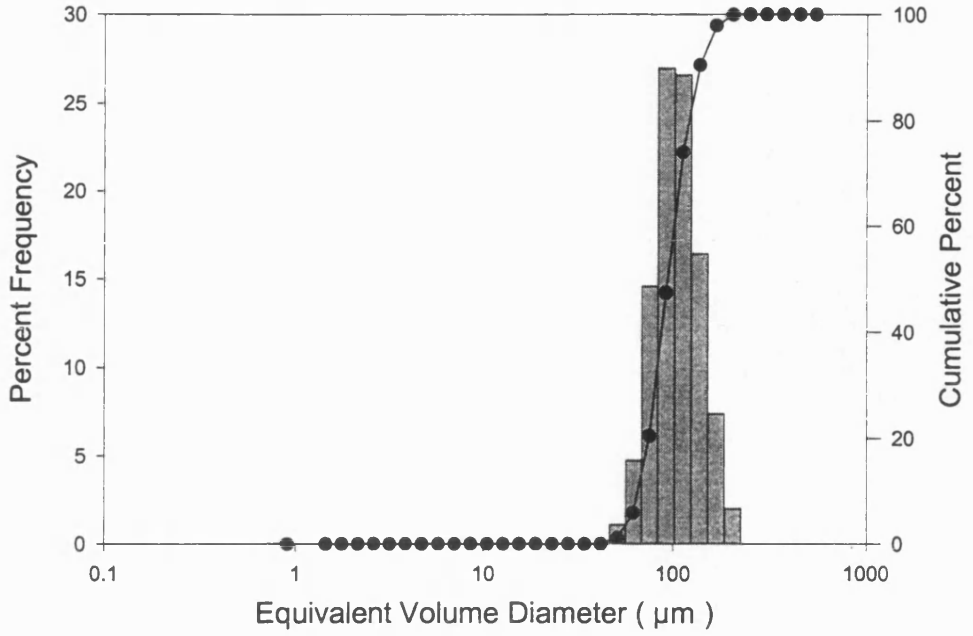

A3 Particle size distribution of Lactose 63-90µm (AJS) (DPF / 300 mm lens)

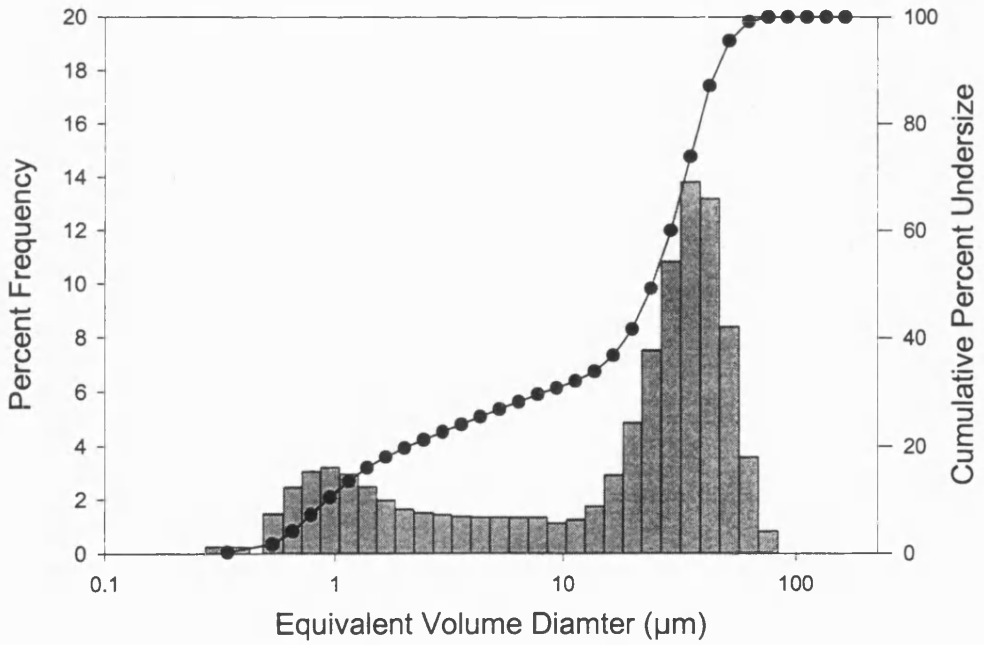

A4 Particle size distribution of lactose sieve size fraction <45 µm) (SVC / 100 mm lens)

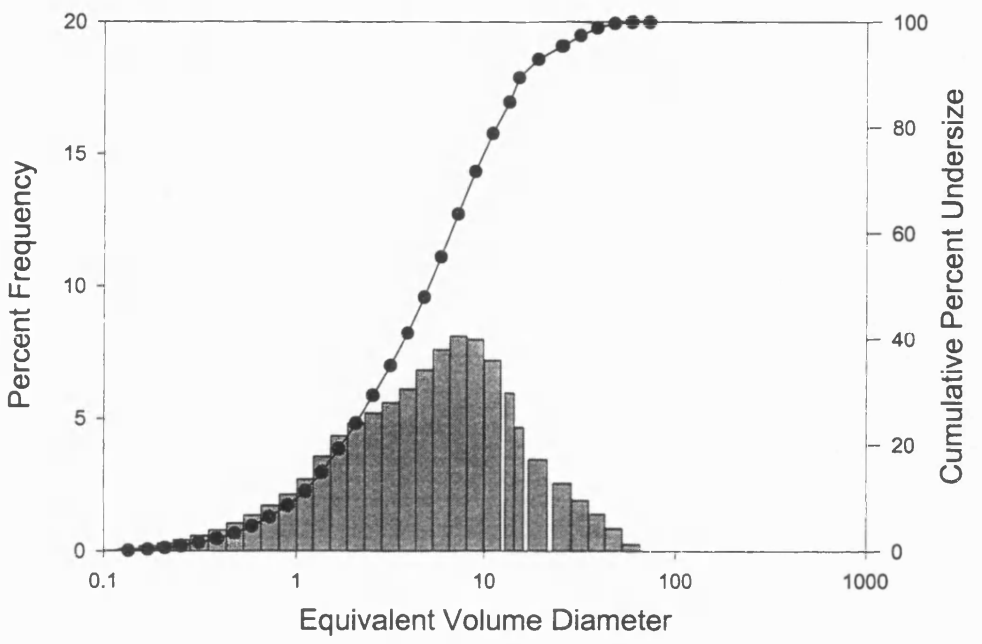

A5 Particle size distribution of FPL (LVC/ 100 mm lens)

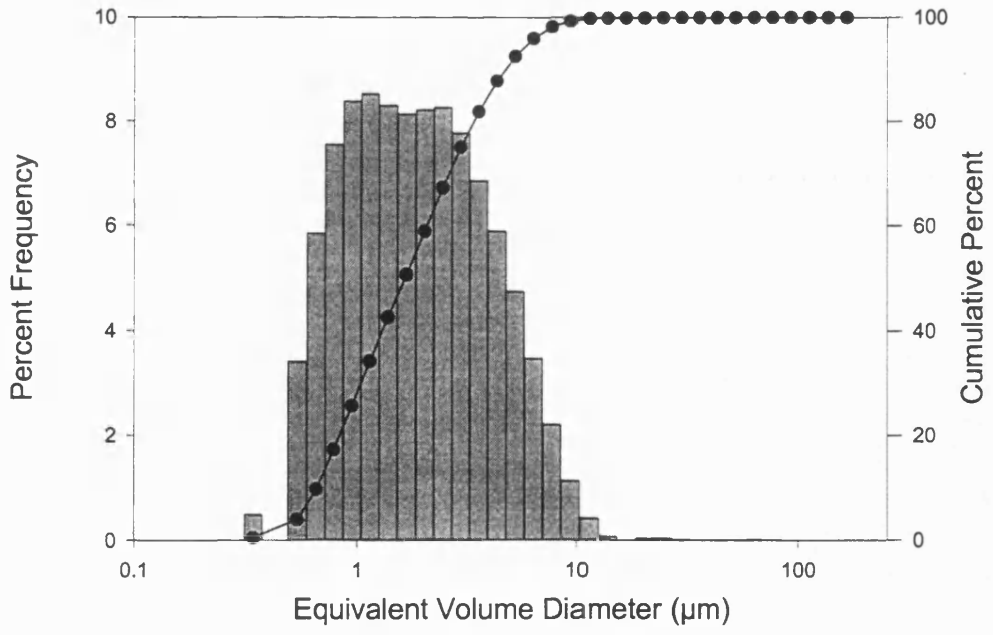

A6 Particle size distribution of micronised TS (SVC / 100 mm)

Appendix II Statistical Analysis

To Determine the Equality of More than Two Estimates of a Parameter (P)

The Bartlett test was used to compare calibration graphs (slopes) for nedocromil sodium trihydrate (stored under various conditions of humidity), nedocromil sodium heptahemihydrate and terbutaline sulphate.

$$\chi^2 = \frac{\sum (P_i - \bar{P})^2}{\hat{\sigma}^2}$$

where $\hat{\sigma}^2$ is given by,

$$\hat{\sigma}^2 = \frac{n_1 s_1^2 + n_2 s_2^2 + \ldots\ldots n_n s_n^2}{n_1 + n_2 + \ldots\ldots n_n}$$

where S_1, S_2 etc. are the standard deviations associated with the estimates P_1, P_2, etc. and n_1 and n_2 are the number of observations used in determining the estimates.

If the estimates all come from the same normal distribution ,

$\frac{\sum (P_i - \bar{P})^2}{\hat{\sigma}^2}$ will have χ^2 distribution with N-1 degrees of freedom,

where N is the number of estimates.

Appendix III

Determination of the Test Flow Rate for the Evaluation of the Cyclohaler at 4 kPa

Equipment

- Hastings Mass Flow Meter model HFM 201, Transducer and model CPD-100 Display Unit (range 1-150 lires min^{-1}).
- 5-Stage Liquid Impinger.
- Differential Pressure Manometer (Digitron P200 H.is).
- Absolute Pressure Manometer (Digitron P200 HA).
- Flow Rate Regulator Unit incorporating regulator valve, timer and solenoid.
- Gast Vacuum Pump Model No. 1023.

Procedure

1. The apparatus was assembled as shown in Figure A7. Rubber bungs were inserted into the MSLI sampling ports in stages 2, 3 and 4. A "special" bung, which allowed connection of the differential pressure meter to the stage 1 sampling port, was also employed.
2. The Cyclohaler® was inserted into the silicone rubber adaptor.
3. The vacuum pump was switched on, the timer-solenoid unit opened and the regulating valve adjusted until the differential pressure at the sidearm was 4 kPa. Two Gast Vacuum Pumps, connected in parallel, were required to achieve the 4 kPa pressure drop across the Cyclohaler®. The pump was then switched off, the manometer, Cyclohaler® and silicone adapter removed and stage-1 sealed with a "normal" bung.
4. The flow rate (litres min^{-1}) was determined by connecting the flow meter to the MSLI.
5. The silicone rubber adaptor and Cyclohaler® were replaced and with the pump running the absolute pressure either side of the timer solenoid (P_2, P_3) measured with the Digitron P200 A11 manometer. The pressure ratio P_3/P_2 was <0.5, confirming critical flow.

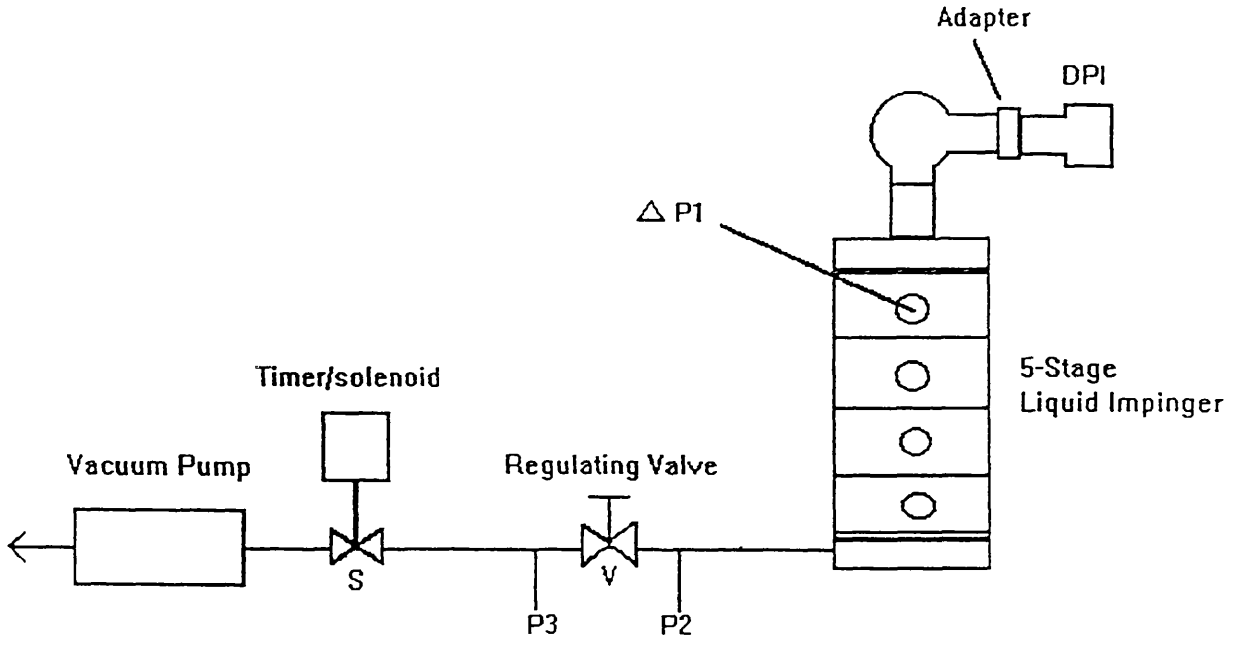

Figure A7 Schematic of apparatus for determination of Cyclohaler® flow rate for 4 kPa pressure drop.

S = CDFS Solenoid/timer control (CDFS, University of Bath, Bath, U.K.)

V = Regulating valve.

ΔP1 = Differential pressure to atmosphere, Digitron P200 H.is.

P2/P3 = Absolute pressure, Digitron P200 HA.

Appendix IV Drug Monolayer Coverage

An approximate concentration (% $^{w}/_{w}$) of micronised NST required to form a theoretical monolayer of particles on the surface of the coarse carrier lactose was calculated based on the assumptions and conclusions of Hersey (1975). Values were obtained based on true density and specific surface area values.

Material	Median Diameter (μm)	True Density (kg m^{-3})	Specific surface Area (m^2 g^{-1})
63-90 μm Lactose	96.5	1.54	0.12
NST Micronised	0.86	1.63	7.1

Table A1. Experimental Data

From surface area data, concentration of NST required for theoretical mono particle layer coverage = 6.0 % $^{w}/_{w}$

From true density data, concentration of NST required for theoretical mono particle layer coverage = 3.5 % $^{w}/_{w}$